MOLECULAR EPIDEMIOLOGY OF FUNGAL INFECTIONS

EDITED BY: Abdullah M. S. Al-Hatmi, G. Sybren De Hoog, Jianping Xu and Min Chen

PUBLISHED IN: Frontiers in Cellular and Infection Microbiology

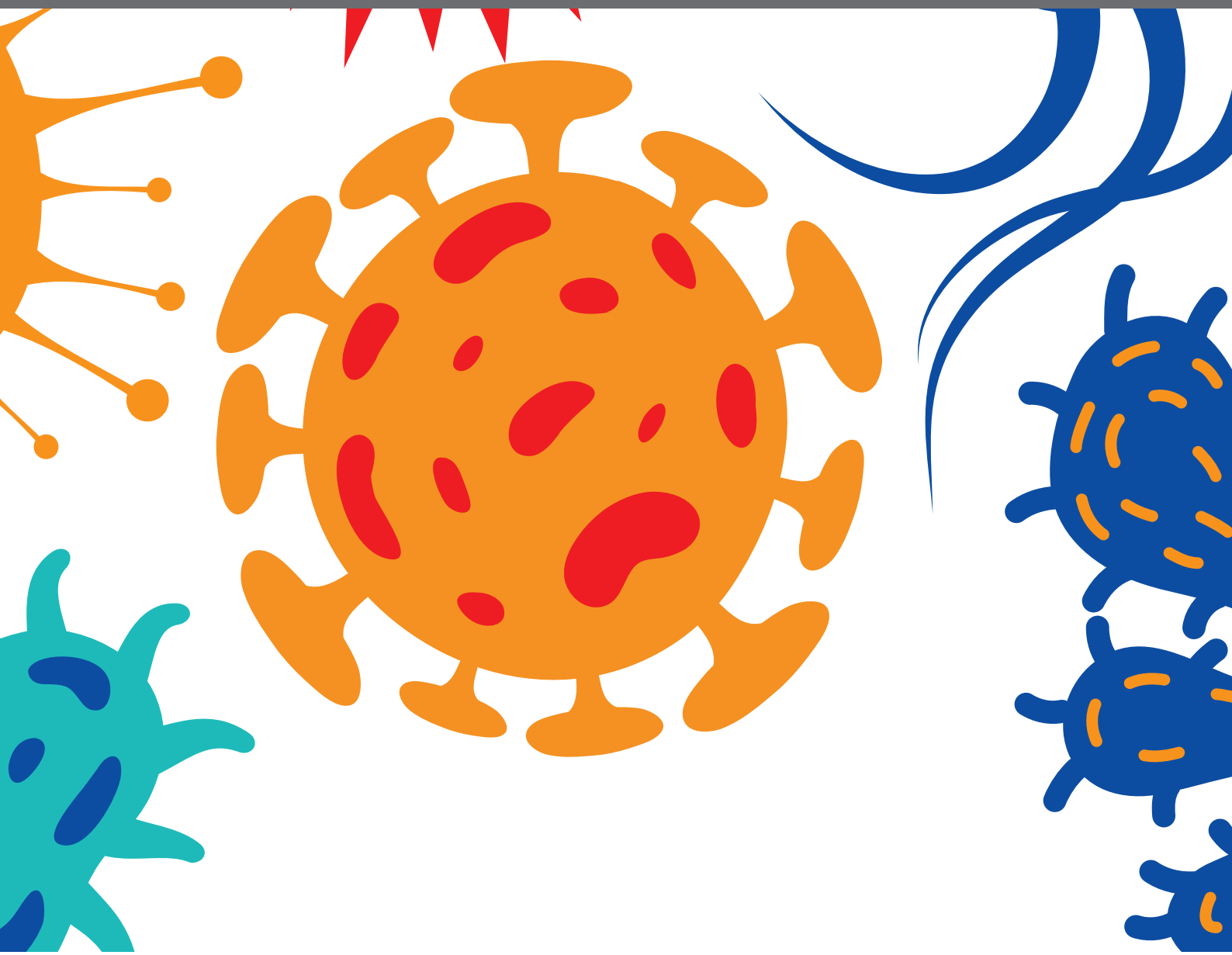

frontiers Research Topics

ISSN 1664-8714
ISBN 978-2-88976-411-2
DOI 10.3389/978-2-88976-411-2

About Frontiers

Frontiers is more than just an open-access publisher of scholarly articles: it is a pioneering approach to the world of academia, radically improving the way scholarly research is managed. The grand vision of Frontiers is a world where all people have an equal opportunity to seek, share and generate knowledge. Frontiers provides immediate and permanent online open access to all its publications, but this alone is not enough to realize our grand goals.

Frontiers Journal Series

The Frontiers Journal Series is a multi-tier and interdisciplinary set of open-access, online journals, promising a paradigm shift from the current review, selection and dissemination processes in academic publishing. All Frontiers journals are driven by researchers for researchers; therefore, they constitute a service to the scholarly community. At the same time, the Frontiers Journal Series operates on a revolutionary invention, the tiered publishing system, initially addressing specific communities of scholars, and gradually climbing up to broader public understanding, thus serving the interests of the lay society, too.

Dedication to Quality

Each Frontiers article is a landmark of the highest quality, thanks to genuinely collaborative interactions between authors and review editors, who include some of the world's best academicians. Research must be certified by peers before entering a stream of knowledge that may eventually reach the public - and shape society; therefore, Frontiers only applies the most rigorous and unbiased reviews.
Frontiers revolutionizes research publishing by freely delivering the most outstanding research, evaluated with no bias from both the academic and social point of view. By applying the most advanced information technologies, Frontiers is catapulting scholarly publishing into a new generation.

What are Frontiers Research Topics?

Frontiers Research Topics are very popular trademarks of the Frontiers Journals Series: they are collections of at least ten articles, all centered on a particular subject. With their unique mix of varied contributions from Original Research to Review Articles, Frontiers Research Topics unify the most influential researchers, the latest key findings and historical advances in a hot research area! Find out more on how to host your own Frontiers Research Topic or contribute to one as an author by contacting the Frontiers Editorial Office: frontiersin.org/about/contact

MOLECULAR EPIDEMIOLOGY OF FUNGAL INFECTIONS

Topic Editors:
Abdullah M. S. Al-Hatmi, University of Nizwa, Oman
G. Sybren De Hoog, Radboud University Nijmegen Medical Centre, Netherlands
Jianping Xu, McMaster University, Canada
Min Chen, Shanghai Changzheng Hospital, China

Citation: Al-Hatmi, A. M. S., De Hoog, G. S., Xu, J., Chen, M., eds. (2022). Molecular Epidemiology of Fungal Infections. Lausanne: Frontiers Media SA. doi: 10.3389/978-2-88976-411-2

Table of Contents

05 ***Editorial: Molecular Epidemiology of Fungal Infections***
Min Chen, Abdullah M. S. Al-Hatmi, Jianping Xu and G. Sybren De Hoog

08 ***Clonal Candidemia Outbreak by* Candida parapsilosis *Carrying Y132F in Turkey: Evolution of a Persisting Challenge***
Amir Arastehfar, Suleyha Hilmioğlu-Polat, Farnaz Daneshnia, Weihua Pan, Ahmed Hafez, Wenjie Fang, Wanqing Liao, Zümrüt Şahbudak-Bal, Dilek Yeşim Metin, João N. de Almeida Júnior, Macit Ilkit, David S. Perlin and Cornelia Lass-Flörl

18 ***Molecular Markers Reveal Epidemiological Patterns and Evolutionary Histories of the Human Pathogenic* Cryptococcus**
Nan Hong, Min Chen and Jianping Xu

33 ***Molecular Epidemiology, Antifungal Susceptibility, and Virulence Evaluation of* Candida *Isolates Causing Invasive Infection in a Tertiary Care Teaching Hospital***
Junzhu Chen, Niya Hu, Hongzhi Xu, Qiong Liu, Xiaomin Yu, Yuping Zhang, Yongcheng Huang, Junjun Tan, Xiaotian Huang and Lingbing Zeng

45 ***Application of Machine Learning Classifier to* Candida auris *Drug Resistance Analysis***
Dingchen Li, Yaru Wang, Wenjuan Hu, Fangyan Chen, Jingya Zhao, Xia Chen and Li Han

55 ***Antifungal Susceptibility Profiles and Resistance Mechanisms of Clinical* Diutina catenulata *Isolates With High MIC Values***
Xin-Fei Chen, Wei Zhang, Xin Fan, Xin Hou, Xiao-Yu Liu, Jing-Jing Huang, Wei Kang, Ge Zhang, Han Zhang, Wen-Hang Yang, Ying-Xing Li, Jin-Wen Wang, Da-Wen Guo, Zi-Yong Sun, Zhong-Ju Chen, Ling-Gui Zou, Xue-Fei Du, Yu-Hong Pan, Bin Li, Hong He and Ying-Chun Xu

63 ***Prevalence of Fungal and Bacterial Co-Infection in Pulmonary Fungal Infections: A Metagenomic Next Generation Sequencing-Based Study***
Zhan Zhao, Junxiu Song, Changqing Yang, Lei Yang, Jie Chen, Xinhui Li, Yubao Wang and Jing Feng

71 ***High Prevalence of HIV-Related Cryptococcosis and Increased Resistance to Fluconazole of the* Cryptococcus neoformans *Complex in Jiangxi Province, South Central China***
Chunxi Yang, Zeyuan Bian, Oliver Blechert, Fengyi Deng, Hui Chen, Yueting Li, Yunhong Yang, Min Chen and Ping Zhan

80 ***First Case of Subcutaneous Mycoses Caused by* Dirkmeia churashimaensis *and a Literature Review of Human* Ustilaginales *Infections***
Fengming Hu, Chong Wang, Peng Wang, Lei Zhang, Qing Jiang, Abdullah M. S. Al-Hatmi, Oliver Blechert and Ping Zhan

88 ***Multilocus Sequence Typing Reveals Extensive Genetic Diversity of the Emerging Fungal Pathogen* Scedosporium aurantiacum**
Azian Harun, Alex Kan, Katharina Schwabenbauer, Felix Gilgado, Haybrig Perdomo, Carolina Firacative, Heidemarie Losert, Sarimah Abdullah, Sandrine Giraud, Josef Kaltseis, Mark Fraser, Walter Buzina, Michaela Lackner, Christopher C. Blyth, Ian Arthur, Johannes Rainer, José F. Cano Lira, Josep Guarro Artigas, Kathrin Tintelnot, Monica A. Slavin, Christopher H. Heath, Jean-Philippe Bouchara, Sharon C. A. Chen and Wieland Meyer

103 ***Genome Sequences of Two Strains of* Prototheca wickerhamii *Provide Insight Into the Protothecosis Evolution***
Jian Guo, Jianbo Jian, Lili Wang, Lijuan Xiong, Huiping Lin, Ziyi Zhou, Eva C. Sonnenschein and Wenjuan Wu

112 ***Molecular Characteristics of Regional Chromoblastomycosis in Guangdong, China: Epidemiological, Clinical, Antifungal Susceptibility, and Serum Cytokine Profiles of 45 Cases***
Hongfang Liu, Jiufeng Sun, Minying Li, Wenying Cai, Yangxia Chen, Yinghui Liu, Huan Huang, Zhenmou Xie, Weiying Zeng and Liyan Xi

123 ***Equine Histoplasmosis in Ethiopia: Phylogenetic Analysis by Sequencing of the Internal Transcribed Spacer Region of rRNA Genes***
Gobena Ameni, Alebachew Messele Kebede, Aboma Zewude, Musse Girma Abdulla, Rahel Asfaw, Mesfin Mamo Gobena, Martina Kyalo, Francesca Stomeo, Balako Gumi and Teshale Sori

frontiers | Frontiers in Cellular and Infection Microbiology

EDITORIAL
published: 31 May 2022
doi: 10.3389/fcimb.2022.939140

Editorial: Molecular Epidemiology of Fungal Infections

Min Chen[1], *Abdullah M. S. Al-Hatmi*[2,3], *Jianping Xu*[4*] *and G. Sybren De Hoog*[3*]

[1] Department of Dermatology, Shanghai Key Laboratory of Medical Mycology, Changzheng Hospital, Shanghai, China, [2] Natural & Medical Sciences Research Center, University of Nizwa, Nizwa, Oman, [3] Center of Expertise in Mycology, Radboud University Medical Center/Canisius Wilhelmina Hospital, Nijmegen, Netherlands, [4] Department of Biology, McMaster University, Hamilton, ON, Canada

Keywords: genetic divercity, molecular epidemiology, fungal infections, antifungal resistance, fungal pathogen

Editorial on the Research Topic

Molecular Epidemiology of Fungal Infections

The term "molecular epidemiology" was first proposed in the 1970s and has since been used to describe any study that uses molecular markers to analyze disease patterns at the population level, including infectious and non-infectious diseases such as SARS-COVID-19 and cancer (Tümmler, 2020). With the rapid development in molecular technology and computer science since the 1990s, molecular epidemiological studies of fungal infections have made tremendous progresses, including studies on plant, animal, and human fungal pathogens (Tarasevich et al., 2003; Tümmler, 2020). Such studies have revealed and refined our understandings of fungal disease outbreaks, transmission dynamics, risk factors, pathogenesis, antifungal resistance, and the genetic and genomic attributes of pathogenic fungi, particularly those that are emerging fungal pathogens. This Special Topic was organized to capture some of the most recent developments and inform the infectious diseases, medical mycology, and public health communities about the progresses and impacts of molecular epidemiology of fungal infections. In the Research Topic on "Molecular Epidemiology of Fungal Infections", a total of 12 articles have been accepted and published, covering a range of human fungal pathogens as well as different aspects of these pathogens. Interestingly, the majority of the papers (75%; 9/12) were written by Chinese researchers, reflecting the overall trend seen in other journals covering similar topics and suggesting the rapid development of this topic in China.

Over the last 30 years, genotyping methods for studying culturable fungal strains has undergone significant changes, from anonymous fingerprinting techniques such as random amplified polymorphic DNA (RAPD) to sequence-based techniques such as multi-locus sequence typing (MLST) and whole-genome sequencing (Tümmler, 2020). Hong et al., reviewed the diversity of molecular marker techniques that has been used for analyzing the human pathogenic *Cryptococcus* species, specifically members of the *Cryptococcus neoformans* and *Cryptococcus gattii* complexes and how such analyses improved our understanding of this group of fungi. Following a thorough discussion of the advantages and disadvantages of individual molecular markers, the authors proposed that MLST and whole genome sequence typing (WGST) will be the gold standards for continued strain genotyping and epidemiological investigations of the human pathogenic *Cryptococcus* species (Hong et al.). As a model organism for medical fungi, this review summarized not only the evolution of molecular techniques for fungal strain typing but also how those techniques improved our understanding of cryptococcal epidemiology and the evolutionary history of human pathogenic *Cryptococcus*.

OPEN ACCESS

Edited and reviewed by:
Anuradha Chowdhary, University of Delhi, India

***Correspondence:**
G. Sybren De Hoog
Sybren.deHoog@radboudumc.nl
Jianping Xu
jpxu@mcmaster.ca

Specialty section:
This article was submitted to Fungal Pathogenesis, a section of the journal Frontiers in Cellular and Infection Microbiology

Received: *08 May 2022*
Accepted: *12 May 2022*
Published: *31 May 2022*

Citation:
Chen M, Al-Hatmi AMS, Xu J and De Hoog GS (2022) Editorial: Molecular Epidemiology of Fungal Infections. Front. Cell. Infect. Microbiol. 12:939140. doi: 10.3389/fcimb.2022.939140

Differences in genotype distribution and antifungal resistance have been observed among clinical and environmental isolates of *C. neoformans* in China (Chen et al., 2018; Chen et al., 2021). Yang et al., analyzed 199 clinical isolates of *C. neoformans* from Jiangxi, China, using the MLST consensus scheme and the Clinical and Laboratory Standards Institute (CLSI) M27-A3 method. The study found that ST5/VNI was the most predominant genotype (approximately 89.5%) of clinical *C. neoformans* isolates in the region, along with three novel genotypes (ST656, ST657, and ST658). A large proportion (approximately 43.2%) of the isolates were not sensitive to fluconazole at a $MIC_{50} \geq 8$ μg/ml.

Harun et al., investigated 188 global clinical, veterinary, and environmental isolates of *Scedosporium aurantiacum* using a 6-locus MLST scheme. A markedly high genetic diversity with 159 unique sequence types (STs) was observed in this important fungal pathogen in a range of clinical settings. The results of phylogenetics, network and linkage disequilibrium analyses revealed evidence of recombination in the species and suggested that *S. aurantiacum* may have originated within the Australian continent and spread to other regions.

Equine histoplasmosis commonly known as epizootic lymphangitis (EL) is a neglected granulomatous disease of equine that is endemic to Ethiopia, and is caused by the *Histoplasma capsulatum* variety *farciminosum* (Scantlebury et al., 2016). Ameni et al., performed a phylogenetic analysis of 54 veterinary isolates from horses in Ethiopia using the internal transcribed spacer region of rRNA genes (ITS) sequence. The study's findings indicated that the Ethiopian isolates were closely aggregated with isolates of the South American A and Eurasian clades, but more distantly related to isolates from the North America 1 and 2 clades and the South American B clade. This study highlights the potential origins and transmission routes of Histoplasmosis in Ethiopia.

The *Prototheca* alga is the only chlorophyte capable of causing infections in humans, with *Prototheca wickerhamii* serving as the main causal agent. Guo et al., used nanopore long-read and Illumina short-read technologies to sequence the genomes of two *P. wickerhamii* isolates, S1 and S931, to investigate the evolution of *Prototheca* and the genetic basis for its pathogenicity. The assembled nuclear genome was 17.57 Mb in size with 19 contigs and 17.45 Mb with 26 contigs for isolates S1 and S931, respectively. There were approximately 5,700 predicted protein-coding genes, with over 96% of these genes could be annotated with a gene function. This study provides in-depth insights into the genome sequences of two clinical isolates of *P. wickerhamii* to contribute to the basic understanding of this species.

Chen et al., analyze 110 clinical *Candida* isolates from a tertiary care teaching hospital from Jiangxi, China using RAPD genotyping and the Sensititre ™ YeastOne YO10 panel. *Candida albicans* was the predominant species (approximately 36.3%), followed by *C. parapsilosis* (approximately 33.6%), *C. tropicalis* (approximately 19.1%), *C. glabrata* (approximately 8.2%), *C. rugosa* (approximately 1.8%), and *C. haemulonii* (approximately 0.9%). Using RAPD typing, *C. albicans* isolates could be grouped into five clusters, *C. parapsilosis* and *C. tropicalis* isolates into seven clusters, and *C. glabrata* isolates into only one cluster comprising six strains. Antifungal testing revealed that the isolates had the highest overall resistance against fluconazole (approximately 6.4%), followed by voriconazole (approximately 4.6%). In the azole-resistant isolates, the most common amino acid substitution was 132aa (Y132H, Y132F) within the *erg11* gene. Cluster F had approximately 75% azole-resistant *C. albicans* isolates, while Cluster Y had two azole-resistant *C. tropicalis* isolates.

To date, few studies have reported the incidence of pulmonary co-infection of fungi and bacteria. Zhao et al., used the mNGS technique to analyze 119 patients with fungal infections, 48 (approximately 40.3%) of which had pulmonary fungal and bacterial co-infection. The most commonly identified fungi species were *Aspergillus*, *Pneumocystis*, and *Rhizopus*, and the most commonly identified bacterial species were *Pseudomonas aeruginosa*, *Acinetobacter baumannii*, and *Stenotrophomonas maltophilia*. The results of the study suggest the incidence of fungal and bacterial co-infection in patients with pulmonary fungal infections could not be ignored, which may also guide the use of antibacterial drugs in these patients.

Studies on antifungal susceptibility and resistance mechanisms also are popular Research Topics in molecular epidemiology of fungal infections. Chen et al., used the CLSI M59 guideline and Sensititre YeastOne™ system to analyze 11 *Diutina catenulata* (*Candida catenulata*) isolates collected from the China Hospital Invasive Fungal Surveillance Net (CHIF-NET) Program. The results showed that itraconazole (0.06-0.12 μg/ml), posaconazole (0.06-0.12 μg/ml), amphotericin B (0.25-1μg/ml), and 5-flucytosine (range, 0.06-0.12 μg/ml) had low MICs, whereas echinocandins had high MICs (≥4 μg/ml) in four isolates. Common ERG11 mutations, including F126L/K143R, were found in isolates with high MIC values for azoles. Two frequent amino acid alterations corresponding to high MIC values of echinocandin, F621I (F641) and S625L (S645), were also found in spot 1 region of FKS1. There was also one new amino acid alteration, I1348S (I1368). The high MIC values for various antifungals in the study suggest that the treatment of invasive infections caused by *D. catenulate* may be challenging.

Arastehfar et al., collected 58 *Candida parapsilosis* isolates that recovered from the bloodstream of 47 patients at Turkey's Ege University Hospital between January 2019 and January 2020. These isolates were genotyped by ITS sequencing and multi-locus microsatellite typing (MLMT). Antifungal susceptibility testing was performed in accordance with the CLSI M60 protocol, and the *ERG11* and HS1/HS2-*FKS1* sequences were sequenced. Results showed that Y132F was the most common mutation in Erg11. All Y132F-positive isolates were found in one large cluster and were mostly recovered from patients admitted to the chest disease and pediatric surgery wards. In Turkey, the study emphasizes the importance of strict infection control strategies, antifungal stewardship, and environmental screening.

Li et al., analyzed the whole genome sequence data from two Chinese *Candida auris* isolates as well as 356 isolates archived in the European Bioinformatics Institute (EBI) databases, which were analyzed by bioinformatics using machine learning

classifiers based on Python 3.8.4 software. Two machine learning algorithms, based on the balanced test and imbalanced test, were designed and evaluated. The results obtained using the balanced test set were superior to those obtained using the imbalanced test set for the majority of drugs. This study suggested that machine learning classifiers are a useful and cost-effective method for identifying fungal drug resistance-related mutations, which could be very important for research into the mechanism underlying antifungal resistance observed in *C. auris*, an emerging fungal pathogen.

Liu et al., investigated the clinical and molecular characteristic of 45 chromoblastomycosis (CBM) cases in Guangdong, China, a CBM hotspot. The mean age of the patients was 61.38 ± 11.20 years and the gender ratio (male to female) was 4.6:1. Approximately 29% of the cases had underlying diseases, and a verrucous form was the most common clinical manifestation (approximately 42%). Approximately 62% of the clinical isolates were identified as *F. monophora*, followed by *F. nubica* (approximately 38%). *In vitro* antifungal susceptibility test revealed that azoles (PCZ 0.015_0.25 μg/ml, VCZ 0.015_0.5 μg/ml, and ITZ 0.03_0.5 μg/ml) and TRB (0.015_1 mg/ml) had low MICs. The main therapeutic strategy used for 31 of 45 cases was itraconazole combined with terbinafine, and approximately 68% of them improved or were cured. The findings of this study are likely to represent regional trends in this subtropical hyper-endemic area of CBM, and they will contribute to better CBM management and clinical therapy.

Hu et al., described a rare subcutaneous infection caused by *Dirkmeia churashimaensis* and reviewed previously published human Ustilaginales infections. Over the course of 2 years, an 80-year-old female farmer developed extensive plaques and nodules on her left arm. Pathological and microbiological examinations revealed that this infections was caused by a new pathological agent, *D. churashimaensi*. The patient was successfully cured by oral itraconazole. A literature review suggested amphotericin B, posaconazole, itraconazole, and voriconazole had good activity against these reported strains, whereas fluconazole, 5-flucytosine, and echinocandins usually showed low susceptibility. Itraconazole was effective against subcutaneous infections. The case report and literature review reveal that *D. churashimaensis* can be a fungal opportunist. A proper identification of fungi and antifungal susceptibility tests can be crucial for clinical treatment.

In summary, the published articles in this Research Topic of "Molecular Epidemiology of Fungal Infections" covered a wide range or research, including: (i) the diverse molecular markers used to investigate genetic diversity and antifungal susceptibility of pathogenic fungi; (ii) molecular epidemiologic investigations of fungal outbreaks/epidemics, routes of spread, risk factors, pathogenesis, and environmental distributions, and (iii) applications of next-generation sequencing in molecular epidemiology of fungal infections to addressing new research questions. We hope that this collection will be useful for future research in the field on molecular epidemiology of fungal infections.

AUTHOR CONTRIBUTIONS

MC was a guest associate editor of the Research Topic and wrote the paper text. AA-H, JX and GH were guest associate editors of the Research Topic and edited the text. All authors contributed to the article and approved the submitted version.

FUNDING

MC is funded in part by the grants from National Natural Science Foundation of China (81720108026 and 82172291). JX is funded in part by grants from Natural Science and Engineering Research Council of Canada (RGPIN-2020-05732) and McMaster University (Global Science Initiative 2020).

ACKNOWLEDGMENTS

We thank authors of the papers published in this Research Topic for their valuable contributions and the referees for their rigorous review.

REFERENCES

Chen, M., Wang, Y., Li, Y., Hong, N., Zhu, X., Pan, W., et al. (2021). Genotypic Diversity and Antifungal Susceptibility of Environmental Isolates of *Cryptococcus Neoformans* From the Yangtze River Delta Region of East China. *Med. Mycol.* 59, 653–663. doi: 10.1093/mmy/myaa096

Chen, M., Xu, Y., Hong, N., Yang, Y., Lei, W., Du, L., et al. (2018). Epidemiology of Fungal Infections in China. *Front. Med.* 12, 58–75. doi: 10.1007/s11684-017-0601-0

Scantlebury, C. E., Pinchbeck, G. L., Loughnane, P., Aklilu, N., Ashine, T., Stringer, A. P., et al. (2016). Development and Evaluation of a Molecular Diagnostic Method for Rapid Detection of *Histoplasma Capsulatum* Var. *Farciminosum*, the Causative Agent of Epizootic Lymphangitis, in Equine Clinical Samples. *J. Clin. Microbiol.* 54, 2990–2999. doi: 10.1128/jcm.00896-16

Tarasevich, I. V., Shaginyan, I. A., and Mediannikov, O. Y. (2003). Problems and Perspectives of Molecular Epidemiology of Infectious Diseases. *Ann. N Y Acad. Sci.* 990, 751–756. doi: 10.1111/j.1749-6632.2003.tb07455.x

Tümmler, B. (2020). Molecular Epidemiology in Current Times. *Environ. Microbiol.* 22, 4909–4918. doi: 10.1111/1462-2920.15238

Conflict of Interest: The authors declare that the research was conducted in the absence of any commercial or financial relationships that could be construed as a potential conflict of interest.

Publisher's Note: All claims expressed in this article are solely those of the authors and do not necessarily represent those of their affiliated organizations, or those of the publisher, the editors and the reviewers. Any product that may be evaluated in this article, or claim that may be made by its manufacturer, is not guaranteed or endorsed by the publisher.

frontiers in Cellular and Infection Microbiology

ORIGINAL RESEARCH
published: 22 April 2021
doi: 10.3389/fcimb.2021.676177

Clonal Candidemia Outbreak by *Candida parapsilosis* Carrying Y132F in Turkey: Evolution of a Persisting Challenge

Amir Arastehfar[1†‡], Suleyha Hilmioğlu-Polat[2†‡], Farnaz Daneshnia[1†], Weihua Pan[3], Ahmed Hafez[4], Wenjie Fang[3†], Wanqing Liao[3], Zümrüt Şahbudak-Bal[5†], Dilek Yeşim Metin[2†], João N. de Almeida Júnior[6,7†], Macit Ilkit[8†], David S. Perlin[1*†] and Cornelia Lass-Flörl[9†]*

[1] Center for Discovery and Innovation, Hackensack Meridian Health, Nutley, NJ, United States, [2] Division of Mycology, Department of Microbiology, Faculty of Medicine, University of Ege, Izmir, Turkey, [3] Shanghai Key Laboratory of Molecular Medical Mycology, Shanghai Institute of Mycology, Shanghai Changzheng Hospital, Second Military Medical University, Shanghai, China, [4] Biotechvana, Valencia, Spain, [5] Division of Pediatric Infectious Diseases, Ege University, Izmir, Turkey, [6] Laboratorio de Micologia Medica (LIM 53), Instituto de Medicina Tropical, Universidade de São Paulo, São Paulo, Brazil, [7] Laboratório Central (LIM 03), Hospital das Clínicas da Faculdade de Medicina da Universidade de São Paulo, São Paulo, Brazil, [8] Division of Mycology, Department of Microbiology, Faculty of Medicine, University of Çukurova, Adana, Turkey, [9] Institute of Hygiene and Medical Microbiology, Medical University of Innsbruck, Innsbruck, Austria

As the second leading etiological agent of candidemia in Turkey and the cause of severe fluconazole-non-susceptible (FNS) clonal outbreaks, *Candida parapsilosis* emerged as a major health threat at Ege University Hospital (EUH). Evaluation of microbiological and pertinent clinical profiles of candidemia patients due to *C. parapsilosis* in EUH in 2019–2020. *Candida parapsilosis* isolates were collected from blood samples and identified by sequencing internal transcribed spacer ribosomal DNA. Antifungal susceptibility testing was performed in accordance with CLSI M60 protocol and *ERG11* and HS1/HS2-*FKS1* were sequenced to explore the fluconazole and echinocandin resistance, respectively. Isolates were typed using a multilocus microsatellite typing assay. Relevant clinical data were obtained for patients recruited in the current study. FNS *C. parapsilosis* isolates were recovered from 53% of the patients admitted to EUH in 2019–2020. Y132F was the most frequent mutation in Erg11. All patients infected with *C. parapsilosis* isolates carrying Y132F, who received fluconazole showed therapeutic failure and significantly had a higher mortality than those infected with other FNS and susceptible isolates (50% *vs*. 16.1%). All isolates carrying Y132F grouped into one major cluster and mainly recovered from patients admitted to chest diseases and pediatric surgery wards. The unprecedented increase in the number of Y132F *C. parapsilosis*, which corresponded with increased rates of fluconazole therapeutic failure and mortality, is worrisome and highlights the urgency for strict infection control strategies, antifungal stewardship, and environmental screening in EUH.

Keywords: antifungal, antifungal agent, molecular type, microdilution, fluconazole

OPEN ACCESS

Edited by:
G. Sybren De Hoog, Radboud University Nijmegen Medical Centre, Netherlands

Reviewed by:
Alexandre Alanio, Université Paris Diderot, France
Marie Desnos-Ollivier, Institut Pasteur, France

****Correspondence:***
Weihua Pan
panweihua9@sina.com
David S. Perlin
david.perlin@hmh-cdi.org

†ORCID:
Amir Arastehfar
0000-0002-4361-4841
Süleyha Hilmioğlu-Polat
0000-0001-8850-2715
Farnaz Daneshnia
0000-0002-8782-2036
Wenjie Fang
0000-0002-6406-5095
Zümrüt Şahbudak-Bal
0000-0001-9189-8220
Dilek Yeşim Metin
0000-0002-7282-5031
João Nóbrega de Almeida Júnior
0000-0002-3766-026X
Macit Ilkit
0000-0002-1174-4182
David S. Perlin
0000-0002-9503-3184
Cornelia Lass-Flörl
0000-0002-2946-7785

‡These authors have contributed equally to this work

Specialty section:
This article was submitted to Fungal Pathogenesis, a section of the journal Frontiers in Cellular and Infection Microbiology

Received: *04 March 2021*
Accepted: *06 April 2021*
Published: *22 April 2021*

INTRODUCTION

Candidemia represents a major global public health concern due to high mortality rates and additional economic burden (Arastehfar et al., 2020f). Although global epidemiological studies characterize *Candida albicans* as the leading cause of candidemia (Pfaller et al., 2019), non-*albicans Candida* (NAC) species, especially *C. parapsilosis*, *C. tropicalis*, *C. glabrata*, and *C. auris*, surpass *C. albicans* in some countries and individual patient population and healthcare institutions (Arastehfar et al., 2020f; Megri et al., 2020). Among these NAC species, *C. parapsilosis* stands out as an important causative agent of invasive candidiasis observed in the last decade (Pfaller et al., 2019). *Candida parapsilosis* is thought to be transferred through direct contact usually involving the hands of healthcare workers (Tóth et al., 2019). Its ability to form tenacious biofilms allows this species to persist avidly in the hospital settings (Tóth et al., 2019). Furthermore, numerous studies from European (Arastehfar et al., 2020b; Martini et al., 2020), Asian (Singh et al., 2019), African (Magobo et al., 2020), and Latin American (Thomaz et al., 2018) countries have reported an unprecedented rate of fluconazole and/or azole resistance due to *C. parapsilosis*, which, combined with the mode of transmission, has led to severe clonal outbreaks and establishment of persistent fluconazole-non-susceptible (FNS) *C. parapsilosis* in previously unknown niches of the hospital environment. Horizontal transmission results in fluconazole-resistant *C. parapsilosis* isolated from azole-naïve patients (Arastehfar et al., 2020b) and subsequent therapeutic failure, which can potentially lead to higher hospital expenses, longer hospitalization times, and poor outcome. To further complicate the matter, the emergence of multidrug-resistant (MDR) *C. parapsilosis* blood isolates showing resistance to both azoles and echinocandins has recently been reported (Arastehfar et al., 2020c; Arastehfar et al., 2021). Therefore, it is highly important to diligently monitor the burden of antifungal resistance and perform genotyping of *C. parapsilosis* blood isolates in clinical settings that have experienced fungal infection outbreaks.

A principal molecular mechanism underlying fluconazole resistance in *Candida* species involves mutations in the *ERG11* gene encoding an enzyme of the ergosterol biosynthetic pathway (Arastehfar et al., 2020f). Residue substitutions Y132F, K143R, and G458S in Erg11 are considered the major cause of fluconazole resistance, followed by the upregulation of *ERG11* and efflux pump genes *MDR1* and *CDR1* due to gain-of-function mutations in the respective transcription factors (Arastehfar et al., 2020f). Resistance to echinocandins develops through acquisition of mutations in hotspot (HS) regions of *FKS* genes (Arastehfar et al., 2020f; Arastehfar et al., 2021).

In our previous studies, we analyzed *C. parapsilosis* blood isolates recovered from Ege University Hospital (EUH) between 2007 and early 2019, and have reported severe clonal outbreaks due to fluconazole-resistant (Arastehfar et al., 2020b) and MDR (Arastehfar et al., 2021) *C. parapsilosis* isolates. The increasing trend of fluconazole-resistant *C. parapsilosis* blood isolates in EUH, especially from 2018 onward, and the lack of detailed clinical data with respect to fluconazole therapeutic failure (FTF) among infected patients from our previous studies prompted us to collect the blood isolates obtained in 2019 to 2020. Furthermore, we applied a multilocus microsatellite typing technique to assess the genetic relatedness of the *C. parapsilosis* blood isolates collected and to identify the wards, where clonal outbreaks are ongoing.

MATERIALS AND METHODS

This was a retrospective study, which included patients with candidemia due to *C. parapsilosis* admitted to EUH between January 2019 and January 2020. There were no exclusion criteria regarding age, sex, underlying conditions, wards, etc. Persistent fever and obtaining *C. parapsilosis* from blood culture despite antifungal treatment were considered as antifungal therapeutic failure and reported by treating physicians. Drug exposure included the recorded data of the preceding six months and if needed records of the previous hospitalizations were checked. Thirty-day mortality was defined when death occurred ≤ 30 days after the first positive blood culture (Kord et al., 2020). *Candida parapsilosis* blood isolates were inoculated onto Sabouraud glucose agar (Merck, Darmstadt, Germany) and chromogenic agar (Candi*Select*™ 4, Bio-Rad, Hercules, CA, USA) plates and incubated at 37°C for 24–48 h. Species identification was performed using primers targeting internal transcribed spacer 1 (ITS1; TCCGTAGGTGAACCTGCGG) and ITS 4 (GCATATCAATAAGCGGA) (Stielow et al., 2015). It has been shown that ITS1 and ITS4 can discriminate species within *C. parapsilosis* species complex (Souza et al., 2012).

Antifungal Susceptibility Testing

Antifungal susceptibility testing was performed by the broth microdilution method according to the CLSI M60 protocol (CLSI, 2017) and included fluconazole, voriconazole, itraconazole, posaconazole, amphotericin B (all from Sigma-Aldrich, St. Louis, MO, USA), caspofungin (bioMérieux SA, Marcy-l'Étoile, France), micafungin (Astellas, Munich, Germany), and anidulafungin (Pfizer, New York, NYC, USA). Isolates were incubated at 35°C for 24 h and minimum inhibitory concentrations (MICs) were visually recorded. *Candida krusei* (ATCC 6258) and *C. parapsilosis* (ATCC 22019) were used for quality control. Resistance to fluconazole, anidulafungin, micafungin, and caspofungin was considered at MICs ≥ 8 μg/mL, whereas that to voriconazole was noted at MICs ≥ 1 μg/mL (Pfaller and Diekema, 2012). Isolates with the fluconazole MICs ≥4 μg/mL were regarded as FNS. Susceptibility to amphotericin B, itraconazole, and posaconazole was reported based on epidemiological cut-off values and isolates showing MICs >2, >0.5, and >0.25 μg/mL were considered non-wild-type (NWT) (Pfaller and Diekema, 2012).

Fluconazole tolerance was defined as incomplete growth inhibition at supra-MICs for 48 h compared to positive control (Arastehfar et al., 2020e; Berman and Krysan, 2020).

DNA Extraction and Sequencing of ERG11 and FKS1

DNA was extracted using a previously described CTAB-based protocol (Arastehfar et al., 2018). ERG11 and HS1 and HS2 of *FKS1* were amplified by PCR using specific primers and sequenced as previously described (Arastehfar et al., 2019b; Arastehfar et al., 2020c). Since echinocandin-susceptible *C. parapsilosis* may occasionally carry mutations in the HS regions (Arastehfar et al., 2020d) and isolates with the susceptible dose-dependent phenotype for fluconazole may have the Y132F mutation (Singh et al., 2019), sequencing was performed for all isolates to detect any potential genetic changes conferring resistance and/or therapeutic failure.

Raw sequence data were edited using SeqMan Pro software (DNASTAR, Madison, WI, USA), and the curated sequences were aligned against WT sequences of *ERG11* (GQ302972) and *FKS* (Garcia-Effron et al., 2008) using MEGA v7.0 (Temple University, Philadelphia, PA, USA).

Genotyping

The genetic relatedness of *C. parapsilosis* strains was evaluated using multilocus microsatellite typing targeting four loci and eight alleles (Trobajo-Sanmartín et al., 2018). Genotyping analysis was performed using BioNumerics software V7.6 (Applied Math Inc., Austin, Texas, USA) and different genotypes were assigned when two given strains differed in more than one allele. Genotypes showing with similar genetic profile were regarded as cluster.

Statistical Analysis

The association between mortality and fluconazole susceptibility profile was assessed by chi-square test using SPSS v24 (SPSS Inc., Chicago, IL, USA). Kaplan-Meier survival curve was plotted using the GraphPad Prism software (GraphPad, San Diego, CA, USA). *P*-values below 0.05 were considered statistically significant.

Deposition of the Generated Sequence Data

The sequences of *ERG11*, *FKS1*-HS1, *FKS1*-HS2 obtained in this study were deposited in the GenBank database under the following accession numbers (MW013584–MW013641), (MW013700–MW013757), and (MW013642–MW013699), respectively.

RESULTS

Clinical Data

Between 2019 and 2020, 58 C. *parapsilosis* isolates were recovered from bloodstream of 47 patients. Multiple *C. parapsilosis* isolates were recovered from five patients: three with four and two – with two sequentially obtained isolates. The median age of the patients was 45 years (range, 40 days–89 years) and the majority of them were men (33/47; 70.2%). The most notable underlying conditions (some patients had more than one) were: cancer (12/47; 25.5%), surgery (10/47; 21.2%), burns (10/47; 21.2%), chronic respiratory diseases (6/47; 12.7%), diabetes mellitus (5/47; 10.6%), hypertension (5/47; 10.6%), neurological diseases (5/47; 10.6%), and cardiovascular diseases (4/47; 8.5%) (details in **Supplementary Table 1**). Central venous catheter was used in 63.8% of patients (30/47) and approximately 40.5% of those patients were admitted in intensive care units (ICUs) (19/47). Twelve patients (25.5%) received prophylactic treatment with azoles, including fluconazole (11/47; 23.4%) and posaconazole (1/47; 2.1%). Fluconazole (20/47; 42.5%), and echinocandins micafungin (15/47; 31.9%), caspofungin (12/47: 25.5%), anidulafungin (8/47; 17%), and amphotericin B (11/47; 23.4%) were used as targeted treatment. The overall mortality rate was 27.6%.

Antifungal Susceptibility Profiles

All *C. parapsilosis* isolates were susceptible to echinocandins (anidulafungin, micafungin, and caspofungin) and were WT to amphotericin B, itraconazole, and posaconazole. The FNS phenotype (MICs ≥4 μg/mL) was detected in 28 isolates (MIC = 4 μg/mL, n = 12; MIC ≥ 8 μg/mL, n = 16) collected from 53% of patients (25/47) (**Tables 1** and **2**). Voriconazole resistance (MICs ≥1 μg/mL) and intermediate phenotypes (MIC = 0.25–0.5 μg/mL) were observed for seven and four isolates, respectively. Of note, the seven voriconazole-resistant isolates were cross-resistant to fluconazole (**Tables 1** and **2**).

ERG11 and *FKS1* Sequencing Results

Consistent with the echinocandin MIC data, none of the *C. parapsilosis* isolates carried any mutations in HS1 or HS2 of *FKS1*. Among fluconazole resistance-related mutations, Y132F was the most prevalent (17/28; 60.7%), followed by G458S (4/28; 14.2%), Y132F+G307A (3/28; 10.7%), and G307A+G458S (1/28; 3.6%) (**Tables 1** and **2**). Interestingly, three FNS isolates recovered from a patient without any exposure to azoles during hospitalization did not carry any mutations in *ERG11* (**Tables 1** and **2**). In order to evaluate the dynamics of *ERG11* mutations in FNS *C. parapsilosis* isolates during the period between 2007 and 2020, we combined the current data with those obtained in our previous study (Arastehfar et al., 2020b) (**Figure 1**). Interestingly, we observed time-dependent shifts in the mutation type and frequency: the number of Y132F-carrying isolates was significantly increased from 2017 onward, whereas isolates with Y132F+K143R and K143R, which were prevalent before 2019, were not detected thereafter (**Figure 1** and **Table 1**). Importantly, isolates with newly emerged mutations (G458S and Y132F+G307A) also showed an increase from 2017 onward and one fluconazole-resistant isolate had a new mutation (G307A+G458S) not detected in our previous studies (**Figure 1** and **Table 1**). However, we did not observe any patients infected with clonal MDR *C. parapsilosis* isolates carrying Y132F+K143R in Erg11 or R658G in HS1 of Fks1, which is in contrast with our previous results (Arastehfar et al., 2021).

To assess the association between the emergence of FNS isolates and the use of antifungals, we analyzed the treatment records of the patients. All patients infected with FNS isolates and treated with fluconazole (17/25, 68%) showed FTF, while the rest of 8 patients carrying FNS *C. parapsilosis* isolates were

TABLE 1 | Comprehensive microbiological and clinical data of candidemic patients infected with *C. parapsilosis* in Ege University Hospital between 2019 to 2020.

Genotype	Ward (patient #)	Isolate #	MIC values (μg/mL)		Erg11p	Azole prophylaxis/ empiric therapy	ATF/ATT	Mortality rate
			FLZ	VRZ				
Fluconazole-non-susceptible isolates containing Y132F mutation								
G19 (*n*= 1), G21 (*n*= 1), G22 (*n*= 3), G28 (*n*= 1)	Chest diseases (*n*= 6)	*n*= 17	4–32	0.032–0.5	Y132F	FLC (*n*= 4)	FLC (*n*= 11)/MFG (*n*= 4), AND (*n*= 3), CSP (*n*= 2), and LAMB (n= 2)	50% (8/16)
G19 (n= 2), G20 (*n*= 1), G21 (*n*= 1), G24 (*n*= 1) G23 (*n*= 1), G25 (*n*= 1) G26 (*n*= 1)	Pediatric surgery (*n*= 5)[A] Pediatric ICU (*n*= 2) Internal medicine (*n*= 1)							
G22 (*n*= 1)	Cardiovascular surgery (*n*= 1)						Azole-naïve (*n*= 5)/CSP (*n*= 2), LAMB (*n*= 2), not treated (*n*= 1)	
G31 (*n*= 1)	ICU burn (*n*= 1)							
C8/G27 (*n*= 3)	Pediatric (*n*= 2), Pediatric ICU (*n*= 1)	*n*= 3	>64	1–2	Y132F +G307A	FLC (*n*= 1)	FLC (*n*= 2)/MFG (*n*=1), LAMB (*n*= 1) Azole-naïve (*n*= 1)/ CSP (*n*=1)	0% (0/3)
Other mutations causing fluconazole resistance G458S								
G13 (*n*= 2)	Pediatric surgery (*n*= 2)	*n*= 4	16–>64	0.25–2	G458S	FLC (*n*= 2)	FLC (*n*= 3)/MFG (*n*= 1), CSP (*n*= 1), LAMB (*n*= 1) Azole-naïve (*n*= 1)/ AND (*n*= 1)	0% (0/4)
G13 (*n*= 1)	Pediatric gastroenterology (*n*= 1)							
G7 (*n*= 1)	Pediatric ICU (*n*= 1)							
G4 (*n*= 1)	Pediatric (*n*= 1)	*n*= 1	>64	4	G307A +G458S	No	FLC (*n*= 1)	0% (0/1)
Other fluconazole-non-susceptible isolates without mutations conferring resistance								
G1 (*n*= 3)	Burn ICU (*n*= 1)[B]	*n*= 3	4–8	0.064–0.125	R398I (n=3)	No	Azole-naïve/MFG and LAMB	0% (0/1)
Fluconazole susceptible isolates								
G1 (*n*= 1), G3 (*n*= 2), G6 (*n*= 1), G9 (*n*= 1), G11 (*n*= 1), G12 (*n*= 1), G16 (*n*= 2)	Burn ICU (*n*= 8)[B*]	*n*= 9[B*]	0.25–2	0.32–0.64	R398I (*n*= 6)	FLC (*n*= 4), POSA (*n*= 1)	FLC (*n*= 2)	22.7% (5/22)
G5 (*n*= 1), G15 (*n*= 4)	Pediatric (*n*= 2)	*n*= 5	0.5	0.32				
G14 (*n*= 1), G18 (*n*= 1)	Chest diseases (*n*= 2)	*n*= 2	0.25–2	0.32–0.64				
G10 (*n*= 1), G17 (*n*= 1)	Neurosurgery services (*n*= 2)	*n*= 2	0.5–1	0.32				
G5 (*n*= 1), G6 (*n*= 1), G7 (*n*= 1), G8 (*n*= 1)	Cardiovascular surgery (*n*= 1)	*n*= 4	0.5	0.32				
G6	Pediatric surgery (*n*= 1)[A*]	*n*= 1[A*]	0.5	0.32				
G6	Cardiology service (*n*= 1)	*n*= 1	0.5	0.32				
G6	Pediatric ICU (*n*= 1)	*n*= 1	0.5	0.32				
G30	General surgery (*n*= 1)	*n*= 1	0.25	0.32				
G6	Urology service (*n*= 1)	*n*= 1	0.5	0.32				
G2	Ear-nose-throat (*n*= 1)	*n*= 1	0.25	0.32				
G29	Infectious diseases (*n*= 1)	*n*= 1	0.5	0.32				
G6	Cardiovascular surgery ICU (*n*= 1)	*n*= 1	0.5	0.32				

[A] *Two patients had duplicate isolates: the first (PA) was infected with two Y132F-carrying isolates and the second (PB) – with one fluconazole-susceptible WT isolate (denoted as* [A*] *and not included in the assessment of the mortality rate) and one fluconazole-non-susceptible Y132F-carrying isolate.* [B] *This patient was infected with four isolates: one WT, one fluconazole-susceptible (denoted as* [B*] *among fluconazole-susceptible isolates), and two fluconazole-resistant isolates not carrying any ERG11 mutations. Abbreviations: ATF, Aazole therapeutic failure; ATT, Alternative targeted treatment; FLC, Fluconazole; POSA, Posaconazole; CSP, Caspofungin; AND, Anidulafungin; MFG, Micafungin.*

azole-naïve (**Tables 1** and **2**). Patients infected with Y132F-carrying *C. parapsilosis* isolates significantly had a higher mortality rate (8/16; 50%) compared to those infected with other FNS and FS (5/31; 16.1%) isolates (**Tables 1** and **2**; **Figure 2**) (Chi-square, two-tailed, *P*= 0.012). FTF was also observed for two patients infected with eight FS isolates (four isolates per patient), but since there was no increase in MICs compared to positive control after 48 h, these isolates were not considered fluconazole-tolerant.

TABLE 2 | Antifungal susceptibility data for *Candida parapsilosis* blood isolates collected from Ege University Hospital, Turkey, 2019–2020.

Antifungaldrugs	Minimum inhibitory concentration values (μg/ml)												Range	GM	MIC50	MIC90
	0.03	0.06	0.125	0.25	0.5	1	2	4	8	16	32	≥64				
Micafungin					23	31	4						0.5–2	0.79	1	2
Anidulafungin					6	46	6						0.5–2	1	1	2
Caspofungin					22	32	4						0.5–2	0.80	1	1–2
Amphotericin B				1	55	2							0.25–1	0.50	0.5	0.5
Fluconazole				6	20	1	3	12	6	2	2	6	0.25–>64	2.22	2	32–64
Voriconazole	31	7	9	2	2	3	3	1					0.03–4	0.07	0.03	1
Itraconazole	44	3	5	6									0.03–0.25	0.04	0.03	1–2
Posaconazole	42	12	3	1									0.03–0.25	0.03	0.03	0.06–0.125

GM, Geometric mean; MIC, Minimum inhibitory concentration value.

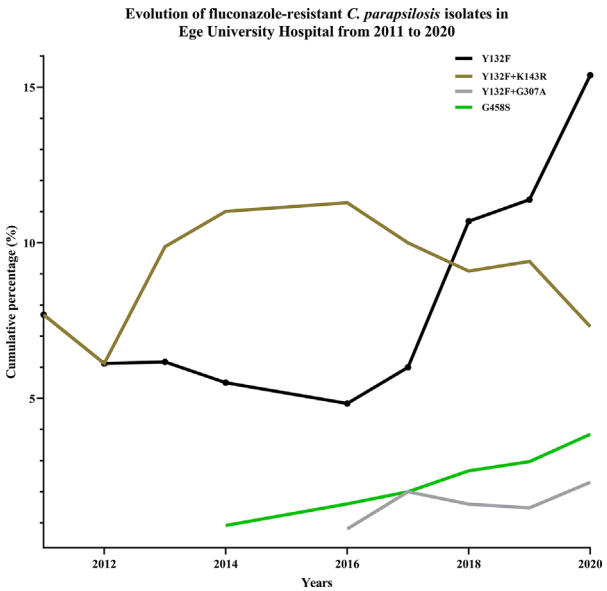

FIGURE 1 | Mutation frequency and types in Erg11 showed a dynamic trend, where new mutations replaced previously dominant ones.

Genotypic Diversity of *C. parapsilosis* Isolates

According to multilocus microsatellite typing, *C. parapsilosis* isolates were distributed into 2 major clusters, 8 sub-clusters (minor clusters), and 31 genotypes (**Figure 2** and **Table 1**). Interestingly, all isolates carrying Y132F or Y132F+G307A grouped into one major cluster and belonged to related genotypes, within which they formed small clonal clusters (**Figure 3** and **Table 1**). Approximately 69% of the patients infected with Y132F *C. parapsilosis* (11/16) were admitted to the chest and pediatric surgery wards, and those infected with Y132F+G307A isolates, which were 100% clonal, were admitted to pediatric wards and pediatric ICU (**Figure 3** and **Table 1**). The second major cluster comprised almost 91% of FS isolates (20/22) and some FNS isolates carrying G458S and G307A+G458S mutations (**Figure 3**, **Table 1**). This cluster contained two sub-clusters of clonal isolates including: FS isolates from seven patients (patients #5, 33, 38, 43, 45, 51, and 53), mainly obtained in burn ICU, and G458S-carrying isolates from three patients of pediatric surgery and gastroenterology wards (patients # 18, 47, and 52), respectively (**Figure 3** and **Table 1**). Details regarding the hospitalization of patients infected with FNS isolates with highly genetic similar profiles and/or clonal are shown in a transmission map in **Figure 4**. Collectively, these data indicate a continuing outbreak due to both FNS isolates with similar genetic profiles and clonal FS *C. parapsilosis* in various wards of EUH.

DISCUSSION

The emergence of clonal outbreaks due to FNS and MDR *C. parapsilosis* in EUH is a matter of clinical concern. Therefore, continuous monitoring of the burden of antifungal resistance as well as analysis of the underlying molecular mechanisms and genotypic diversity of the isolates in relation to clinical data are of

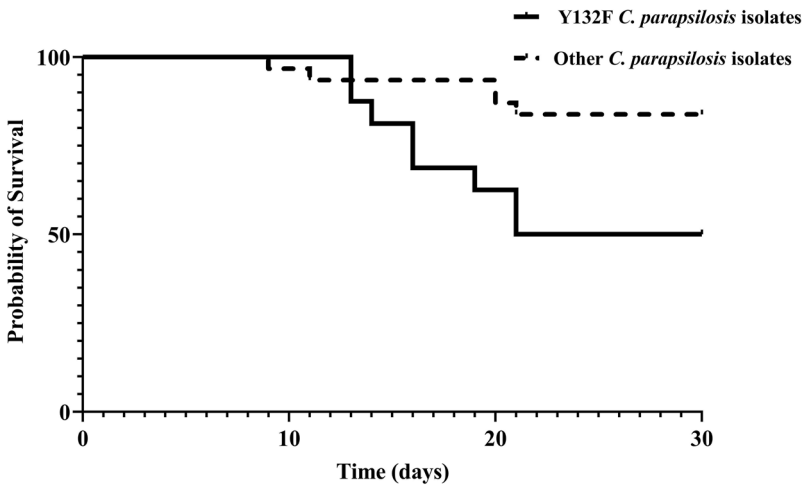

FIGURE 2 | 30-day survival of patients infected with azole-susceptible and azole-resistant *C. parapsilosis* isolates carrying Y132F in Erg11.

paramount importance. An alarming finding is that approximately 53% of patients with candidemia in this study were infected with FNS *C. parapsilosis* and all of them showed FTF when treated with azoles. We observed a dynamic shift in the mutation type and frequency among FNS *C. parapsilosis* isolates, when some previously prevalent mutations disappeared and were replaced by new ones. Beyond FTF, the Y132F-carrying *C. parapsilosis* isolates were associated with the highest mortality rate compared to patients infected with other isolates.

Overall, the 53% of the patients infected with FNS *C. parapsilosis* represented 48% of all analyzed isolates. Moreover, almost 15% of the FNS isolates were also cross-resistant to voriconazole. Analysis of the burden of FNS isolates in EUH in 2007–2020 based on the combined results of this and the previous study (Arastehfar et al., 2020b) revealed its highest rate in 2019. An increased number of studies report a high rate of FNS *C. parapsilosis* blood isolates, which ranges from 22% and 32% in Italy and India (Singh et al., 2019; Martini et al., 2020) to 71% and 78% in Brazil and South Africa (Thomaz et al., 2018; Magobo et al., 2020). Consistent with these data, a recent global study showed increasing prevalence of FNS *C. parapsilosis* in Latin American countries (Pfaller et al., 2019). In contrast to our earlier study (Arastehfar et al., 2021) but in line with the global trend, in this study we did not detect any isolates showing resistance against echinocandins or the NWT phenotype to amphotericin B. Unfortunately, most reports on the clonal expansion of FNS *C. parapsilosis* are from developing countries, where high cost of echinocandins promotes the popularity of fluconazole as the main treatment of invasive *Candida* infections (Arastehfar et al., 2019a; Arastehfar et al., 2019c; Arastehfar et al., 2020a; Megri et al., 2020) which can undermine the clinical efficacy of fluconazole and may have detrimental consequences. Altogether, these data point to the danger of the increasing burden of FNS *C. parapsilosis* blood isolates in clinical centers.

To analyze the molecular mechanisms of antifungal resistance in our isolates, we sequenced *ERG11* and *FKS1* genes. In agreement with the drug susceptibility profiles, we did not identify any mutations in *FKS1* HS1 and HS2 but found numerous mutations in *ERG11* of FNS isolates, which showed dynamic changes over time. Interestingly, in contrast to our previous study indicating that Y132F+K143R was one of the most prevalent residue substitutions in Erg11p (Arastehfar et al., 2020b), here we did not find any isolates carrying Y132F+K143R or K143R, Q250K+R398I+G458S, and G458S+T519A, which were replaced by the emerging mutations Y132F+G307A, G458S, and G307A+G458S. Y132F was found in almost 60% of the current FNS isolates and its prevalence was higher in this study (2019–2020) compared to our previous study (2007–2019) (Arastehfar et al., 2020b). Our previous analysis using a large cohort of patients infected with *C. parapsilosis* showed that azole use in the hospital was higher from 2015 onward, which was speculated to be the cause behind this surge (Arastehfar et al., 2020b). Moreover, environmental contamination could be another factor further contributing in continuous outbreak and increasing number patients infected with *C. parapsilosis* isolates carrying Y132F isolates. Our data confirming Y132F as the leading mutation underlying azole resistance is consistent with reports from India (Singh et al., 2019), Brazil (Thomaz et al., 2018), South Korea (Choi et al., 2018), South Africa (Magobo et al., 2020), Italy (Martini et al., 2020), the United States (Grossman et al., 2015), and Kuwait (Asadzadeh et al., 2017), where other Erg11p mutations have rarely been identified, except for K143R detected in India (Singh et al., 2019). On the other hand, the extreme variety of *ERG11* mutations observed in our settings compared to the other studies (Grossman et al., 2015; Asadzadeh et al., 2017; Choi et al., 2018; Thomaz et al., 2018; Singh et al., 2019; Magobo et al., 2020; Martini et al., 2020) may highlight potential hypermutability of Turkish *C. parapsilosis* isolates and the presence of certain genetic mechanisms

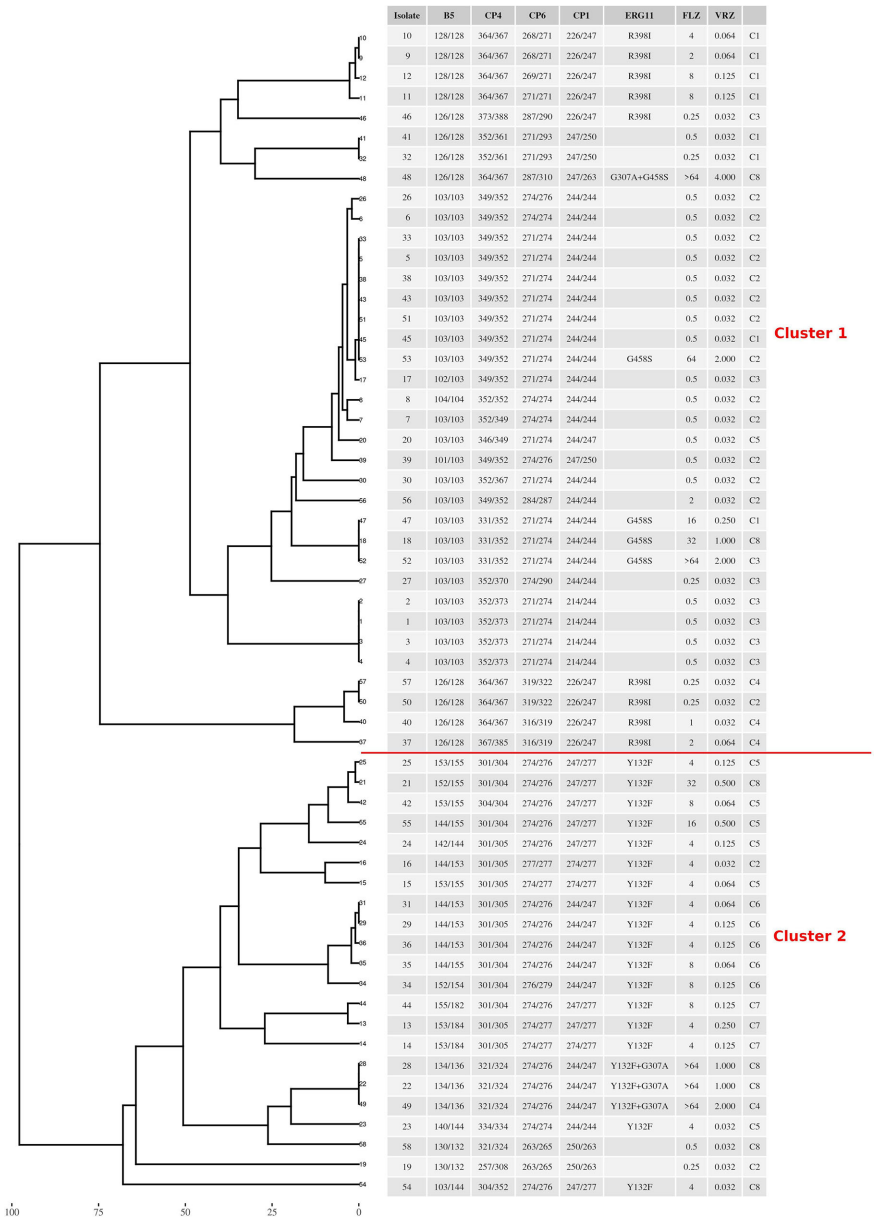

Isolate	B5	CP4	CP6	CP1	ERG11	FLZ	VRZ	
10	128/128	364/367	268/271	226/247	R398I	4	0.064	C1
9	128/128	364/367	268/271	226/247	R398I	2	0.064	C1
12	128/128	364/367	269/271	226/247	R398I	8	0.125	C1
11	128/128	364/367	271/271	226/247	R398I	8	0.125	C1
46	126/128	373/388	287/290	226/247	R398I	0.25	0.032	C3
41	126/128	352/361	271/293	247/250		0.5	0.032	C1
32	126/128	352/361	271/293	247/250		0.25	0.032	C1
48	126/128	364/367	287/310	247/263	G307A+G458S	>64	4.000	C8
26	103/103	349/352	274/276	244/244		0.5	0.032	C2
6	103/103	349/352	274/274	244/244		0.5	0.032	C2
33	103/103	349/352	271/274	244/244		0.5	0.032	C2
5	103/103	349/352	271/274	244/244		0.5	0.032	C2
38	103/103	349/352	271/274	244/244		0.5	0.032	C2
43	103/103	349/352	271/274	244/244		0.5	0.032	C2
51	103/103	349/352	271/274	244/244		0.5	0.032	C2
45	103/103	349/352	271/274	244/244		0.5	0.032	C1
53	103/103	349/352	271/274	244/244	G458S	64	2.000	C2
17	102/103	349/352	271/274	244/244		0.5	0.032	C3
8	104/104	352/352	274/274	244/244		0.5	0.032	C2
7	103/103	352/349	274/274	244/244		0.5	0.032	C2
20	103/103	346/349	271/274	244/247		0.5	0.032	C5
39	101/103	349/352	274/276	247/250		0.5	0.032	C2
30	103/103	352/367	271/274	244/244		0.5	0.032	C2
56	103/103	349/352	284/287	244/244		2	0.032	C2
47	103/103	331/352	271/274	244/244	G458S	16	0.250	C1
18	103/103	331/352	271/274	244/244	G458S	32	1.000	C8
52	103/103	331/352	271/274	244/244	G458S	>64	2.000	C3
27	103/103	352/370	274/290	244/244		0.25	0.032	C3
2	103/103	352/373	271/274	214/244		0.5	0.032	C3
1	103/103	352/373	271/274	214/244		0.5	0.032	C3
3	103/103	352/373	271/274	214/244		0.5	0.032	C3
4	103/103	352/373	271/274	214/244		0.5	0.032	C3
57	126/128	364/367	319/322	226/247	R398I	0.25	0.032	C4
50	126/128	364/367	319/322	226/247	R398I	0.25	0.032	C2
40	126/128	364/367	316/319	226/247	R398I	1	0.032	C4
37	126/128	367/385	316/319	226/247	R398I	2	0.064	C4
25	153/155	301/304	274/276	247/277	Y132F	4	0.125	C5
21	152/155	301/304	274/276	247/277	Y132F	32	0.500	C8
42	153/155	304/304	274/276	247/277	Y132F	8	0.064	C5
55	144/155	301/304	274/276	247/277	Y132F	16	0.500	C5
24	142/144	301/305	274/276	247/277	Y132F	4	0.125	C5
16	144/153	301/305	277/277	274/277	Y132F	4	0.032	C2
15	153/155	301/305	274/277	274/277	Y132F	4	0.064	C5
31	144/153	301/305	274/276	244/247	Y132F	4	0.064	C6
29	144/153	301/305	274/276	244/247	Y132F	4	0.125	C6
36	144/153	301/304	274/276	244/247	Y132F	4	0.125	C6
35	144/155	301/304	274/276	244/247	Y132F	8	0.064	C6
34	152/154	301/304	276/279	244/247	Y132F	8	0.125	C6
44	155/182	301/304	274/276	247/277	Y132F	8	0.125	C7
13	153/184	301/305	274/277	247/277	Y132F	4	0.250	C7
14	153/184	301/305	274/277	274/277	Y132F	4	0.125	C7
28	134/136	321/324	274/276	244/247	Y132F+G307A	>64	1.000	C8
22	134/136	321/324	274/276	244/247	Y132F+G307A	>64	1.000	C8
49	134/136	321/324	274/276	244/247	Y132F+G307A	>64	2.000	C4
23	140/144	334/334	274/274	244/244	Y132F	4	0.032	C5
58	130/132	321/324	263/265	250/263		0.5	0.032	C8
19	130/132	257/308	263/265	250/263		0.25	0.032	C2
54	103/144	304/352	274/276	247/277	Y132F	4	0.032	C8

FIGURE 3 | The genotypic relatedness of *C. parapsilosis* blood isolates recovered during 2019 to 2020 in Ege University Hospital reveals clonal outbreak due to both azole-susceptible and azole-non-susceptible isolates. C denotes minor cluster containing similar genotypes (difference ≥ 2 alleles).

promoting the establishment and persistence of such outstanding genetic diversity.

To evaluate the clinical significance of our molecular data, we analyzed their association with patient outcome, specifically focusing on mortality and FTF. The overall mortality rate was 27.6%; however, it was significantly higher for patients infected with Y132F-carrying *C. parapsilosis* than for those infected with the other FNS and FS isolates, which is consistent with the trend reported in our previous study (Arastehfar et al., 2020b; Thomaz et al., 2021). Unfortunately, the retrospective nature of our study did not allow us to obtain detailed clinical data on the severity of the diseases, which directly impacts the mortality rate. Among other host- and drug-related factors involved, this phenomenon may be attributed to the presence of some unknown compensatory genetic mutations accompanying Y132F and/or higher virulence of Y132F strains compared to other isolates, which, consequently, may explain the exponential increase in the incidence of Y132F-carrying *C. parapsilosis* observed in our and other studies (Grossman et al., 2015; Asadzadeh et al., 2017; Choi et al., 2018; Thomaz et al., 2018; Singh et al., 2019; Arastehfar et al., 2020b; Magobo et al., 2020; Martini et al., 2020). Of note, our most recent study involving *Galleria mellonella* have shown

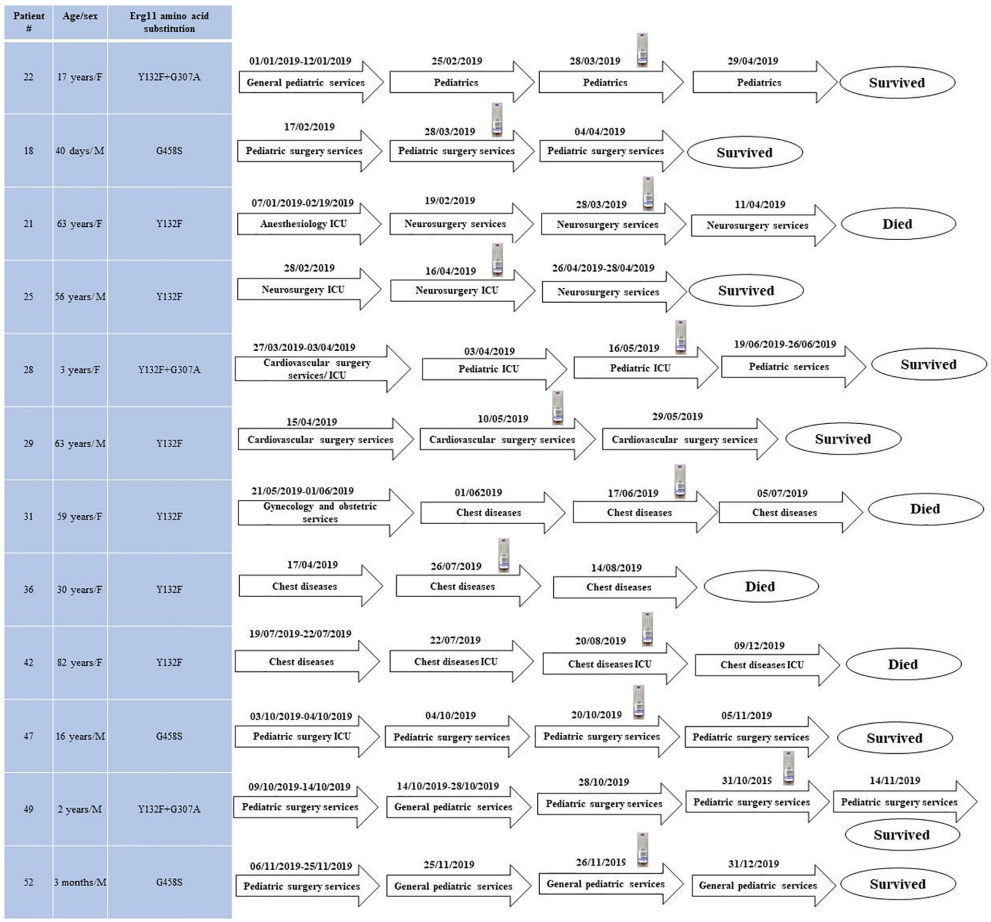

FIGURE 4 | The transmission map of patients infected with fluconazole non-susceptible clonal isolates and/or with those showing high genetic similarity during the study period. Blood bottle symbol denotes the positive blood bottle date.

the lack of a higher virulence attributes of *C. parapsilosis* isolates carrying Y132F compared to other FNS and FS isolates (Binder et al., 2020). However, comprehensive studies involving mice model using a large number of *C. parapsilosis* isolates are required to investigate if Y132F possess a higher virulence and if such isolates are associated with a higher mortality rate.

FTF was found in 100% and 9% of fluconazole-treated patients infected with FNS and FS *C. parapsilosis* isolates, respectively. Although FTF can also occur because of fluconazole tolerance (Arastehfar et al., 2020e; Berman and Krysan, 2020), none of the FS isolates showed a fluconazole-tolerant phenotype and FTF could be explained by the involvement of other mechanisms such as host- and drug-related factors (Arastehfar et al., 2020e; Arastehfar et al., 2020f; Berman and Krysan, 2020). Consistent with other studies, we found that 32% of the patients infected with FNS isolates were also azole-naïve (Arastehfar et al., 2020b), which raises the question whether such isolates have emerged through clonal expansion. Therefore, we analyzed the genetic relatedness of *C. parapsilosis* isolates by multilocus microsatellite typing, which allowed identification of two major clusters: one predominated by FNS and the other – by FS isolates, among which a few FNS isolates were scattered. Interestingly, all FNS *C. parapsilosis* isolates carrying Y132F and Y132F+G307 grouped together in genetically similar minor clusters and were mostly obtained from patients in chest diseases and pediatric surgery wards, whereas other FNS isolates carrying G458S were clonal and dispersed among FS isolates. Clonality was observed for FS *C. parapsilosis* and almost 37% of patients infected with such isolates were admitted to the burn ICU, which is similar to our previous observations. These data are important to consider, since some studies have focused on the genetic relatedness of FNS *C. parapsilosis* assuming that Y132F isolates are mostly associated with persistent clonal outbreaks, (Choi et al., 2018) while here we have shown that both FNS and FS *C. parapsilosis* isolates formed clonal clusters and consequently caused outbreak. The observation of expanding genetically similar and/or clonal ones is similar to what have been observed for the multidrug-resistant *Candida auris*, where cross-transmission among several patients were recorded during the course of infection (Al Maani et al.,

2019; Mohsin et al., 2020). Our findings emphasize the continuous expansion of clonal FNS and FS *C. parapsilosis* outbreaks in EUH, which requires prompt implementation of infection control strategies and establishment of antifungal stewardship to prevent further spread and emergence of *C. parapsilosis* in this hospital. Of note, the lack of AMB resistance in our huge collection of *C. parapsilosis* isolates collected over 14 years and its well-tolerability among neonates and children is in line with the *in-vivo* efficacy data obtained from *G. mellonella* where the larvae were infected with MDR and FNS *C. parapsilosis* blood isolates showed excellent efficacy when AMB compared with fluconazole (Binder et al., 2020).

The major limitations of the current study are the lack of expression analysis of efflux pumps (*CDR1* and *MDR1*) and *ERG11* in FNS compared to FS *C. parapsilosis* isolates and their association with gain-of-function mutations occurring in their transcription factors, namely *TAC1*, *MRR1*, and *UPC2*. Moreover, the continual clonal expansion of FNS and FS *C. parapsilosis* isolates in EUH requires the environmental screening to find the source of infection, which will be addressed in the future.

DATA AVAILABILITY STATEMENT

The datasets presented in this study can be found in online repositories. The sequences of ERG11, FKS1-HS1, FKS1-HS2 obtained in this study were deposited in the GenBank database under the following accession numbers (MW013584–MW013641), (MW013700–MW013757), and (MW013642–MW013699), respectively.

ETHICS STATEMENT

This study was approved by the ethical committee of EUH (ethical approval number: 20-2T/30). Written informed consent to participate in this study was provided by the participants' legal guardian/next of kin.

AUTHOR CONTRIBUTIONS

Conceptualization, AA, CL-F, DP, and SH-P. Methodology, AA, CL-F, SH-P, FD, WP, AH, WF, WL, ZŞ-B, and DM. Software, AA, SH-P, FD, and AH. Validation, AA, SH-P, FD, WP, DP, and CL-F. Formal analysis, AA and SH-P. Investigation, AA, CL-F, FD, WP, AH, WF, WL, ZŞ-B, and DM. Resources, WF, WL, ZŞ-B, DM, SH-P, MI, and WP. Data curation, AA, SH-P, FD, and AH. Writing – original draft preparation draft, AA. Writing – review & editing, All co-authors. Visualization, AA, AH, and JA. Supervision, AA, SH-P, DP, and WP. Project administration, AA. Funding acquisition, DP, WP, and SH-P. All authors contributed to the article and approved the submitted version.

FUNDING

This work was supported by the Major National R&D Projects of the National Health Department [2018ZX10101003], National Natural Science Foundation of China [31770161], Shanghai Science and Technology Committee [17DZ2272900 and 14495800500], Shanghai Municipal Commission of Health and Family Planning [2017ZZ01024-001], Shanghai Sailing Program [19YF1448000], and the Chinese Academy of Engineering [2019-XY-33].

SUPPLEMENTARY MATERIAL

The Supplementary Material for this article can be found online at: https://www.frontiersin.org/articles/10.3389/fcimb.2021.676177/full#supplementary-material

REFERENCES

Al Maani, A., Paul, H., Al-Rashdi, A., Al Wahaibi, A., Al-Jardani, A., Al Abri, A. M. A., et al. (2019). Ongoing Challenges With Healthcare-Associated *Candida Auris* Outbreaks in Oman. *J. Fungi* 5, 101. doi: 10.3390/jof5040101

Arastehfar, A., Daneshnia, F., Hafez, A., Khodavaisy, S., Najafzadeh, M. J., Charsizadeh, A., et al. (2020a). Antifungal Susceptibility, Genotyping, Resistance Mechanism, and Clinical Profile of *Candida Tropicalis* Blood Isolates. *Med. Mycol.* 58, 766–773. doi: 10.1093/mmy/myz124

Arastehfar, A., Daneshnia, F., Hilmioğlu-Polat, S., Fang, W., Yaşar, M., Polat, F., et al. (2020b). First Report of Candidemia Clonal Outbreak Caused by Emerging Fluconazole-Resistant *Candida Parapsilosis* Isolates Harboring Y132F and/or Y132F+K143R in Turkey. *Antimicrob. Agents Chemother.* 64, e01001–e01020. doi: 10.1128/AAC.01001-20

Arastehfar, A., Daneshnia, F., Hilmioglu-Polat, S., Ilkit, M., Yaşar, M., Polat, F., et al. (2021). Genetically-Related Micafungin-Resistant *C. Parapsilosis* Blood Isolates Harboring a Novel Mutation R658G in Hotspot1-Fks1p: A New Challenge? *J. Antimicrob. Chemother.* 76, 418–422. doi: 10.1093/jac/dkaa419

Arastehfar, A., Daneshnia, F., Najafzadeh, M. J., Hagen, F., Mahmoudi, S., Salehi, M., et al. (2020c). Evaluation of Molecular Epidemiology, Clinical Characteristics, Antifungal Susceptibility Profiles, and Molecular Mechanisms of Antifungal Resistance of Iranian *Candida Parapsilosis* Species Complex Blood Isolates. *Front. Cell. Infect. Microbiol.* 10, 206. doi: 10.3389/fcimb.2020.00206

Arastehfar, A., Daneshnia, F., Salehi, M., Yaşar, M., Hoşbul, T., Ilkit, M., et al. (2020d). Low Level of Antifungal Resistance of *Candida Glabrata* Blood Isolates in Turkey: Fluconazole Minimum Inhibitory Concentration and FKS Mutations can Predict Therapeutic Failure. *Mycoses* 63, 911–920. doi: 10.1111/myc.13104

Arastehfar, A., Daneshnia, F., Zomorodian, K., Najafzadeh, M. J., Khodavaisy, S., Zarrinfar, H., et al. (2019a). Low Level of Antifungal Resistance in Iranian Isolates of *Candida Glabrata* Recovered From Blood Samples in a Multicenter Study From 2015 to 2018 and Potential Prognostic Values of Genotyping and Sequencing of PDR1. *Antimicrob. Agents Chemother.* 63, e02503–e02518. doi: 10.1128/AAC.02503-18

Arastehfar, A., Fang, W., Pan, W., Liao, W., Yan, L., and Boekhout, T. (2018). Identification of Nine Cryptic Species of *Candida Albicans*, *C. Glabrata*, and *C. Parapsilosis* Complexes Using One-Step Multiplex PCR. *BMC Infect. Dis.* 18, 480. doi: 10.1186/s12879-018-3381-5

Arastehfar, A., Hilmioğlu-Polat, S., Daneshnia, F., Hafez, A., Salehi, M., Polat, F., et al. (2020e). Recent Increase in the Prevalence of Fluconazole-non-Susceptible *Candida Tropicalis* Blood Isolates in Turkey: Clinical

Implication of Azole-non-Susceptible and Fluconazole Tolerant Phenotypes and Genotyping. *Front. Microbiol.* 11, 587278. doi: 10.3389/fmicb.2020.587278

Arastehfar, A., Khodavaisy, S., Daneshnia, F., Najafzadeh, M. J., Mahmoudi, S., Charsizadeh, A., et al. (2019b). Molecular Identification, Genotypic Diversity, Antifungal Susceptibility, and Clinical Outcomes of Infections Caused by Clinically Underrated Yeasts, *Candida Orthopsilosis*, and *Candida Metapsilosis*: An Iranian Multicenter Study, (2014–2019). *Front. Cell. Infect. Microbiol.* 9, 264. doi: 10.3389/fcimb.2019.00264

Arastehfar, A., Lass-Flörl, C., Garcia-Rubio, R., Daneshnia, F., Ilkit, M., Boekhout, T., et al. (2020f). The Quiet and Underappreciated Rise of Drug Resistant Invasive Fungal Pathogens. *J. Fungi* 6, E138. doi: 10.3390/jof6030138

Arastehfar, A., Wickes, B. L., Ilkit, M., Pincus, D. H., Daneshnia, F., Pan, W., et al. (2019c). Identification of Mycoses in Developing Countries. *J. Fungi* 5, 90. doi: 10.3390/jof5040090

Asadzadeh, M., Ahmad, S., Al-Sweih, N., and Khan, Z. (2017). Epidemiology and Molecular Basis of Resistance to Fluconazole Among Clinical *Candida Parapsilosis* Isolates in Kuwait. *Microb. Drug Resist.* 23, 966–972. doi: 10.1089/mdr.2016.0336

Berman, J., and Krysan, D. J. (2020). Drug Resistance and Tolerance in Fungi. *Nat. Rev. Microbiol.* 18, 319–331. doi: 10.1038/s41579-019-0322-2

Binder, U., Arastehfar, A., Schnegg, L., Hörtnagl, C., Hilmioğlu-Polat, S., Perlin, D. S., et al. (2020). Efficacy of LAMB Against Emerging Azole- and Multidrug-Resistant *Candida Parapsilosis* İsolates İn the *Galleria Mellonella* Model. *J. Fungi* 6, 4. doi: 10.3390/jof6040377

Choi, Y. J., Kim, Y. J., Yong, D., Byun, J. H., Kim, T. S., Chang, Y. S., et al. (2018). Fluconazole-Resistant *Candida Parapsilosis* Bloodstream Isolates With Y132F Mutation in ERG11 Gene, South Korea. *Emerg. Infect. Dis.* 24, 1768–1770. doi: 10.3201/eid2409.180625

Clinical and Laboratory Standards Institute (2017). *Reference Method for Broth Dilution Antifungal Susceptibility Testing of Yeasts; Approved Standard. 3rd ed.* (Wayne, PA, USA: M60. CLSI).

Garcia-Effron, G., Katiyar, S. K., Park, S., Edlind, T. D., and Perlin, D. S. (2008). A Naturally Occurring Proline-to-Alanine Amino Acid Change in Fks1p in *Candida Parapsilosis*, *Candida Orthopsilosis*, and *Candida Metapsilosis* Accounts for Reduced Echinocandin Susceptibility. *Antimicrob. Agents Chemother.* 52, 2305–2312. doi: 10.1128/AAC.00262-08

Grossman, N. T., Pham, C. D., Cleveland, A. A., and Lockhart, S. R. (2015). Molecular Mechanisms of Fluconazole Resistance in *Candida Parapsilosis* Isolates From a U.S. Surveillance System. *Antimicrob. Agents Chemother.* 59, 1030–1037. doi: 10.1128/AAC.04613-14

Kord, M., Salehi, M., Khodavaisy, S., Hashemi, S. J., Daei-Ghazvini, R., Rezaei, S., et al. (2020). Epidemiology of Yeast Species Causing Bloodstream Infection in Tehran, Iran, (2015–2017); Superiority of 21-Plex PCR Over the Vitek 2 System for Yeast Identification. *J. Med. Microbiol.* 69, 712–720. doi: 10.1099/jmm.0.001189

Magobo, R. E., Lockhart, S. R., and Govender, N. P. (2020). Fluconazole-Resistant *Candida Parapsilosis* Strains With a Y132F Substitution in the ERG11 Gene Causing Invasive Infections in a Neonatal Unit, South Africa. *Mycoses* 63, 471–477. doi: 10.1111/myc.13070

Martini, C., Torelli, R., de Groot, T., de Carolis, E., Morandotti, G. A., de Angelis, G., et al. (2020). Prevalence and Clonal Distribution of Azole-Resistant *Candida Parapsilosis* Isolates Causing Bloodstream Infections in a Large Italian Hospital. *Front. Cell. Infect. Microbiol.* 10, 232. doi: 10.3389/fcimb.2020.00232

Megri, Y., Arastehfar, A., Boekhout, T., Daneshnia, F., Hörtnagl, C., Sartori, B., et al. (2020). *Candida Tropicalis* is the Most Prevalent Yeast Species Causing Candidemia in Algeria: The Urgent Need for Antifungal Stewardship and Infection Control Measures. *Antimicrob. Resist. Infect. Control* 9, 50. doi: 10.1186/s13756-020-00710-z

Mohsin, J., Weerakoon, S., Ahmed, S., Puts, Y., Al Balushi, Z., Meis, J. F., et al. (2020). A Cluster of *Candida Auris* Blood Stream Infections in a Tertiary Care Hospital in Oman From 2016 to 2019. *Antibiotics* 9, 638. doi: 10.3390/antibiotics9100638

Pfaller, M. A., and Diekema, D. J. (2012). Progress in Antifungal Susceptibility Testing of *Candida* Spp. by Use of Clinical and Laboratory Standards Institute Broth Microdilution Methods 2010 to 2012. *J. Clin. Microbiol.* 50, 2846–2856. doi: 10.1128/JCM.00937–12

Pfaller, M. A., Diekema, D. J., Turnidge, J. D., Castanheira, M., and Jones, R. N. (2019). Twenty Years of the SENTRY Antifungal Surveillance Program: Results for *Candida* Species From 1997–2016. *Open Forum Infect. Dis.* 6, S79–S94. doi: 10.1093/ofid/ofy358

Singh, A., Singh, P. K., de Groot, T., Kumar, A., Mathur, P., Tarai, B., et al. (2019). Emergence of Clonal Fluconazole-Resistant *Candida Parapsilosis* Clinical Isolates in a Multicentre Laboratory-Based Surveillance Study in India. *J. Antimicrob. Chemother.* 74, 1260–1268. doi: 10.1093/jac/dkz029

Souza, A. C. R., Ferreira, R. C., Gonçalves, S. S., Quindós, G., Eraso, E., Bizerra, F. C., et al. (2012). Accurate Identification of *Candida Parapsilosis* (*Sensu Lato*) by Use of Mitochondrial DNA and Real-Time PCR. *J. Clin. Microbiol.* 50, 2310–2314. doi: 10.1128/JCM.00303-12

Stielow, J. B., Lévesque, C. A., Seifert, K. A., Meyer, W., Iriny, L., Smits, D., et al. (2015). One Fungus, Which Genes? Development and Assessment of Universal Primers for Potential Secondary Fungal DNA Barcodes. *Persoonia* 35, 242–263. doi: 10.3767/003158515X689135

Thomaz, D. Y., de Almeida, J. N., Lima, G. M. E., de Oliveira Nunes, M., Camargo, C. H., de Carvalho-Grenfell, R., et al. (2018). An Azole-Resistant *Candida Parapsilosis* Outbreak: Clonal Persistence in the Intensive Care Unit of a Brazilian Teaching Hospital. *Front. Microbiol.* 9, 2997. doi: 10.3389/fmicb.2018.02997

Thomaz, D. Y., de Almeida, J. N. , Jr., Sejas, O. N. E., Del Negro, G. M. B., Carvalho, G. O. M. H., Gimenes, V. M. F., et al. (2021). Environmental Clonal Spread of Azole-Resistant *Candida Parapsilosis* With Erg11-Y132F Mutation Causing a Large Candidemia Outbreak in a Brazilian Cancer Referral Center. *J. Fungi* 7, 259. doi: 10.3390/jof7040259

Tóth, R., Nosek, J., Mora-Montes, H. M., Gabaldon, T., Bliss, J. M., Nosanchuk, J. D., et al. (2019). *Candida Parapsilosis*: From Genes to the Bedside. *Clin. Microbiol. Rev.* 32, e00111–e00118. doi: 10.1128/CMR.00111-18

Trobajo-Sanmartín, C., Ezpeleta, G., Pais, C., Eraso, E., and Quindós, G. (2018). Design and Validation of a Multiplex PCR Protocol for Microsatellite Typing of *Candida Parapsilosis Sensu Stricto* Isolates. *BMC Genomics* 19, 718. doi: 10.1186/s12864-018-50653

Conflict of Interest: Author AH was employed by company Biotechvana.

The remaining authors declare that the research was conducted in the absence of any commercial or financial relationships that could be construed as a potential conflict of interest.

Citation: *Arastehfar A, Hilmioğlu-Polat S, Daneshnia F, Pan W, Hafez A, Fang W, Liao W, Şahbudak-Bal Z, Metin DY, Júnior JNdA, Ilkit M, Perlin DS and Lass-Flörl C (2021) Clonal Candidemia Outbreak by* Candida parapsilosis *Carrying Y132F in Turkey: Evolution of a Persisting Challenge.*
Front. Cell. Infect. Microbiol. 11:676177. doi: 10.3389/fcimb.2021.676177

frontiers in Cellular and Infection Microbiology

REVIEW
published: 06 May 2021
doi: 10.3389/fcimb.2021.683670

Molecular Markers Reveal Epidemiological Patterns and Evolutionary Histories of the Human Pathogenic *Cryptococcus*

Nan Hong[1,2†], *Min Chen*[1†] *and Jianping Xu*[3*]

[1] Department of Dermatology, Shanghai Key Laboratory of Medical Mycology, Changzheng Hospital, Naval Medical University, Shanghai, China, [2] Department of Burn and Plastic Surgery, Jinling Hospital, School of Medicine, Nanjing University, Nanjing, China, [3] Department of Biology, McMaster University, Hamilton, ON, Canada

OPEN ACCESS

Edited by:
Li-Jun Ma,
University of Massachusetts Amherst, United States

Reviewed by:
Shira Milo,
University of Massachusetts Amherst, United States
Neta Shlezinger,
The Hebrew University of Jerusalem, Israel

***Correspondence:**
Jianping Xu
jpxu@mcmaster.ca

[†]These authors have contributed equally to this work and share first authorship

Specialty section:
This article was submitted to Fungal Pathogenesis, a section of the journal Frontiers in Cellular and Infection Microbiology

Received: 21 March 2021
Accepted: 22 April 2021
Published: 06 May 2021

Citation:
Hong N, Chen M and Xu J (2021) Molecular Markers Reveal Epidemiological Patterns and Evolutionary Histories of the Human Pathogenic Cryptococcus. Front. Cell. Infect. Microbiol. 11:683670. doi: 10.3389/fcimb.2021.683670

The human pathogenic *Cryptococcus* species are the main agents of fungal meningitis in humans and the causes of other diseases collectively called cryptococcosis. There are at least eight evolutionary divergent lineages among these agents, with different lineages showing different geographic and/or ecological distributions. In this review, we describe the main strain typing methods that have been used to analyze the human pathogenic *Cryptococcus* and discuss how molecular markers derived from the various strain typing methods have impacted our understanding of not only cryptococcal epidemiology but also its evolutionary histories. These methods include serotyping, multilocus enzyme electrophoresis, electrophoretic karyotyping, random amplified polymorphic DNA, restriction fragment length polymorphism, PCR-fingerprinting, amplified fragment length polymorphism, multilocus microsatellite typing, single locus and multilocus sequence typing, matrix-assisted laser desorption/ionization time of flight mass spectrometry, and whole genome sequencing. The major findings and the advantages and disadvantages of each method are discussed. Together, while controversies remain, these strain typing methods have helped reveal (i) the broad phylogenetic pattern among these agents, (ii) the centers of origins for several lineages and their dispersal patterns, (iii) the distributions of genetic variation among geographic regions and ecological niches, (iv) recent hybridization among several lineages, and (v) specific mutations during infections within individual patients. However, significant challenges remain. Multilocus sequence typing and whole genome sequencing are emerging as the gold standards for continued strain typing and epidemiological investigations of cryptococcosis.

Keywords: *Cryptococcus neoformans* species complex, *Cryptococcus gattii* species complex, genetic variation, gene flow, discrimination power, microevolution

INTRODUCTION

The human pathogenic *Cryptococcus* species are among the biggest causes of mobility and mortality in humans. Globally, there are ~223,100 cases of cryptococcal meningitis per year, primarily in HIV-infected patients, resulting in ~181,100 deaths (Rajasingham et al., 2017). Strains in two sibling species complexes, the *Cryptococcus neoformans* species complex (CNSC) and the *Cryptococcus gattii* species complex (CGSC), are the primary causative agents of cryptococcosis (Kwon-Chung et al., 2014; May et al., 2016). CNSC has a worldwide distribution, occurring naturally in the soil, avian excreta, and decayed wood inside trunk hollows of many tree species (Lazera et al., 2000; Randhawa et al., 2008; Taverna et al., 2020), and is responsible for over 80% of the global cryptococcal infections (Park et al., 2009). CGSC has been mainly reported from the decayed wood in trunk hollows of various trees in tropical and subtropical regions and is observed to cause diseases in apparently healthy individuals (Byrnes et al., 2009; Mcculloh et al., 2011; Chen et al., 2014).

Since the 1980s, several molecular typing methods have been developed to study the epidemiology and genetic diversity of these two species complexes (**Table 1**). These methods primarily assay DNA sequence variations among strains and lineages and include random amplified polymorphic DNA (RAPD), PCR-fingerprinting, amplified fragment length polymorphisms (AFLP), PCR-restriction fragment length polymorphisms (PCR-RFLP), single locus sequence typing (SLST), multilocus sequence typing (MLST), multilocus microsatellite typing (MLMT), and whole genome sequencing (Sidrim et al., 2010; Li et al., 2013; Cuomo et al., 2018). The pros and cons of each of these methods are briefly summarized in **Table 1**. Together, these methods have allowed the identifications of individual and/or groups of strains, clarified the phylogenetic diversity within and between the two species complexes, revealed both recent and ancient hybridizations among lineages, and identified both broad geographic patterns of strain genotype distributions and local transmissions and microevolutions. In the sections below, we briefly describe each molecular typing method, point out their advantages and disadvantages, and summarize the main epidemiological findings based on each method. We also discuss how the methods have enabled other types of studies on the origins, virulence, and drug resistance in this important group of fungal pathogens.

SEROTYPING METHODS

Serotypes of CNSC and CGSC reflect the antigenic differences resulting from variation in capsular polysaccharides (Cherniak and Sundstrom, 1994). A diagnostic medium containing L-canavanine, glycine and bromothymol blue (CGB test) was first used to identify two species complexes including four serotypes: CNSC for serotypes A and D, and CGSC for serotypes B and C (Kwon-Chung et al., 1982). However, it was reported that a positive CGB reaction alone was not sufficient for accurate serotyping (Khan et al., 2003). Subsequently, antisera raised from strains of four different serotypes were developed into a commercial capsular agglutination test kit to identify cryptococcal serotypes. Based on the capsular agglutination reactions, an additional serotype AD that reacted with both serotypes A and D antisera was identified (Belay et al., 1996).

Serotyping was a quick and widely used epidemiological tool in cryptococcal research until the early part of the 21st century. Those studies identified that globally, the most frequent serotype in both environmental and clinical samples belonged to serotype A. In contrast, other serotypes showed more patchy distributions. For example, serotypes B and C were mainly found in tropical and subtropical regions while serotype D was mainly found in southern Europe (Dromer et al., 1996; Tortorano et al., 1997; Viviani et al., 2006). Further research revealed that different serotypes each had unique microbiological and biochemical characteristics (Nakamura et al., 1998). However, there were several limitations in using serotyping as the only strain typing method. For example, there were natural isolates without any capsular polysaccharides and thus were not reacting with any of the specific antisera and were deemed not typable (Fromtling et al., 1982; Kwon-Chung and Rhodes, 1986). In addition, the discrimination power of serotyping method is comparatively low which makes it unable to meet the demand of modern epidemiological studies of CNSC and CGSC.

At the turn of the century, DNA sequence analyses revealed significant divergence among strains and serotypes of the human pathogenic *Cryptococcus*. Those sequence analyses revealed restriction site polymorphism within specific genes that could be readily used to distinguish strains of different serotypes. For example, PCR amplification of a fragment of *CAP59*, a gene required for capsule biosynthesis, followed by restriction enzyme digest, enabled successful identification of the serotypes of CNSC and CGSC (Nakamura, 2001; Enache-Angoulvant et al., 2007). Later on, a multiplex PCR based on a set of four primers was created for serotype identification (Ito-Kuwa et al., 2007). These PCR-based methods showed high concordance with immunological serotyping methods. The cost-effectiveness and convenience of PCR-based methods for serotype identification resulted in the disuse of antisera serotyping kits as a common tool for epidemiological studies.

MULTILOCUS ENZYME ELECTROPHORESIS

Multilocus enzyme electrophoresis (MLEE) is a molecular typing method that detects differences in gel electrophoretic migration patterns of enzymes. The differences in mobility through gel matrixes are due to non-synonymous substitutions in genes encoding for enzymes. Since many enzymes are polymorphic among individuals in most species, MLEE was a very popular molecular typing method from the 1960s to the 1990s for assaying genetic variation in a diversity of organisms, from bacteria to fungi, plants and animals, including humans. For each metabolic enzyme, each individual haploid organism has a

TABLE 1 | Comparison of major molecular methods used for typing the human pathogenic *Cryptococcus*.

Methods	Genes/Molecules	Cost	Specificity	Convenience	Reproducibility	Discriminating Power	Resolution	First report
Serotyping	Capsular surface antigen	Medium	Medium	Medium	High	Low	Five serotypes A, B, C, D, AD	Kwon-Chung et al., 1982
RAPD	Random sequence in genome	Low	Low	High	Low	High	Strain-level	Welsh and McClelland, 1990
PCR fingerprinting	Random sequence in genome	Low	Low	High	Medium	Medium	Medium	Jeffreys et al., 1985
AFLP	Random sequence in genome	Medium	Low	Low	Medium	High	High	Vos et al., 1995
MLMT	Specific loci in genome	Medium	High	Medium	High	Medium to high depending on loci	Medium to high depending on loci	De Valk et al., 2007
MLST	Specific loci in genome	Medium	High	Medium	High	Medium to high depending on loci	Medium to high depending on loci	Xu et al., 2000b
MALDI-TOF MS	Whole-cell proteome	Medium	Low	Medium	Medium	Medium to high	Medium to high	Firacative et al., 2012
WGST	Whole genome sequence	High	High	Low	High	High	High	Fraser et al., 2005

specific amino acid sequence, exhibiting a specific mobility during gel electrophoresis. For diploid organisms, each individual would typically contain two copies of each gene. If the two copies are identical to each other within an individual, the individual is called a homozygote at the locus and only one enzyme band would be found during gel electrophoresis for the specific enzyme in this individual. In contrast, if the two copies of a metabolic enzyme have different amino acid sequences that change the mobility of the enzyme, the individual is called a heterozygote at the locus and two enzyme bands would be found during gel electrophoresis for the specific enzyme in the individual. After electrophoresis, specific colorimetric substrates are added to the gel to detect the mobility of individual enzymes. The mobility patterns of multiple enzymes constitute the individual organism's electrophoretic profile. MLEE offers higher discriminatory power than serotyping for detecting clones of many human microbial pathogens.

In 1995, Brandt et al. investigated the usefulness of MLEE in subtyping human pathogenic *Cryptococcus* clinical isolates (Bertout et al., 1999). They assayed the following 10 enzymes: alcohol dehydrogenase (EC 1.1.1.1), glucose 6-phosphate dehydrogenase (EC 1.1.1.49), 6-phosphogluconate dehydrogenase (EC 1.1.1.44), glutamate dehydrogenase (EC 1.4.1.4), glutamate oxaloacetic transaminase (EC 2.6.1.1), malate dehydrogenase (EC 1.1.1.37), phosphoglucose isomerase (EC 5.3.1.9), phosphoglyceromutase (EC 2.7.5.1), phenylalanine-leucine peptidase (EC 3.4.X.X), and leucine-alanine peptidase (EC 3.4.X.X). All 10 enzymes were found to be polymorphic in the analyzed *Cryptococcus* population. Based on the electrophoretic patterns of these 10 enzymes, they separated 344 isolates into 19 MLEE electrophoretic types (ETs): serotype A strains were grouped into 10 ETs; and three ETs each were found for strains of serotype D, serotype AD, and serotype B respectively (Brandt et al., 1995). The applications of the MLEE method allowed them to infer the epidemiological patterns of cryptococcal infections in four U.S. metropolitan areas between 1992 to 1994 (Brandt et al., 1995). Specifically, though some of the ETs were broadly distributed, they found several geographic specificities. For example, ET-1, the predominant ET throughout the US, was recovered in significantly greater proportion from Atlanta (Georgia), Houston (Texas), and all major metropolitan areas of Alabama than from San Francisco (California). In contrast, ET-2 and ET-7 (serotype AD) isolates were recovered predominantly from San Francisco (Brandt et al., 1995). Multiple isolates from the same patient always had the same ET, consistent with the stability of these markers and the persistence of cryptococcal strains in these patients. Furthermore, no significant difference in ET type distribution was found when isolates from HIV-infected patients were compared with those without HIV-infections, indicating no evidence of selection by the host or the pathogen in the genotype of cryptococcal strains causing cryptococcosis among patient groups in the US (Brandt et al., 1995).

While MLEE played a major role for studying a wide variety of practical and theoretical questions relating to epidemiology, population genetics, and systematics of microbial pathogens, it has ceased to be a routine strain typing technique of clinical or environmental microorganisms, including those of the human pathogenic *Cryptococcus*. Several reasons have likely contributed to its limited use, including: (i) technical complexity of MLEE; (ii) difficulties in comparing mobility results among laboratories; (iii) inability to assess nucleotide substitutions that do not cause amino acid changes (synonymous substitutions) due to redundancy in genetic code; and (iv) inability to assess amino acid substitutions that do not alter the overall charge or obvious molecular weight among alleles. Both (iii) and (iv) will cause different alleles with either different DNA sequences and/or different amino acid sequence to have the same or indistinguishable electrophoretic mobilities on gels. In addition, MLEE can only detect polymorphisms within the coding region of each gene. Mutations in promoter regions or introns of a gene cannot be assayed by MLEE. Methods that directly assay DNA sequence variations could help eliminate the limitations intrinsic to MLEE.

ELECTROPHORETIC KARYOTYPING

Karyotyping is a classical technology by which photographs of chromosomes are taken in order to determine the chromosome

complement of an individual organism, including the number, size, and staining patterns of chromosomes. Any abnormalities in the number, size, and staining patterns of chromosomes among individuals can all be theoretically determined. In humans, chromosomal karyotyping is most commonly used for prenatal screening and to diagnose chromosomal abnormalities that cause infertility. In fungi, due to the small sizes of their chromosomes, karyotyping is not accomplished by staining and microscopy but by pulsed-field gel electrophoresis (PFGE). The application of PFGE for studying the human pathogenic *Cryptococcus* began in the early 1990s. Indeed, it was commonly used as an epidemiological tool for clinical and environmental isolates of CNSC and CGSC during the period of 1990s to 2000s (Kwon-Chung et al., 1992; Boekhout et al., 1993; Perfect et al., 1993; Saracli et al., 2006; Esposto et al., 2009). For example, Boekhout et al. reported that the electrophoretic karyotypes of CNSC and CGSC consist of seven to fourteen bands of chromosomal DNA, and that there was no obvious correlation between chromosomal number and serotypes, geographic origin or ecological habitat (Boekhout et al., 1993). In addition, while differences among isolates were observed, the karyotype patterns of individual CNSC or CGSC isolates were shown to be stable during both *in vitro* passage and *in vivo* infections (Boekhout et al., 1993). Those analyses revealed no specific pattern of karyotypes of CNSC or CGSC isolates being associated with site of infection [e.g., isolates from cerebral spinal fluid (CSF) vs blood] or with the hosts' underlying conditions (e.g., isolates from HIV-infected patients compared with patterns in non-HIV-infected patients) (Perfect et al., 1993). Moreover, results of PFGE karyotyping supported the hypothesis that serotype AD isolates of CNSC often contained most chromosomal complements of both serotypes A and D strains (Esposto et al., 2009). In addition, PFGE karyotyping helped provide estimates of genome size and chromosome numbers in individual strains. For example, using PFGE, Perfect *et al.* provided the first estimate of the genome size of CNSC as between 15 and 17 Mb, with the number of chromosomes ranging between 10 and 12 (Perfect et al., 1993). Later, also using PFGE, Wickes *et al.* derived larger and more accurate genome size estimates at 21 to 24.5 Mb, with 13 chromosomes on average in CGSC and 12 chromosomes in CNSC (Wickes et al., 1994).

Notably, PFGE revealed significant electrophoretic karyotype polymorphisms among clinical and environmental isolates of CNSC and CGSC (Kwon-Chung et al., 1992; Perfect et al., 1993). For instances, Currie *et al.* reported 18 different karyotypes among 25 environmental and clinical isolates of CNSC from New York, USA (Currie et al., 1994). Similarly, six and three karyotypes were identified among 21 clinical isolates and eight environmental isolates of CNSC from Nagasaki, Japan (Yamamoto et al., 1995). In the study by Perfect *et al.* (Perfect et al., 1993), 41 different karyotypes were found among 46 clinical or environmental CNSC or CGSC isolates. Similarly, a high karyotype polymorphisms were found by Dromer et al. (Dromer et al., 1994) who reported 39 different karyotypes among 40 clinical isolates of CNSC (serotype D). Further, Perfect et al. noted that PFGE karyotyping could be used to exclude the possibility of nosocomial spread of CNSC in one clinical situation and supported relapse in two other cases due to its variable chromosome sizes between isolates (Perfect et al., 1993). Together, these results indicated the PFGE karyotyping can be a powerful method for discriminating strains and for epidemiological studies of CNSC and CGSC.

Even in the omics era, the PFGE karyotyping can still be a useful tool for genetic and epidemiological studies on CNSC and CGSC, particularly for determining chromosomal structural changes associated with environmental outbreaks or distinguishing the clinical isolates between relapse and reinfection. For example, drug resistance can be caused by duplication of whole chromosomes or chromosomal segments. Such duplications can often be detected through PFGE while other DNA sequence – based methods may miss such genetic changes. Together with other methods such as targeted gene sequencing or whole genome sequencing, PFGE will continue to help understand the epidemiology and evolution of CNSC and CGSC in the future.

RESTRICTION FRAGMENT LENGTH POLYMORPHISM

Restriction fragment length polymorphism (RFLP) is a classic molecular genotyping technique originally developed for genetic studies and for constructing restriction maps of large DNA molecules such as plasmids and mitochondrial genomes. RFLP has been broadly employed for mapping human disease genes beginning in the late 1970s (Botstein et al., 1980). The RFLP-based molecular markers provide an ability to detect DNA fragments of different lengths after digestion of DNA samples from various sources by restriction endonucleases. Depending on our prior information, RFLP can be detected using different approaches. When the DNA sequence of the target gene is not known and PCR amplification is not possible, RFLP is typically determined based on the restriction digest of whole-genome DNA, followed by agarose gel electrophoresis, Southern blotting, hybridization of the labeled target DNA molecule to the Southern blot, and visualization of the hybridization products through autoradiography (Grover and Sharma, 2016). Although the procedure described above for assaying RFLP is reliable for distinguishing different genotypes and does not require knowledge of the genome sequence (Gebhardt et al., 1989), the entire procedure is very time-consuming and requires special training and equipment.

When the specific DNA sequence containing the restriction polymorphic site is known, PCR primers can be designed and RFLP can be effectively combined with PCR to quickly assay RFLP for many samples. For the human pathogenic *Cryptococcus*, Xu et al. in 2000 identified an RFLP within the mitochondrial large ribosomal subunit that distinguished serotypes A and D strains (Xu et al., 2000a). After 2001, Velegraki et al., Xu et al., Meyer et al. and Latouche et al. successively used PCR-RFLP in molecular epidemiological

studies of clinical isolates of CNSC and CGSC, which targeted different genes including orotidine monophosphate pyrophosphorylase gene (*URA5*) (Velegraki et al., 2001; Xu, 2002; Meyer et al., 2003), the mitochondrial large ribosomal subunit (Velegraki et al., 2001; Xu, 2002; Meyer et al., 2003), and phospholipase B gene (*PLB1*) (Latouche et al., 2003). Commendably, the RFLP assays clustered CNSC and CGSC isolates into eight major molecular types, which have since found a good concordance with results of serotyping, PCR fingerprinting, and multilocus sequence typing, and whole-genome sequencing (please see below) of isolates of CNSC and CGSC. Additional PCR-RFLP markers based on other genes such as *CAP1* and *GEF1* allowed simultaneous identification of both the molecular type and mating type of CNSC and CGSC (Feng et al., 2008). Because of the ease of application, the PCR-RFLP markers will continue to be used for targeted epidemiological studies and genetic analyses of the human pathogenic *Cryptococcus*.

RANDOM AMPLIFIED POLYMORPHIC DNA

PCR-fingerprinting is a series of PCR-based techniques using arbitrary primers to amplify regions of genomes. These techniques are versatile for detecting DNA sequence polymorphisms for a variety of purposes, including genetic mapping, phylogenetics, and molecular epidemiology (Welsh and Mcclelland, 1990; Williams et al., 1990). Among the PCR-fingerprinting techniques, random amplified polymorphic DNA (RAPD) is a molecular marker technique that uses a single short arbitrary oligonucleotide primer (generally 10 bp) to randomly amplify DNA fragments within individual genomes (Welsh and Mcclelland, 1990; Williams et al., 1990). Because the single primer is short, there are potentially many regions in the genome with similar or identical sequences that the primer can anneal to and amplify. Consequently, RAPD can potentially generate a large number of amplified fragments from different parts of the genome. Polymorphisms among individuals are generated when there are differences among individuals in nucleotide sequences at the primer sites and/or when there are insertions/deletions within the regions of DNA flanked by the primer recognition sites. The polymorphism information on target genomic DNA can be generated independent of any prior knowledge of the target DNA sequence. RAPD was broadly used in the early 1990s (Williams et al., 1990; Hadrys et al., 1992) when no whole-genome sequence was available. An appropriate primer may yield distinctive RAPD patterns of DNA fragments among species and strains. Most studies using RAPD markers for genotyping employ multiple primers, with one in each PCR. Together, a large number of polymorphic DNA bands can be generated and detected through agarose gel electrophoresis to distinguish strains. However, because of the short primer length and low annealing temperature, RAPD is sensitive to minor variations in many factors such as annealing temperature, buffer solution, template DNA concentration, and the PCR machine used. Consequently, it's often necessary to standardize the procedures such as the quality and quantity of genomic DNA (Koebner, 1995; Mohan et al., 1995) and the specific PCR instrument used (Schierwater and Ender, 1993) in order to ensure reproducibility of RAPD results (Williams et al., 1990; Hadrys et al., 1992).

The RAPD technique was employed for several molecular epidemiological studies on CNSC and CGSC, using a series of primer combinations in the 1990s (Chen et al., 1996; Sorrell et al., 1996; Chen et al., 1997). Brandt et al. compared RAPD and MLEE and found they each had advantages, resolving the relationships among strains of CNSC and CGSC to different degrees (Brandt et al., 1995). Ruma et al. distinguished CNSC isolates between serotypes A, D or AD, and revealed further differentiation among strains within each serotype using seven RAPD primers (Ruma et al., 1996). In their study, four RAPD profiles were clearly distinguished within CGSC, among which two primers 5SOR and CNl differentiated their collection of CGSC isolates between serotypes B and C (Ruma et al., 1996). With primers ERICl and ERIC2, Boekhout et al. also reported that the RAPD technique could distinguish CNSC and CGSC isolates at the level of serotypes (Boekhout et al., 1997). Furthermore, RAPD markers have been successfully used in combination with other molecular typing methods. For example, Boekhout et al. showed that RAPD in combination with PFGE karyotyping were more useful in epidemiological studies of CNSC and CGSC than either technique alone (Boekhout et al., 1997). In other studies, the combination of long primer PCR-fingerprinting and RAPD revealed abundant genetic diversity of more than 400 isolates of CNSC and CGSC in two studies (Sorrell et al., 1996; Meyer et al., 1999), clustering the CNSC and CGSC isolates into four major groups, respectively.

In general, while RAPD markers have generated useful information for epidemiological studies on CNSC and CGSC, its high sensitivity to experimental conditions and low reproducibility among experiments make comparing results among labs difficult (Williams et al., 1990; Hadrys et al., 1992). Indeed, there has been a continuous decline in using RAPD markers alone for epidemiological studies on CNSC and CGSC (and other organisms) since the early 1990s (**Figure 1**).

PCR-FINGERPRINTING

As described in the last section, PCR fingerprinting is a common strain typing technique, first described in 1985 (Jeffreys et al., 1985). Different from RAPD, this strain typing technique typically refers to the detection of hypervariable repetitive sequences (minisatellite and microsatellite or simple repetitive DNAs) using specific oligonucleotides individually as PCR primers. These oligonucleotides were originally designed as hybridization probes for classical DNA fingerprinting experiments through Southern hybridization (Meyer et al., 1993a; Meyer et al., 1993b). Since 1993, Meyer et al. started to use a series of oligonucleotides hybridization probes such as $(CA)_8$, $(CT)_8$, $(CAC)_5$, $(GTG)_5$, $(GACA)_4$, $(GATA)_4$, and the

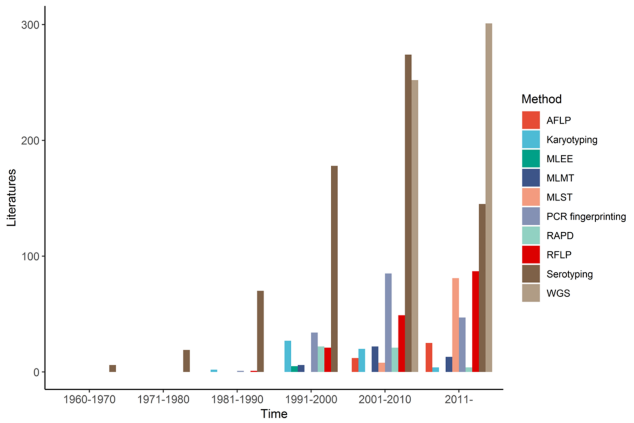

FIGURE 1 | Number of publications using different molecular typing methods for studying the human pathogenic *Cryptococcus* from 1960 to 2021, by decade.

phage M13 core sequence (5'-GAGGGTGGXGGXTCT-3') as primers for PCR fingerprinting for strain typing and for molecular epidemiological analyses of fungal pathogens, including the human pathogenic *Cryptococcus* (Meyer et al., 1993a; Meyer et al., 1993b; Meyer and Mitchell, 1995). Because of the long primers and more stringent PCR amplification conditions, DNA fingerprints produced by PCR using primers such as $(GTG)_5$, $(GACA)_4$, or the M13 core sequence were much more reproducible than RAPD. Indeed, PCR fingerprinting reliably and successfully differentiated several lineages within CNSC and CGSC; with many isolates showing unique PCR fingerprint patterns (Meyer et al., 1993b). Since then, primers $(GTG)_5$, $(GACA)_4$, and the M13 core sequence have been widely recognized as standard PCR fingerprinting primers for studies on CNSC and CGSC (Meyer et al., 1993b; Meyer and Mitchell, 1995; Cogliati et al., 2000; Meyer et al., 2003). For example, in 1999, Meyer et al. used PCR fingerprinting to genotype 356 clinical isolates of CNSC and CGSC from around the globe (Meyer et al., 1999). They clustered these isolates into eight major molecular types, namely VNI (Serotype A), VNII (Serotype A), VNIII (Serotype AD), and VNIV (Serotype D) in CNSC; VGI, VGII, VGIII, and VGIV in CGSC (Meyer et al., 1999). These molecular types were later used for higher level taxonomy. Additionally, a unique molecular type (VNB) of CNSC, a new lineage of CGSC (VGV), and several hybrids between CNSC and CGSC have been found in recent years, all of which were at least partly based on data from PCR fingerprinting (Bovers et al., 2008a; Sidrim et al., 2010; Farrer et al., 2019).

Indeed, PCR fingerprinting using the M13 core sequence as a primer has become a major strain typing tool in the ongoing molecular epidemiological surveys of CNSC and CGSC. Although PCR fingerprinting requires high-quality DNA template and highly standardized conditions to ensure comparability among experiments and labs (Meyer et al., 1999), it combines the specificity of classical DNA hybridization fingerprinting with the speed and simplicity of the PCR reaction (Meyer et al., 1999; Kidd et al., 2004). Furthermore, PCR fingerprinting is of high reproducibility due to the high degree of homology between the primers and the template DNA, which allows the use of high annealing temperatures during the PCR amplification (Meyer and Mitchell, 1995). It is likely that PCR fingerprinting using the M13 core sequence as primer will remain a valuable technique in molecular epidemiological surveys of CNSC and CGSC.

AMPLIFIED FRAGMENT LENGTH POLYMORPHISM

Amplified fragment length polymorphism (AFLP) is a powerful genotyping technique that can discriminate closely related strains and individuals in many groups of organisms, including microorganisms (Vos et al., 1995). This technique can quickly generate a large number of DNA fragments for any organism, with high degrees of reproducibility and discriminatory power (Janssen et al., 1996; Savelkoul et al., 1999; Paun and Schönswetter, 2012). Briefly, AFLP is a PCR-based molecular technique that uses selective amplification of a subset of restriction enzyme digested DNA fragments from any source to generate and compare unique electrophoretic patterns among genomes (Sheeja et al., 2021). Thus, AFLP requires limited amounts of materials but combines the advantages of both RFLP and RAPD in terms of reproducibility and resolution (Janssen et al., 1996; Savelkoul et al., 1999; Paun and Schönswetter, 2012). In addition, it does not require any prior genome information (Sheeja et al., 2021). Overall, despites its higher labor intensity and higher cost than other methods such as RFLP, RAPD and PCR-fingerprinting, the AFLP technique is generally more discriminatory than other molecular typing methods (Savelkoul et al., 1999; Paun and Schönswetter, 2012; Grover and Sharma, 2016). Moreover, several previous studies suggested that the AFLP technique could be used for linkage mapping and for locating genomic regions within the CNSC and CGSC genomes that are related to pathogen virulence, drug susceptibility, and human immune responses (Wiesner et al., 2012; Thompson et al., 2014). Since the 1990s, Boekhout et al. and Hagen et al. have also reported the use of AFLP markers in studies on the taxonomy, molecular epidemiology, genetic diversity, phylogenetic analysis, etc. of the human pathogenic *Cryptococcus* (Kidd et al., 2004; Hagen et al., 2010; Day et al., 2011; Pakshir et al., 2018; van de Wiele et al., 2020).

Similar to PCR fingerprinting, the AFLP technique has been commonly used for epidemiological studies on CNSC and CGSC. Compared to PCR fingerprinting, AFLP has more discriminating power in epidemiological studies of CNSC and CGSC (Ngamskulrungroj et al., 2009; Hagen et al., 2015). For example, a total of 11 AFLP major types have been identified within the human pathogenic Cryptococcus (Hagen et al., 2015), including AFLP1 (CNSC, Serotype A, VNI) (Franzot et al., 1999), AFLP1A (CNSC, Serotype A, VNII/VNB) (Franzot et al., 1999), AFLP1B (CNSC, Serotype A, VNII), AFLP2 (CNSC, Serotype D, VNIV), AFLP3 (CNSC, Serotype AD, VNIII), AFLP4 (CGSC, VGI), AFLP5 (CGSC, VGIII), AFLP6 (CGSC, VGII), AFLP7

(CGSC, VGIV), AFLP8 (CNSC VNIV × CGSC VGI, hybrid) (Bovers et al., 2006), AFLP9 (CNSC VNI × CGSC VGI, hybrid) (Bovers et al., 2008b), AFLP10 (CGSC, VGIV/VGIIIc) (Springer et al., 2014; Trilles et al., 2014), AFLP11 (CNSC VNI × CGSC VGII, hybrid) (Aminnejad et al., 2012). Furthermore, strains' AFLP patterns have shown overall concordance with results from other strain typing methods such as serotyping, RAPD and PCR fingerprinting among isolates of CNSC and CGSC. For instance, AFLP markers clustered isolates of CNSC and CGSC into the same eight major molecular types as PCR fingerprinting, namely AFLP1 (=VNI), AFLP1A/AFLP1B (=VNII), AFLP2 (=VNIII), and AFLP3 (=VNIV) in CNSC; AFLP4 (=VGI), AFLP5 (=VGIII), AFLP6 (=VGII), and AFLP7 (=VGIV) in CGSC (Meyer et al., 1999; Bovers et al., 2008a; Hagen et al., 2015). AFLP markers contributed to the identification of rare but unique hybrids and to our overall understanding of the diversity and distribution of the human pathogenic *Cryptococcus*. One drawback of AFLP is that DNA banding patterns on gels can be difficult to compare between results from different labs and that fragments of the same size may not be homologous, i.e., containing the same DNA sequences. A summary comparison of results between AFLP with other strain typing methods regarding the major molecular type identifications of the human pathogenic *Cryptococcus* is shown in **Table 2**.

MULTILOCUS MICROSATELLITE TYPING

Multilocus microsatellite typing (MLMT) is a common genotyping method for population genetics and molecular ecology studies of many eukaryotic species, including fungi. MLMT has been used to analyze CNSC and CGSC (De Valk et al., 2007; Karaoglu et al., 2008; Illnait-Zaragozi et al., 2010; Rudramurthy et al., 2011; Pan et al., 2012). Microsatellites (also referred to as short tandem repeats, STRs) are genomic sequences consisting of tandemly repeated short motifs up to 6 nucleotides, which are abundantly present in the genomes of most eukaryotes, including eukaryotic microorganisms. Due to the higher mutation rate of the short repeats during DNA replication (due to strand slippage) than base substitutions, microsatellite markers are especially powerful for analyzing recently expanding populations of organisms (Van Belkum et al., 1998). Microsatellite analysis is usually performed in two steps: (i) amplification of STR loci by PCR and (ii) detection and sizing of amplification products followed by the assignment of repeat numbers. Assignment of repeat numbers is established by comparing the relative electrophoretic mobility of the fragments to the mobility of reference fragments with established repeat numbers (De Valk et al., 2007).

The application of MLMT to analyze CNSC and CGSC samples has resulted in the identification of a large number of genotypes within both CNSC and CGSC (Garcia-Hermoso et al., 2010; Prakash et al., 2020). The power of MLMT in strain discrimination was also shown in a recently emerged human fungal pathogen *Candida auris* where results based on MLMT markers showed similar discrimination power as that based on single nucleotide polymorphisms at the whole genome level (De Groot et al., 2020). Different from RAPD, PCR-finger printing and AFLP, MLMT marker polymorphisms can be directly compared among labs. For example, an MLMT analysis based on 426 Asian clinical CNSC isolates showed a different distribution of genotypes of CNSC isolates from various countries in Asia. The study also identified a correlation between microsatellite genotypes with the original source of strains and their susceptibilities to 5-flucytosine (Pan et al., 2012). Another MLMT analysis of 523 CNSC isolates collected from India showed that environmental isolates were genetically more diverse than clinical isolates (Prakash et al., 2020). However, an MLMT study based on 89 CNSC isolates from Brazil found no differences in antifungal susceptibility and capsule size between major environmental and clinical MLMT types (Zhu et al., 2010). In general, MLMT provides cost-effective genotyping with fast turn-around times and on an individual locus basis, is generally much more discriminatory than MLST. However, there is no global public database for CNSC and CGSC based on MLMT markers. The establishment of such a

TABLE 2 | Summarized classification of CNSC and CGSC based on different molecular markers.

Species complex	Variety	Serotype	PCR finger-printing	AFLP	IGS1	ITS	Proposed species name	Reference strain	Accession ID of reference assembly
CNSC	var. *grubii*	A	VNI	1	1a/1b	1	*C. neoformans*	H99	ASM301198v1
		A	VNB	1A	1a	1	*C. neoformans*	Bt88	BROAD_CneoA_Bt88_1
		A	VNII	1B	1c	1	*C. neoformans*	PMHc1023.ENR	BROAD_CneoA_PMHc1023.Enr_1
	var. *neoformans*	D	VNIV	2	2a/2b/2c	2	*C. deneoformans*	JEC21	ASM9104v1
	AD hybrid	AD	VNIII	3			*C. neoformans* × *C. deneoformans hybrid*		
CGSC		B/C	VGI	4A	4c	7	*C. gattii*	WM276	ASM18594v1
		B/C	VGI	4B	4a/4b	3/7	*C. gattii*	Ru294	Cryp_gatt_Ru294_V1
		B/C	VGII	6	3	4	*C. deuterogattii*	R265	R265.1
		B/C	VGIII	5A/5C	5	5	*C. bacillisporus*	CA1280	Cryp_gatt_CA1280_V1
		B	VGIII	5B	5	5	*C. bacillisporus*	CA1873	Cryp_gatt_CA1873_V1
		B/C	VGIV	7	6	6	*C. tetragattii*	IND107	Cryp_gatt_IND107_V2
		B	VGV					MF34	Cryp_gatt_MF34

centralized database would increase its adoption by more researchers and consequently increase our understanding of the recent evolution, gene flow, and epidemiology of the human pathogenic *Cryptococcus*.

SINGLE LOCUS AND MULTILOCUS SEQUENCE TYPING

Revolutions in DNA sequencing techniques have taken the discovery and application of molecular markers to high-throughput and ultrahigh-throughput levels for a variety of studies (Grover and Sharma, 2016). Sequencing single DNA fragments such as the internal transcribed spacer (ITS) region and the intergenic spacer region (IGS) of the ribosomal RNA gene cluster have been broadly used to identify fungal species and strains. For the human pathogenic *Cryptococcus*, ITS, IGS, the *RPR8* gene, and the mitochondrial cytochrome b gene have been commonly used for species and lineage identifications (Diaz et al., 2000; Butler and Poulter, 2005; Diaz et al., 2005). Indeed, ITS region sequence is the universal DNA barcode for fungal species identification, including in many instances for investigating intra-specific variations among strains from different geographic regions and ecological niches (Schoch et al., 2012). Compared to the limited variations in ITS sequences among molecular types within CNSC (Katsu et al., 2004), IGS sequences are more variable with variations represented by nucleotide base substitutions and the presence of long insertions/deletions (indels) (Diaz et al., 2000; Diaz et al., 2005). Some of the differences between IGS and ITS with regard to variations in CNSC are shown in **Table 2**. The pros and cons of using single locus sequences for species and strain identifications have been extensively discussed (Xu, 2016; Xu, 2020).

The limited variation at an individual locus such as ITS and IGS within some species can be overcome by sequencing multiple loci located in different parts of the genome. Indeed, MLST is a commonly used method for genotyping strains of many common human microbial pathogens. With the use of sequence information from multiple loci, MLST can provide high discriminatory power and allow reproducible results to be shared among laboratories. The first MLST study of the human pathogenic *Cryptococcus* was published in 2000 (Xu et al., 2000b). Since then, MLST has been applied to many studies on the epidemiology of CNSC and CGSC (Sugita et al., 2001; Taylor and Fisher, 2003; Fraser et al., 2005; Litvintseva et al., 2006). For example, both single locus and multilocus sequence typing of serotype AD strains identified that these strains were recent hybrids and revealed evidence for sexual reproduction in natural populations of both the VNI (serotype A) and VNIV (serotype D) lineages within CNSC (Xu et al., 2002; Xu and Mitchell, 2003).

Early MLST studies of the human pathogenic *Cryptococcus* often sequenced different loci and resulted in inconsistent numbers and nomenclatures of those sub-groups (Sugita et al., 2001; Bovers et al., 2008b). Consequently, there were difficulties in comparing epidemiological results among studies. In 2009, the International Society for Human and Animal Mycology (ISHAM) *Cryptococcus* Working Group agreed upon MLST using seven loci: *CAP59*, *GPD1*, *LAC1*, *PLB1*, *SOD1*, *URA5* and *IGS1* region as the standardized genotyping approach (Meyer et al., 2009). The application of a standardized set of loci for sequence typing of strains led to an expanding dataset and the establishment of a reference database from which future studies could continuously build on (https://mlst.mycologylab.org/). MLST analyses based on the shared DNA sequences provided a comprehensive view on the global distribution of genotypes (Litvintseva et al., 2006; Bovers et al., 2008b; Ngamskulrungroj et al., 2009), including unique clades and sub-clades within CNSC and CGSC in specific regions in the world (Chowdhary et al., 2011; Beale et al., 2015). For example, MLST analysis detected higher genetic diversity in the South African *C. neoformans* var. *grubii* isolates than those from other geographic regions, which led to the 'Out of Africa' hypothesis for the origin and dispersal of *C. neoformans* var. *grubii* around the globe (Litvintseva et al., 2011; Simwami et al., 2011; Litvintseva and Mitchell, 2012). In addition, MLST analyses identified that the East Asian clinical population of *C. neoformans* var. *grubii* was highly clonal and dominated by one sequence type ST5 and its closely related sequence types (Simwami et al., 2011; Khayhan et al., 2013; Dou et al., 2015; Fan et al., 2016; Day et al., 2017; Chen et al., 2018; Hong et al., 2019). For CGSC, comparisons of genetic diversity of isolates from different locations based on MLST analyses indicated northern Brazil was likely the source for the global expansion of the VGII lineage, including for strains causing the outbreak in the Pacific Northwest of North America (Hagen et al., 2013; Souto et al., 2016), and revealing a possible introduction of Australian VGII into Vancouver Island in western Canada (Fraser et al., 2005; Byrnes et al., 2009; Byrnes et al., 2010). Moving forward, MLST will continue to be a major strain typing method for epidemiological studies of the human pathogenic *Cryptococcus*.

MALDI-TOF MS

Aside from the DNA fragment-based sequencing and targeted protein-based molecular strain typing methods described above, there is another common molecular method for identifying fungal species called matrix-assisted laser desorption/ionization time of flight mass spectrometry (MALDI-TOF MS). This method is based on species-specific spectra of the masses of peptides and proteins in colonies of microbial cells. It was first developed for bacterial identification (Claydon et al., 1996; Krishnamurthy and Ross, 1996) and subsequently extended to fungal identification (Li et al., 2000; Van Veen et al., 2010; Alshawa et al., 2012; De Carolis et al., 2012). MALDI-TOF MS has become a rapid, easy-to-use, and inexpensive method for identifying clinically important microorganisms (Claydon et al., 1996; Krishnamurthy and Ross, 1996; Seng et al., 2009). Indeed, this technology has been used to identify hundreds of CNSC and CGSC strains isolated from both humans and animals (Firacative

et al., 2012; Posteraro et al., 2012; Jin et al., 2020; Zvezdanova et al., 2020; Florek et al., 2021). In a recent study, an expanded database allowed the MALDI-TOF MS technology to separate the two major lineages within CNSC, VNI (*C. neoformans*) and VNIV (*C. deneoformans*), including identifying most of their hybrids (VNIII) when the authors used a hierarchical clustering approach and focused on five selected biomarkers in the dataset (Zvezdanova et al., 2020). However, the reproducibility of MALDI_TOF MS for either lineage or strain identifications have not been critically evaluated by different labs for the same set of strains.

In addition to (potentially) allow direct identification of pathogens based on protein profiles, MALDI-TOF MS holds great promise for diagnosing and genotyping pathogenic fungal species based on other cellular molecules. For example, due to their essential roles in cell integrity, growth, and reproduction, lipids such as membrane phospholipids are found in all cellular organisms, including strains of CNSC and CGSC. However, different fungal species and strains can differ in their lipid profiles, thus making lipids a promising group of molecules to potentially serve as biomarkers for taxonomic and metabolic characterization of fungal pathogens (Stübiger et al., 2016). For example, because fungal membrane lipids such as ergosterol are targets of several commonly used antifungal drugs, lipid analysis can potentially help identify medically important features such as antifungal resistance among clinical strains, thus benefiting patient treatments. Overall, due to its simplicity, high efficiency and increasing availability, the MALDI-TOF MS technology can be a valuable tool for molecular lineage identification within CNSC and CGSC, and thus representing a potential future alternative for screening drug susceptibilities among strains.

WHOLE-GENOME SEQUENCE TYPING (WGST)

With rapidly falling cost, whole genome sequencing typing (WGST) has been applied for epidemiological studies of a variety of organisms, including for CNSC and CGSC. Compared to epidemiological studies of CNSC and CGSC utilizing other strain typing methods, whole-genome sequencing is capable of capturing the complete genetic variation, including single nucleotide polymorphisms, insertions and deletion, gene copy number variations, and genome structural rearrangements. However, to reveal all of the above genetic variations, very high sequence coverages employing sequencing platforms capable of generating both short and long sequence reads are needed. At present, most epidemiological surveys of microbial pathogens using the whole-genome sequencing approach rely on the Illumina MiSeq or HiSeq platforms to obtain short-read DNA sequences. Such short reads at greater than 50X coverage are generally sufficient for robust identification of SNPs for inferences of strain relationships and epidemiological patterns (Beale et al., 2015; Cuomo et al., 2018).

However, for most genomic epidemiological comparisons to be informative, well-annotated reference genome assemblies are generally needed. Fortunately, within the human pathogenic *Cryptococcus*, reference genomes representing *C. neoformans* var. *grubii* (VNI, VNII, VNB) and var. *neoformans* (VNIV), and each of the five molecular types of CGSC (VGI, VGII, VGIII, VGIV and VGV) are available (Fraser et al., 2005; Galagan et al., 2005; Loftus et al., 2005; D'souza et al., 2011; Janbon et al., 2014; Farrer et al., 2015; Rhodes et al., 2017a). Indeed, to date, three *C. neoformans* var. *neoformans* genomes, 58 C. *neoformans* var. *grubii* genomes and 7 CGSC genomes have been assembled and annotated, providing nearly complete catalogs of genes within both CNSC and CGSC (**Table 2**). These genome assemblies provide genomic resources for the community and enable a wide array of downstream studies. Genome sequence comparisons between different molecular types of CGSC revealed a sequence divergence of >3% among the major lineages and molecular types (D'souza et al., 2011; Farrer et al., 2016). In addition to the average nucleotide identity in among the genomes, there were several other notable findings. For example, gene structure comparisons revealed that genes of CNSC have more introns with more alternative splicing (Loftus et al., 2005; Janbon et al., 2014) than those of CGSC (Farrer et al., 2016). In addition, strains of the VGII clade responsible for the cryptococcal outbreak on Vancouver Island seemed to have lost the genes involved in RNA interference (Loftus et al., 2005; Janbon et al., 2014). Furthermore, these well-annotated reference assemblies have enabled the construction of functional genomic resources, such as a deletion collection of *C. neoformans* var. *grubii* genes in the H99 strain background (Liu et al., 2008). Such resources make it easier for the community to studying the relationships between specific genes and phenotypic differences between strains and populations.

In addition to revealing the similarities and differences among natural strains from within and between different lineages, whole genome sequencing can help identify microevolution of infecting strains within patients by comparing cryptococcal genomes at initial presentation and later such as during relapse of infection (Ormerod et al., 2013; Chen et al., 2017; Rhodes et al., 2017a). For example, in one study, the deletion of a transcriptional regulator and changes in the copy number of genes on chromosome 12 were found between a pair of initial and relapse isolates, with such changes correlated with marked virulence-related phenotypic differences between the strains (Ormerod et al., 2013). Similarly, based on genome sequencing of 38 initial and relapse isolates from 18 patients, specific mutations were found in genes involved in growth at 39°C, stress response, and capsule production (Chen et al., 2017). Indeed, microevolution studies have revealed that clinical isolates are capable of rapid adaptation through hypermutation, frequently due to mutations in mismatch repair gene *MSH2* in CGSC (Billmyre et al., 2014; Billmyre et al., 2017) and CNSC (Boyce et al., 2017; Rhodes et al., 2017a).

With the increasing availability of whole genome sequencing, both CNSC and CGSC have now had hundreds of individual isolates sequenced, providing fine-scale insights into their evolution and diversification (Desjardins et al., 2017; Rhodes et al., 2017b; Vanhove et al., 2017; Ashton et al., 2019). Population genomic methods, such as principal component

analysis (PCA), admixture analysis and phylogenetic analysis based on whole genome sequencing, are playing an increasingly important role in clustering cryptococcal isolates and tracing the origin of individual strains and/or groups of strains (Billmyre et al., 2014; Engelthaler et al., 2014; Desjardins et al., 2017). In combination with other methods, population genomics can help identify genes related to the evolution of virulence and pathogenicity, including putative novel drug targets (Farrer et al., 2015; Desjardins et al., 2017).

For CGSC, genome-level phylogenetic studies have suggested VGII strains, the main strains responsible for the cryptococcal outbreak in the Pacific Northwest of North America, can be divided into three main subgroups: VGIIa, VGIIb and VGIIc. Furthermore, the analyses provided evidence that the main outbreak lineage might have an origin in South America (Billmyre et al., 2014; Engelthaler et al., 2014). In addition, whole-genome comparisons recently revealed a new lineage of CGSC isolates (VGV) in Zambia (Farrer et al., 2019). For CNSC, a recent population genomic study found evidence for two sub-lineages within VNB, VNBI and VNBII. Such a finding helped reveal phenotypic differences between these two subgroups (Desjardins et al., 2017). Though there were some differences, results from mitochondrial exon sequence analyses were largely consistent with the existence of two subgroups VNBI and VNBII within VNB, as inferred based on nuclear genome SNPs (Wang and Xu, 2020). However, the distributions of mitochondrial introns were quite mixed within CNSC, suggesting their frequent gains and losses during evolution (Wang and Xu, 2020). Several population genomic studies have found a highly clonal cluster of VNI isolates capable of infecting HIV-negative patients in east Asia (Day et al., 2017; Ashton et al., 2019). Multidrug transporters, aconitases (iron-sulfur proteins), capsule genes, heat-shock proteins and protein kinases were found to be under positive selection in multiple sub-lineages of CGSC, which suggested that these genes might play an important role in the adaptation of CGSC isolates to host environments (Farrer et al., 2015; Farrer et al., 2016). Finally, the large number of publicly available genomes provides a fertile ground for genome-wide association studies (GWAS) between genetic variants and phenotypic differences among strains. A recent GWAS study found that the loss-of-function mutation in the transcription factor *BZP4* was linked to melanization capacity among VNB isolates (Desjardins et al., 2017).

Overall, epidemiological studies utilizing whole genome sequencing have significantly improved our understanding of genetic divergence between lineages, gene flows across geographic regions, and gene gains and losses during the evolution of different lineages within both CNSC and CGSC. However, as mentioned above, most currently available genome sequences of CNSC and CGSC strains were generated using the short-read Illumina platforms, the quality and utility of which could be affected by sequencing depth, library preparation chemistry, and sequencing bias (Rhodes et al., 2014). Previous studies have shown that most cryptococcal assemblies generated from the Illumina platform contain many sequencing gaps, making it difficult to infer chromosomal structural polymorphisms in these genomes (Day et al., 2017; Rhodes et al., 2017b). In the future, the incorporation of long reads generated by Pacific Biosciences or Oxford Nanopore Technologies will allow more complete genome assemblies and provide robust foundations for other types of genomic comparisons such as chromosomal reversions and translocations (Van Der Straaten, 2015; Cuomo et al., 2018).

CONCLUSIONS AND FUTURE DIRECTIONS

Our literature review above showed that many molecular techniques have been successfully used for *Cryptococcus* epidemiological studies. Over the past 30 years, we have seen a rapid development of strain typing methods to differentiate species and strains of this group of important human fungal pathogens (**Figure 1**). These studies have helped resolve species boundaries, identify hybrids, reveal both local and global genetic diversities and gene flows, and pinpoint specific mutations accumulated during the microevolution of strains within patients. As shown above, all techniques have helped improve our understanding of cryptococcal epidemiology and each technique has its advantages and limitations (**Table 1**). For example, though relatively crude, PCR fingerprinting and AFLP analysis established the most widely used taxonomy and nomenclature system for CNSC and CGSC. Though there are still controversies (Hagen et al., 2015; Hagen et al., 2017; Kwon-Chung et al., 2017), the applications of more precise molecular typing methods, especially WGST have moved the taxonomy and nomenclature system to become increasingly clear for the human pathogenic *Cryptococcus*. Resolution of the controversies in these organisms could potentially serve as a model for other fungal species (Xu, 2020). For cryptococcal epidemiological studies, we expect the increasing use of MLST, MLMT, MALDI-TOF MS, and WGST in the future with different methods serving slightly different but complementary purposes.

AUTHOR CONTRIBUTIONS

Writing—original draft preparation: NH, MC, and JX. Writing—review and editing: JX. All authors contributed to the article and approved the submitted version.

FUNDING

This review was funded by National Natural Science Foundation of China (grant numbers 81201269 and 81720108026), Innovation Team Foundation of Jiangsu Province (grant number CXTDA2017038), National Medicine Foundation of China (grant number CLB20J022), Natural Science and Engineering Research Council of Canada (grant number RGPIN-2020-05732), and McMaster University (Global Science Initiative-2020-03).

REFERENCES

Alshawa K., Beretti J. L., Lacroix C., Feuilhade M., Dauphin B., Quesne G., et al. (2012). Successful Identification of Clinical Dermatophyte and Neoscytalidium Species by Matrix-Assisted Laser Desorption Ionization-Time of Flight Mass Spectrometry. *J. Clin. Microbiol.* 50, 2277–2281. doi: 10.1128/jcm.06634-11

Aminnejad M., Diaz M., Arabatzis M., Castañeda E., Lazera M., Velegraki A., et al. (2012). Identification of Novel Hybrids Between *Cryptococcus Neoformans* Var. *Grubii* VNI and *Cryptococcus Gattii* VGII. *Mycopathologia* 173, 337–346. doi: 10.1007/s11046-011-9491-x

Ashton P. M., Thanh L. T., Trieu P. H., Van Anh D., Trinh N. M., Beardsley J., et al. (2019). Three Phylogenetic Groups Have Driven the Recent Population Expansion of *Cryptococcus Neoformans*. *Nat. Commun.* 10, 2035. doi: 10.1038/s41467-019-10092-5

Beale M. A., Sabiiti W., Robertson E. J., Fuentes-Cabrejo K. M., O'hanlon S. J., Jarvis J. N., et al. (2015). Genotypic Diversity is Associated With Clinical Outcome and Phenotype in Cryptococcal Meningitis Across Southern Africa. *PloS Negl. Trop. Dis.* 9, e0003847. doi: 10.1371/journal.pntd.0003847

Belay T., Cherniak R., O'neill E. B., and Kozel T. R. (1996). Serotyping of *Cryptococcus Neoformans* by Dot Enzyme Assay. *J. Clin. Microbiol.* 34, 466–470. doi: 10.1128/jcm.34.2.466-470.1996

Bertout S., Renaud F., Swinne D., Mallié M., and Bastide J. M. (1999). Genetic Multilocus Studies of Different Strains of *Cryptococcus Neoformans*: Taxonomy and Genetic Structure. *J. Clin. Microbiol.* 37, 715–720. doi: 10.1128/jcm.37.3.715-720.1999

Billmyre R. B., Clancey S. A., and Heitman J. (2017). Natural Mismatch Repair Mutations Mediate Phenotypic Diversity and Drug Resistance in Cryptococcus Deuterogattii. *Elife* 6, e28802. doi: 10.7554/eLife.28802

Billmyre R. B., Croll D., Li W., Mieczkowski P., Carter D. A., Cuomo C. A., et al. (2014). Highly Recombinant VGII *Cryptococcus Gattii* Population Develops Clonal Outbreak Clusters Through Both Sexual Macroevolution and Asexual Microevolution. *mBio* 5, e01494–e01414. doi: 10.1128/mBio.01494-14

Boekhout T., Renting M., Scheffers W. A., and Bosboom R. (1993). The Use of Karyotyping in the Systematics of Yeasts. *Antonie Van Leeuwenhoek* 63, 157–163. doi: 10.1007/bf00872390

Boekhout T., Van Belkum A., Leenders A. C., Verbrugh H. A., Mukamurangwa P., Swinne D., et al. (1997). Molecular Typing of *Cryptococcus Neoformans*: Taxonomic and Epidemiological Aspects. *Int. J. Syst. Bacteriol.* 47, 432–442. doi: 10.1099/00207713-47-2-432

Botstein D., White R. L., Skolnick M., and Davis R. W. (1980). Construction of a Genetic Linkage Map in Man Using Restriction Fragment Length Polymorphisms. *Am. J. Hum. Genet.* 32, 314–331.

Bovers M., Hagen F., and Boekhout T. (2008a). Diversity of the *Cryptococcus neoformans-Cryptococcus Gattii* Species Complex. *Rev. Iberoam. Micol.* 25, S4–12. doi: 10.1016/s1130-1406(08)70019-6

Bovers M., Hagen F., Kuramae E. E., and Boekhout T. (2008b). Six Monophyletic Lineages Identified Within *Cryptococcus Neoformans* and *Cryptococcus Gattii* by Multi-Locus Sequence Typing. *Fungal Genet. Biol.* 45, 400–421. doi: 10.1016/j.fgb.2007.12.004

Bovers M., Hagen F., Kuramae E. E., Diaz M. R., Spanjaard L., Dromer F., et al. (2006). Unique Hybrids Between the Fungal Pathogens *Cryptococcus Neoformans* and *Cryptococcus Gattii*. *FEMS Yeast Res.* 6, 599–607. doi: 10.1111/j.1567-1364.2006.00082.x

Boyce K. J., Wang Y., Verma S., Shakya V. P. S., Xue C., and Idnurm A. (2017). Mismatch Repair of DNA Replication Errors Contributes to Microevolution in the Pathogenic Fungus *Cryptococcus Neoformans*. *mBio* 8, e28802. doi: 10.1128/mBio.00595-17

Brandt M. E., Hutwagner L. C., Kuykendall R. J., and Pinner R. W. (1995). Comparison of Multilocus Enzyme Electrophoresis and Random Amplified Polymorphic DNA Analysis for Molecular Subtyping of *Cryptococcus Neoformans*. The Cryplococcal Disease Active Surveillance Group. *J. Clin. Microbiol.* 33, 1890–1895. doi: 10.1128/jcm.33.7.1890-1895.1995

Butler M. I., and Poulter R. T. (2005). The PRP8 Inteins in Cryptococcus are a Source of Phylogenetic and Epidemiological Information. *Fungal Genet. Biol.* 42, 452–463. doi: 10.1016/j.fgb.2005.01.011

Byrnes E. J.,. 3., Bildfell R. J., Frank S. A., Mitchell T. G., Marr K. A., and Heitman J. (2009). Molecular Evidence That the Range of the Vancouver Island Outbreak of *Cryptococcus Gattii* Infection has Expanded Into the Pacific Northwest in the United States. *J. Infect. Dis.* 199, 1081–1086. doi: 10.1086/597306

Byrnes E. J.,. 3., Li W., Lewit Y., Ma H., Voelz K., Ren P., et al. (2010). Emergence and Pathogenicity of Highly Virulent *Cryptococcus Gattii* Genotypes in the Northwest United States. *PloS Pathog.* 6, e1000850. doi: 10.1371/journal.ppat.1000850

Chen S. C., Brownlee A. G., Sorrell T. C., Ruma P., and Nimmo G. (1996). Identification by Random Amplification of Polymorphic DNA of a Common Molecular Type of *Cryptococcus Neoformans* Var. Neoformans in Patients With AIDS or Other Immunosuppressive Conditions. *J. Infect. Dis.* 173, 754–758. doi: 10.1093/infdis/173.3.754

Chen S. C., Currie B. J., Campbell H. M., Fisher D. A., Pfeiffer T. J., Ellis D. H., et al. (1997). *Cryptococcus Neoformans* Var. Gattii Infection in Northern Australia: Existence of an Environmental Source Other Than Known Host Eucalypts. *Trans. R. Soc Trop. Med. Hyg.* 91, 547–550. doi: 10.1016/s0035-9203(97)90021-3

Chen Y., Farrer R. A., Giamberardino C., Sakthikumar S., Jones A., Yang T., et al. (2017). Microevolution of Serial Clinical Isolates of *Cryptococcus Neoformans* Var. *Grubii* and C. Gattii. *mBio* 8, e00166-17. doi: 10.1128/mBio.00166-17

Chen S. C., Meyer W., and Sorrell T. C. (2014). *Cryptococcus Gattii* Infections. *Clin. Microbiol. Rev.* 27, 980–1024. doi: 10.1128/cmr.00126-13

Chen Y. H., Yu F., Bian Z. Y., Hong J. M., Zhang N., Zhong Q. S., et al. (2018). Multilocus Sequence Typing Reveals Both Shared and Unique Genotypes of *Cryptococcus Neoformans* in Jiangxi Province, China. *Sci. Rep.* 8, 1495. doi: 10.1038/s41598-018-20054-4

Cherniak R., and Sundstrom J. B. (1994). Polysaccharide Antigens of the Capsule of *Cryptococcus Neoformans*. *Infect. Immun.* 62, 1507–1512. doi: 10.1128/iai.62.5.1507-1512.1994

Chowdhary A., Hiremath S. S., Sun S., Kowshik T., Randhawa H. S., and Xu J. (2011). Genetic Differentiation, Recombination and Clonal Expansion in Environmental Populations of *Cryptococcus Gattii* in India. *Environ. Microbiol.* 13, 1875–1888. doi: 10.1111/j.1462-2920.2011.02510.x

Claydon M. A., Davey S. N., Edwards-Jones V., and Gordon D. B. (1996). The Rapid Identification of Intact Microorganisms Using Mass Spectrometry. *Nat. Biotechnol.* 14, 1584–1586. doi: 10.1038/nbt1196-1584

Cogliati M., Allaria M., Tortorano A. M., and Viviani M. A. (2000). Genotyping *Cryptococcus Neoformans* Var. Neoformans With Specific Primers Designed From PCR-fingerprinting Bands Sequenced Using a Modified PCR-based Strategy. *Med. Mycol.* 38, 97–103. doi: 10.1080/mmy.38.2.97.103

Cuomo C. A., Rhodes J., and Desjardins C. A. (2018). Advances in Cryptococcus Genomics: Insights Into the Evolution of Pathogenesis. *Mem. Inst. Oswaldo. Cruz.* 113, e170473. doi: 10.1590/0074-02760170473

Currie B. P., Freundlich L. F., and Casadevall A. (1994). Restriction Fragment Length Polymorphism Analysis of *Cryptococcus Neoformans* Isolates From Environmental (Pigeon Excreta) and Clinical Sources in New York City. *J. Clin. Microbiol.* 32, 1188–1192. doi: 10.1128/jcm.32.5.1188-1192.1994

Day J. N., Hoang T. N., Duong A. V., Hong C. T., Diep P. T., Campbell J. I., et al. (2011). Most Cases of Cryptococcal Meningitis in HIV-uninfected Patients in Vietnam are Due to a Distinct Amplified Fragment Length Polymorphism-Defined Cluster of *Cryptococcus Neoformans* Var. *Grubii* VN1. *J. Clin. Microbiol.* 49, 658–664. doi: 10.1128/jcm.01985-10

Day J. N., Qihui S., Thanh L. T., Trieu P. H., Van A. D., Thu N. H., et al. (2017). Comparative Genomics of *Cryptococcus Neoformans* Var. *Grubii* Associated With Meningitis in HIV Infected and Uninfected Patients in Vietnam. *PloS Negl. Trop. Dis.* 11, e0005628. doi: 10.1371/journal.pntd.0005628

De Carolis E., Posteraro B., Lass-Flörl C., Vella A., Florio A. R., Torelli R., et al. (2012). Species Identification of Aspergillus, Fusarium and Mucorales With Direct Surface Analysis by Matrix-Assisted Laser Desorption Ionization Time-of-Flight Mass Spectrometry. *Clin. Microbiol. Infect.* 18, 475–484. doi: 10.1111/j.1469-0691.2011.03599.x

De Groot T., Puts Y., Berrio I., Chowdhary A., and Meis J. F. (2020). Development of *Candida Auris* Short Tandem Repeat Typing and Its Application to a Global Collection of Isolates. *mBio* 11, e02971-19. doi: 10.1128/mBio.02971-19

Desjardins C. A., Giamberardino C., Sykes S. M., Yu C. H., Tenor J. L., Chen Y., et al. (2017). Population Genomics and the Evolution of Virulence in the Fungal Pathogen *Cryptococcus Neoformans*. *Genome Res.* 27, 1207–1219. doi: 10.1101/gr.218727.116

De Valk H. A., Meis J. F., and Klaassen C. H. (2007). Microsatellite Based Typing of *Aspergillus Fumigatus*: Strengths, Pitfalls and Solutions. *J. Microbiol. Methods* 69, 268–272. doi: 10.1016/j.mimet.2007.01.009

Diaz M. R., Boekhout T., Kiesling T., and Fell J. W. (2005). Comparative Analysis of the Intergenic Spacer Regions and Population Structure of the Species Complex of the Pathogenic Yeast *Cryptococcus Neoformans*. *FEMS Yeast Res.* 5, 1129–1140. doi: 10.1016/j.femsyr.2005.05.005

Diaz M. R., Boekhout T., Theelen B., and Fell J. W. (2000). Molecular Sequence Analyses of the Intergenic Spacer (IGS) Associated With rDNA of the Two Varieties of the Pathogenic Yeast, *Cryptococcus Neoformans*. *Syst. Appl. Microbiol.* 23, 535–545. doi: 10.1016/s0723-2020(00)80028-4

Dou H. T., Xu Y. C., Wang H. Z., and Li T. S. (2015). Molecular Epidemiology of *Cryptococcus Neoformans* and *Cryptococcus Gattii* in China Between 2007 and 2013 Using Multilocus Sequence Typing and the DiversiLab System. *Eur. J. Clin. Microbiol. Infect. Dis.* 34, 753–762. doi: 10.1007/s10096-014-2289-2

Dromer F., Mathoulin S., Dupont B., Letenneur L., and Ronin O. (1996). Individual and Environmental Factors Associated With Infection Due to *Cryptococcus Neoformans* Serotype D. French Cryptococcosis Study Group. *Clin. Infect. Dis.* 23, 91–96. doi: 10.1093/clinids/23.1.91

Dromer F., Varma A., Ronin O., Mathoulin S., and Dupont B. (1994). Molecular Typing of *Cryptococcus Neoformans* Serotype D Clinical Isolates. *J. Clin. Microbiol.* 32, 2364–2371. doi: 10.1128/jcm.32.10.2364-2371.1994

D'souza C. A., Kronstad J. W., Taylor G., Warren R., Yuen M., Hu G., et al. (2011). Genome Variation in *Cryptococcus Gattii*, an Emerging Pathogen of Immunocompetent Hosts. *mBio* 2, e00342–e00310. doi: 10.1128/mBio.00342-10

Enache-Angoulvant A., Chandenier J., Symoens F., Lacube P., Bolognini J., Douchet C., et al. (2007). Molecular Identification of *Cryptococcus Neoformans* Serotypes. *J. Clin. Microbiol.* 45, 1261–1265. doi: 10.1128/jcm.01839-06

Engelthaler D. M., Hicks N. D., Gillece J. D., Roe C. C., Schupp J. M., Driebe E. M., et al. (2014). *Cryptococcus Gattii* in North American Pacific Northwest: Whole-Population Genome Analysis Provides Insights Into Species Evolution and Dispersal. *mBio* 5, e01464–e01414. doi: 10.1128/mBio.01464-14

Esposto M. C., Cogliati M., Tortorano A. M., and Viviani M. A. (2009). Electrophoretic Karyotyping of *Cryptococcus Neoformans* AD-hybrid Strains. *Mycoses* 52, 16–23. doi: 10.1111/j.1439-0507.2008.01532.x

Fan X., Xiao M., Chen S., Kong F., Dou H. T., Wang H., et al. (2016). Predominance of *Cryptococcus Neoformans* Var. *Grubii* Multilocus Sequence Type 5 and Emergence of Isolates With non-Wild-Type Minimum Inhibitory Concentrations to Fluconazole: A Multi-Centre Study in China. *Clin. Microbiol. Infect.* 22, 887.e881–887.e889. doi: 10.1016/j.cmi.2016.07.008

Farrer R. A., Chang M., Davis M. J., Van Dorp L., Yang D. H., Shea T., et al. (2019). A New Lineage of *Cryptococcus Gattii* (VGV) Discovered in the Central Zambezian Miombo Woodlands. *mBio* 10, e02306-19. doi: 10.1128/mBio.02306-19

Farrer R. A., Desjardins C. A., Sakthikumar S., Gujja S., Saif S., Zeng Q., et al. (2015). Genome Evolution and Innovation Across the Four Major Lineages of *Cryptococcus Gattii*. *mBio* 6, e00868–e00815. doi: 10.1128/mBio.00868-15

Farrer R. A., Voelz K., Henk D. A., Johnston S. A., Fisher M. C., May R. C., et al. (2016). Microevolutionary Traits and Comparative Population Genomics of the Emerging Pathogenic Fungus *Cryptococcus Gattii*. *mBio* 6, e00868-15. doi: 10.1098/rstb.2016.0021

Feng X., Yao Z., Ren D., and Liao W. (2008). Simultaneous Identification of Molecular and Mating Types Within the Cryptococcus Species Complex by PCR-RFLP Analysis. *J. Med. Microbiol.* 57, 1481–1490. doi: 10.1099/jmm.0.2008/003665-0

Firacative C., Trilles L., and Meyer W. (2012). Maldi-Tof MS Enables the Rapid Identification of the Major Molecular Types Within the *Cryptococcus Neoformans*/C. Gattii Species Complex. *PloS One* 7, e37566. doi: 10.1371/journal.pone.0037566

Florek M., Nawrot U., Korzeniowska-Kowal A., Włodarczyk K., Wzorek A., Woźniak-Biel A., et al. (2021). An Analysis of the Population of *Cryptococcus Neoformans* Strains Isolated From Animals in Poland, in the Years 2015-2019. *Sci. Rep.* 11, 6639. doi: 10.1038/s41598-021-86169-3

Franzot S. P., Salkin I. F., and Casadevall A. (1999). *Cryptococcus Neoformans* Var. *Grubii*: Separate Varietal Status for *Cryptococcus Neoformans* Serotype A Isolates. *J. Clin. Microbiol.* 37, 838–840. doi: 10.1128/jcm.37.3.838-840.1999

Fraser J. A., Giles S. S., Wenink E. C., Geunes-Boyer S. G., Wright J. R., Diezmann S., et al. (2005). Same-Sex Mating and the Origin of the Vancouver Island *Cryptococcus Gattii* Outbreak. *Nature* 437, 1360–1364. doi: 10.1038/nature04220

Fromtling R. A., Shadomy H. J., and Jacobson E. S. (1982). Decreased Virulence in Stable, Acapsular Mutants of *Cryptococcus Neoformans*. *Mycopathologia* 79, 23–29. doi: 10.1007/bf00636177

Galagan J. E., Henn M. R., Ma L. J., Cuomo C. A., and Birren B. (2005). Genomics of the Fungal Kingdom: Insights Into Eukaryotic Biology. *Genome Res.* 15, 1620–1631. doi: 10.1101/gr.3767105

Garcia-Hermoso D., Maccallum D. M., Lott T. J., Sampaio P., Serna M. J., Grenouillet F., et al. (2010). Multicenter Collaborative Study for Standardization of *Candida Albicans* Genotyping Using a Polymorphic Microsatellite Marker. *J. Clin. Microbiol.* 48, 2578–2581. doi: 10.1128/jcm.00040-10

Gebhardt C., Ritter E., Debener T., Schachtschabel U., Walkemeier B., Uhrig H., et al. (1989). RFLP Analysis and Linkage Mapping in Solanum Tuberosum. *Theor. Appl. Genet.* 78, 65–75. doi: 10.1007/bf00299755

Grover A., and Sharma P. C. (2016). Development and Use of Molecular Markers: Past and Present. *Crit. Rev. Biotechnol.* 36, 290–302. doi: 10.3109/07388551.2014.959891

Hadrys H., Balick M., and Schierwater B. (1992). Applications of Random Amplified Polymorphic DNA (RAPD) in Molecular Ecology. *Mol. Ecol.* 1, 55–63. doi: 10.1111/j.1365-294x.1992.tb00155.x

Hagen F., Ceresini P. C., Polacheck I., Ma H., Van Nieuwerburgh F., Gabaldón T., et al. (2013). Ancient Dispersal of the Human Fungal Pathogen *Cryptococcus Gattii* From the Amazon Rainforest. *PloS One* 8, e71148. doi: 10.1371/journal.pone.0071148

Hagen F., Illnait-Zaragozi M. T., Bartlett K. H., Swinne D., Geertsen E., Klaassen C. H., et al. (2010). In Vitro Antifungal Susceptibilities and Amplified Fragment Length Polymorphism Genotyping of a Worldwide Collection of 350 Clinical, Veterinary, and Environmental *Cryptococcus Gattii* Isolates. *Antimicrobial. Agents Chemother.* 54, 5139–5145. doi: 10.1128/aac.00746-10

Hagen F., Khayhan K., Theelen B., Kolecka A., Polacheck I., Sionov E., et al. (2015). Recognition of Seven Species in the *Cryptococcus Gattii*/*Cryptococcus Neoformans* Species Complex. *Fungal Genet. Biol.* 78, 16–48. doi: 10.1016/j.fgb.2015.02.009

Hagen F., Lumbsch H. T., Arsic Arsenijevic V., Badali H., Bertout S., Billmyre R. B., et al. (2017). Importance of Resolving Fungal Nomenclature: The Case of Multiple Pathogenic Species in the Cryptococcus Genus. *mSphere* 2, e00238-17. doi: 10.1128/mSphere.00238-17

Hong N., Chen M., Xu N., Al-Hatmi A. M. S., Zhang C., Pan W. H., et al. (2019). Genotypic Diversity and Antifungal Susceptibility of *Cryptococcus Neoformans* Isolates From Paediatric Patients in China. *Mycoses* 62, 171–180. doi: 10.1111/myc.12863

Illnait-Zaragozi M. T., Martínez-Machín G. F., Fernández-Andreu C. M., Boekhout T., Meis J. F., and Klaassen C. H. (2010). Microsatellite Typing of Clinical and Environmental *Cryptococcus Neoformans* Var. *Grubii* Isolates From Cuba Shows Multiple Genetic Lineages. *PloS One* 5, e9124. doi: 10.1371/journal.pone.0009124

Ito-Kuwa S., Nakamura K., Aoki S., and Vidotto V. (2007). Serotype Identification of *Cryptococcus Neoformans* by Multiplex PCR. *Mycoses* 50, 277–281. doi: 10.1111/j.1439-0507.2007.01357.x

Janbon G., Ormerod K. L., Paulet D., Byrnes E. J.,. 3., Yadav V., Chatterjee G., et al. (2014). Analysis of the Genome and Transcriptome of *Cryptococcus Neoformans* Var. *Grubii* Reveals Complex RNA Expression and Microevolution Leading to Virulence Attenuation. *PloS Genet.* 10, e1004261. doi: 10.1371/journal.pgen.1004261

Janssen P., Coopman R., Huys G., Swings J., Bleeker M., Vos P., et al. (1996). Evaluation of the DNA Fingerprinting Method AFLP as an New Tool in Bacterial Taxonomy. *Microbiol. (Reading)* 142 (Pt 7), 1881–1893. doi: 10.1099/13500872-142-7-1881

Jeffreys A. J., Wilson V., and Thein S. L. (1985). Hypervariable 'Minisatellite' Regions in Human DNA. *Nature* 314, 67–73. doi: 10.1038/314067a0

Jin L., Cao J. R., Xue X. Y., Wu H., Wang L. F., Guo L., et al. (2020). Clinical and Microbiological Characteristics of *Cryptococcus Gattii* Isolated From 7 Hospitals in China. *BMC Microbiol.* 20, 73. doi: 10.1186/s12866-020-01752-4

Karaoglu H., Lee C. M., Carter D., and Meyer W. (2008). Development of Polymorphic Microsatellite Markers for *Cryptococcus Neoformans*. *Mol. Ecol. Resour.* 8, 1136–1138. doi: 10.1111/j.1755-0998.2008.02196.x

Katsu M., Kidd S., Ando A., Moretti-Branchini M. L., Mikami Y., Nishimura K., et al. (2004). The Internal Transcribed Spacers and 5.8S rRNA Gene Show

Extensive Diversity Among Isolates of the *Cryptococcus Neoformans* Species Complex. *FEMS Yeast Res.* 4, 377–388. doi: 10.1016/s1567-1356(03)00176-4

Khan Z. U., Al-Anezi A. A., Chandy R., and Xu J. (2003). Disseminated Cryptococcosis in an AIDS Patient Caused by a Canavanine-Resistant Strain of *Cryptococcus Neoformans* Var. *Grubii*. *J. Med. Microbiol.* 52, 271–275. doi: 10.1099/jmm.0.05097-0

Khayhan K., Hagen F., Pan W., Simwami S., Fisher M. C., Wahyuningsih R., et al. (2013). Geographically Structured Populations of *Cryptococcus Neoformans* Variety *Grubii* in Asia Correlate With HIV Status and Show a Clonal Population Structure. *PloS One* 8, e72222. doi: 10.1371/journal.pone.0072222

Kidd S. E., Hagen F., Tscharke R. L., Huynh M., Bartlett K. H., Fyfe M., et al. (2004). A Rare Genotype of *Cryptococcus Gattii* Caused the Cryptococcosis Outbreak on Vancouver Island (British Columbia, Canada). *Proc. Natl. Acad. Sci. U. S. A.* 101, 17258–17263. doi: 10.1073/pnas.0402981101

Koebner R. M. (1995). Predigestion of DNA Template Improves the Level of Polymorphism of Random Amplified Polymorphic DNAs in Wheat. *Genet. Anal.* 12, 63–67. doi: 10.1016/1050-3862(95)00102-6

Krishnamurthy T., and Ross P. L. (1996). Rapid Identification of Bacteria by Direct Matrix-Assisted Laser Desorption/Ionization Mass Spectrometric Analysis of Whole Cells. *Rapid Commun. Mass Spectrom.* 10, 1992–1996. doi: 10.1002/(sici)1097-0231(199612)10:15<1992::Aid-rcm789>3.0.Co;2-v

Kwon-Chung K. J., Bennett J. E., Wickes B. L., Meyer W., Cuomo C. A., Wollenburg K. R., et al. (2017). The Case for Adopting the "Species Complex" Nomenclature for the Etiologic Agents of Cryptococcosis. *mSphere* 2, e00357-16. doi: 10.1128/mSphere.00357-16

Kwon-Chung K. J., Fraser J. A., Doering T. L., Wang Z., Janbon G., Idnurm A., et al. (2014). *Cryptococcus Neoformans* and *Cryptococcus Gattii*, the Etiologic Agents of Cryptococcosis. *Cold Spring Harb. Perspect. Med.* 4:a019760. doi: 10.1101/cshperspect.a019760

Kwon-Chung K. J., Polacheck I., and Bennett J. E. (1982). Improved Diagnostic Medium for Separation of *Cryptococcus Neoformans* Var. Neoformans (Serotypes A and D) and *Cryptococcus Neoformans* Var. Gattii (Serotypes B and C). *J. Clin. Microbiol.* 15, 535–537. doi: 10.1128/jcm.15.3.535-537.1982

Kwon-Chung K. J., and Rhodes J. C. (1986). Encapsulation and Melanin Formation as Indicators of Virulence in *Cryptococcus Neoformans*. *Infect. Immun.* 51, 218–223. doi: 10.1128/iai.51.1.218-223.1986

Kwon-Chung K. J., Wickes B. L., Stockman L., Roberts G. D., Ellis D., and Howard D. H. (1992). Virulence, Serotype, and Molecular Characteristics of Environmental Strains of *Cryptococcus Neoformans* Var. Gattii. *Infect. Immun.* 60, 1869–1874. doi: 10.1128/iai.60.5.1869-1874.1992

Latouche G. N., Huynh M., Sorrell T. C., and Meyer W. (2003). PCR-Restriction Fragment Length Polymorphism Analysis of the Phospholipase B (PLB1) Gene for Subtyping of *Cryptococcus Neoformans* Isolates. *Appl. Environ. Microbiol.* 69, 2080–2086. doi: 10.1128/aem.69.4.2080-2086.2003

Lazera M. S., Salmito Cavalcanti M. A., Londero A. T., Trilles L., Nishikawa M. M., and Wanke B. (2000). Possible Primary Ecological Niche of *Cryptococcus Neoformans*. *Med. Mycol.* 38, 379–383. doi: 10.1080/mmy.38.5.379.383

Li M., Chen M., and Pan W. (2013). Approaches on Genetic Polymorphism of Cryptococcus Species Complex. *Front. Biosci. (Landmark Ed)* 18, 1227–1236. doi: 10.2741/4174

Li T. Y., Liu B. H., and Chen Y. C. (2000). Characterization of Aspergillus Spores by Matrix-Assisted Laser Desorption/Ionization Time-of-Flight Mass Spectrometry. *Rapid Commun. Mass Spectrom.* 14, 2393–2400. doi: 10.1002/1097-0231(20001230)14:24<2393::Aid-rcm178>3.0.Co;2-9

Litvintseva A. P., Carbone I., Rossouw J., Thakur R., Govender N. P., and Mitchell T. G. (2011). Evidence That the Human Pathogenic Fungus *Cryptococcus Neoformans* Var. *Grubii* may Have Evolved in Africa. *PloS One* 6, e19688. doi: 10.1371/journal.pone.0019688

Litvintseva A. P., and Mitchell T. G. (2012). Population Genetic Analyses Reveal the African Origin and Strain Variation of *Cryptococcus Neoformans* Var. *Grubii*. *PloS Pathog.* 8, e1002495. doi: 10.1371/journal.ppat.1002495

Litvintseva A. P., Thakur R., Vilgalys R., and Mitchell T. G. (2006). Multilocus Sequence Typing Reveals Three Genetic Subpopulations of *Cryptococcus Neoformans* Var. *Grubii* (Serotype A), Including a Unique Population in Botswana. *Genetics* 172, 2223–2238. doi: 10.1534/genetics.105.046672

Liu O. W., Chun C. D., Chow E. D., Chen C., Madhani H. D., and Noble S. M. (2008). Systematic Genetic Analysis of Virulence in the Human Fungal Pathogen *Cryptococcus Neoformans*. *Cell* 135, 174–188. doi: 10.1016/j.cell.2008.07.046

Loftus B. J., Fung E., Roncaglia P., Rowley D., Amedeo P., Bruno D., et al. (2005). The Genome of the Basidiomycetous Yeast and Human Pathogen *Cryptococcus Neoformans*. *Science* 307, 1321–1324. doi: 10.1126/science.1103773

May R. C., Stone N. R., Wiesner D. L., Bicanic T., and Nielsen K. (2016). Cryptococcus: From Environmental Saprophyte to Global Pathogen. *Nat. Rev. Microbiol.* 14, 106–117. doi: 10.1038/nrmicro.2015.6

Mcculloh R. J., Phillips R., Perfect J. R., Byrnes E. J.,. 3., Heitman J., and Dufort E. (2011). *Cryptococcus Gattii* Genotype VGI Infection in New England. *Pediatr. Infect. Dis. J.* 30, 1111–1114. doi: 10.1097/INF.0b013e31822d14fd

Meyer W., Aanensen D. M., Boekhout T., Cogliati M., Diaz M. R., Esposto M. C., et al. (2009). Consensus Multi-Locus Sequence Typing Scheme for *Cryptococcus Neoformans* and *Cryptococcus Gattii*. *Med. Mycol.* 47, 561–570. doi: 10.1080/13693780902953886

Meyer W., Castañeda A., Jackson S., Huynh M., and Castañeda E. (2003). Molecular Typing of IberoAmerican *Cryptococcus Neoformans* Isolates. *Emerg. Infect. Dis.* 9, 189–195. doi: 10.3201/eid0902.020246

Meyer W., Lieckfeldt E., Kuhls K., Freedman E. Z., Börner T., and Mitchell T. G. (1993a). DNA- and PCR-fingerprinting in Fungi. *Exs* 67, 311–320. doi: 10.1007/978-3-0348-8583-6_28

Meyer W., Marszewska K., Amirmostofian M., Igreja R. P., Hardtke C., Methling K., et al. (1999). Molecular Typing of Global Isolates of *Cryptococcus Neoformans* Var. Neoformans by Polymerase Chain Reaction Fingerprinting and Randomly Amplified Polymorphic DNA-a Pilot Study to Standardize Techniques on Which to Base a Detailed Epidemiological Survey. *Electrophoresis* 20, 1790–1799. doi: 10.1002/(sici)1522-2683(19990101)20:8<1790::Aid-elps1790>3.0.Co;2-2

Meyer W., and Mitchell T. G. (1995). Polymerase Chain Reaction Fingerprinting in Fungi Using Single Primers Specific to Minisatellites and Simple Repetitive DNA Sequences: Strain Variation in *Cryptococcus Neoformans*. *Electrophoresis* 16, 1648–1656. doi: 10.1002/elps.11501601273

Meyer W., Mitchell T. G., Freedman E. Z., and Vilgalys R. (1993b). Hybridization Probes for Conventional DNA Fingerprinting Used as Single Primers in the Polymerase Chain Reaction to Distinguish Strains of *Cryptococcus Neoformans*. *J. Clin. Microbiol.* 31, 2274–2280. doi: 10.1128/jcm.31.9.2274-2280.1993

Mohan D., Rao K. B., Dixit A., and Ali S. (1995). Assessment of Amplicons in the DNA From Boiled Tissue by PCR and AP-PCR Amplification. *Genet. Anal.* 12, 57–62. doi: 10.1016/1050-3862(95)00103-4

Nakamura Y. (2001). Molecular Analyses of the Serotype of *Cryptococcus Neoformans*. *Nihon Ishinkin Gakkai Zasshi* 42, 69–74. doi: 10.3314/jjmm.42.69

Nakamura Y., Kano R., Sato H., Watanabe S., Takahashi H., and Hasegawa A. (1998). Isolates of *Cryptococcus Neoformans* Serotype A and D Developed on Canavanine-Glycine-Bromthymol Blue Medium. *Mycoses* 41, 35–40. doi: 10.1111/j.1439-0507.1998.tb00373.x

Ngamskulrungroj P., Gilgado F., Faganello J., Litvintseva A. P., Leal A. L., Tsui K. M., et al. (2009). Genetic Diversity of the Cryptococcus Species Complex Suggests That *Cryptococcus Gattii* Deserves to Have Varieties. *PloS One* 4, e5862. doi: 10.1371/journal.pone.0005862

Ormerod K. L., Morrow C. A., Chow E. W., Lee I. R., Arras S. D., Schirra H. J., et al. (2013). Comparative Genomics of Serial Isolates of *Cryptococcus Neoformans* Reveals Gene Associated With Carbon Utilization and Virulence. *G3 (Bethesda)* 3, 675–686. doi: 10.1534/g3.113.005660

Pakshir K., Fakhim H., Vaezi A., Meis J. F., Mahmoodi M., Zomorodian K., et al. (2018). Molecular Epidemiology of Environmental Cryptococcus Species Isolates Based on Amplified Fragment Length Polymorphism. *J. Mycol. Med.* 28, 599–605. doi: 10.1016/j.mycmed.2018.09.005

Pan W., Khayhan K., Hagen F., Wahyuningsih R., Chakrabarti A., Chowdhary A., et al. (2012). Resistance of Asian *Cryptococcus Neoformans* Serotype A is Confined to Few Microsatellite Genotypes. *PloS One* 7, e32868. doi: 10.1371/journal.pone.0032868

Park B. J., Wannemuehler K. A., Marston B. J., Govender N., Pappas P. G., and Chiller T. M. (2009). Estimation of the Current Global Burden of Cryptococcal Meningitis Among Persons Living With HIV/AIDS. *Aids* 23, 525–530. doi: 10.1097/QAD.0b013e328322ffac

Paun O., and Schönswetter P. (2012). Amplified Fragment Length Polymorphism: An Invaluable Fingerprinting Technique for Genomic, Transcriptomic, and Epigenetic Studies. *Methods Mol. Biol.* 862, 75–87. doi: 10.1007/978-1-61779-609-8_7

Perfect J. R., Ketabchi N., Cox G. M., Ingram C. W., and Beiser C. L. (1993). Karyotyping of *Cryptococcus Neoformans* as an Epidemiological Tool. *J. Clin. Microbiol.* 31, 3305–3309. doi: 10.1128/jcm.31.12.3305-3309.1993

Posteraro B., Vella A., Cogliati M., De Carolis E., Florio A. R., Posteraro P., et al. (2012). Matrix-Assisted Laser Desorption Ionization-Time of Flight Mass Spectrometry-Based Method for Discrimination Between Molecular Types of *Cryptococcus Neoformans* and *Cryptococcus Gattii*. *J. Clin. Microbiol.* 50, 2472–2476. doi: 10.1128/jcm.00737-12

Prakash A., Sundar G., Sharma B., Hagen F., Meis J. F., and Chowdhary A. (2020). Genotypic Diversity in Clinical and Environmental Isolates of *Cryptococcus Neoformans* From India Using Multilocus Microsatellite and Multilocus Sequence Typing. *Mycoses* 63, 284–293. doi: 10.1111/myc.13041

Rajasingham R., Smith R. M., Park B. J., Jarvis J. N., Govender N. P., Chiller T. M., et al. (2017). Global Burden of Disease of HIV-associated Cryptococcal Meningitis: An Updated Analysis. *Lancet Infect. Dis.* 17, 873–881. doi: 10.1016/s1473-3099(17)30243-8

Randhawa H. S., Kowshik T., Chowdhary A., Preeti Sinha K., Khan Z. U., Sun S., et al. (2008). The Expanding Host Tree Species Spectrum of *Cryptococcus Gattii* and *Cryptococcus Neoformans* and Their Isolations From Surrounding Soil in India. *Med. Mycol.* 46, 823–833. doi: 10.1080/13693780802124026

Rhodes J., Beale M. A., and Fisher M. C. (2014). Illuminating Choices for Library Prep: A Comparison of Library Preparation Methods for Whole Genome Sequencing of *Cryptococcus Neoformans* Using Illumina Hiseq. *PloS One* 9, e113501. doi: 10.1371/journal.pone.0113501

Rhodes J., Beale M. A., Vanhove M., Jarvis J. N., Kannambath S., Simpson J. A., et al. (2017a). A Population Genomics Approach to Assessing the Genetic Basis of Within-Host Microevolution Underlying Recurrent Cryptococcal Meningitis Infection. *G3 (Bethesda)* 7, 1165–1176. doi: 10.1534/g3.116.037499

Rhodes J., Desjardins C. A., Sykes S. M., Beale M. A., Vanhove M., Sakthikumar S., et al. (2017b). Tracing Genetic Exchange and Biogeography of *Cryptococcus Neoformans* Var. *Grubii* At the Global Population Level. *Genetics* 207, 327–346. doi: 10.1534/genetics.117.203836

Rudramurthy S. M., De Valk H. A., Chakrabarti A., Meis J. F., and Klaassen C. H. (2011). High Resolution Genotyping of Clinical *Aspergillus Flavus* Isolates From India Using Microsatellites. *PloS One* 6, e16086. doi: 10.1371/journal.pone.0016086

Ruma P., Chen S. C., Sorrell T. C., and Brownlee A. G. (1996). Characterization of *Cryptococcus Neoformans* by Random DNA Amplification. *Lett. Appl. Microbiol.* 23, 312–316. doi: 10.1111/j.1472-765x.1996.tb00197.x

Saracli M. A., Yildiran S. T., Sener K., Gonlum A., Doganci L., Keller S. M., et al. (2006). Genotyping of Turkish Environmental *Cryptococcus Neoformans* Var. Neoformans Isolates by Pulsed Field Gel Electrophoresis and Mating Type. *Mycoses* 49, 124–129. doi: 10.1111/j.1439-0507.2006.01203.x

Savelkoul P. H., Aarts H. J., De Haas J., Dijkshoorn L., Duim B., Otsen M., et al. (1999). Amplified-Fragment Length Polymorphism Analysis: The State of an Art. *J. Clin. Microbiol.* 37, 3083–3091. doi: 10.1128/jcm.37.10.3083-3091.1999

Schierwater B., and Ender A. (1993). Different Thermostable DNA Polymerases may Amplify Different RAPD Products. *Nucleic Acids Res.* 21, 4647–4648. doi: 10.1093/nar/21.19.4647

Schoch C. L., Seifert K. A., Huhndorf S., Robert V., Spouge J. L., Levesque C. A., et al. (2012). Nuclear Ribosomal Internal Transcribed Spacer (its) Region as a Universal DNA Barcode Marker for Fungi. *Proc. Natl. Acad. Sci. U. S. A.* 109, 6241–6246. doi: 10.1073/pnas.1117018109

Seng P., Drancourt M., Gouriet F., La Scola B., Fournier P. E., Rolain J. M., et al. (2009). Ongoing Revolution in Bacteriology: Routine Identification of Bacteria by Matrix-Assisted Laser Desorption Ionization Time-of-Flight Mass Spectrometry. *Clin. Infect. Dis.* 49, 543–551. doi: 10.1086/600885

Sheeja T. E., Kumar I. P. V., Giridhari A., Minoo D., Rajesh M. K., and Babu K. N. (2021). Amplified Fragment Length Polymorphism: Applications and Recent Developments. *Methods Mol. Biol.* 2222, 187–218. doi: 10.1007/978-1-0716-0997-2_12

Sidrim J. J., Costa A. K., Cordeiro R. A., Brilhante R. S., Moura F. E., Castelo-Branco D. S., et al. (2010). Molecular Methods for the Diagnosis and Characterization of Cryptococcus: A Review. *Can. J. Microbiol.* 56, 445–458. doi: 10.1139/w10-030

Simwami S. P., Khayhan K., Henk D. A., Aanensen D. M., Boekhout T., Hagen F., et al. (2011). Low Diversity *Cryptococcus Neoformans* Variety *Grubii* Multilocus Sequence Types From Thailand are Consistent With an Ancestral African Origin. *PloS Pathog.* 7, e1001343. doi: 10.1371/journal.ppat.1001343

Sorrell T. C., Chen S. C., Ruma P., Meyer W., Pfeiffer T. J., Ellis D. H., et al. (1996). Concordance of Clinical and Environmental Isolates of *Cryptococcus Neoformans* Var. Gattii by Random Amplification of Polymorphic DNA Analysis and PCR Fingerprinting. *J. Clin. Microbiol.* 34, 1253–1260. doi: 10.1128/jcm.34.5.1253-1260.1996

Souto A. C., Bonfietti L. X., Ferreira-Paim K., Trilles L., Martins M., Ribeiro-Alves M., et al. (2016). Population Genetic Analysis Reveals a High Genetic Diversity in the Brazilian *Cryptococcus Gattii* VGII Population and Shifts the Global Origin From the Amazon Rainforest to the Semi-arid Desert in the Northeast of Brazil. *PloS Negl. Trop. Dis.* 10, e0004885. doi: 10.1371/journal.pntd.0004885

Springer D. J., Billmyre R. B., Filler E. E., Voelz K., Pursall R., Mieczkowski P. A., et al. (2014). *Cryptococcus Gattii* VGIII Isolates Causing Infections in HIV/AIDS Patients in Southern California: Identification of the Local Environmental Source as Arboreal. *PloS Pathog.* 10, e1004285. doi: 10.1371/journal.ppat.1004285

Stübiger G., Wuczkowski M., Mancera L., Lopandic K., Sterflinger K., and Belgacem O. (2016). Characterization of Yeasts and Filamentous Fungi Using MALDI Lipid Phenotyping. *J. Microbiol. Methods* 130, 27–37. doi: 10.1016/j.mimet.2016.08.010

Sugita T., Ikeda R., and Shinoda T. (2001). Diversity Among Strains of *Cryptococcus Neoformans* Var. Gattii as Revealed by a Sequence Analysis of Multiple Genes and a Chemotype Analysis of Capsular Polysaccharide. *Microbiol. Immunol.* 45, 757–768. doi: 10.1111/j.1348-0421.2001.tb01312.x

Taverna C. G., Bosco-Borgeat M. E., Mazza M., Vivot M. E., Davel G., and Canteros C. E. (2020). Frequency and Geographical Distribution of Genotypes and Mating Types of *Cryptococcus Neoformans* and *Cryptococcus Gattii* Species Complexes in Argentina. *Rev. Argent. Microbiol.* 52, 183–188. doi: 10.1016/j.ram.2019.07.005

Taylor J. W., and Fisher M. C. (2003). Fungal Multilocus Sequence Typing–It's Not Just for Bacteria. *Curr. Opin. Microbiol.* 6, 351–356. doi: 10.1016/s1369-5274(03)00088-2

Thompson G. R.,. 3., Albert N., Hodge G., Wilson M. D., Sykes J. E., Bays D. J., et al. (2014). Phenotypic Differences of Cryptococcus Molecular Types and Their Implications for Virulence in a Drosophila Model of Infection. *Infect. Immun.* 82, 3058–3065. doi: 10.1128/iai.01805-14

Tortorano A. M., Viviani M. A., Rigoni A. L., Cogliati M., Roverselli A., and Pagano A. (1997). Prevalence of Serotype D in *Cryptococcus Neoformans* Isolates From HIV Positive and HIV Negative Patients in Italy. *Mycoses* 40, 297–302. doi: 10.1111/j.1439-0507.1997.tb00235.x

Trilles L., Wang B., Firacative C., Lazéra Mdos S., Wanke B., and Meyer W. (2014). Identification of the Major Molecular Types of *Cryptococcus Neoformans* and C. Gattii by Hyperbranched Rolling Circle Amplification. *PloS One* 9, e94648. doi: 10.1371/journal.pone.0094648

Van Belkum A., Scherer S., Van Alphen L., and Verbrugh H. (1998). Short-Sequence DNA Repeats in Prokaryotic Genomes. *Microbiol. Mol. Biol. Rev.* 62, 275–293. doi: 10.1128/MMBR.62.2.275-293.1998

Van Der Straaten T. (2015). Next-Generation Sequencing: Current Technologies and Applications. Edited by Jianping Xu. *Chem. Med. Chem.* 10, 419–420. doi: 10.1002/cmdc.201402456

Van De Wiele N., Neyra E., Firacative C., Gilgado F., Serena C., Bustamante B., et al. (2020). Molecular Epidemiology Reveals Low Genetic Diversity Among *Cryptococcus Neoformans* Isolates From People Living With HIV in Lima, Peru, During the Pre-HAART Era. *Pathogens* 9, 665. doi: 10.3390/pathogens9080665

Vanhove M., Beale M. A., Rhodes J., Chanda D., Lakhi S., Kwenda G., et al. (2017). Genomic Epidemiology of Cryptococcus Yeasts Identifies Adaptation to Environmental Niches Underpinning Infection Across an African HIV/AIDS Cohort. *Mol. Ecol.* 26, 1991–2005. doi: 10.1111/mec.13891

Van Veen S. Q., Claas E. C., and Kuijper E. J. (2010). High-Throughput Identification of Bacteria and Yeast by Matrix-Assisted Laser Desorption Ionization-Time of Flight Mass Spectrometry in Conventional Medical Microbiology Laboratories. *J. Clin. Microbiol.* 48, 900–907. doi: 10.1128/jcm.02071-09

Velegraki A., Kiosses V. G., Kansouzidou A., Smilakou S., Mitroussia-Ziouva A., and Legakis N. J. (2001). Prospective Use of RFLP Analysis on Amplified *Cryptococcus Neoformans* URA5 Gene Sequences for Rapid Identification of Varieties and Serotypes in Clinical Samples. *Med. Mycol.* 39, 409–417. doi: 10.1080/mmy.39.5.409.417

Viviani M. A., Cogliati M., Esposto M. C., Lemmer K., Tintelnot K., Colom Valiente M. F., et al. (2006). Molecular Analysis of 311 *Cryptococcus Neoformans* Isolates From a 30-Month ECMM Survey of Cryptococcosis in Europe. *FEMS Yeast Res.* 6, 614–619. doi: 10.1111/j.1567-1364.2006.00081.x

Vos P., Hogers R., Bleeker M., Reijans M., Van De Lee T., Hornes M., et al. (1995). AFLP: A New Technique for DNA Fingerprinting. *Nucleic Acids Res.* 23, 4407–4414. doi: 10.1093/nar/23.21.4407

Wang Y., and Xu J. (2020). Mitochondrial Genome Polymorphisms in the Human Pathogenic Fungus *Cryptococcus Neoformans*. *Front. Microbiol.* 11:706. doi: 10.3389/fmicb.2020.00706

Welsh J., and Mcclelland M. (1990). Fingerprinting Genomes Using PCR With Arbitrary Primers. *Nucleic Acids Res.* 18, 7213–7218. doi: 10.1093/nar/18.24.7213

Wickes B. L., Moore T. D., and Kwon-Chung K. J. (1994). Comparison of the Electrophoretic Karyotypes and Chromosomal Location of Ten Genes in the Two Varieties of *Cryptococcus Neoformans*. *Microbiol. (Reading)* 140 (Pt 3), 543–550. doi: 10.1099/00221287-140-3-543

Wiesner D. L., Moskalenko O., Corcoran J. M., Mcdonald T., Rolfes M. A., Meya D. B., et al. (2012). Cryptococcal Genotype Influences Immunologic Response and Human Clinical Outcome After Meningitis. *mBio* 3, e00196-12. doi: 10.1128/mBio.00196-12

Williams J. G., Kubelik A. R., Livak K. J., Rafalski J. A., and Tingey S. V. (1990). DNA Polymorphisms Amplified by Arbitrary Primers are Useful as Genetic Markers. *Nucleic Acids Res.* 18, 6531–6535. doi: 10.1093/nar/18.22.6531

Xu J. (2002). Mitochondrial DNA Polymorphisms in the Human Pathogenic Fungus *Cryptococcus Neoformans*. *Curr. Genet.* 41, 43–47. doi: 10.1007/s00294-002-0282-2

Xu J. (2016). Fungal DNA Barcoding. *Genome* 59, 913–932. doi: 10.1139/gen-2016-0046

Xu J. (2020). Fungal Species Concepts in the Genomics Era. *Genome* 63, 459–468. doi: 10.1139/gen-2020-0022

Xu J., Ali R. Y., Gregory D. A., Amick D., Lambert S. E., Yoell H. J., et al. (2000a). Uniparental Mitochondrial Transmission in Sexual Crosses in *Cryptococcus Neoformans*. *Curr. Microbiol.* 40, 269–273. doi: 10.1007/s002849910053

Xu J., Luo G., Vilgalys R. J., Brandt M. E., and Mitchell T. G. (2002). Multiple Origins of Hybrid Strains of *Cryptococcus Neoformans* With Serotype AD. *Microbiol. (Reading)* 148, 203–212. doi: 10.1099/00221287-148-1-203

Xu J., and Mitchell T. G. (2003). Comparative Gene Genealogical Analyses of Strains of Serotype AD Identify Recombination in Populations of Serotypes A and D in the Human Pathogenic Yeast *Cryptococcus Neoformans*. *Microbiol. (Reading)* 149, 2147–2154. doi: 10.1099/mic.0.26180-0

Xu J., Vilgalys R., and Mitchell T. G. (2000b). Multiple Gene Genealogies Reveal Recent Dispersion and Hybridization in the Human Pathogenic Fungus *Cryptococcus Neoformans*. *Mol. Ecol.* 9, 1471–1481. doi: 10.1046/j.1365-294x.2000.01021.x

Yamamoto Y., Kohno S., Koga H., Kakeya H., Tomono K., Kaku M., et al. (1995). Random Amplified Polymorphic DNA Analysis of Clinically and Environmentally Isolated *Cryptococcus Neoformans* in Nagasaki. *J. Clin. Microbiol.* 33, 3328–3332. doi: 10.1128/jcm.33.12.3328-3332.1995

Zhu J., Kang Y., Uno J., Taguchi H., Liu Y., Ohata M., et al. (2010). Comparison of Genotypes Between Environmental and Clinical Isolates of *Cryptococcus Neoformans* Var. *Grubii* Based on Microsatellite Patterns. *Mycopathologia* 169, 47–55. doi: 10.1007/s11046-009-9230-8

Zvezdanova M. E., Arroyo M. J., Méndez G., Guinea J., Mancera L., Muñoz P., et al. (2020). Implementation of MALDI-TOF Mass Spectrometry and Peak Analysis: Application to the Discrimination of *Cryptococcus Neoformans* Species Complex and Their Interspecies Hybrids. *J. Fungi (Basel)* 6, 330. doi: 10.3390/jof6040330

Conflict of Interest: The authors declare that the research was conducted in the absence of any commercial or financial relationships that could be construed as a potential conflict of interest.

frontiers in Cellular and Infection Microbiology

ORIGINAL RESEARCH
published: 15 September 2021
doi: 10.3389/fcimb.2021.721439

Molecular Epidemiology, Antifungal Susceptibility, and Virulence Evaluation of *Candida* Isolates Causing Invasive Infection in a Tertiary Care Teaching Hospital

Junzhu Chen[1,2†], Niya Hu[1†], Hongzhi Xu[1,3†], Qiong Liu[2], Xiaomin Yu[2], Yuping Zhang[2], Yongcheng Huang[3], Junjun Tan[2], Xiaotian Huang[1,2] and Lingbing Zeng[1,3*]*

[1] Department of Clinical Laboratory, The First Affiliated Hospital of Nanchang University, Nanchang, China, [2] Department of Medical Microbiology, School of Medicine, Nanchang University, Nanchang, China, [3] Department of Preventive Medicine and Public Health, School of Public Health, Nanchang University, Nanchang, China

OPEN ACCESS

Edited by:
Min Chen,
Shanghai Changzheng Hospital, China

Reviewed by:
Mohammad Javad Najafzadeh,
Mashhad University of Medical Sciences, Iran
Farnaz Daneshnia,
Hackensack University Medical Center, United States

***Correspondence:**
Xiaotian Huang
xthuang@ncu.edu.cn
Lingbing Zeng
lingbing_zeng@163.com

†These authors have contributed equally to this work

Specialty section:
This article was submitted to Fungal Pathogenesis, a section of the journal Frontiers in Cellular and Infection Microbiology

Received: *07 June 2021*
Accepted: *09 August 2021*
Published: *15 September 2021*

Citation:
Chen J, Hu N, Xu H, Liu Q, Yu X, Zhang Y, Huang Y, Tan J, Huang X and Zeng L (2021) Molecular Epidemiology, Antifungal Susceptibility, and Virulence Evaluation of Candida Isolates Causing Invasive Infection in a Tertiary Care Teaching Hospital. Front. Cell. Infect. Microbiol. 11:721439. doi: 10.3389/fcimb.2021.721439

Background: The incidence of invasive candidiasis is increasing worldwide. However, the epidemiology, antifungal susceptibility, and virulence of *Candida* spp. in most hospitals remain unclear. This study aimed to evaluate invasive candidiasis in a tertiary care hospital in Nanchang City, China.

Methods: MALDI-TOF MS and 18S rDNA ITS sequencing were used to identify *Candida* strains. Randomly amplified polymorphic DNA analysis was used for molecular typing; biofilm production, caseinase, and hemolysin activities were used to evaluate virulence. The Sensititre™ YeastOne YO10 panel was used to examine antifungal susceptibility. Mutations in *ERG11* and the hotspot regions of *FKS1* of drug-resistant strains were sequenced to evaluate the possible mechanisms of antifungal resistance.

Results: We obtained 110 *Candida* strains, which included 40 *Candida albicans* (36.36%), 37 C. *parapsilosis* (33.64%), 21 C. *tropicalis* (19.09%), 9 C. *glabrata* (8.18%), 2 C. *rugose* (1.82%), and 1 C. *haemulonii* (0.91%) isolates. At a limiting point of 0.80, *C. albicans* isolates could be grouped into five clusters, *C. parapsilosis* and *C. tropicalis* isolates into seven clusters, and *C. glabrata* isolates into only one cluster comprising six strains by RAPD typing. Antifungal susceptibility testing revealed that the isolates showed the greatest overall resistance against fluconazole (6.36%), followed by voriconazole (4.55%). All *C. albicans* and *C. parapsilosis* isolates exhibited 100% susceptibility to echinocandins (i.e., anidulafungin, caspofungin, and micafungin), whereas one *C. glabrata* strain was resistant to echinocandins. The most common amino acid substitutions noted in our study was 132aa (Y132H, Y132F) in the azole-resistant strains. No missense mutation was identified in the hotpot regions of *FKS1*. Comparison of the selected virulence factors detectable in a laboratory environment, such as biofilm, caseinase, and hemolysin production, revealed that most *Candida* isolates were caseinase and hemolysin producers with a strong activity ($Pz < 0.69$). Furthermore, *C. parapsilosis* had greater total biofilm biomass (average $Abs_{620} = 0.712$) than *C. albicans* (average $Abs_{620} = 0.214$, $p < 0.01$) or *C. tropicalis* (average $Abs_{620} =$

0.450, $p < 0.05$), although all *C. glabrata* strains were either low- or no-biofilm producers. The virulence level of the isolates from different specimen sources or clusters showed no obvious correlation. Interesting, 75% of the *C. albicans* from cluster F demonstrated azole resistance, whereas two azole-resistant *C. tropicalis* strains belonged to the cluster Y.

Conclusion: This study provides vital information regarding the epidemiology, pathogenicity, and antifungal susceptibility of *Candida* spp. in patients admitted to Nanchang City Hospital.

Keywords: *Candida* species, RAPD, caseinase, hemolysin, biofilm, antifungal susceptibility

INTRODUCTION

Fungal infections in humans are relatively common and range from common or mild superficial infections to life-threatening invasive infections. In recent years, the widespread use of broad-spectrum antibiotics, hormones, immunosuppressive agents, chemotherapy, and central venous catheters have led to an increase in the incidence of invasive fungal infections. More than 1.6 million people worldwide have been reported to suffer from serious fungal diseases that have a profound impact on patients and can even be fatal (Bongomin et al., 2017).

Infections caused by *Candida* spp. can be divided into superficial, cutaneous, mucosal, and invasive infections (deep and extensive). Up to date, *Candida* spp. have become the third most common cause of bloodstream infections, including candidemia (Wisplinghoff et al., 2004). *Candida albicans* is responsible for approximately 50% of all candidiasis, and the other species account for the remaining *Candida* infections. Specifically, infections caused by *C. tropicalis*, *C. glabrata*, *C. parapsilosis*, *C. krusei*, and *C. auris* have attracted significant scientific attention (Mba and Nweze, 2020). Invasive candidiasis has been attributed to 40%–50% mortality in intensive care units (ICUs) (De Rosa et al., 2009). Candidemia is currently the fourth most common nosocomial bloodstream infection in America (Wisplinghoff et al., 2004; Li et al., 2016). In Europe, the incidence of candidemia was estimated to be approximately 79 cases per day, of which 29 patients were estimated to have a fatal outcome on Day 30 (Koehler et al., 2019).

As the mortality rate in candidiasis is high, identifying the relationship among the various *Candida* species and assessing disease epidemiology, species distribution, and drug resistance to facilitate the control of nosocomial candidiasis is crucial. This study describes the results from an analysis of 110 *Candida* strains isolated from sterile body fluid samples obtained between 2014 and 2019 from patients in a tertiary hospital in Nanchang City. *Candida* spp. in the samples were identified, tested, and analyzed to evaluate the prevalence of *Candida* infection and determine virulence profiles.

MATERIALS AND METHODS

Strains

This retrospective study was conducted between September 2014 and September 2019. *Candida* spp. were isolated from sterile fluid samples (i.e., blood, ascites, bile, secretions, and abscess) of patients admitted in the First Affiliated Hospital of Nanchang University, China. The ethics committee of the university hospital approved this study (approval no. 2014036).

Separation and Identification

The desired strains were isolated and purified on Sabouraud's dextrose agar (SDA; 1% peptone, 4% dextrose, and 2% agar) plates and cultured at 30°C for 24 h. The first crucial step in our study is the correct identification of the *Candida* species. The strains were initially identified by MALDI-TOF mass spectrometry analyses using a Clin-ToF-II mass spectrometer (Bioyong, China). To ensure accuracy, 18S rDNA ITS sequencing was performed for further identification. Briefly, the contiguous ITS1-5.8S rDNA-ITS2 region was amplified with the universal fungal primers ITS1 (5′-TCCGTAGGTGAACCTGCGG-3′) and ITS4 (5′-TCCTCCGCTTATTGATATGC-3′) (Salehi et al., 2017). PCR reactions were performed using the Bio-Rad S1000 thermal cycler in 50 μL volumes containing 1 μL of extracted DNA, 47 μL of T3 Super PCR mix (TSINGKE, China), and 1 μL of each ITS1 and ITS4 primers. Amplification was performed with cycles of 3 min at 98°C for primary denaturation, followed by 35 cycles at 98°C (10 s), 55°C (10 s), and 72°C (20 s), along with a final extension at 72°C for 5 min. The PCR amplification products were sequenced by Tsingke Biological Company (Changsha, China). The sequences were analyzed using the NCBI BLAST searches (http://blast.ncbi.nlm.nih.gov/Blast.cgi).

Randomly Amplified Polymorphic DNA Analysis

DNA from individual strains was extracted as described by Jain et al. but with certain modifications (Jain et al., 2001). Briefly, overnight-cultured *Candida* strains were harvested *via* centrifugation at 12000 rpm after washing with sterile PBS, and the precipitate was resuspended in 100 μL STES buffer (0.2 M Tris-HCl, 0.5 M NaCl, 0.1% SDS, and 0.01 M EDTA, pH = 8.0) and 20 μL TE buffer (0.01 M Tris-HCl and 0.001 M EDTA, pH = 8.0). Acid-washed glass beads (Sigma-Aldrich, USA) and 120 μL phenol–chloroform–isoamyl alcohol mixture (25:24:1 v/v/v) were added to lyse cells and release DNA. After 10 min of vortexing, lysates were centrifuged at 12000 rpm and 4°C for 10 min. DNA from the aqueous phase was precipitated with 2 times the volume of absolute ethanol at −20°C for 15 min, centrifuged at 12000 rpm and 4°C for 10 min, dried, and resuspended in

50 μL TE buffer. The concentration of nucleic acids was measured using a NanoDrop-2000 spectrophotometer (Thermo Fisher Scientific, USA).

Genomic DNA was amplified using previously described primers for five genes, namely, CD16AS (5′-CTCTTGAAA CTGGGGAGACTTGA-3′), HP1247 (5′-AAGAGCCCGT-3′), ERIC-2 (5′-AAGTAAGTGACTGGGGTGAGCG-3′), OPE-3 (5′-CCAGATGCAC-3′), and OPE-18 (5′-GGACTGCAGA-3′) (Paluchowska et al., 2014). The primers used were synthesized by the Tsingke Biological Technology Company. Randomly amplified polymorphic DNA (RAPD) reactions were performed in a final volume of 50 μL, which included 1 μL of the DNA template (approximately 50 ng), 1 μL of each primer (10 μM), and the T3 Super PCR mix. Amplification reactions were performed for 40 cycles using a Bio-Rad S1000 thermal cycler under the following conditions: initial denaturation at 98°C for 3 min, followed by denaturation at 98°C for 10 s, annealing at 36°C for 1 min, and extension at 72°C for 2 min, along with a final extension at 72°C for 5 min. The DNA fragments were separated by electrophoresis in a 1% agarose gel run at 100 V for 30 min. Fragment sizes were determined by comparison with a DL5000 DNA Marker (Vazyme, China), and bands were visualized in the ChemiDocXRS+ system (Bio-Rad, USA). Similarity analysis of RAPD patterns was performed using NTSYS 2.10 software.

Drug Sensitivity Test

In vitro susceptibility of *Candida* strains to nine antifungal drugs, namely, 5-flucytosine, anidulafungin, caspofungin, itraconazole, micafungin, posaconazole, voriconazole, amphotericin B, and fluconazole, was determined using the Sensititre™ YeastOne YO10 panel (Thermo Scientific, USA) based on manufacturer's instructions. *C. krusei* ATCC 6258 and *C. parapsilosis* ATCC 22019 were used as controls, as per the Clinical and Laboratory Standards Institute guidelines. Plates were incubated at 35°C for 24 h, and minimum inhibitory concentrations (MICs) were interpreted according to documents M27-A3 and M27-S4 (Institut, C.a.L.S 2008; Institute, C.a.L.S 2012).

Sequencing of *ERG11* and *FKS1*

The entire open reading frame (ORF) of *ERG11* from azole-resistant strains were amplified and sequenced with specific primers (**Supplementary Table S1**). The hotspot 1 (HS1) and hotspot 2 (HS2) sequences of *FKS1* were amplified using PCR with specific primers shown in **Supplementary Table S1** based on their key role in echinocandin resistance. Conventional PCRs were performed in a 50 μL reaction mixture containing 47 μL of T3 Super PCR mix, 0.2 μM of each primer, and 100 ng of the extracted DNA. The amplification conditions were as follows: initial denaturation at 98°C for 3 min followed by 35 cycles of denaturation (98°C, 10 s), annealing (52°C, 20 s), and extension (72°C, 5 min), followed by a final extension of 72°C for 10 min. The PCR products were purified and sequenced by the Tsingke Biological Technology Company. The *ERG11* sequences were aligned using BLAST and compared with the related published GenBank sequence for *C. albicans* SC5314 (Gene ID: 3641571), *C. parapsilosis* ATCC 22019 (Gene ID GQ302972.1), *C. tropicalis* ATCC 750 (Gene ID: M23673), *C. glabrata* CBS138 (Gene ID: XM 445876), and *C. haemulonis* (Gene ID: XM_025486744.1). The *FKS1* sequences were compared with the reference sequences of *C. tropicalis* ATCC 750 (Gene ID: EU676168) and *C. glabrata* (Gene ID: XM_446406).

Caseinase Activity

Caseinase activity was measured by the single diffusion technique in SDA plates containing 1% casein (Ramesh et al., 2011). A standard inoculum (10^6 cells/mL) was prepared in saline solution from an overnight yeast culture for each isolate and 10 μL of this standard inoculum was plated. Plates were incubated at 37°C for 5 days. Three independent replicates were tested for each strain. Colony diameter (a) and colony diameter plus precipitation zone (b) were measured using a vernier caliper (Guanglu, China). Phospholipase index (defined as Pz = a/b, based on the study by Price et al) was used to evaluate the extent of hydrolytic enzyme production by various *Candida* species (Price et al., 1982). According to this definition, a lower Pz value indicates a greater enzymatic activity, which was scored into four categories as follows: Pz = 1.00 was defined as no enzymatic activity, Pz = 0.90–0.99 as weak enzymatic activity, Pz = 0.89–0.70 as moderate activity, and Pz < 0.69 as strong enzymatic activity (Price et al., 1982).

Hemolysin Activity

Hemolysin assay for *Candida* strains was measured using blood agar plates that were prepared by adding 6% human blood to 100 mL of SDA supplemented with 3% glucose (final concentration, wt/vol; pH = 5.6) (Neji et al., 2017). Standard inoculum (10 μL of 10^6 cells/mL) was spotted onto the blood plates, plates were incubated at 37°C for 5 days, and hemolytic activity was measured and evaluated using the method described by Price et al. (1982). The assay was performed in triplicate for each isolate.

Biofilm Formation

Biofilm production in *Candida* species was evaluated using a modified crystal violet assay described elsewhere (Silva et al., 2009; Mancera et al., 2015; Neji et al., 2017). Briefly, biofilm formation was spectrophotometrically determined wherein each well of a 96-well polystyrene plate was treated with 200 μL of 5% BSA (dissolved in sterilized PBS) at 4°C for 48 h and washed once with sterile PBS. Each experimental condition was designed such that five replicates were distributed in one column of the microplate. Sterility controls, i.e., without cell suspension, were used as a negative control to ensure no accidental contamination during treatment. Clinical isolates and the control strain Sc5314 were first cultured on SDA plates at 30°C for 24 h and then in 5 mL SDA medium overnight at 30°C with shaking. Cells were collected by centrifugation at 2458 g for 5 min, washed twice with sterilized PBS, and resuspended in spider medium (20 g/L nutrient broth, 20 g/L mannitol, and 4 g/L K_2HPO4; pH 7.2). The turbidity of each strain suspension was spectrophotometrically adjusted to OD_{600} = 0.5; 200 μL of the cell suspension (OD_{600} = 0.5) was transferred to each well of the 96-well plates, which were incubated at 37°C for 90 min. Next, the strain suspension was removed, 200 μL of fresh spider medium was added, and the plates were incubated at 37°C for 48 h without shaking (static culture). Plates were washed twice

with PBS to remove nonadherent cells after the adhesion stage and biofilms were fixed by incubation with 200 µL methanol for 30 min. Afterward, the plates were dried at room temperature and 200-µL 1% crystal violet (Solarbio, China) was added to each well and incubated for 30 min. The wells were then gently washed with water until the washing was colorless and incubated with 200 µL of acetic acid for 1 h to dissolve the biofilm. The absorbance of the obtained solution was read at 620 nm in a microtiter plate reader (Molecular Devices, USA). Absorbance values of the controls were subtracted from test values to eliminate background interference.

Statistical Analysis

Data were analyzed with SPSS (version 25.0) and GraphPad Prism (version 5.0). Unless otherwise mentioned, data are presented as mean ± standard deviation (SD). The normality of data distribution was evaluated using the D' Agostino-Pearson omnibus normality test. Differences between two independent groups were performed with the nonparametric Mann–Whitney U test or the Kolmogorov–Smirnov Z test for the relative values. A p value of ≤0.05 was defined as statistically significant.

RESULTS

Prevalence of Invasive *Candida* spp. Isolates

A total of 105 patients were enrolled in this study. The study population comprised 77 (73.3%) males and 28 (26.7%) females with a median age of 53 years (range 0–87 years). Although most isolates were obtained from patients hospitalized in the ICU (n = 31, 28.18%), 26 (23.6%) came from the department of gastroenterology, 14 (12.73%) from the burns unit, 11 (10.0%) from emergency services unit, 5 (4.54%) from infectious diseases unit, 4 (3.6%) from the hematology department, and 17 (15.5%) from other non-ICU departments (**Table 1**). Overall, 22.9% (24/105) of the patients died, mainly from acute pancreatitis, which accounted for approximately 37.5% of all mortality cases. Antifungal use (oral or injected) was reported for 42.9% (45/105) of the patients. In our study, the most common antifungal drug used was fluconazole (44.4%, 20/45), followed by voriconazole (40.0%, 18/45) and caspofungin (15.6%, 7/45).

A total of 110 clinical isolates (40 C. *albicans*, 37 C. *parapsilosis*, 21 C. *tropicalis*, 9 C. *glabrata*, 2 C. *rugose*, and 1 C. *haemulonii* isolates) were studied (**Figure 1**). Each isolate was obtained from different patients, with the following exceptions: *C. albicans* NCU_B040, NCU_B049, and NCU_B059, and *C. tropicalis* NCU_B047 and NCU_B050 strains, were acquired from the blood of one patient and three strains of *C. glabrata* (NCU_B103, NCU_O109, and NCU_O145) were isolated from different source sites of the same patient.

Sources of the 110 isolates (**Table 2**) were predominantly blood (n = 64, 58.18%), followed by catheter tips (n = 9, 8.18%) and drainage fluid (n = 17, 15.45%), and also included abscesses (1.82%), secretions (1.82%), and other sources (14.55%). Furthermore, as shown in **Table 2** and **Figure 2**, *C. albicans* could be isolated from a wider range of specimens than other species. However, *C. haemulonii* and *C. rugose* were isolated only from blood.

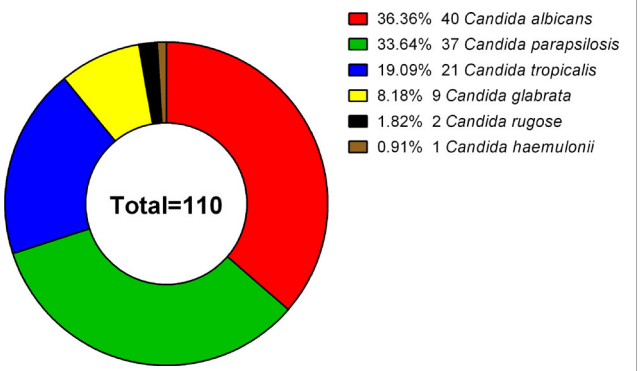

FIGURE 1 | Species distribution of 110 clinical isolates. The 110 *Candida* strains analyzed included 40 C. *albicans* (36.36%), 37 C. *parapsilosis* (33.64%), 21 C. *tropicalis* (19.09%), 9 C. *glabrata* (8.18%), 2 C. rugose (1.82%), and 1 C. *haemulonii* (0.91%) isolate.

TABLE 1 | Distribution of *Candida* isolates by a source of isolation.

	C. albicans	*C. parapsilosis*	*C. tropicalis*	*C. glabrata*	*C. rugosa*	*C. haemulonii*	Total
ICUs	9 (8.18%)	11 (10.00%)	4 (3.64%)	6 (5.45%)	1 (0.91%)	0	31 (28.18%)
Department of gastroenterology	12 (10.91%)	7 (6.36%)	5 (4.54%)	2 (1.82%)	0	0	26 (23.64)
Department of burn wound	5 (4.54%)	4 (3.64%)	4 (3.64%)	0	1 (0.91%)	0	14 (12.73)
Department of emergency	6 (5.45%)	1 (0.91%)	3 (2.73%)	1 (0.91%)	0	0	11 (10.00%)
Department of infectious diseases	0	4 (3.64%)	1 (0.91%)	0	0	0	5 (4.54%)
Department of hematology	0	0	4 (3.64%)	0	0	0	4 (3.64%)
Department of orthopedics	1 (0.91%)	1 (0.91%)	0	0	0	0	2 (1.82%)
Department of urology	3 (2.73%)	0	0	0	0	0	3 (2.73%)
Department of general surgery	1 (0.91%)	2 (1.82%)	0	0	0	0	3 (2.73%)
Department of Nephrology	0	2 (1.82%)	0	0	0	0	2 (1.82%)
Department of neonatal pediatrics	1 (0.91%)	1 (0.91%)	0	0	0	1 (0.91%)	3 (2.73%)
Department of ENT	1 (0.91%)	0	0	0	0	0	1 (0.91%)
Department of maternity	1 (0.91%)	0	0	0	0	0	1 (0.91%)
Plastic Surgery	0	1 (0.91%)	0	0	0	0	1 (0.91%)
Cardiothoracic Surgery	0	3 (2.73%)	0	0	0	0	3 (2.73%)
Total	40 (36.36%)	37 (33.64%)	21 (19.09%)	9 (8.18%)	2 (1.82%)	1 (0.91%)	110 (100%)

Molecular Phylogenetic Analysis of the Invasive *Candida* Spp. Isolates

To explore the diversity of the isolated *Candida* spp., RAPD analysis of the four major species of clinical isolates was performed with five random primers using the UPGMA method. *C. rugose* and *C. haemulonii* strains were not analyzed because of their low isolation rates. The number of patterns generated by *C. albicans*, *C. parapsilosis*, *C. tropicalis*, and *C. glabrata* isolates with each primer changed between 3–10, 4–12, 3–10, and 6–10, respectively. All primers were used for the dendrogram construction.

We recognized 32 distinct RAPD profiles among the 40 C. *albicans* isolates analyzed. **Figure 2A** shows the cluster analysis of the electrophoretic bands of the *C. albicans* isolates, and the Sj value ranged from 0.58 to 1.00. Four strains presented unique patterns (C1, G1, H1, and I1) and were considered to be unrelated. At a limiting point of 0.80, 36 C. *albicans* isolates could be allocated into five clusters (A, B, and D–F). For *C. parapsilosis*, the primers produced up to 12 bands, and therefore, this set displayed the greatest discriminatory power. In their dendrogram, *C. parapsilosis* isolates could be grouped into seven clusters (K–P, and R) when 0.80 was assumed as the limiting value, whereas three isolates (NCU_B023, NCU_O082, and NCU_B148) were deemed unrelated (**Figure 2B**). Among the 21 C. *tropicalis* isolates, 18 RAPD profiles could be distinguished, and they were accommodated into seven clusters (T–Z) (**Figure 2C**). Six genotypes (a1– a3, b1, c1, and d1) were observed upon the RAPD analysis of the nine *C. glabrata* isolates. A total of 6 C. *glabrata* isolates with a similarity level >80% were allocated into the same cluster; of these, NCU_B103, NCU_O109, and NCU_O145 were different sites of the same patient and were grouped in the same cluster. Three genotypes (b1, c1, and d1) were represented by only one isolate each, and they were considered unrelated (**Figure 2D**).

Antifungal Susceptibility for the Invasive *Candida* spp. Isolates

Table 3 shows the susceptibility profiles of the *Candida* species to the nine antifungal drugs tested. MICs were also determined for two rare yeast species (one *C. haemulonii* and two *C. rugose* isolates); however, fewer than five isolates were studied for these two *Candida* spp. Furthermore, drug-resistant strains of *C. haemulonii* and *C. rugose* could not be accurately determined because of a lack of validated clinical breakpoints. Nevertheless, on the basis of CLSI document M27-S4, we found that nine isolates were resistant to azoles. The MIC_{90} values for fluconazole were 1–2, 1, 4, and 32 μg/mL for *C. albicans*, *C. parapsilosis*, *C. tropicalis*, and *C. glabrata*, respectively. MIC_{90} values for voriconazole, itraconazole, and posaconazole were in the range of ≤0.08–1, 0.12–1, and 0.06–2 μg/mL, respectively, for *C. albicans*, *C. parapsilosis*, *C. tropicalis*, and *C. glabrata*, respectively. In addition, MIC for fluconazole ranged from 4 to 16 μg/mL for *C. rugose* isolates, whereas that for *C. haemulonii* was high at 128 μg/mL. MIC_{90} values of echinocandins (anidulafungin, caspofungin, and micafungin) against *C. parapsilosis* were higher than those for *C. albicans*, *C. tropicalis*, and *C. glabrata*.

TABLE 2 | Comparison of the virulence factors among *Candida* strains isolated from different sources (mean optical density ± SD).

		C. albicans			*C. parapsilosis*			*C. tropicalis*			*C. glabrata*			*C. rugosa*			*C. haemulonii*		
		N	Mean Abs ± SD	Range	N	Mean Abs ± SD	Range	N	Mean Abs ± SD	Range	N	Mean Abs ± SD	Range	N	Range		N	Range	
Blood (N=64)	Biofilm	22	0.139 ± 0.094	0.027-0.295	21	0.646 ± 0.778	0.007-2.492	13	0.438 ± 0.454	0.059-1.546	5	0.112 ± 0.011	0.095-0.123	2	0.085-0.098		1	0.061-0.061	
	Caseinase		0.357 ± 0.078	0.257-0.504		0.484 ± 0.112	0.330-0.703		0.417 ± 0.139	0.310-0.669		0.325 ± 0.024	0.300-0.355		0.516-0.657			0.453-0.453	
	Hemolysin		0.309 ± 0.047	0.233-0.456		0.420 ± 0.135	0.325-0.555		0.357 ± 0.049	0.287-0.457		0.221 ± 0.019	0.207-0.246		0.514-0.555			0.336-0.336	
Catheter tips (N=9)	Biofilm	7	0.312 ± 0.291	0.065-0.768	2	0.110 ± 0.141	0.010-0.209	0	0		0	0		0			0	0	
	Caseinase		0.311 ± 0.031	0.277-0.363		0.473 ± 0.076	0.419-0.527												
	Hemolysin		0.318 ± 0.052	0.336-0.373		0.390 ± 0.042	0.360-0.420												
Drainage fluid (N=17)	Biofilm	3	0.203 ± 0.181	0.040-0.399	6	0.986 ± 1.157	0.004-2.514	6	0.150 ± 0.121	0.051-0.358	2	0.178 ± 0.098	0.109-0.247	0			0		
	Caseinase		0.316 ± 0.016	0.298-0.329		0.456 ± 0.045	0.415-0.536		0.380 ± 0.053	0.330-0.471		0.328 ± 0.015	0.317-0.338						
	Hemolysin		0.347 ± 0.059	0.304-0.414		0.394 ± 0.028	0.361-0.440		0.348 ± 0.049	0.287-0.418		0.313 ± 0.090	0.249-0.376						
Abscess (N=2)	Biofilm	1	0.127	0.127-0.127	1	0.522	0.522-0.522	0	0		0	0		0			0		
	Caseinase		0.295	0.295-0.295		0.403	0.403-0.403												
	Hemolysin		0.383	0.383-0.383		0.44	0.440-0.440												
Secretion (N=2)	Biofilm	2	0.296 ± 0.010	0.289-0.303	0	0	0	0	0		0	0		0			0		
	Caseinase		0.325 ± 0.017	0.313-0.337															
	Hemolysin		0.291 ± 0.024	0.274-0.308															
Others (N=16)	Biofilm	5	0.174 ± 0.103	0.049-0.328	7	0.876 ± 0.940	0.016-2.006	2	1.432 ± 1.667	0.253-2.611	2		0.109-0.109	0			0		
	Caseinase		0.319 ± 0.018	0.300-0.344		0.425 ± 0.072	0.345-0.558		0.365 ± 0.083	0.306-0.423		0.309 ± 0.004	0.306-0.311						
	Hemolysin		0.358 ± 0.034	0.312-0.396		0.389 ± 0.042	0.302-0.434		0.374 ± 0.024	0.357-0.391		0.241 ± 0.014	0.231-0.251						

N, number of tested isolates; SD, standard deviation.

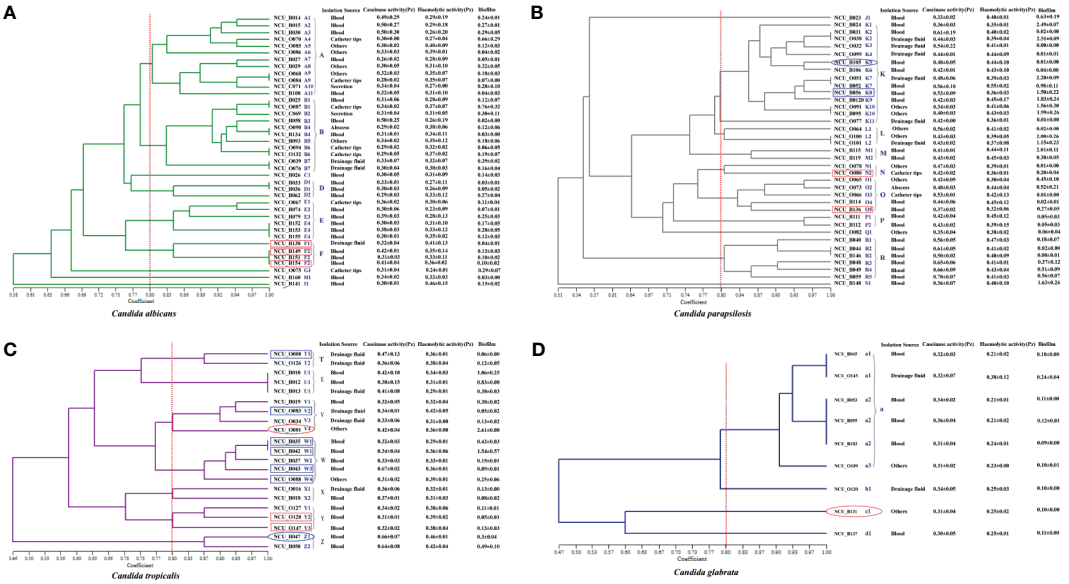

FIGURE 2 | Dendrogram presenting the genetic relatedness of 107 *Candida* spp. based on the random amplified polymorphic DNA (RAPD) data. The virulence factors (i.e., caseinase, hemolysin, and biofilm), drug resistance, and specimen sources are indicated in the figure. The vertical line divides the strains based on the level of genetic similarity into related and unrelated strains. The red boxes indicate azole resistance (fluconazole and voriconazole), whereas the blue boxes indicate azole-susceptible (S) dose dependence (SDD). Red ellipses represent resistance to echinocandins, while the blue ellipses represent intermediate resistance to micafungin. **(A)** Dendrogram of 40 *C. albicans* isolates. **(B)** Dendrogram of 37 *C. parapsilosis* isolates. **(C)** Dendrogram of 21 *C. tropicalis* isolates. **(D)** Dendrogram of 9 *C. glabrata* isolates.

Table 4 shows the overall drug susceptibility pattern of these four *Candia* species against the five antifungal drug types tested. All *C. albicans* and *C. parapsilosis* isolates exhibited 100% of susceptibility to echinocandins, whereas one strain of *C. glabrata* was resistant (**Table 4**). Overall resistance was greatest against fluconazole (6.36%), followed by voriconazole (4.55%). As far as species-specific antifungal resistance rates were concerned, *C. tropicalis* was resistant to almost all drugs tested (except for caspofungin), with the least resistance rate of 4.76%. Isolates of *C. tropicalis* were susceptible to fluconazole and voriconazole with sensitivity rates of 80.95% and 61.90%, respectively. It is worth noting that the current data were insufficient for distinguishing between drug-resistant and -sensitive strains of *C. glabrata* based on the CLSI document M27-S4 (Institute, 2012). One (11.11%) of the nine *C. glabrata* strains was resistant to echinocandins, and all *C. glabrata* isolates met the criteria for "susceptible-dose dependence (S-DD)" for fluconazole (**Table 4**).

Mutations In *ERG11* and the HS Regions of *FKS1*

Comparison of the complete ORF of *ERG11* of the eight isolates with that of the published wild-type sequences revealed 12 mutations, of which five were silent without any amino acid changes (data not shown). Seven missense mutations were detected in these seven strains. Of the seven distinct amino acid substitutions identified, three (i.e., A114S, Y132H, and Y132F) have been reported previously (Morio et al., 2010). One strains (NCU_O080) only showed a synonymous mutation. Mutations in *ERG11* and the resultant amino acid changes are indicated in the **Table 5**. DNA sequencing of HS1 and HS2 of the drug target *FKS1* that is known to confer echinocandin resistance was performed on one *C. tropicalis* isolate (NCU_O081) and one *C. glabrata* isolate (NCU_B131). However, no mutation was detected in the hotspot regions of *FKS1* (**Supplementary Table 2**).

Virulence Evaluation of the Invasive *Candida* spp. Isolates

Several virulence factors are involved in the pathogenesis of candidiasis, and they allow the fungal cells to escape or evade host defense mechanisms. These include phenotypic switching, biofilm formation, and secretion of multiple hydrolases (Neji et al., 2017). We investigated three virulence factors, namely, biofilm, caseinase, and hemolysin.

Caseinase Activity

All 110 isolates were caseinase positive and 109 displayed strong activity. The mean Pz value in caseinase-positive *C. albicans* and *C. parapsilosis* isolates was 0.34 ± 0.06 and 0.47 ± 0.10, respectively, indicating a lower enzymatic activity in *C. parapsilosis* than that in *C. albicans* (**Table 2** and **Figure 2**). Of the 37 C. *parapsilosis* isolates, 36 displayed strong enzymatic activity, whereas one had moderate activity. All *C. tropicalis* (mean Pz = 0.40 ± 0.11) *and C. glabrata* isolates (mean Pz = 0.32 ± 0.02) were strong caseinase producers. No appreciable

TABLE 3 | Minimum inhibitory concentration values (μg/mL) for the *Candida* isolates.

Antifungals	*C. albicans*			*C. parapsilosis*			*C. tropicalis*			*C. glabrata*			*C. rugosa*	*C. haemulonii*
	MIC range	MIC50	MIC90	MIC range	MIC50	MIC90	MIC range	MIC50	MIC90	MIC range	MIC50	MIC90	MIC range	MIC range
Anidulafungin	≤0.015-0.12	0.03	0.12	0.06-2	1	1	0.03-2	0.12	0.25	≤0.015-0.12	0.03	0.06	0.25-2	0.06-0.06
Caspofungin	0.015-0.25	0.06	0.12	0.03-2	0.5	1	0.06-0.5	0.06	0.12	0.03-0.5	0.06	0.06-0.12	0.5-8	0.06-0.06
Micafungin	≤0.008-0.12	≤0.008	0.015	0.12-4	1	1	0.015-2	0.03	0.06	≤0.008-2	0.015	0.015	0.06-0.5	0.12-0.12
Fluconazole	≤0.12-32	0.25	1-2	0.5-64	0.5	1	0.5->256	2	4	1-32	16	32	4-16	128-128
Voriconazole	≤0.008-1	≤0.008	≤0.008-1	≤0.008-2	≤0.008	0.03	≤0.008->8	0.12	0.25	0.06-2	1	1	0.06-0.25	8-8
Itraconazole	≤0.015-0.12	0.03-0.06	0.12	≤0.015-0.5	0.06-0.12	0.12	0.03-1	0.25	0.5	0.12-2	1	1	0.12-0.25	16-16
5-Flucytosine	≤0.06-8	≤0.06	0.12	≤0.06-0.5	≤0.06	≤0.06	≤0.06-0.12	≤0.06	≤0.06	≤0.06-0.5	≤0.06	≤0.06	0.12-0.25	64-64
Amphotericin B	≤0.12-0.5	0.5	0.5	≤0.12-2	0.25	0.25	≤0.12-1	0.5	1	≤0.12-2	0.5	0.5-1	0.5-1	0.5-0.5
Posaconazole	≤0.008-1	0.015-0.03	0.06	0.015-0.5	0.06	0.06	0.015-1	0.25	0.5	0.5-8	2	2	0.06-0.12	8-8

difference was noted in the caseinase activity from any of the specimen sources (**Figure 3**).

Hemolytic Activity

All of the tested isolates demonstrated strong hemolytic activity on human blood SDA plates with Pz values <0.69 (**Figure 2**). The mean Pz values for hemolytic activity were 0.32 ± 0.05, 0.41 ± 0.04, 0.36 ± 0.05, 0.25 ± 0.05, and 0.47 ± 0.10 for *C. albicans*, *C. parapsilosis*, *C. tropicalis*, and *C. glabrata*, respectively (**Table 2**). No noticeable differences were detected in the hemolytic activity of the strains from different sources (**Figure 3**).

Biofilm Formation

Figure 2 and **Table 2** shows the results of biofilm quantification. Although *C. parapsilosis* isolates produced greater total biomass (average Abs_{620} = 0.712) than did *C. albicans* (average Abs_{620} = 0.186, $p < 0.05$) or *C. tropicalis* isolates (average Abs_{620} = 0.450; **Figure 4**), one *C. tropicalis* isolate (NCU_O081) yielded the greatest biomass (Abs_{620} = 2.611 ± 0.087), and this was significantly higher than that of *C. parapsilosis*. By contrast, all *C. glabrata* strains were low biofilm producers with Abs_{620} values ranging between 0.095 and 0.247. No significant differences were found in the extent of biofilm formation among all *C. glabrata* isolates ($p > 0.05$). Among *C. rugose* and *C. haemulonii*, it was impossible to derive any conclusions because of the small sample size. Furthermore, strains isolated from drainage fluid generally produced more biofilm than those isolated from blood, except for *C. tropicalis* species. *C. albicans* isolates obtained from catheter tips were the highest biofilm producers, whereas, for *C. parapsilosis*, these were the isolates obtained from drainage fluids (**Figure 3** and **Table 2**).

DISCUSSION

Invasive candidiasis is an emerging infection that is closely related to advances in medical technology, and it is widely recognized as a major cause of morbidity and mortality in high-risk groups such as immunosuppressed patients and those admitted to ICUs. At least 15 different species of *Candida* can cause human diseases, but a majority of the invasive infections are caused by five pathogens—*C. albicans*, *C. parapsilosis*, *C. glabrata*, *C. tropicalis*, and *C. krusei* (Pappas et al., 2018). Although *C. albicans* is currently the most common pathogen, non-*albicans Candida* spp. could collectively represent >50% of all bloodstream isolates in some regions (Pappas et al., 2018). A study of 141 clinical *Candida* specimens in Brazil reported that *C. albicans* is the most frequently isolated species (45.4%), followed by *C. parapsilosis* (28.4%), *C. tropicalis* (14.2%), and *C. glabrata* (1.4%) (Neufeld et al., 2015). A 6-year retrospective analysis of 351 patients with candidiasis showed that 48.1% of the candidemia episodes were due to *C. albicans*, followed by *C. parapsilosis* (25.1%) and *C. glabrata* (11.7%) (Ulu Kilic et al., 2017). In recent years, studies have described an increase in the incidence of *C. parapsilosis* infection (Ulu Kilic et al., 2017). We also show that *C. albicans* is the most prevalent disease-causing *Candida* spp., followed by

TABLE 4 | Antifungal susceptibility testing results of four main *Candida* species against five antifungal drugs.

Antifungal	*C. albicans* (N = 40)				*C. parapsilosis* (N = 37)				*C. tropicalis* (N = 21)				*C. glabrata* (N = 9)			
	S	S-DD	I	R	S	S-DD	I	R	S	S-DD	I	R	S	S-DD	I	R
Anidulafungin	40		0	0	37		0	0	20		0	1	8		0	1
Caspofungin	40		0	0	37		0	0	20		1	0	8		0	1
Micafungin	40		0	0	36		1	0	19		1	1	8		0	1
Fluconazole	37	0		3	34	1		2	17	2		2	0	9	0	0
Voriconazole	37	1		2	35	1		1	13	6		2				

S, susceptible; SDD, susceptible-dose dependent; I, intermediate; R, resistant.

TABLE 5 | Polymorphic sites in *ERG11* sequences.

Species	Strains number	Resistance to fungal drugs	Gene	Base mutation sits	Amino acid substitution
C. albicans	NCU_B138	Fluconazole	*ERG11*	C368T/T394C	T123I/Y132H
	NCU_B149	Voriconazole, Fluconazole	*ERG11*	G340T/T768C	A114S
	NCU_B154	Voriconazole, Fluconazole	*ERG11*	G340T/T768C	A114S
C. parapsilosis	NCU_O080	Voriconazole, Fluconazole	*ERG11*	T591C	None
	NCU_B136	Fluconazole	*ERG11*	A395T/T591C/G1193T	Y132F/R398I
C. tropicalis	NCU_B128	Voriconazole, Fluconazole	*ERG11*	T225C/G264A/A395T/C461T	Y132F/S154F
	NCU_B147	Voriconazole, Fluconazole	*ERG11*	G264A/C461T/G1362A/G1504A	S154F/D454N
C. haemulonii	NCU_B011	Voriconazole, Fluconazole	*ERG11*	A395T	Y132H

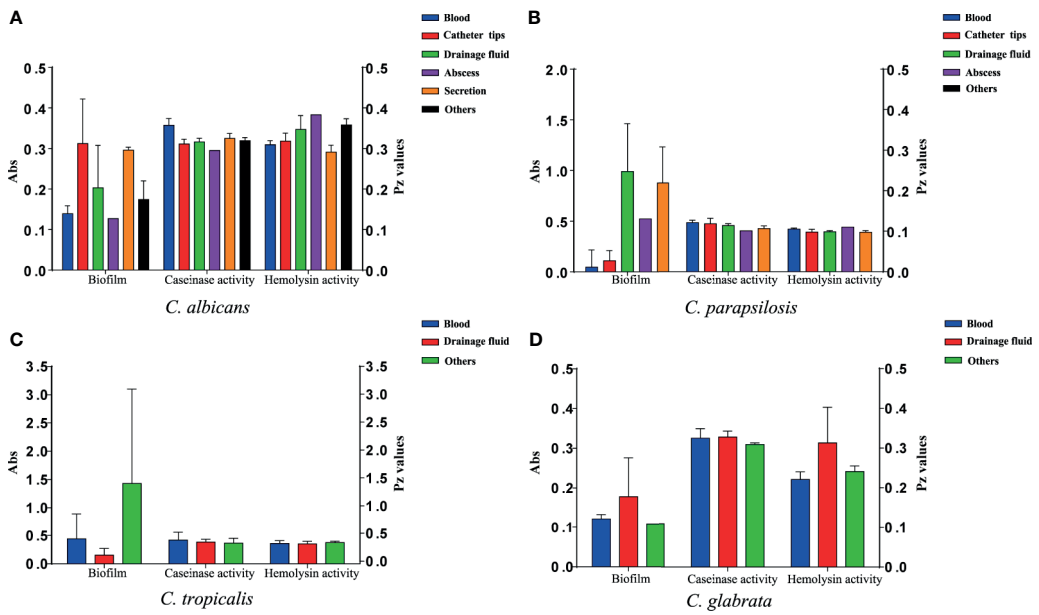

FIGURE 3 | Virulence level (biofilm biomass, caseinase activity, and hemolysin activity) of the 107 *Candida* species isolates from different specimen sources. Y-axis (far left panel): biofilm biomass (positively correlated with virulence); Y-axis (far right panel): the Pz values of caseinase and hemolysin activities (negatively correlated with virulence). No significant differences were noted in these factors. **(A)** The virulence level of 40 *C. albicans* isolates from different specimen sources. **(B)** The virulence level of 37 *C. parapsilosis* isolates from different specimen sources. **(C)** The virulence level of 21 *C. tropicalis* isolates from different specimen sources. **(D)** The virulence level of 9 *C. glabrata* isolates from different specimen sources.

C. parapsilosis, *C. tropicalis*, and *C. glabrata*, and that most isolates were obtained from patients hospitalized in ICUs.

RAPD analysis is a valuable tool for studying the genetic epidemiology of *Candida* infections, and multiple studies have confirmed its applicability and high discriminatory power for *Candida* genotyping at a local level (Paluchowska et al., 2014). Such accurate identification and molecular typing of *Candida* species provide valuable information for the prevention and

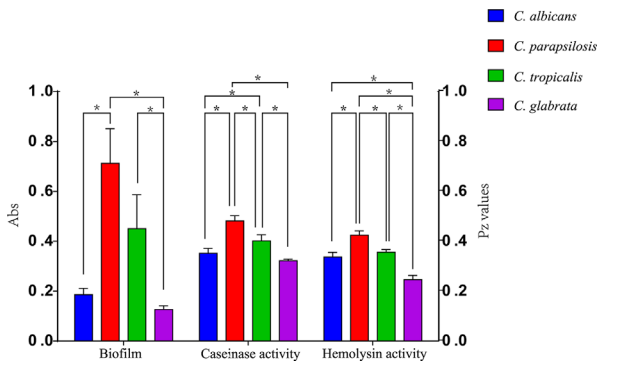

FIGURE 4 | Comparison of the virulence levels (biofilm biomass, casein activity and hemolysin activity) of four *Candida* species. * indicates statistically significant ($p < 0.05$).

control of nosocomial infections caused by these yeasts. Thus, the genetic diversity of 107 *Candida* species comprising *C. albicans* (n = 40), *C. parapsilosis* (n = 37), *C. tropicalis* (n = 21), and *C. glabrata* (n = 9), when an Sj value of 0.80 was defined as the limiting point, showed that *C. parapsilosis* and *C. tropicalis* isolates were more diverse than *C. albicans* isolates because of the greater range of Sj values in the dendrogram generated using the five primer pairs. The present study revealed two identical *C. albicans* isolates (NCU_B153 and NCU_B155) from the blood of two different patients admitted to ICU from different admission years. In addition, two *C. glabrata* isolates (NCU_B045 and NCU_B055) from different patients sharing the same ward showed similar genotype profiles. Notably, the aforementioned *C. glabrata* strains were isolated within the same month. These isolates may have come either from the patients, hospital personnel, medical devices, or environment, suggesting that *Candida* infection can spread exogenously.

Establishing antifungal susceptibility patterns among *Candida* species isolates from clinical specimens was an important aspect of our study. Fluconazole has remained the drug of choice for treating candidemia over several years now because of its efficacy against clinical *Candida* infection (Pappas et al., 2004; Autmizguine et al., 2018). However, the current treatment guidelines recommend the use of echinocandins as the first-line empirical treatment because of the increased resistance and treatment failure associated with the use of fluconazole (Bassetti et al., 2018; Zeng et al., 2019). Although we found that most isolates were sensitive to the echinocandins, one *C. glabrata* isolate was simultaneously resistant to three echinocandins and one *C. tropicalis* isolate was resistant to both anidulafungin and micafungin. Resistance to fluconazole (6.36%, 7/110) was high among the isolates tested here, and some strains displayed multiazole resistance, i.e., simultaneous resistance to both fluconazole and voriconazole among *C. albicans*, *C. parapsilosis*, and *C. tropicalis* isolates were 5% (2/40), 2.70% (1/37), and 9.52% (2/21), respectively. The appearance of multiazole-resistant strains could be associated with the high rates of azole usage in hospitals (36.2%, 38/105). The azole-resistant rates of patients with azole treatment to *C. albicans*, *C. parapsilosis*, *C. tropicalis* and *C. glabrata* were 30.0% (3/10), 25.0% (2/8), 25.0% (2/8), and 33.3% (1/3). Among these, 37.5% of the patients received long-course azole treatment for >15 days, which may be a risk factor for azole resistance. Although only two *C. rugose* strains and one *C. haemulonii* strain were isolated in our study, their high MICs against antifungal drugs could have been a cause for concern. In our study, the azole-resistance rate of *C. albicans* (7.5%, 3/10), *C. parapsilosis* (5.4%, 2/37), and *C. tropicalis* (9.5%, 2/21) were similar to those reported by Maubon et al. (Maubon et al., 2014). However, the resistance rate of *C. albicans* (7.5%) was significantly lower than that reported for a hospital in Southwest China (>20.0%) (Zeng et al., 2019). This discrepancy may be induced by the difference in the regional population, medical resources, and distribution of patient types.

DNA sequencing of the two drug target genes, *ERG11* and *FKS1*, was performed using drug-resistant strains. The pharmacological target of azoles is the enzyme 14-α-demethylase (encoded by *ERG11*), which is an enzyme for ergosterol biosynthesis (Spettel et al., 2019). The mutation leading to amino acid substitution in the *ERG11* sequence is one of the main mechanisms contributing to azole resistance in clinical isolates (Morio et al., 2010). As observed in previous studies, all *ERG11* mutations in the present study also occurred at three diffuse hotspot regions: amino acids 105–165, 266–287, and 405–488 (Marichal et al., 1999). The most common amino acid substitution in our study was 132aa (50%, 4/8) in the azole-resistant strains. A single Y132H substitution has been shown to reduce susceptibility to voriconazole and fluconazole, with MIC increased by four and eight times, respectively (Wang et al., 2005). The Y132H substitution was detected in one *C. albicans* isolate (NCU_B138) and one *C. haemulonii* isolate (NCU_B011). The Y132F substitution was also detected in a *C. parapsilosis* isolate (NCU_B136) and a *C. tropicalis* isolate (NCU_B128). A previous study confirmed that the Y132H substitution interfered with the interaction between the heme center of the enzyme and fluconazole, thereby reducing the affinity of the target enzyme to fluconazole, leading to fluconazole resistance (Kelly et al., 1999). Hence, our data support the involvement of Y132F and Y132H in azole resistance and their potential use as predictive markers of azole resistance. *FKS1* encode the β-1,3-glucan synthase, which is responsible for the synthesis of fungal cell wall and is the target enzyme of echinocandin (Sfeir et al., 2020). The most common cause of resistance is the serine-to-proline mutation in the HS1 region of *FKS1* at the position 654 (Sfeir et al., 2020). No mutation was detected in the HS1 and HS2 regions of *FKS1*, although some mutations in other regions of this gene may have been missed because of sequencing only the HS1 and HS2 regions. Notably, the finding of amino acid substitutions in these isolates does not indicate that there may not be other coexisting mechanisms of antifungal resistance, such as the overexpression of *ERG11*, *CDR1*, and/or *MDR1*, although these points were not proved in our study.

Several virulence factors in *Candida* species are indispensable for their ability to cause disease, and these include extracellular hydrolytic enzymes, particularly proteases, phospholipases, and

hemolysins, which facilitate food acquisition, adherence, colonization, invasion, diffusion, and escape from host immune responses (Abbes et al., 2017; Figueiredo-Carvalho et al., 2017). Accurate identification of putative virulence factors in *Candida* spp. is critical for predicting the response of antifungal drugs and detecting the emergence of strains with greater resistance. França et al. have reported that although 68% of patients with candidiasis had been prescribed antifungal therapy with a favorable susceptibility profile, the mortality rate was 56%, implying that other factors are involved in determining patient prognosis (França et al., 2008). Two such factors may be biofilm formation and the expression of virulence-associated factors. Biofilm formation is a major virulence factor (Mba and Nweze, 2020) because, when generated on host tissues and indwelling medical devices such as central venous catheters, they hinder drug diffusion and render infection eradication extremely difficult (Chen et al., 2020). We compared certain virulence factors among *Candida* species that are detectable in a laboratory environment, such as caseinase, hemolysin, and biofilm production, to assess the pathogenic potential of *Candida* species.

Proteases can degrade the host epithelial and mucosal barrier proteins such as albumin, collagen, and mucin. They also help *Candida* resist attacks by host immune system thorough the degradation of antibodies, complements, and cytokines (Borst and Fluit, 2003; Neji et al., 2017). Casein has also been widely reported as a substrate to evaluate the protease activity of pathogenic strains (Fernandes et al., 2012; Neji et al., 2017). Our results show that all the *Candida* spp. were caseinase producers with a strong enzymatic activity (99.09%). Furthermore, all *C. glabrata* strains showed a strong enzymatic activity and our results are consistent with findings reported by Abbes et al. who also tested *C. glabrata* isolates (Abbes et al., 2017). However, these results are in contrast to those described by Figueiredo-Carvalho et al. who reported no caseinase activity in 91 C. *glabrata* isolates (Figueiredo-Carvalho et al., 2017). Using casein as a substrate, all isolates of *C. albicans*, *C. parapsilosis*, *C. tropicalis*, *C. haemulonii*, and *C. rugose* were found to be proteinase positive. Lower caseinase activities were detected for *C. parapsilosis* than for *C. albicans*, *C. tropicalis*, and C. *glabrata* isolates with a statistically significant difference (**Figure 4**); these differences were independent of the specimen sources and genotypes (**Figure 4**; **Supplementary Figure 1**).

Hemolytic activity is another virulence factor exhibited by pathogenic microorganisms, which enables fungal pathogens to utilize hemoglobin as an iron source for growth in the iron-scarce host environment (Weissman et al., 2021). Previous studies have shown a close relationship between cellular iron and drug susceptibility in *C. albicans* (Prasad et al., 2006), and iron uptake mechanisms have also been reported to be necessary for the virulence of C. *glabrata* (Figueiredo-Carvalho et al., 2017). In our study, all *Candida* spp. showed strong hemolytic activity. Moreover, *C. tropicalis* exhibited greater hemolysin production than *C. glabrata*. We noted that the hemolytic activity of *C. albicans* isolates was higher than that of *C. parapsilosis* isolates; these findings are inconsistent with those of previous studies (**Figure 4**) (Chin et al., 2013; Neji et al., 2017).

Several studies have established the importance of biofilm formation in clinical infections due to *Candida* strains (Nett and Andes, 2006; Akers et al., 2015). Estivill et al. found that biofilm formation was observed on implantable medical devices and all *Candida* strains tested (including *C. albicans*, *C. parapsilosis*, *C. tropicalis*, *C. glabrata*, and *C. krusei*) were able to form biofilms (Estivill et al., 2011). Our results correspond with those reported previously, especially that *C. glabrata* showed no biofilm production (Marak and Dhanashree, 2018). This is likely, in part, to be related to its intrinsic inability to form hyphae (Seidler et al., 2006). More *C. albicans* isolates produced biofilms than *C. parapsilosis* or *C. tropicalis* isolates, but *C. rugose* and *C. haemulonii* showed no biofilm production in our study. We also performed subgroup analyses by specimen source and found that isolates from drainage fluids exhibited greater biofilm formation than those originating from blood, except among *C. tropicalis* isolates.

The association between clusters and virulence factors was compared (**Supplementary Figure 1**). No significant difference was noted in the hemolytic and caseinase activities among the strains of different genotypes, although their biofilm production was found to vary with the different clusters. For instance, for *C. parapsilosis*, three clusters (K–M) showed higher biofilm formation ability than the others (**Supplementary Figure 1B**). A similar situation was also noted for *C. tropicalis*, although the difference failed to reach a statistical significance (**Supplementary Figure 1C**). We also compared the virulence factors of the isolates from different specimen sources, although no obvious correlation was recorded. Interestingly, a correlation was noted between the RAPD genotypes and antifungal resistance. Moreover, 75% of the *C. albicans* from cluster F demonstrated azole resistance, whereas only two azole-resistant *C. tropicalis* strains belonged to the cluster Y (**Figure 2A**). Moreover, 66.7% of the *C. tropicalis* strains, which were S-DD to azole drugs, were allocated into cluster W (**Figure 2C**). These findings together suggest that RAPD results allow the selection of drug-resistant isolates with diverse genetic backgrounds, which has significance in clinical medication and applications.

CONCLUSION

To summarize, this study is able to investigate the molecular relationship and genetic diversity among 110 clinical *Candida* isolates obtained from hospital inpatients admitted in the Nanchang region of China. Although these data are expected to help understand the epidemiology of *Candida* species in Nanchang City, our results also contribute toward a greater understanding of the pathogenicity of *Candida* species in patients with candidiasis and the susceptibility of *Candida* strains to the most commonly used antifungal drugs; the latter may also help prevent the occurrence and outbreak of *Candida* infections. Furthermore, our data provide experimental evidence for designing appropriate clinical monitoring and treatment strategies for candidiasis. Because of the rising incidence of *Candida* infections and their resistance to antifungal drugs,

further studies are required to develop treatment strategies against *Candida* strains.

DATA AVAILABILITY STATEMENT

The sequencing results of ERG11 and FKS1 in the study are deposited in the NCBI BankIt database under accession numbers MZ711431 to MZ711438 and MZ711439 to MZ711442, respectively.

ETHICS STATEMENT

The ethics committee of the First Affiliated Hospital of Nanchang University approved this study (approval no. 2014036).

AUTHOR CONTRIBUTIONS

LZ, NH, QL, XY, and XH designed the study. JC, NH, HX, YZ, YH, and JT performed the experiments and analyses, and wrote the original draft. LZ and XH edited the manuscript. All authors contributed to the article and approved the submitted version.

FUNDING

This work was supported by the National Natural Science Foundation of China (32060040 and 31760261), the Natural Science Foundation of Jiangxi Province (20202BABL216084, 20192ACBL21042, 20202BAB216045, 20192BBG70067, and 20204BCJL23054), the Science and Technology Research Project of Education Department of Jiangxi Province (GJJ180130), and the Major Science and Technology Project of Jiangxi Province (20181BBG70030).

ACKNOWLEDGMENTS

We wish to thank Nanchang University Medical School, for providing the space and equipment necessary to conduct the present study.

SUPPLEMENTARY MATERIAL

The Supplementary Material for this article can be found online at: https://www.frontiersin.org/articles/10.3389/fcimb.2021.721439/full#supplementary-material

Supplementary Figure 1 | Comparison of the virulence levels (biofilm biomass, casein activity, and hemolysin activity) of three *Candida* species isolates by genotypic relatedness. Y-axis (far left panel): biofilm biomass (positively correlated with virulence); Y-axis (far right panel): the Pz values of caseinase and hemolysin activities (negatively correlated with virulence). No significant differences can be noted in this figure. **(A)** The virulence level of 40 *C. albicans* isolates from different gene clusters; **(B)** The virulence level of 37 *C. parapsilosis* isolates from different gene clusters; **(C)** The virulence level of 21 *C. tropicalis* isolates from different gene clusters.

REFERENCES

Abbes, S., Amouri, I., Trabelsi, H., Neji, S., Sellami, H., Rahmouni, F., et al. (2017). Analysis of Virulence Factors and *In Vivo* Biofilm-Forming Capacity of Yarrowia Lipolytica Isolated From Patients With Fungemia. *Med. Mycology* 55, 193–202. doi: 10.1093/mmy/myw028

Akers, K. S., Cardile, A. P., Wenke, J. C., and Murray, C. K. (2015). Biofilm Formation by Clinical Isolates and its Relevance to Clinical Infections. *Adv. Exp. Med. Biol.* 830, 1–28. doi: 10.1007/978-3-319-11038-7_1

Autmizguine, J., Smith, P. B., Prather, K., Bendel, C., Natarajan, G., Bidegain, M., et al. (2018). Effect of Fluconazole Prophylaxis on Candida Fluconazole Susceptibility in Premature Infants. *J. Antimicrobial. Chemother.* 73, 3482–3487. doi: 10.1093/jac/dky353

Bassetti, M., Righi, E., Montravers, P., and Cornely, O. A. (2018). What has Changed in the Treatment of Invasive Candidiasis? A Look at the Past 10 Years and Ahead. *J. Antimicrobial. Chemother.* 73, i14–i25. doi: 10.1093/jac/dkx445

Bongomin, F., Gago, S., Oladele, R., and Denning, D. (2017). Global and Multi-National Prevalence of Fungal Diseases—Estimate Precision. *J. Fungi* 3, 57. doi: 10.3390/jof3040057

Borst, A., and Fluit, A. C. (2003). High Levels of Hydrolytic Enzymes Secreted by Candida Albicans Isolates Involved in Respiratory Infections. *J. Med. Microbiol.* 52, 971–974. doi: 10.1099/jmm.0.05228-0

Chen, J., Liu, Q., Zeng, L., and Huang, X. (2020). Protein Acetylation/Deacetylation: A Potential Strategy for Fungal Infection Control. *Front. Microbiol.* 11, 574736. doi: 10.3389/fmicb.2020.574736

Chin, V. K., Foong, K. J., Maha, A., Rusliza, B., Norhafizah, M., Ng, K. P., et al. (2013). Candida Albicans Isolates From a Malaysian Hospital Exhibit More Potent Phospholipase and Haemolysin Activities Than Non-Albicans Candida Isolates. *Trop. Biomed* 30, 654–662.

Clinical and Laboratory Standards Institut (2008). *Reference method for broth dilution antifungal susceptibility testing of yeasts; third edition, M27-A3*. Wayne, PA, USA.

Clinical and Laboratory Standards Institute (2012). *Reference method for broth dilution antifungal susceptibility testing of yeasts; fourth informational* supplement, M27–S4. Wayne, PA, USA.

De Rosa, F. G., Garazzino, S., Pasero, D., Di Perri, G., and Ranieri, V. M. (2009). Invasive Candidiasis and Candidemia: New Guidelines. *Minerva Anestesiologica* 75, 453–458.

Desnos-Ollivier, M., Bretagne, S., Raoux, D., Hoinard, D., Dromer, F., and Dannaoui, E. (2008). Mutations in the Fks1 Gene in Candida Albicans, C. Tropicalis and C. Krusei Correlate With Elevated Caspofungin MICs Uncovered in AM3 Medium Using the Method of the European Committee on Antibiotic Susceptibility Testing. *Antimicrobial. Agents Chemother.* 52, 3092–3098. doi: 10.1128/AAC.00088-08

Estivill, D., Arias, A., Torres-Lana, A., Carrillo-Muñoz, A. J., and Arévalo, M. P. (2011). Biofilm Formation by Five Species of Candida on Three Clinical Materials. *J. Microbiol. Methods* 86, 238–242. doi: 10.1016/j.mimet.2011.05.019

Fernandes, E. G., Valério, H. M., Feltrin, T., and van der Sand, S. T. (2012). Variability in the Production of Extracellular Enzymes by Entomopathogenic Fungi Grown on Different Substrates. *Braz. J. Microbiol. [publication Braz. Soc. Microbiology]* 43, 827–833. doi: 10.1590/S1517-83822012000200049

Figueiredo-Carvalho, M. H. G., Ramos, L. S., Barbedo, L. S., de Oliveira, J. C. A., Dos Santos, A. L. S., Almeida-Paes, R., et al. (2017). Relationship Between the Antifungal Susceptibility Profile and the Production of Virulence-Related Hydrolytic Enzymes in Brazilian Clinical Strains of Candida Glabrata. *Mediators Inflamm.* 2017, 8952878. doi: 10.1155/2017/8952878

França, J. C., Ribeiro, C. E., and Queiroz-Telles, F. (2008). [Candidemia in a Brazilian Tertiary Care Hospital: Incidence, Frequency of Different Species, Risk Factors and Antifungal Susceptibility]. *Rev. da Sociedade Bras. Medicina Trop.* 41, 23–28. doi: 10.1590/s0037-86822008000100005

Jain, P., Khan, Z. K., Bhattacharya, E., and Ranade, S. A. (2001). Variation in Random Amplified Polymorphic DNA (RAPD) Profiles Specific to Fluconazole-Resistant and -Sensitive Strains of Candida Albicans. *Diagn. Microbiol. Infect. Dis.* 41, 113–119. doi: 10.1016/s0732-8893(01)00292-9

Kelly, S. L., Lamb, D. C., and Kelly, D. E. (1999). Y132H Substitution in Candida Albicans Sterol 14alpha-Demethylase Confers Fluconazole Resistance by Preventing Binding to Haem. *FEMS Microbiol. Lett.* 180, 171–175. doi: 10.1111/j.1574-6968.1999.tb08792.x

Koehler, P., Stecher, M., Cornely, O. A., Koehler, D., Vehreschild, M. J. G. T., Bohlius, J., et al. (2019). Morbidity and Mortality of Candidaemia in Europe: An Epidemiologic Meta-Analysis. *Clin. Microbiol. Infect.* 25, 1200–1212. doi: 10.1016/j.cmi.2019.04.024

Li, Y., Du, M., Chen, L. A., Liu, Y., and Liang, Z. (2016). Nosocomial Bloodstream Infection Due to Candida Spp. In China: Species Distribution, Clinical Features, and Outcomes. *Mycopathologia* 181, 485–495. doi: 10.1007/s11046-016-9997-3

Mancera, E., Porman, A. M., Cuomo, C. A., Bennett, R. J., and Johnson, A. D. (2015). Finding a Missing Gene: EFG1 Regulates Morphogenesis in Candida Tropicalis. *G3 (Bethesda Md.)* 5, 849–856. doi: 10.1534/g3.115.017566

Marak, M. B., and Dhanashree, B. (2018). Antifungal Susceptibility and Biofilm Production of Candida Spp. Isolated From Clinical Samples. *Int. J. Microbiol.* 2018, 7495218. doi: 10.1155/2018/7495218

Marichal, P., Koymans, L., Willemsens, S., Bellens, D., Verhasselt, P., Luyten, W., et al. (1999). Contribution of Mutations in the Cytochrome P450 14alpha-Demethylase (Erg11p, Cyp51p) to Azole Resistance in Candida Albicans. *Microbiol. (Reading)* 145 (Pt 10), 2701–2713. doi: 10.1099/00221287-145-10-2701

Maubon, D., Garnaud, C., Calandra, T., Sanglard, D., and Cornet, M. (2014). Resistance of Candida Spp. To Antifungal Drugs in the ICU: Where Are We Now? *Intensive Care Med.* 40, 1241–1255. doi: 10.1007/s00134-014-3404-7

Mba, I. E., and Nweze, E. I. (2020). Mechanism of Candida Pathogenesis: Revisiting the Vital Drivers. *Eur. J. Clin. Microbiol. Infect. Dis. Off. Publ. Eur. Soc. Clin. Microbiol.* 39, 1797–1819. doi: 10.1007/s10096-020-03912-w

Morio, F., Loge, C., Besse, B., Hennequin, C., and Le Pape, P. (2010). Screening for Amino Acid Substitutions in the Candida Albicans Erg11 Protein of Azole-Susceptible and Azole-Resistant Clinical Isolates: New Substitutions and a Review of the Literature. *Diagn. Microbiol. Infect. Dis.* 66, 373–384. doi: 10.1016/j.diagmicrobio.2009.11.006

Neji, S., Hadrich, I., Trabelsi, H., Abbes, S., Cheikhrouhou, F., Sellami, H., et al. (2017). Virulence Factors, Antifungal Susceptibility and Molecular Mechanisms of Azole Resistance Among Candida Parapsilosis Complex Isolates Recovered From Clinical Specimens. *J. Biomed. Sci.* 24, 67. doi: 10.1186/s12929-017-0376-2

Nett, J., and Andes, D. (2006). Candida Albicans Biofilm Development, Modeling a Host-Pathogen Interaction. *Curr. Opin. Microbiol.* 9, 340–345. doi: 10.1016/j.mib.2006.06.007

Neufeld, P. M., Melhem Mde, S., Szeszs, M. W., Ribeiro, M. D., Amorim Ede, L., da Silva, M., et al. (2015). Nosocomial Candidiasis in Rio De Janeiro State: Distribution and Fluconazole Susceptibility Profile. *Braz. J. Microbiol. [publication Braz. Soc. Microbiology]* 46, 477–484. doi: 10.1590/s1517-838246220120023

Paluchowska, P., Tokarczyk, M., Bogusz, B., Skiba, I., and Budak, A. (2014). Molecular Epidemiology of Candida Albicans and Candida Glabrata Strains Isolated From Intensive Care Unit Patients in Poland. *Memorias do Instituto Oswaldo Cruz* 109, 436–441. doi: 10.1590/0074-0276140099

Pappas, P. G., Lionakis, M. S., Arendrup, M. C., Ostrosky-Zeichner, L., and Kullberg, B. J. (2018). Invasive Candidiasis. *Nat. Rev. Dis. Primers* 4, 18026. doi: 10.1038/nrdp.2018.26

Pappas, P. G., Rex, J. H., Sobel, J. D., Filler, S. G., Dismukes, W. E., Walsh, T. J., et al. (2004). Guidelines for Treatment of Candidiasis. *Clin. Infect. Dis.* 38, 161–189. doi: 10.1086/380796

Prasad, T., Chandra, A., Mukhopadhyay, C. K., and Prasad, R. (2006). Unexpected Link Between Iron and Drug Resistance of Candida Spp.: Iron Depletion Enhances Membrane Fluidity and Drug Diffusion, Leading to Drug-Susceptible Cells. *Antimicrobial Agents Chemother.* 50, 3597–3606. doi: 10.1128/aac.00653-06

Price, M. F., Wilkinson, I. D., and Gentry, L. O. (1982). Plate Method for Detection of Phospholipase Activity in Candida Albicans. *Sabouraudia* 20, 7–14. doi: 10.1080/00362178285380031

Ramesh, N., Priyadharsini, M., Sumathi, C. S., Balasubramanian, V., Hemapriya, J., and Kannan, R. (2011). Virulence Factors and Anti Fungal Sensitivity Pattern of Candida Sp. Isolated From HIV and TB Patients. *Indian J. Microbiol.* 51, 273–278. doi: 10.1007/s12088-011-0177-3

Salehi, F., Esmaeili, M., and Mohammadi, R. (2017). Isolation of Candida Species From Gastroesophageal Lesions Among Pediatrics in Isfahan, Iran: Identification and Antifungal Susceptibility Testing of Clinical Isolates by E-Test. *Adv. BioMed. Res.* 6, 103. doi: 10.4103/2277-9175.213662

Seidler, M., Salvenmoser, S., and Müller, F. M. (2006). *In Vitro* Effects of Micafungin Against Candida Biofilms on Polystyrene and Central Venous Catheter Sections. *Int. J. Antimicrobial. Agents* 28, 568–573. doi: 10.1016/j.ijantimicag.2006.07.024

Sfeir, M. M., Jiménez-Ortigosa, C., Gamaletsou, M. N., Schuetz, A. N., Soave, R., Van Besien, K., et al. (2020). Breakthrough Bloodstream Infections Caused by Echinocandin-Resistant: An Emerging Threat to Immunocompromised Patients With Hematological Malignancies. *J. Fungi (Basel)* 6, 20. doi: 10.3390/jof6010020

Silva, S., Henriques, M., Martins, A., Oliveira, R., Williams, D., and Azeredo, J. (2009). Biofilms of non-Candida Albicans Candida Species: Quantification, Structure and Matrix Composition. *Med. Mycology* 47, 681–689. doi: 10.3109/13693780802549594

Spettel, K., Barousch, W., Makristathis, A., Zeller, I., Nehr, M., Selitsch, B., et al. (2019). Analysis of Antifungal Resistance Genes in Candida Albicans and Candida Glabrata Using Next Generation Sequencing. *PloS One* 14, e0210397. doi: 10.1371/journal.pone.0210397

Ulu Kilic, A., Alp, E., Cevahir, F., Ture, Z., and Yozgat, N. (2017). Epidemiology and Cost Implications of Candidemia, a 6-Year Analysis From a Developing Country. *Mycoses* 60, 198–203. doi: 10.1111/myc.12582

Vatanshenassan, M., Arastehfar, A., Boekhout, T., Berman, J., Lass-Flörl, C., Sparbier, K., et al. (2019). Anidulafungin Susceptibility Testing of Candida Glabrata Isolates From Blood Cultures by the MALDI Biotyper Antibiotic (Antifungal) Susceptibility Test Rapid Assay. *Antimicrobial. Agents Chemother.* 63(9). doi: 10.1128/AAC.00554-19

Wang, Y.-b., Wang, H., Guo, H.-y., Zhao, Y.-z., and Luo, S.-q. (2005). Analysis of ERG11 Gene Mutation in Candida Albicans. *Di Yi Jun Yi Da Xue Xue Bao* 25, 1390–1393.

Weissman, Z., Pinsky, M., Donegan, R. K., Reddi, A. R., and Kornitzer, D. (2021). Using Genetically Encoded Heme Sensors to Probe the Mechanisms of Heme Uptake and Homeostasis in Candida Albicans. *Cell. Microbiol.* 23, e13282. doi: 10.1111/cmi.13282

Wisplinghoff, H., Bischoff, T., Tallent, S. M., Seifert, H., Wenzel, R. P., and Edmond, M. B. (2004). Nosocomial Bloodstream Infections in US Hospitals: Analysis of 24,179 Cases From a Prospective Nationwide Surveillance Study. *Clin. Infect. Dis.* 39, 309–317. doi: 10.1086/421946

Zeng, Z.-R., Tian, G., Ding, Y.-H., Yang, K., Liu, J.-B., and Deng, J. (2019). Surveillance Study of the Prevalence, Species Distribution, Antifungal Susceptibility, Risk Factors and Mortality of Invasive Candidiasis in a Tertiary Teaching Hospital in Southwest China. *BMC Infect. Dis.* 19, 939. doi: 10.1186/s12879-019-4588-9

Conflict of Interest: The authors declare that the research was conducted in the absence of any commercial or financial relationships that could be construed as a potential conflict of interest.

Publisher's Note: All claims expressed in this article are solely those of the authors and do not necessarily represent those of their affiliated organizations, or those of the publisher, the editors and the reviewers. Any product that may be evaluated in this article, or claim that may be made by its manufacturer, is not guaranteed or endorsed by the publisher.

frontiers in Cellular and Infection Microbiology

ORIGINAL RESEARCH
published: 15 October 2021
doi: 10.3389/fcimb.2021.742062

Application of Machine Learning Classifier to *Candida auris* Drug Resistance Analysis

Dingchen Li[1†], *Yaru Wang*[1,2†], *Wenjuan Hu*[1,2], *Fangyan Chen*[1], *Jingya Zhao*[1], *Xia Chen*[2*] *and Li Han*[1*]

[1] Department of Disinfection and Infection Control, Chinese People's Liberation Army (PLA) Center for Disease Control and Prevention, Beijing, China, [2] School of Mathematics and Statistics, Shaanxi Normal University, Xi'an, China

Candida auris (C. auris) is an emerging fungus associated with high morbidity. It has a unique transmission ability and is often resistant to multiple drugs. In this study, we evaluated the ability of different machine learning models to classify the drug resistance and predicted and ranked the drug resistance mutations of *C. auris*. Two *C. auris* strains were obtained. Combined with other 356 strains collected from the European Bioinformatics Institute (EBI) databases, the whole genome sequencing (WGS) data were analyzed by bioinformatics. Machine learning classifiers were used to build drug resistance models, which were evaluated and compared by various evaluation methods based on AUC value. Briefly, two strains were assigned to Clade III in the phylogenetic tree, which was consistent with previous studies; nevertheless, the phylogenetic tree was not completely consistent with the conclusion of clustering according to the geographical location discovered earlier. The clustering results of *C. auris* were related to its drug resistance. The resistance genes of *C. auris* were not under additional strong selection pressure, and the performance of different models varied greatly for different drugs. For drugs such as azoles and echinocandins, the models performed relatively well. In addition, two machine learning algorithms, based on the balanced test and imbalanced test, were designed and evaluated; for most drugs, the evaluation results on the balanced test set were better than on the imbalanced test set. The mutations strongly be associated with drug resistance of *C. auris* were predicted and ranked by Recursive Feature Elimination with Cross-Validation (RFECV) combined with a machine learning classifier. In addition to known drug resistance mutations, some new resistance mutations were predicted, such as Y501H and I466M mutation in the *ERG11* gene and R278H mutation in the *ERG10* gene, which may be associated with fluconazole (FCZ), micafungin (MCF), and amphotericin B (AmB) resistance, respectively; these mutations were in the "hot spot" regions of the ergosterol pathway. To sum up, this study suggested that machine learning classifiers are a useful and cost-effective method to identify fungal drug resistance-related mutations, which is of great significance for the research on the resistance mechanism of *C. auris*.

Keywords: *Candida auris*, phylogenetic analysis, drug resistance, whole genome sequencing, machine learning, antifungal drugs, ergosterol pathway

Edited by:
Jianping Xu,
McMaster University, Canada

Reviewed by:
Yue Wang,
McMaster University, Canada
Marie Desnos-Ollivier,
Institut Pasteur, France
Kin-Ming (Clement) Tsui,
University of British Columbia, Canada

***Correspondence:**
Li Han
hanlicdc@163.com
Xia Chen
xchen80@snnu.edu.cn

†These authors have contributed equally to this work and share first authorship

Specialty section:
This article was submitted to Fungal Pathogenesis, a section of the journal Frontiers in Cellular and Infection Microbiology

Received: *15 July 2021*
Accepted: *22 September 2021*
Published: *15 October 2021*

Citation:
Li D, Wang Y, Hu W, Chen F, Zhao J, Chen X and Han L (2021) Application of Machine Learning Classifier to Candida auris Drug Resistance Analysis. Front. Cell. Infect. Microbiol. 11:742062. doi: 10.3389/fcimb.2021.742062

INTRODUCTION

Candida auris (*C. auris*) is an emerging fungal pathogen first isolated from the external ear canal of a 70-year-old female inpatient in Tokyo hospital (Satoh et al., 2009). *C. auris* can persist for weeks in a nosocomial environment, and survive high-end disinfections, thus presenting a serious global health threat (Chaabane et al., 2019; Du et al., 2020). To date, *C. auris* outbreak has been reported in more than 30 countries worldwide (Rhodes et al., 2018; Tian et al., 2018; Escandon et al., 2019; Rhodes and Fisher, 2019). *C. auris*, also known as "super fungus", is a multidrug-resistant species associated with high mortality (Wang et al., 2018).

So far, four specific clades of *C. auris* have been identified by phylogenetic analysis based on whole-genome sequencing (WGS): South Asia (Clade I), East Asia (Clade II), South Africa (Clade III), and South America (Clade IV). A potential fifth clade of Iranian origin was described by few studies (Chow et al., 2019; Di Pilato et al., 2021). All clades are characterized by distinct single nucleotide polymorphisms (SNPs), highlighting this pathogen's independent and worldwide emergence (Lockhart et al., 2017). Except for Clade II, the other three clusters have been associated with an outbreak of invasive infection and multiple resistance. Clade II is predominantly an ear canal infection, and presents either single fluconazole resistance or susceptible (Kwon et al., 2019; Welsh et al., 2019).

Clinically, invasive fungal infections are usually treated with three classes of antifungal agents: echinocandins, azoles, and polyenes (ElBaradei, 2020). Fluconazole (FCZ) resistance is the most common. Resistance to other azoles like voriconazole (VCZ), itraconazole (ICZ), and posaconazole (PZ) might vary (Montoya et al., 2019; ElBaradei, 2020).

Ergosterol is a key component of the fungal cell membrane. In *Candida*, ergosterol is mediated by lanosterol 14-alpha-demethylase (*ERG11*), which is involved in an important step in the biosynthesis of ergosterol. Antifungal agents effectively inhibit ergosterol biosynthesis by inhibiting the enzyme's function, thereby compromising membrane integrity (Sanglard et al., 1998). Different mechanisms, including mutations in the *ERG11* gene, overexpression of the ATP-binding Cassette (*ABC*) exogenous pump transporter, which is encoded by the *CDR1* gene, and duplication and overexpression of the *ERG11* gene, contribute to the reduction of the sensitivity of *C. auris* to azole drugs (Puri et al., 1999; de Micheli et al., 2002; Coste et al., 2004; Cannon et al., 2009; Noel, 2012; Spampinato and Leonardi, 2013; Medici and Del Poeta, 2015; Nami et al., 2019; Bing et al., 2020). Point mutations in the *ERG11* gene, associated with FCZ resistance in *Candida albicans*, are also one of the mechanisms of FCZ resistance in *C. auris*. Point mutations in *ERG11* can reduce the azole sensitivity of *Candida*, particularly in the "hot spots" located between 105-165, 266-287, and 405-488 (Lamb et al., 1995; Sanglard et al., 1998; Mellado et al., 2004; Vandeputte et al., 2012). Moreover, Lockhart et al. described three major mutations in *ERG11* that influence FCZ resistance, namely, F126T, Y132F, and K143R (Lockhart et al., 2017). Furthermore, Healey et al. found that Y132F mutations significantly reduce the sensitivity of *C. auris* to azole drugs. Also, it has been reported that these mutations are associated with geographic cues, with mutations leading to Y132F and K143R associated with isolates belonging to South Asian and South American groups (Healey et al., 2018). In addition, Rybak et al. reported new mutations on the zinc-cluster transcription factor-encoding gene (*TAC1B*) associated with FCZ resistance (Rybak et al., 2020). This study showed that mutations on *TAC1B* could be produced rapidly *in vitro* after exposure to FCZ. Most FCZ-resistant isolates have many drug-related *TAC1B* mutations in a specific global lineage or group of *C. auris*, and the identification of new resistance determinants has significantly increased the understanding of clinical antifungal resistance in *C. auris* (Rybak et al., 2020).

C. auris resistance to echinocandins is less common. Caspofungin (CSF), micafungin (MCF), and anidulafungin (AND) are often recommended as first-line treatments for candidemia (ElBaradei, 2020). *In vitro* studies have demonstrated that CSF and AND have a certain inhibitory effect on the growth of *C. auris* (Dudiuk et al., 2019). Interestingly, one study reported that among all echinocandins, micafungin has the highest inhibitory effect against *C. auris* (Kordalewska et al., 2018).

Echinocandins inhibit the 1, 3-beta-D-glucan synthetase required for cell wall synthesis, encoded by the genes *FKS1* and *FKS2*. Several mutations ("hot spots 1 and 2") in the *FKS1* and *FKS2* genes in *Candida albicans* and other non-auris *Candida* species have been associated with the echinocandins resistance. In the *FKS1* gene of *C. albicans*, these "hot spots" lie between the amino acids 641-649 and 1,345-1,365 (Park et al., 2005). Resistance to the echinocandins involves mutations in the *FKS1* gene, with changes in the hot spot 1 region leading to amino acid substitution from serine to proline at 639 (S639P) (Biagi et al., 2019). Moreover, a multicenter study in India reported another mutation in the same position 639 of the *FKS1* gene, involving a change from serine to phenylalanine (S639F or S639Y) (Chowdhary et al., 2018). Sharma et al. also found *FKS2* in a single copy of the *C. auris* genome; yet, no mutation associated with echinocandins resistance has been found in this gene (Sharma et al., 2016; Chaabane et al., 2019).

Among polyenes, *C. auris* and *C. lusitaniae* have shown high resistance to amphotericin B (AmB). However, the molecular mechanism of polyene drug resistance is not clear (ElBaradei, 2020) and more research may be needed to reveal how non-synonymous mutations promote resistance to AmB in *C. auris* (Escandon et al., 2019). Kordalewska and Perlin suggested that resistance to AmB is regulated at the transcriptional level rather than mutations (Kordalewska and Perlin, 2019).

Predictive models based on machine learning can explore multiple associations between genetic variations. Machine learning is the scientific discipline that focuses on how computers learn from data (Deo, 2015). As an essential component in artificial intelligence (AI), it has been integrated into many fields, such as data generation, analytics and knowledge mining (Handelman et al., 2018; Patel et al., 2020). Several previous studies have used machine learning algorithms

to predict microbial resistance. For example, Zhang et al. collected 161 strains of *Mycobacterium tuberculosis* (MTB) from China and used logistic regression and random forest to find and predict new genes associated with drug resistance of seven drugs (Zhang et al., 2013). Furthermore, using a more geographically diverse data set, Farhat et al. studied the performance of the random forest algorithm based 1,397 isolates (Farhat et al., 2016). Her et al. proposed a pan-genome-based method to characterize antibiotic-resistant microbial strains; the method was tested on *Escherichia coli*. The drug resistance gene was predicted by identifying the core and accessory gene clusters on *Escherichia coli* pan-genomic (Her and Wu, 2018). In addition, Yang et al. considered 1,839 bacterial isolates from the UK and compared the performance of more machine learning classifiers, including Logistic Regression, Support Vector Classifier (based on linear and Gaussian kernel functions), product-of-marginals model (PM), Random Forest, gradient tree boosting (GBT), and Adaboost. Finally, mutations associated with drug resistance of MTB ranked and were predicted (Yang et al., 2018; Kouchaki et al., 2019). However, most of the microbes studied were bacteria, while only a few studies applied this method to study fungi. Moreover, currently, there are no studies on the classification of fungi drug resistance and the evaluation of drug resistance mutations by mathematical models.

In this study, we collected *C. auris* isolates from different countries or regions, analyzed their whole genome sequencing data, constructed the phylogenetic relationship, evaluated the ability of different machine learning models to classify the drug resistance, and predicted and ranked the drug resistance mutations of *C. auris*.

MATERIALS AND METHODS

WGS and Pre-processing

As of April 2020, the whole genome sequencing (WGS) data of *C. auris* published by the European Bioinformatics Institute (EBI, https://www.ebi.ac.uk/) has 796 isolates in total. Among them, 356 strains have undergone antifungal susceptibility testing. According to these results, resistant or susceptible strains were determined according to the Clinical and Laboratory Standards Institute (CLSI) guidelines.

In this study, WGS data of 356 strains containing drug resistance information on the EBI website were collected, and two strains named C1921 and C1922, which showed FCZ resistance from the Chinese PLA Center for Disease Control & Prevention were combined (Chen et al., 2018). This study involved WGS data of 358 C. *auris* strains (see **Supplementary Materials File**), all of which were sequenced using Illumina sequencing technology platform; the sequencing data obtained were double-ended WGS data in FASTQ data format. The drug resistance of 358 strains above was collected, including fluconazole, itraconazole, voriconazole, posaconazole, amphotericin B, micafungin, anifenqine and caspofunqine. The statistics of drug resistance of the strains are shown in **Table 1**.

WGS data of 358 C. *auris* strains were collected and analyzed using the following steps: FastQC (http://www.bioinformatics.babraham.ac.uk/projects/fastqc/) checked the data quality of each strain's sequence and divided the data according to different types of sequencing adapters for quality control [Trimmomatic (Bolger et al., 2014)]. All data were aligned and sorted with the reference strain B8441 using Bwa-0.7.17 (Munoz et al., 2018). Duplicates in the file were marked using MarkDuplicates module in GATK (DePristo et al., 2011) v4.1.4.1, and were ignored during the mutation detection. In BaseRecalibrator, 246,258 sites were jointly detected by GATK HaplotypeCaller and Bcftools (Li et al., 2009) mpileup, which were finally used as SNP reference sets.

The recalibration of base mass values mainly involved two steps: GATK BaseRecalibrator and GATK ApplyBQSR. Then, the mutation detection was performed by GATK HaplotypeCaller. Finally, VCFtools (Danecek et al., 2011) software was used to filter the samples and detection sites, respectively. Two samples with high deletion rates (max-missing ≥ 50%) (SRR10461133 and SRR10461145) were removed from the filtering of the samples. The sites with minQ ≤ 30, max-missing ≥ 0.5, mac ≤ 3, and minDP ≤ 3 were deleted, respectively, using VCFtools, and the number of sites after filtering was 229,262. The filtered files were annotated using SNPEff (Cingolani et al., 2012), and the annotated files were used for phylogenetic analysis and machine learning resistance analysis. Three antifungals (FCZ, MCF and AmB) and point mutations (Y132F, K143R and F126L in ERG11, S639Y/S639F and S639P in FKS1) was also depicted in the phylogenetic NJ tree. This process is shown in **Figure S1** and **Table S1**.

Selection and Extraction of Gene Sets

A total of 229,262 SNP mutation sites were found in 358 *C. auris* isolates. Candidate genes that may have a strong correlation with drug resistance of *C. auris* in previous studies were selected; this was performed in order to reduce its dimension, facilitate machine learning classification, eliminate redundant sites, and improve the accuracy of the analysis for the complex dimension.

TABLE 1 | Classification of all *C. auris* strains' drug-resistant phenotypes.

Drugs	FCZ	AmB	MCF	VCZ	ICZ	PZ	AND	CSF
Resistant	254	80	24	19	10	39	3	3
Susceptible	104	273	321	104	108	70	113	119
Missing	0	5	13	235	240	249	242	236

In addition, only missense mutations were extracted for further analysis since they accounted for only a small part of the original mutations, but affected the type of amino acids, i.e., the function of proteins.

Three candidate gene sets were selected in this study (Lockhart et al., 2017; Munoz et al., 2018; Chaabane et al., 2019; Rybak et al., 2020) (**Table S2**). F3 set included genes that were previously reported to be associated with drug resistance and may contain determinants of drug resistance information in *C. auris*; F2 set was a list of seven genes specific in C. *auris*, which have been associated with drug resistance in *C. albicans*, but are highly conserved in *C. auris* (Munoz et al., 2018). F1 set combined the F2 and F3 genes. All the missense mutations were extracted in the three gene sets and filtered. The samples and sites with too many missing values for each set were deleted, and the dimension of the data set after processing the missing values (samples × mutations) was respectively: F1: 350 x 579; F2: 353 x 202; F3: 352 x 377.

Machine Learning Algorithms

Two algorithms were designed by using Python 3.8.4 (https://www.python.org/downloads/): the classifier on the balanced test set and on the imbalanced test set (**Figures S2**, **S3**). The F1, F2, and F3 sets were used as the classification feature sets, and the drug resistance of *C. auris* was taken as the classification target. Ten machine learning classifiers (**Table S3**), Logistic Regression (LR), Support Vector Classifier (SVC, including SVC RBF and SVC linear), K-Nearest Neighbors (KNN), Decision Tree (DT), Ensemble Learning (including RandomForest, AdaBoost and GradientBoosting), and Naive Bayes (including BernoulliNB and GaussianNB) were used to build the model (Breiman, 1996; Breiman, 2001) by using Python 3.8.4. For AdaBoost, the Decision Tree Classifier was the base estimator whose number was 200 and the max depth was 1. There were 100 trees set in the random forest classifier. The neighbor was 5 (the value of K) for the KNN classifier. In both algorithms, principal component analysis (PCA) was used to reduce dimensionality based on retaining 99% of the original information. The number of principal components after dimension reduction with PCA method when 99% of the variance is retained is in supplementary material **Table S4**. Upsampling and downsampling were mainly adopted to balance the data set and repeated sampling 100 times. Downsampling means, for a dataset from the majority classification, creating a new subset with the same sample number as the minority classification from the original set by random sampling. Upsampling means, for a dataset from the minority classification, creating a new dataset with the same sample number as the majority classification from the original set by random sampling. The data were divided into test set and training set according to 5-fold cross-validation (5-CV), which accounted for 20% and 80%, respectively. The model parameters were adjusted on a training set, and the model was retrained using 5-CV. Finally, the model was evaluated on the test set. The area under the ROC (the Receiver operating characteristic curve) curve (AUC), was used as evaluation standard of a model's performance. A classifier with a larger AUC (closer to 1.0) performed better.

Recursive Feature Elimination With Cross-Validation

The Recursive Feature Elimination with Cross-validation (RFECV) functions in Python's Scikit-Learn established in mutation sequencing were based on the F1 data set, which contained all candidate genes selected before machine learning modeling. All features were standardized before ranking, and the training model was the classifier above. The standardized method used was StandardScaler() function in Python. The number of features discarded in each iteration was 1, indicating elimination one by one, and the model was built repeatedly through 5-CV.

RESULTS

Phylogenetic Analysis of *Candida auris*

Phylogenetic NJ-tree was constructed using MEGA-X (Kumar et al., 2018), and boostrap test was repeated 500 times. Then, the phylogenetic tree was annotated using the iTOL online tool (https://itol.embl.de/). The phylogenetic NJ tree was divided into four clades starting from the root (**Figure 1**): Clade I (orange), Clade II (blue), Clade III (purple), and Clade IV (green), which was consistent with the conclusions reported in previous literatures (Lockhart et al., 2017). The clustering results are shown in **Table S5**. However, strain B16401 (SRR10852068, Kenya) was assigned to Clade I in this study; in a previous study, strain B16401 was assigned to Clade III (Chow et al., 2020). In the NJ tree, C1921 and C1922 from our laboratory were in Clade III, which was consistent with the phylogenetic tree constructed using Internal Transcribed Spacer (ITS) and D1/D2 Large Ribosomal Subunit Region previously (Chen et al., 2018). In addition, the mutations associated with azoles and echinocandins resistance detected were consistent with the previous conclusions (Chow et al., 2020). According to these results, F126L mutation in lanosterol 14-alpha-demethylase *ERG11* occurred in C1921 and C1922 strains, which is closely related to their FCZ resistance observed in clinical practice. It was also shown that the phylogenetic tree constructed by the drug-resistant gene set F3 was very similar to the phylogenetic tree constructed by the WGS of *C. auris*, and there was no difference in the clustering results of the strains (**Figure S4**), indicating that the evolution of *C. auris* resistance genes was consistent with the overall evolution of the strains (at the level of the whole genome). It was speculated that the resistance genes of *C. auris* were not under additional strong selection pressure, which may be related to the clinical use of drugs.

Evaluation of Classification Models

The performances of machine learning classifiers, constructed by the two algorithms described above on F1, F2, and F3, were evaluated and compared by several evaluation methods. The best model for each set and drug was listed in **Table 2**. For most drugs, the evaluation results on the balanced test set were better than on the imbalanced test set. The classifiers established using two algorithms achieved better results for azoles, like FCZ, ICZ

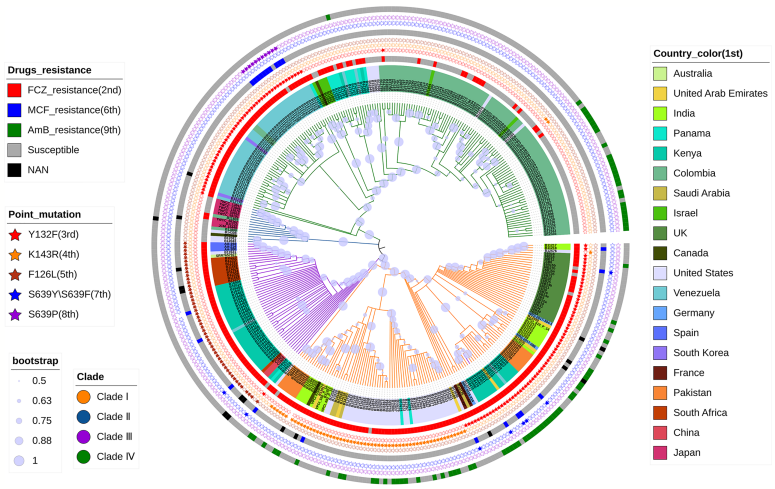

FIGURE 1 | Phylogenetic NJ tree based on WGS of *C. auris*. The tree describes the phylogeny of 356 strains of *C. auris* from different regions, divided into four clades. The 1st to 9th indicates a concentric circle from the inner-most to the outer-most, respectively. It also shows the correlation between the resistance of these strains to FCZ, AmB, and MCF and the reported point mutations with Y132F, K143R, and F126L in *ERG11*, S639Y/S639F, and S639P in *FKS1*.

TABLE 2 | Model evaluation results under two different algorithms: on the balanced test set (the upper table) and on the imbalanced test set (the lower table).

The best model	AUC value	Sensitivity	Specificity	Accuracy	Recall	F1 score	Threshold
F1AmB_AdaBoost_Upsampling	0.9507 ± 0.0082	0.9504 ± 0.0178	0.8554 ± 0.0096	0.9019 ± 0.0140	0.9502 ± 0.0179	0.9066 ± 0.0138	0.5012 ± 0.0002
F2AmB_KNeighbors_Upsampling	0.8719 ± 0.0249	0.8057 ± 0.0671	0.8025 ± 0.0093	0.7992 ± 0.0323	0.8057 ± 0.0671	0.7920 ± 0.0406	0.7187 ± 0.0532
F3AmB_RF_Upsampling	0.9026 ± 0.0285	0.8711 ± 0.0465	0.7818 ± 0.0395	0.8227 ± 0.0435	0.8710 ± 0.0465	0.8303 ± 0.0423	0.5851 ± 0.0316
F1MCF_KNeighbors_Upsampling	0.9971 ± 0.0007	0.9926 ± 0.0060	0.9908 ± 0.0068	0.9865 ± 0.0072	0.9926 ± 0.0060	0.9867 ± 0.0071	0.9561 ± 0.0247
F2MCF_KNeighbors_Upsampling	0.9648 ± 0.0127	0.9691 ± 0.0130	0.8882 ± 0.0345	0.9078 ± 0.0253	0.9691 ± 0.0129	0.9140 ± 0.0228	0.8026 ± 0.0281
F3MCF_RF_Upsampling	0.9914 ± 0.0044	0.9401 ± 0.0365	0.9825 ± 0.0100	0.9604 ± 0.0231	0.9395 ± 0.0370	0.9586 ± 0.0245	0.8755 ± 0.0564
F1FCZ_RF_Upsampling	0.9908 ± 0.0043	0.9542 ± 0.0138	0.9769 ± 0.0173	0.9615 ± 0.0156	0.9483 ± 0.0129	0.9609 ± 0.0155	0.6040 ± 0.0136
F2FCZ_AdaBoost_Upsampling	0.9621 ± 0.0048	0.9129 ± 0.0144	0.9860 ± 0.0061	0.9502 ± 0.0110	0.9120 ± 0.0143	0.9478 ± 0.0118	0.5436 ± 0.0217
F3FCZ_RF_Upsampling	0.9787 ± 0.0076	0.9380 ± 0.0124	0.9703 ± 0.0207	0.9533 ± 0.0171	0.9377 ± 0.0126	0.9527 ± 0.0170	0.7207 ± 0.0567
F1VCZ_KNeighbors_Upsampling	0.9690 ± 0.0094	0.9710 ± 0.0077	0.9089 ± 0.0243	0.9262 ± 0.0157	0.9704 ± 0.0078	0.9306 ± 0.0147	0.8061 ± 0.0567
F2VCZ_LR_Downsampling	0.9381 ± 0.0025	0.8924 ± 0.0030	0.9477 ± 0.0009	0.8753 ± 0.0016	0.8567 ± 0.0023	0.8721 ± 0.0021	0.5064 ± 0.0016
F3VCZ_AdaBoost_Upsampling	0.9485 ± 0.0056	0.9959 ± 0.0048	0.8587 ± 0.0052	0.9272 ± 0.0043	0.9959 ± 0.0048	0.9320 ± 0.0040	0.5016 ± 0.0003
F1PZ_DecisionTree_Upsampling	0.9251 ± 0.0429	0.9099 ± 0.0479	0.8347 ± 0.0577	0.8689 ± 0.0534	0.9087 ± 0.0485	0.8735 ± 0.0522	0.7408 ± 0.0563
F2PZ_RF_Upsampling	0.7872 ± 0.0605	0.7496 ± 0.1100	0.8173 ± 0.0116	0.7822 ± 0.0616	0.7496 ± 0.1100	0.7628 ± 0.0807	0.7732 ± 0.0515
F3PZ_RF_Upsampling	0.8919 ± 0.0472	0.9057 ± 0.0660	0.8010 ± 0.0455	0.8350 ± 0.0571	0.9057 ± 0.0660	0.8442 ± 0.0566	0.7275 ± 0.0626
F1ICZ_KNeighbors_Upsampling	0.9651 ± 0.0099	0.9945 ± 0.0036	0.9220 ± 0.0220	0.9528 ± 0.0106	0.9944 ± 0.0036	0.9563 ± 0.0095	0.8884 ± 0.0332
F2ICZ_AdaBoost_Downsampling	0.9874 ± 0.0032	1.0000 ± 0.0000	0.9749 ± 0.0064	0.9800 ± 0.0048	1.0000 ± 0.0000	0.9840 ± 0.0038	1.0000 ± 0.0000
F3ICZ_BernoulliNB_Downsampling	0.9701 ± 0.0014	1.0000 ± 0.0000	0.9000 ± 0.0000	0.9500 ± 0.0000	1.0000 ± 0.0000	0.9600 ± 0.0000	0.9995 ± 0.0000
The best model	AUC value	Sensitivity	Specificity	Accuracy	Recall	F1 score	Threshold
F1AmB_RF_Downsampling	0.9136 ± 0.0144	0.7365 ± 0.0935	0.9024 ± 0.0154	0.8565 ± 0.0116	0.7335 ± 0.0945	0.6908 ± 0.0472	0.6003 ± 0.0018
F2AmB_GB_Downsampling	0.8008 ± 0.0033	0.1980 ± 0.0278	0.9997 ± 0.0005	0.8118 ± 0.0084	0.1980 ± 0.0278	0.3214 ± 0.0410	0.9759 ± 0.0264
F3AmB_RF_Downsampling	0.8116 ± 0.0244	0.4220 ± 0.0278	0.9230 ± 0.0325	0.8009 ± 0.0226	0.4150 ± 0.0300	0.4904 ± 0.0223	0.5949 ± 0.0076
F1MCF_SVC_RBF_Upsampling	0.9807 ± 0.0162	0.9186 ± 0.0764	0.9911 ± 0.0033	0.9825 ± 0.0034	0.9186 ± 0.0764	0.8540 ± 0.0433	0.9516 ± 0.0188
F2MCF_GB_Upsampling	0.7565 ± 0.0179	0.6240 ± 0.0698	0.8086 ± 0.0128	0.7846 ± 0.0086	0.6240 ± 0.0698	0.2615 ± 0.0291	0.6777 ± 0.0155
F3MCF_LRL2_Upsampling	0.9510 ± 0.0089	0.8121 ± 0.0485	0.9750 ± 0.0065	0.9010 ± 0.0064	0.8121 ± 0.0485	0.5121 ± 0.0215	0.9735 ± 0.0136
F1FCZ_RF_Downsampling	0.9593 ± 0.0043	0.9707 ± 0.0029	0.8700 ± 0.0213	0.9312 ± 0.0112	0.9695 ± 0.0030	0.9527 ± 0.0075	0.5901 ± 0.0097
F2FCZ_RF_Upsampling	0.9314 ± 0.0095	0.9053 ± 0.0065	0.9294 ± 0.0154	0.9076 ± 0.0087	0.9026 ± 0.0077	0.9328 ± 0.0065	0.6716 ± 0.0356
F3FCZ_RF_Downsampling	0.9531 ± 0.0090	0.2122 ± 0.0792	0.8966 ± 0.0412	0.9049 ± 0.0080	0.9225 ± 0.0101	0.9321 ± 0.0050	0.5903 ± 0.0207
F1VCZ_RF_Downsampling	0.9341 ± 0.0441	0.8222 ± 0.0628	0.9270 ± 0.0462	0.8921 ± 0.0340	0.8218 ± 0.0631	0.7092 ± 0.0693	0.7420 ± 0.0211
F2VCZ_LRL2_Upsampling	0.9136 ± 0.0498	0.9204 ± 0.0699	0.8978 ± 0.0377	0.8731 ± 0.0509	0.9202 ± 0.0702	0.7159 ± 0.1058	0.5389 ± 0.0053
F3VCZ_SVC_Linear_Upsampling	0.9434 ± 0.0300	0.9211 ± 0.0693	0.9247 ± 0.0198	0.8594 ± 0.0211	0.8775 ± 0.0760	0.6554 ± 0.0550	0.7265 ± 0.0689
F1PZ_RF_Downsampling	0.7846 ± 0.0270	0.5016 ± 0.0285	0.8447 ± 0.0156	0.7090 ± 0.0117	0.4967 ± 0.0285	0.5429 ± 0.0211	0.5986 ± 0.0088
F2PZ_LRL2_Downsampling	0.6595 ± 0.0296	0.3707 ± 0.0148	0.8793 ± 0.0290	0.6950 ± 0.0201	0.3707 ± 0.0148	0.4596 ± 0.0312	0.5617 ± 0.0386
F3PZ_RF_Downsampling	0.6737 ± 0.0346	0.4131 ± 0.0409	0.8787 ± 0.0279	0.6831 ± 0.0045	0.4068 ± 0.0366	0.4712 ± 0.0172	0.6173 ± 0.0275
F1ICZ_KNeighbors_Upsampling	0.9696 ± 0.0168	0.9585 ± 0.0261	0.9388 ± 0.0224	0.9404 ± 0.0204	0.9585 ± 0.0261	0.7479 ± 0.0457	0.7861 ± 0.0461
F2ICZ_LRL2_Upsampling	0.9375 ± 0.0112	1.0000 ± 0.0000	0.8750 ± 0.0224	0.8838 ± 0.0231	1.0000 ± 0.0000	0.6040 ± 0.0382	0.8403 ± 0.0281
F3ICZ_BernoulliNB_Upsampling	0.9657 ± 0.0144	1.0000 ± 0.0000	0.9276 ± 0.0226	0.9323 ± 0.0207	1.0000 ± 0.0000	0.7310 ± 0.0477	0.9997 ± 0.0000

The number after ± indicates the standard deviation after 100 repeated samplings.

and VCZ, since their AUC values were above 0.9. However, compared with other drug models, the evaluation results of AmB needed to be improved; we speculated that this might be closely related to the selection of candidate genes. For well-studied drugs (azoles and echinocandins), the selected three gene sets contained more information about determinants associated with drug resistance, but there were few determinants of polyenes resistance.

The model with the highest AUC value was extracted and compared (**Figure 2** and **Table S6**). Random forest, logistic regression, and K-nearest neighbors ranked in the top and for several times. Under two algorithms, the classifier models performed well on F1 for all drugs, of which the AUC values were above 0.85. While on F2 and F3, classifiers performed well only on some drugs; for example, models performed well on F2 for azoles like FCZ, ICZ, and VCZ, and they performed well on F3 for MCF, but they all had poor classification effect on AmB and PZ. It may be that the correlation between the three sets and classification targets was not very strong, and the information collected for these two drugs was insufficient.

Mutation Ranking

Using RFECV, three antifungal drugs, including FCZ, MCF, and AmB, were ranked and predicted, respectively. The mutation ranking results are shown in **Tables 3–5**. Previously reported mutations (bolded in the table), such as Y132F, K143R, and F126L on the *ERG11*, mutations on the *TAC1B* (Rybak et al., 2020), and S639Y/S639F and S639P on the *FKS1* gene, were detected and listed as important mutations. In addition, several novel mutations were detected (marked by an asterisk). Particularly, mutations in the "hot spot" regions of the ergosterol pathway, such as I466M, G459S, and Y501H in *ERG11*, and R278H in *ERG10*, were detected. These mutations were frequently and

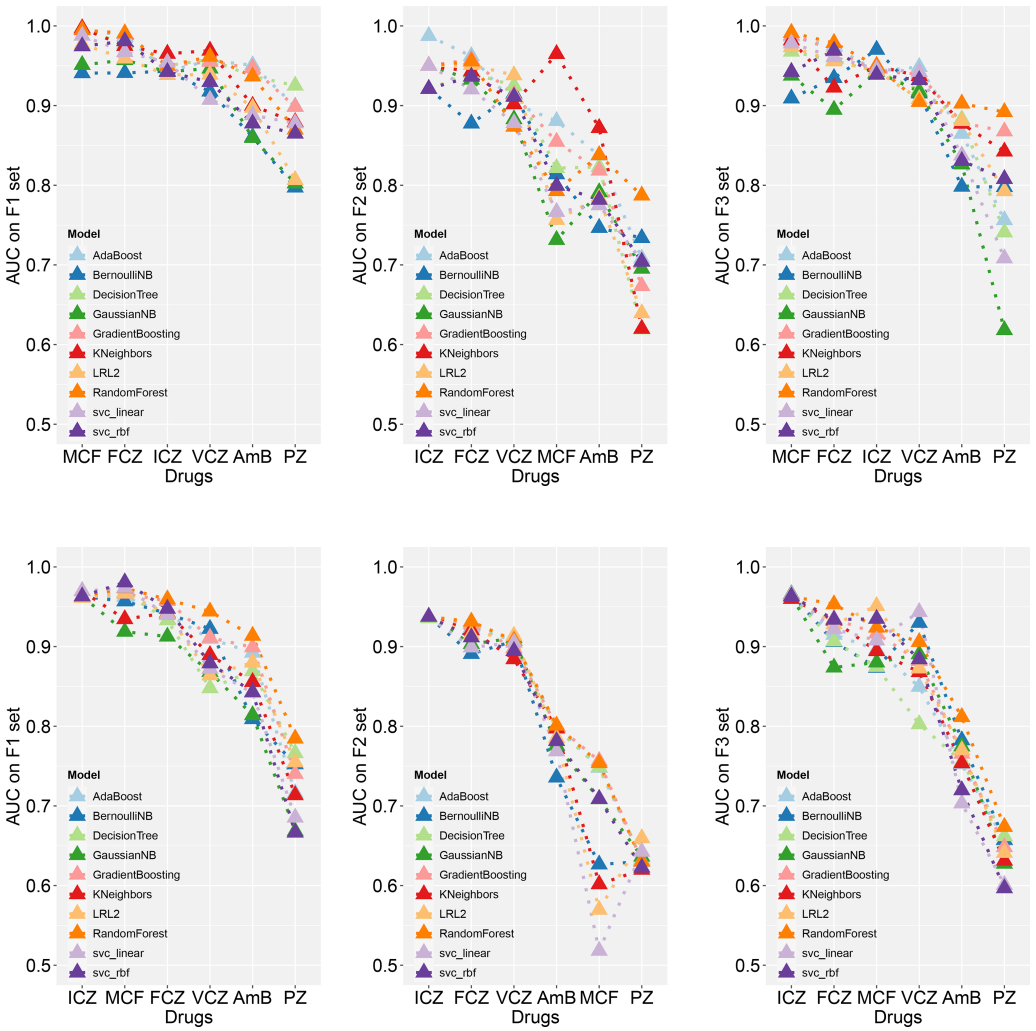

FIGURE 2 | Comparison of the best AUC values using different machine learning classifiers.The best models on the balanced (the upper three) and imbalanced (the lower three) test set are shown, respectively. Please see supplementary materials **Table S6** for detailed evaluation results.

TABLE 3 | Top 20 mutations ranked by RFECV for FCZ on F1 set.

NO.	AdaBoost	GradientBoosting	DecisionTree	SVC_linear
1	**FKS1_S639P**	B9J08_003739_G672S	B9J08_003735_K325N	**ERG11_K143R**
2	FKBP12_S4N*	B9J08_003902_G126R	B9J08_003902_G126R	**ERG11_Y132F**
3	B9J08_000267_Y114D	B9J08_003902_S24P	CDR1_G995S*	ERG11_V125A
4	ERG11_Y501H*	CDR1_H771R*	ERG11_Y501H*	B9J08_004578_A202T
5	ERG11_G459S*	ERG11_Y501H*	**ERG11_K143R**	**TAC1B_K247E**
6	**ERG11_K143R**	B9J08_004467_ G22E	**TAC1B_A651T**	B9J08_004467_G22E
7	**ERG11_Y132F**	CDR1_G995S*	B9J08_004468_F82V	**ERG11_F126L**
8	B9J08_004578_M245V	**TAC1B_A651T**	**ERG11_Y132F**	B9J08_001033_L136F
9	**TAC1B_E200K**	**ERG11_K143R**	**TAC1B_F214S**	ERG11_Y501H*
10	**TAC1B_F214S**	B9J08_004468_F82V	B9J08_004467_G22E	MRR1_N647T
11	**TAC1B_K247E**	**TAC1B_F214S**	PGA7_E49D*	B9J08_004468_K506R
12	**TAC1B_A583S**	B9J08_003735_K325N	B9J08_000267_Y114D	B9J08_004818_D671N
13	**TAC1B_A651T**	**ERG11_Y132F**	UPC2_E229K	B9J08_004818_E749K
14	**TAC1B_M653V**	UPC2_E229K	**TAC1B_K247E**	B9J08_004578_E289G
15	B9J08_004468_F82V	B9J08_001033_L136F	B9J08_001033_L136F	B9J08_001030_E534K
16	PGA7_A18P*	B9J08_000267_Y114D	ERG11_I466M*	B9J08_000962_H59L
17	PGA7_E49D*	**TAC1B_K247E**	ERG10_R278H*	CDR1_E709G
18	CDR1_G995S*	B9J08_001030_E2Q	**TAC1B_M653V**	B9J08_004468_F82V
19	**TAC1B_S195C**	B9J08_003902_T917I	**FKS1_S639P**	B9J08_000961_K330N
20	**TAC1B_S192N**	PGA7_E49D*	ERG3_Y279H	FKS1_M1267I

Bolded means previously reported mutations.
**Represents drug resistance mutation should be paid special attention to.*

TABLE 4 | Top 20 mutations ranked by RFECV for AmB on F1 set.

NO.	AdaBoost	DecisionTree	GradientBoosting	SVC_Linear	RandomForest
1	ERG10_R278H*	ERG10_R278H*	ERG10_R278H*	ERG10_R278H*	ERG10_R278H*
2	ERG3_D283N	B9J08_003902_G126R	B9J08_003902_G126R	B9J08_003902_G126R	B9J08_003736_N36H
3	B9J08_003902_G126R	MRR1_H417L	MRR1_H417L	B9J08_005341_K374R	B9J08_003902_G126R
4	**TAC1B_S195C**	B9J08_000267_Y114D	B9J08_000267_Y114D	B9J08_000267_Y114D	B9J08_005338_V621F
5	B9J08_005341_A592D	ERG11_I466M*	ERG11_I466M*	ERG11_I466M*	B9J08_005341_N279H
6	B9J08_000962_G41E	ERG11_G459S*	ERG11_G459S*	ERG11_G459S*	CDR1_H771R*
7	**FKS1_S639Y/S639F**	**ERG11_K143R**	**ERG11_K143R**	**ERG11_K143R**	B9J08_000267_Y114D
8	FKS1_F219V	**ERG11_Y132F**	B9J08_004576_L747F	**ERG11_Y132F**	B9J08_001445_S430N
9	FKBP12_S4N*	B9J08_004818_S745P	B9J08_004818_S745P	**TAC1B_A651T**	ERG11_I466M*
10	B9J08_001033_L136F	**TAC1B_A651T**	B9J08_004818_P67H	PGA7_A18P	ERG11_G459S*
11	CDR1_G995S*	PGA7_A18P*	**TAC1B_S192N**	PGA7_E49D	**ERG11_K143R**
12	CDR1_E709G	**TAC1B_F214S**	**TAC1B_A640V**	CDR1_G995S*	**TAC1B_A651T**
13	B9J08_000267_Y114D	**TAC1B_S192N**	**TAC1B_A651T**	B9J08_005341_K918R	**TAC1B_A657V**
14	UPC2_E229K	B9J08_001445_L368F	**TAC1B_A657V**	**TAC1B_K247E**	PGA7_A18P*
15	B9J08_001445_L368F	**TAC1B_A15T**	PGA7_A18P*	**TAC1B_F214S**	PGA7_E49D*
16	B9J08_001445_V317L	**TAC1B_A583S**	B9J08_001445_L368F	**TAC1B_A657V**	B9J08_000166_V641D
17	ERG11_I466M*	B9J08_005341_A592D	**TAC1B_S195C**	B9J08_001033_L136F	**ERG11_Y132F**
18	ERG11_G459S*	PGA7_E49D*	B9J08_000268_I6F	B9J08_003735_E275G	UPC2_E229K
19	**ERG11_K143R**	ERG3_D283N	FKS1_K848R	B9J08_001030_E2Q	**TAC1B_S192N**
20	**ERG11_Y132F**	UPC2_E229K	**ERG11_Y132F**	CDR1_H771R*	B9J08_004818_S745P

Bolded means previously reported mutations.
**Represents drug resistance mutation should be paid special attention to.*

highly ranked mutations. *FKBP12* has been reported to be associated with multiple resistance in *Candida* spp., and the S4N mutation was detected in this gene. Two frequently occurring mutations, H771R and G995S, were identified in *CDR1*, the gene encoding the ATP-Binding Cassette efflux pump transporter. Two high-frequency mutations, E49D and A18P, were also found in a specific gene (*PGA7*, *C. albicans* homolog) of *C. Auris*. These mutations should be paid special attention to in the following research.

DISCUSSION

C. auris strains C1921 and C1922 sequenced in our laboratory were classified into Clade III from the phylogenetic tree, which was consistent with the tree constructed using Internal Transcribed Spacer and D1/D2 Large Ribosomal Subunit Region in the previous study (Chen et al., 2018). Previous studies classified *C. auris* into four clades: South Asia (Clade I), East Asia (Clade II), South Africa (Clade III), and South America

TABLE 5 | Top 20 mutations ranked by RFECV for MCF on F1 set.

NO.	AdaBoost	DecisionTree	GradientBoosting	SVC_Linear	RandomForest
1	B9J08_003489_D695V	**FKS1_S639Y/S639F**	**FKS1_S639Y/S639F**	B9J08_003902_G126R	**FKS1_S639Y/S639F**
2	B9J08_003726_T631S	**FKS1_S639P**	**FKS1_S639P**	**FKS1_S639Y/S639F**	**FKS1_S639P**
3	ABC_T37A	B9J08_000274_V248F	B9J08_001033_L136F	**FKS1_S639P**	B9J08_000274_F180V
4	**FKS1_S639Y/S639F**	B9J08_000274_F180V	ERG11_I466M*	CDR1_H771R*	FKBP12_S4N*
5	**FKS1_S639P**	ERG11_I466M*	B9J08_000274_V248F	ERG11_I466M*	**ERG11_Y132F**
6	FKS1_F219V	B9J08_001033_L136F	FKS1_D979N	B9J08_000274_V248G	B9J08_001033_L136F
7	CDR1_E709D	PGA7_E49D*	FKS1_K848R	FKS1_L972M	**TAC1B_A657V**
8	CDR1_V704L	**ERG11_F126L**	B9J08_000274_F180V	MRR1_R249K	ERG11_I466M*
9	UPC2_E229K	CDR1_V704L	B9J08_000274_V248G	FKBP12_S4N*	B9J08_000161_N244K
10	B9J08_000274_F180V	**TAC1B_A640V**	B9J08_003735_H8Q	B9J08_000162_D109G	ERG3_L262I
11	ERG11_I466M*	B9J08_003726_G756V	PGA7_E49D*	B9J08_000162_P110S	CDR1_V704L
12	**TAC1B_A640V**	FKS1_F219V	FKS1_S846A	MRR1_I211V	PGA7_E49D*
13	PGA7_E49D*	PGA7_A18P*	ABC_Y504H	B9J08_000274_F180V	B9J08_004009_E641K
14	B9J08_003726_G756V	B9J08_001445_L368F	B9J08_000274_N243K	B9J08_003489_D695V	FKS1_L972M
15	CDR1_E709G	ABC_V3I	MRR1_N647T	B9J08_000162_E475K	PGA7_A131T
16	B9J08_001033_L136F	B9J08_003726_N248H	B9J08_003726_K299R	**ERG11_Y132F**	**ERG11_K143R**
17	**ERG11_Y132F**	B9J08_000166_V641D	B9J08_000274_A245G	CDR1_E709D	PGA7_A18P*
18	CDR1_H771R*	B9J08_003726_S279N	**TAC1B_A640V**	B9J08_003726_P586S	FKS1_K848R
19	ABC_V3I	B9J08_000166_S685N	**ERG11_F126L**	B9J08_003622_V132L	CDR1_H771R*
20	PGA7_A18P*	B9J08_003726_K299R	B9J08_000274_A231D	B9J08_003622_S249T	ERG3_V258I

Bolded means previously reported mutations.

**Represents drug resistance mutation should be paid special attention to.*

(Clade IV) (potential fifth clade of Iranian origin), and it was emphasized that each clade has a great relationship with geographical location. The clustering results from the phylogenetic tree in this study illustrated that these strains could be divided into four clades, but the conclusion of clustering according to geographical location was not very prominent.

Machine learning technology has great potential in classifying drug resistance of strains with WGS data and analyzing high-dimensional data sets, which is very important for predicting mutations associated with drug resistance. Our model evaluation results illustrated that the machine learning classifiers performed quite different when testing different drugs. The classifier model showed excellent performance for azoles and echinocandins such as FCZ, ICZ, VCZ, and MCF, but not for others like AmB and PZ. It was speculated that there might be more information about determinants associated with azoles and echinocandins resistance but less for AmB and PZ in the three sets. This was directly indicative of the fact that the correlation between feature sets and classification targets was stronger for azoles and echinocandins, but was weaker for the two drugs. In addition, there were some deficiencies in model optimization so that only several models were optimized in the process of constructing classifier models and adjusting parameters. Therefore, optimizing models through a large number of experiments and tests should be performed in future work in order to achieve better performance.

In this study, RFECV combined with a machine learning classifier was used to predict and rank the mutations of *C. auris* related to antifungal drug resistance. In the RFECV process, different ranked mutation results were obtained by combining different classifiers. Overall, the results indicated that the RFECV method could not only rank several known mutations as important, especially for well-studied drugs but also predict some new important mutations on the genes closely related to drug resistance. Some of the predicted mutations were known to be important resistance mutations, which to some extent demonstrated the validity of our classification model. The model could obtain more reliable conclusions for well-studied drugs, such as azoles and echinocandins, while for amphotericin B, the model also predicted some resistance-related mutations. Based on these results, further research and verification are needed on the specific mutations and drug resistance mechanisms of *C. auris*.

Machine learning models can improve the prediction of important genetic mutation sites related to drug resistance in fungi, particularly beneficially for less-studied drugs. The amount of test data, or sample size, is one of the keys to the performance of machine learning methods. We speculate that 500 to 1,000 fungal samples may get satisfactory results according to previous studies. Random forest, logistic regression, and K-nearest neighbors classifier performed relatively better in this study. While in another study, PM (product-of-marginal model) and SVC-RBF ranked as the top two best-performing classifiers on MTB (Yang et al., 2018). The most common issues in machine learning lie around overfitting, underfitting, noisy data and inappropriate validation. Hence, considering all available variants and allowing machine learning methods to reduce the dimension can improve the performance. In the future, it is necessary to conduct systematic verification and related functional studies on these mutations.

This study may help to analyze the drug resistance mechanism of *C. auris*, and provide a scientific basis for developing prevention and control strategies against drug resistance and the search for possible new drug targets.

DATA AVAILABILITY STATEMENT

The datasets presented in this study can be found in online repositories. The names of the repository/repositories and accession number(s) can be found in the article/**Supplementary Material**.

AUTHOR CONTRIBUTIONS

LH and XC conceived the project. JZ and FC collected the samples. DL, YW, and WH conducted the NGS. YW and DL conducted the RNA analysis, analyzed data and wrote manuscript. LH evaluated all results. All authors contributed to the article and approved the submitted version.

FUNDING

This study was supported by Scientific Research Project of National Natural Science Foundation of China (81971914, 81772163, 82172293), the State Key Program of National Natural Science Foundation of China (12031016), Project of Natural Science Foundation of Liaoning Province (20180550255) and Fundamental Research Funds for the Central Universities (GK201901008).

ACKNOWLEDGMENTS

We thank all the subjects who participated in this study.

SUPPLEMENTARY MATERIAL

The Supplementary Material for this article can be found online at: https://www.frontiersin.org/articles/10.3389/fcimb.2021.742062/full#supplementary-material

REFERENCES

Biagi, M. J., Wiederhold, N. P., Gibas, C., Wickes, B. L., Lozano, V., Bleasdale, S. C., et al. (2019). Development of High-Level Echinocandin Resistance in a Patient With Recurrent Candida Auris Candidemia Secondary to Chronic Candiduria. *Open Forum Infect. Dis.* 6 (7), ofz262. doi: 10.1093/ofid/ofz262

Bing, J., Hu, T., Zheng, Q., Munoz, J. F., Cuomo, C. A., and Huang, G. (2020). Experimental Evolution Identifies Adaptive Aneuploidy as a Mechanism of Fluconazole Resistance in Candida Auris. *Antimicrob. Agents Chemother.* 65 (1). doi: 10.1128/AAC.01466-20

Bolger, A. M., Lohse, M., and Usadel, B. (2014). Trimmomatic: A Flexible Trimmer for Illumina Sequence Data. *Bioinformatics* 30 (15), 2114–2120. doi: 10.1093/bioinformatics/btu170

Breiman, L. (1996). Stacked Regressions. *Mach. Learn.* 24 (1), 49–64. doi: 10.1007/BF00117832

Breiman, L. (2001). Random Forests. *Mach. Learn.* 45 (1), 5–32. doi: 10.1023/A:1010933404324

Cannon, R. D., Lamping, E., Holmes, A. R., Niimi, K., Baret, P. V., Keniya, M. V., et al. (2009). Efflux-Mediated Antifungal Drug Resistance. *Clin. Microbiol. Rev.* 22 (2), 291–321. doi: 10.1128/CMR.00051-08

Chaabane, F., Graf, A., Jequier, L., and Coste, A. T. (2019). Review on Antifungal Resistance Mechanisms in the Emerging Pathogen Candida Auris. *Front. Microbiol.* 10, 2788. doi: 10.3389/fmicb.2019.02788

Chen, Y., Zhao, J., Han, L., Qi, L., Fan, W., Liu, J., et al. (2018). Emergency of Fungemia Cases Caused by Fluconazole-Resistant Candida Auris in Beijing, China. *J. Infect.* 77 (6), 561–571. doi: 10.1016/j.jinf.2018.09.002

Chow, N. A., de Groot, T., Badali, H., Abastabar, M., Chiller, T. M., and Meis, J. F. (2019). Potential Fifth Clade of Candida Auris, Ira. *Emerg. Infect. Dis.* 25 (9), 1780–1781. doi: 10.3201/eid2509.190686

Chow, N. A., Munoz, J. F., Gade, L., Berkow, E. L., Li, X., Welsh, R. M., et al. (2020). Tracing the Evolutionary History and Global Expansion of Candida Auris Using Population Genomic Analyses. *mBio* 11 (2). doi: 10.1128/mBio.03364-19

Chowdhary, A., Prakash, A., Sharma, C., Kordalewska, M., Kumar, A., Sarma, S., et al. (2018). A Multicentre Study of Antifungal Susceptibility Patterns Among 350 Candida Auris Isolate-17) in India: Role of the ERG11 and FKS1 Genes in Azole and Echinocandin Resistance. *J. Antimicrob. Chemother.* 73 (4), 891–899. doi: 10.1093/jac/dkx480

Cingolani, P., Platts, A., Wang le, L., Coon, M., Nguyen, T., Wang, L., et al. (2012). A Program for Annotating and Predicting the Effects of Single Nucleotide Polymorphisms, SnpEff: SNPs in the Genome of Drosophila Melanogaster Strain W1118; Iso-2; Iso-3. *Fly (Austin)* 6 (2), 80–92. doi: 10.4161/fly.19695

Coste, A. T., Karababa, M., Ischer, F., Bille, J., and Sanglard, D. (2004). TAC1, Transcriptional Activator of CDR Genes, Is a New Transcription Factor Involved in the Regulation of Candida Albicans ABC Transporters CDR1 and CDR2. *Eukaryot Cell* 3 (6), 1639–1652. doi: 10.1128/EC.3.6.1639-1652.2004

Danecek, P., Auton, A., Abecasis, G., Albers, C. A., Banks, E., DePristo, M. A., et al. (2011). The Variant Call Format and VCFtools. *Bioinformatics* 27 (15), 2156–2158. doi: 10.1093/bioinformatics/btr330

de Micheli, M., Bille, J., Schueller, C., and Sanglard, D. (2002). A Common Drug-Responsive Element Mediates the Upregulation of the Candida Albicans ABC Transporters CDR1 and CDR2, Two Genes Involved in Antifungal Drug Resistance. *Mol. Microbiol.* 43 (5), 1197–1214. doi: 10.1046/j.1365-2958.2002.02814.x

Deo, R. C. (2015). Machine Learning in Medicine. *Circulation* 132 (20), 1920–1930. doi: 10.1161/CIRCULATIONAHA.115.001593

DePristo, M. A., Banks, E., Poplin, R., Garimella, K. V., Maguire, J. R., Hartl, C., et al. (2011). A Framework for Variation Discovery and Genotyping Using Next-Generation DNA Sequencing Data. *Nat. Genet.* 43 (5), 491–498. doi: 10.1038/ng.806

Di Pilato, V., Codda, G., Ball, L., Giacobbe, D. R., Willison, E., Mikulska, M., et al. (2021). Molecular Epidemiological Investigation of a Nosocomial Cluster of C. Auris: Evidence of Recent Emergence in Italy and Ease of Transmission During the COVID-19 Pandemic. *J. Fungi (Basel)* 7 (2). doi: 10.3390/jof7020140

Du, H., Bing, J., Hu, T., Ennis, C. L., Nobile, C. J., and Huang, G. (2020). Candida Auris: Epidemiology, Biology, Antifungal Resistance, and Virulence. *PloS Pathog.* 16 (10), e1008921. doi: 10.1371/journal.ppat.1008921

Dudiuk, C., Berrio, I., Leonardelli, F., Morales-Lopez, S., Theill, L., Macedo, D., et al. (2019). Antifungal Activity and Killing Kinetics of Anidulafungin, Caspofungin and Amphotericin B Against Candida Auris. *J. Antimicrob. Chemother.* 74 (8), 2295–2302. doi: 10.1093/jac/dkz178

ElBaradei, A. (2020). A Decade After the Emergence of Candida Auris: What do We Know? *Eur. J. Clin. Microbiol. Infect. Dis.* 39 (9), 1617–1627. doi: 10.1007/s10096-020-03886-9

Escandon, P., Chow, N. A., Caceres, D. H., Gade, L., Berkow, E. L., Armstrong, P., et al. (2019). Molecular Epidemiology of Candida Auris in Colombia Reveals a Highly Related, Countrywide Colonization With Regional Patterns in Amphotericin B Resistance. *Clin. Infect. Dis.* 68 (1), 15–21. doi: 10.1093/cid/ciy411

Farhat, M. R., Sultana, R., Iartchouk, O., Bozeman, S., Galagan, J., Sisk, P., et al. (2016). Genetic Determinants of Drug Resistance in Mycobacterium Tuberculosis and Their Diagnostic Value. *Am. J. Respir. Crit. Care Med.* 194 (5), 621–630. doi: 10.1164/rccm.201510-2091OC

Handelman, G. S., Kok, H. K., Chandra, R. V., Razavi, A. H., Lee, M. J., and Asadi, H. (2018). Edoctor: Machine Learning and the Future of Medicine. *J. Intern. Med.* 284 (6), 603–619. doi: 10.1111/joim.12822

Healey, K. R., Kordalewska, M., Jimenez Ortigosa, C., Singh, A., Berrio, I., Chowdhary, A., et al. (2018). Limited ERG11 Mutations Identified in Isolates of Candida Auris Directly Contribute to Reduced Azole Susceptibility. *Antimicrob. Agents Chemother.* 62 (10). doi: 10.1128/AAC.01427-18

Her, H. L., and Wu, Y. W. (2018). A Pan-Genome-Based Machine Learning Approach for Predicting Antimicrobial Resistance Activities of the Escherichia Coli Strains. *Bioinformatics* 34 (13), i89–i95. doi: 10.1093/bioinformatics/bty276

Kordalewska, M., Lee, A., Park, S., Berrio, I., Chowdhary, A., Zhao, Y., et al. (2018). Understanding Echinocandin Resistance in the Emerging Pathogen Candida Auris. *Antimicrob. Agents Chemother.* 62 (6). doi: 10.1128/AAC.00238-18

Kordalewska, M., and Perlin, D. S. (2019). Identification of Drug Resistant Candida Auris. *Front. Microbiol.* 10, 1918. doi: 10.3389/fmicb.2019.01918

Kouchaki, S., Yang, Y., Walker, T. M., Sarah Walker, A., Wilson, D. J., Peto, T. E. A., et al. (2019). Application of Machine Learning Techniques to Tuberculosis Drug Resistance Analysis. *Bioinformatics* 35 (13), 2276–2282. doi: 10.1093/bioinformatics/bty949

Kumar, S., Stecher, G., Li, M., Knyaz, C., and Tamura, K. (2018). MEGA X: Molecular Evolutionary Genetics Analysis Across Computing Platforms. *Mol. Biol. Evol.* 35 (6), 1547–1549. doi: 10.1093/molbev/msy096

Kwon, Y. J., Shin, J. H., Byun, S. A., Choi, M. J., Won, E. J., Lee, D., et al. (2019). Candida Auris Clinical Isolates From South Korea: Identification, Antifungal Susceptibility, and Genotyping. *J. Clin. Microbiol.* 57 (4). doi: 10.1128/JCM.01624-18

Lamb, D. C., Corran, A., Baldwin, B. C., Kwon-Chung, J., and Kelly, S. L. (1995). Resistant P45051A1 Activity in Azole Antifungal Tolerant Cryptococcus Neoformans From AIDS Patients. *FEBS Lett.* 368 (2), 326–330. doi: 10.1016/0014-5793(95)00684-2

Li, H., Handsaker, B., Wysoker, A., Fennell, T., Ruan, J., Homer, N., et al. (2009). The Sequence Alignment/Map Format and SAMtools. *Bioinformatics* 25 (16), 2078–2079. doi: 10.1093/bioinformatics/btp352

Lockhart, S. R., Etienne, K. A., Vallabhaneni, S., Farooqi, J., Chowdhary, A., Govender, N. P., et al. (2017). Simultaneous Emergence of Multidrug-Resistant Candida Auris on 3 Continents Confirmed by Whole-Genome Sequencing and Epidemiological Analyses. *Clin. Infect. Dis.* 64 (2), 134–140. doi: 10.1093/cid/ciw691

Medici, N. P., and Del Poeta, M. (2015). New Insights on the Development of Fungal Vaccines: From Immunity to Recent Challenges. *Mem Inst Oswaldo Cruz* 110 (8), 966–973. doi: 10.1590/0074-02760150335

Mellado, E., Garcia-Effron, G., Alcazar-Fuoli, L., Cuenca-Estrella, M., and Rodriguez- Tudela, J. L. (2004). Substitutions at Methionine 220 in the 14alpha-Sterol Demethylase (Cyp51A) of Aspergillus Fumigatus Are Responsible for Resistance *In Vitro* to Azole Antifungal Drugs. *Antimicrob. Agents Chemother.* 48 (7), 2747–2750. doi: 10.1128/AAC.48.7.2747-2750.2004

Montoya, M. C., Moye-Rowley, W. S., and Krysan, D. J. (2019). Candida Auris: The Canary in the Mine of Antifungal Drug Resistance. *ACS Infect. Dis.* 5 (9), 1487–1492. doi: 10.1021/acsinfecdis.9b00239

Munoz, J. F., Gade, L., Chow, N. A., Loparev, V. N., Juieng, P., Berkow, E. L., et al. (2018). Genomic Insights Into Multidrug-Resistance, Mating and Virulence in Candida Auris and Related Emerging Species. *Nat. Commun.* 9 (1), 5346. doi: 10.1038/s41467-018-07779-6

Nami, S., Mohammadi, R., Vakili, M., Khezripour, K., Mirzaei, H., and Morovati, H. (2019). Fungal Vaccines, Mechanism of Actions and Immunology: A Comprehensive Review. *BioMed. Pharmacother.* 109, 333–344. doi: 10.1016/j.biopha.2018.10.075

Noel, T. (2012). The Cellular and Molecular Defense Mechanisms of the Candida Yeasts Against Azole Antifungal Drugs. *J. Mycol Med.* 22 (2), 173–178. doi: 10.1016/j.mycmed.2012.04.004

Park, S., Kelly, R., Kahn, J. N., Robles, J., Hsu, M. J., Register, E., et al. (2005). Specific Substitutions in the Echinocandin Target Fks1p Account for Reduced Susceptibility of Rare Laboratory and Clinical Candida Sp. Isolates. *Antimicrob. Agents Chemother.* 49 (8), 3264–3273. doi: 10.1128/AAC.49.8.3264-3273.2005

Patel, L., Shukla, T., Huang, X., Ussery, D. W., and Wang, S. (2020). Machine Learning Methods in Drug Discovery. *Molecules* 25 (22). doi: 10.3390/molecules25225277

Puri, N., Krishnamurthy, S., Habib, S., Hasnain, S. E., Goswami, S. K., and Prasad, R. (1999). CDR1, A Multidrug Resistance Gene From Candida Albicans, Contains Multiple Regulatory Domains in Its Promoter and the Distal AP-1 Element Mediates Its Induction by Miconazole. *FEMS Microbiol. Lett.* 180 (2), 213–219. doi: 10.1111/j.1574-6968.1999.tb08798.x

Rhodes, J., Abdolrasouli, A., Farrer, R. A., Cuomo, C. A., Aanensen, D. M., Armstrong-James, D., et al. (2018). Genomic Epidemiology of the UK Outbreak of the Emerging Human Fungal Pathogen Candida Auris. *Emerg. Microbes Infect.* 7 (1), 43. doi: 10.1038/s41426-018-0045-x

Rhodes, J., and Fisher, M. C. (2019). Global Epidemiology of Emerging Candida Auris. *Curr. Opin. Microbiol.* 52, 84–89. doi: 10.1016/j.mib.2019.05.008

Rybak, J. M., Munoz, J. F., Barker, K. S., Parker, J. E., Esquivel, B. D., Berkow, E. L., et al. (2020). Mutations in TAC1B: A Novel Genetic Determinant of Clinical Fluconazole Resistance in Candida Auris. *mBio* 11 (3). doi: 10.1128/mBio.00365-20

Sanglard, D., Ischer, F., Koymans, L., and Bille, J. (1998). Amino Acid Substitutions in the Cytochrome P-450 Lanosterol 14alpha-Demethylase (CYP51A1) From Azole-Resistant Candida Albicans Clinical Isolates Contribute to Resistance to Azole Antifungal Agents. *Antimicrob. Agents Chemother.* 42 (2), 241–253. doi: 10.1128/AAC.42.2.241

Satoh, K., Makimura, K., Hasumi, Y., Nishiyama, Y., Uchida, K., and Yamaguchi, H. (2009). Candida Auris Sp. Nov., a Novel Ascomycetous Yeast Isolated From the External Ear Canal of an Inpatient in a Japanese Hospital. *Microbiol. Immunol.* 53 (1), 41–44. doi: 10.1111/j.1348-0421.2008.00083.x

Sharma, C., Kumar, N., Pandey, R., Meis, J. F., and Chowdhary, A. (2016). Whole Genome Sequencing of Emerging Multidrug Resistant Candida Auris Isolates in India Demonstrates Low Genetic Variation. *New Microbes New Infect.* 13, 77–82. doi: 10.1016/j.nmni.2016.07.003

Spampinato, C., and Leonardi, D. (2013). Candida Infections, Causes, Targets, and Resistance Mechanisms: Traditional and Alternative Antifungal Agents. *BioMed. Res. Int.* 2013, 204237. doi: 10.1155/2013/204237

Tian, S., Rong, C., Nian, H., Li, F., Chu, Y., Cheng, S., et al. (2018). First Cases and Risk Factors of Super Yeast Candida Auris Infection or Colonization From Shenyang, China. *Emerg. Microbes Infect.* 7 (1), 128. doi: 10.1038/s41426-018-0131-0

Vandeputte, P., Ferrari, S., and Coste, A. T. (2012). Antifungal Resistance and New Strategies to Control Fungal Infections. *Int. J. Microbiol.* 2012, 713687. doi: 10.1155/2012/713687

Wang, X., Bing, J., Zheng, Q., Zhang, F., Liu, J., Yue, H., et al. (2018). The First Isolate of Candida Auris in China: Clinical and Biological Aspects. *Emerg. Microbes Infect.* 7 (1), 93. doi: 10.1038/s41426-018-0095-0

Welsh, R. M., Sexton, D. J., Forsberg, K., Vallabhaneni, S., and Litvintseva, A. (2019). Insights Into the Unique Nature of the East Asian Clade of the Emerging Pathogenic Yeast Candida Auris. *J. Clin. Microbiol.* 57 (4). doi: 10.1128/JCM.00007-19

Yang, Y., Niehaus, K. E., Walker, T. M., Iqbal, Z., Walker, A. S., Wilson, D. J., et al. (2018). Machine Learning for Classifying Tuberculosis Drug-Resistance From DNA Sequencing Data. *Bioinformatics* 34 (10), 1666–1671. doi: 10.1093/bioinformatics/btx801

Zhang, H., Li, D., Zhao, L., Fleming, J., Lin, N., Wang, T., et al. (2013). Genome Sequencing of 161 Mycobacterium Tuberculosis Isolates From China Identifies Genes and Intergenic Regions Associated With Drug Resistance. *Nat. Genet.* 45 (10), 1255–1260. doi: 10.1038/ng.2735

Conflict of Interest: The authors declare that the research was conducted in the absence of any commercial or financial relationships that could be construed as a potential conflict of interest.

Publisher's Note: All claims expressed in this article are solely those of the authors and do not necessarily represent those of their affiliated organizations, or those of the publisher, the editors and the reviewers. Any product that may be evaluated in this article, or claim that may be made by its manufacturer, is not guaranteed or endorsed by the publisher.

frontiers in Cellular and Infection Microbiology

ORIGINAL RESEARCH
published: 29 October 2021
doi: 10.3389/fcimb.2021.739496

Antifungal Susceptibility Profiles and Resistance Mechanisms of Clinical *Diutina catenulata* Isolates With High MIC Values

*Xin-Fei Chen[1,2,3†], Wei Zhang[1,2,3,4†], Xin Fan[3,5], Xin Hou[1,3], Xiao-Yu Liu[1,3], Jing-Jing Huang[1,2,3], Wei Kang[1,3], Ge Zhang[1,3], Han Zhang[1,3], Wen-Hang Yang[1,2,3], Ying-Xing Li[3,6], Jin-Wen Wang[7], Da-Wen Guo[8], Zi-Yong Sun[9], Zhong-Ju Chen[9], Ling-Gui Zou[10], Xue-Fei Du[10], Yu-Hong Pan[11], Bin Li[11], Hong He[12] and Ying-Chun Xu[1,3]**

[1] Department of Laboratory Medicine, State Key Laboratory of Complex Severe and Rare Diseases, Peking Union Medical College Hospital, Chinese Academy of Medical Science and Peking Union Medical College, Beijing, China, [2] Graduate School, Chinese Academy of Medical Science and Peking Union Medical College, Beijing, China, [3] Department of Laboratory Medicine, Beijing Key Laboratory for Mechanisms Research and Precision Diagnosis of Invasive Fungal Diseases (BZ0447), Beijing, China, [4] Clinical Microbiology Laboratory, The First Affiliated Hospital of Hebei North University, Zhangjiakou, China, [5] Department of Infectious Diseases and Clinical Microbiology, Beijing Chaoyang Hospital, Beijing, China, [6] Department of Medical Research Center, Peking Union Medical College Hospital, Chinese Academy of Medical Science & Peking Union Medical College, Beijing, China, [7] Department of Laboratory Medicine, Daqing Oilfield General Hospital, Daqing, China, [8] Department of Laboratory Medicine, The First Affiliated Hospital of Harbin Medical University, Harbin, China, [9] Department of Laboratory Medicine, Tongji Hospital, Tongji Medical College, Huazhong University of Science and Technology, Wuhan, China, [10] Department of Laboratory Medicine, The Fourth Affiliated Hospital of Harbin Medical University, Harbin, China, [11] Department of Clinical Laboratory, Fujian Medical University Union Hospital, Fuzhou, China, [12] Department of Clinical Laboratory, The Affiliated Hospital of Qingdao University, Qingdao, China

Diutina catenulata (*Candida catenulata*) is an ascomycete yeast species widely used in environmental and industrial research and capable of causing infections in humans and animals. At present, there are only a few studies on *D. catenulata*, and further research is required for its more in-depth characterization and analysis. Eleven strains of *D. catenulata* collected from China Hospital Invasive Fungal Surveillance Net (CHIF-NET) and the CHIF-NET North China Program were identified using matrix-assisted laser desorption ionization–time of flight mass spectrometry and internal transcribed spacer sequencing. The antifungal susceptibility of the *Diutina catenulata* strains was tested using the Clinical and Laboratory Standards Institute broth microdilution method and Sensititre YeastOne™. Furthermore, ERG11 and FKS1 were sequenced to determine any mutations related to azole and echinocandin resistance in *D. catenulata*. All isolates exhibited low minimum inhibitory concentration (MIC) values for itraconazole (0.06–0.12 μg/ml), posaconazole (0.06–0.12 μg/ml), amphotericin B (0.25–1 μg/ml), and 5-flucytosine (range, <0.06–0.12 μg/ml), whereas four isolates showed high MICs (≥4 μg/ml) for echinocandins. Strains with high MIC values for azoles showed common *ERG11* mutations, namely, F126L/K143R. In addition, L139R mutations may be linked to high MICs of fluconazole. Two amino acid alterations reported to correspond to high MIC values of echinocandin, namely, F621I (F641) and S625L (S645), were found in the hot

OPEN ACCESS

Edited by:
Min Chen,
Shanghai Changzheng Hospital, China

Reviewed by:
Shuwen Deng,
Suzhou High-tech Zone People's Hospital, China
Aylin Döğen,
Mersin University, Turkey
Amir Arastehfar,
Westerdijk Fungal Biodiversity Institute, Netherlands

***Correspondence:**
Ying-Chun Xu
xycpumch@139.com

[†]*These authors have contributed equally to this work and share first authorship*

Specialty section:
This article was submitted to Fungal Pathogenesis, a section of the journal Frontiers in Cellular and Infection Microbiology

Received: *11 July 2021*
Accepted: *28 September 2021*
Published: *29 October 2021*

Citation:
Chen X-F, Zhang W, Fan X, Hou X, Liu X-Y, Huang J-J, Kang W, Zhang G, Zhang H, Yang W-H, Li Y-X, Wang J-W, Guo D-W, Sun Z-Y, Chen Z-J, Zou L-G, Du X-F, Pan Y-H, Li B, He H and Xu Y-C (2021) Antifungal Susceptibility Profiles and Resistance Mechanisms of Clinical Diutina catenulata Isolates With High MIC Values. Front. Cell. Infect. Microbiol. 11:739496. doi: 10.3389/fcimb.2021.739496

spot 1 region of *FKS1*. In addition, one new amino acid alteration, I1348S (I1368), was found outside of the *FKS1* hot spot 2 region, and its contribution to echinocandin resistance requires future investigation. *Diutina catenulata* mainly infects patients with a weak immune system, and the high MIC values for various antifungals exhibited by these isolates may represent a challenge to clinical treatment.

Keywords: *Diutina catenulata* (*Candida catenulata*), antifungal susceptibility, *ERG11*, *FKS1*, gene mutation, drug resistance mechanisms

INTRODUCTION

In recent years, *Candida* infections have been on the rise worldwide (Sanguinetti et al., 2015; Pristov and Ghannoum, 2019). Although *Candida albicans* remains the main causative agent of these infections, the rate of non–*C. albicans* candidial infections is increasing (Sanguinetti et al., 2015). Candida infections are not usually multidrug-resistant, but there are notable cases of drug resistance among non-albicans Candida (NAC) species. *Candida auris* shows *in vitro* multidrug resistance and is associated with outbreaks. *Candida glabrata* is the most common cause of candidemia and is resistant to azoles and echinocandins. *Candida parapsilosis* is another notorious pathogen isolated from patients, which causes outbreaks and multidrug resistance (Arastehfar et al., 2021). These *Candida* species, though rare, are clinically common and necessitate a better understanding of their pathogenic mechanisms. *Diutina catenulata* (*C. catenulata*), an ascomycete, can colonize the digestive tract of animals and humans and cause superficial or deep infections (Crozier, 1977; Radosavljevic et al., 1999; Ha et al., 2018; Cafarchia et al., 2019). *Diutina catenulata* is usually utilized in the production of industrial products (Joo et al., 2008; Subramanya et al., 2017; Babaei and Habibi, 2018; Cafarchia et al., 2019). *Diutina catenulata* belongs to the CTG-Ser clade and is closely related to *Saccharomyces cerevisiae* (O'Brien et al., 2018). The first time describing *D. catenulata* associated with disease in humans in 1977, and *D. catenulata* was recovered from the nail of a 50-year-old male Australian patient (Crozier, 1977). Subsequently, the first case of candidemia was diagnosed in a patient with cancer (Radosavljevic et al., 1999).

There are few reports of human infection with *D. catenulata*, and only a small number of studies are available to guide clinical treatment. *Diutina catenulata* generally exhibits antifungal sensitivity (Radosavljevic et al., 1999; Ha et al., 2018); however, some strains showing resistance to azoles and echinadines have been isolated from eggs and feces (Glushakova et al., 2021). Thus, it is important to consider the potential antifungal resistance of *D. catenulata*. However, the resistance mechanism of *D. catenulata* is poorly understood. Amino acid alternations in Erg11p and Fks1p are responsible for causing azole and echinocandin resistance in pathogenic *Candida* spp. (Berkow and Lockhart, 2017; Toutounji et al., 2019). However, the complete open reading frames of both *ERG11* and *FKS1* genes have not been revealed, and the gene polymorphisms of *ERG11* and *FKS1* in clinical *D. catenulata* isolates remain unknown.

Despite the three cases reported worldwide, the occurrence of *D. catenulata* in clinical specimens of the Chinese population remains unelucidated. Thus, we studied the antifungal susceptibility and potential drug resistance mechanisms of the clinical isolates of *D. catenulata* obtained in China over a period of 9 years.

MATERIAL AND METHODS

Ethics Statement

This study was approved by the Human Research Ethics Committee of Peking Union Medical College Hospital (No. S-263). A written informed consent was obtained from all study participants to examine the isolates cultured from them for scientific research.

Isolates

During the period from 2010 to 2018 (**Table 1**), 11 *D. catenulata* isolates were collected from seven different hospitals in five provinces from the China Hospital Invasive Fungal Surveillance Net (CHIF-NET) and the CHIF-NET North China Program. These isolates were mainly from invasive fungal infection specimens. Most specimens were obtained from patients with bloodstream infections, which indicates the seriousness of the situation for these patients.

Identification

All isolates were identified at the species level using matrix-assisted laser desorption ionization–time of flight mass spectrometry (MALDI-TOF MS) conducted with Autof MS 1000 (Autobio, Zhengzhou, China) and Vitek MS (Bio Merieux, Marcy-l'Étoile, France). The species identification was confirmed *via* the sequencing of the rDNA internal transcribed spacer (ITS) region (ABI 3730XL, Thermo Fisher Scientific, Cleveland, OH, USA). PCR and sequencing of the amplicons were performed using the forward primers, V9G and ITS1 (5′-TCCGTAGGTGAACCTGCGG-3′), and the reverse primers, LS266 and ITS4 (5′-TCCTCCGCTT ATTGATATGC-3′) (Zhang et al., 2014; Hou et al., 2016). The phylogenetic tree of *D. catenulata* was constructed by alignment with the ITS gene sequences of the common *Candida* species in the NCBI gene library. Maximum-likelihood phylogenetic trees were constructed with IQ-TREE using an ultrafast bootstrap approximation approach with 1,000 replicates (Trifinopoulos et al., 2016).

TABLE 1 | List of isolates included in the study.

Strain	Gender/Age	Year	Department	Source of isolate	Identity	Clinical diagnosis
1	F/75	2010	ICU	Blood	100	Pneumonia
2	M/56	2010	ICU	Blood	100	Coronary heart disease, lung infection
3	M/54	2013	Organ transplantation	Ascites	100	Primary liver cancer
4	M/60	2016	Neurosurgery	Cerebrospinal fluid	100	Hydrocephalus
6	M/79	2016	ICU	Blood	100	Coronary heart disease
11	M/2	2015	Hematopathy	Blood	100	Infectious fever
12	F/59	2018	ICU	Blood	100	Cerebral hemorrhage
13	M/45	2017	Organ transplantation	Ascites	100	Liver transplantation
15	M/84	2016	ICU	Urine	100	Subarachnoid hemorrhage
16	M/81	2017	ICU	Urine	100	Fever
17	F/78	2017	ICU	Urine	100	Closed abdominal trauma

Antifungal Susceptibility Testing

Minimum inhibitory concentrations (MICs, μg/ml) of nine antifungal agents, namely, anidulafungin, micafungin, caspofungin, fluconazole, posaconazole, voriconazole, itraconazole, amphotericin B, fluorocytosine, were determined for all isolates using the Sensititre YeastOne™ system (SYO, Trek Diagnostic Systems, Thermo Fisher Scientific, Cleveland, OH, USA) according to the manufacturer's instructions. MICs of micafungin (Astellas, Japan), caspofungin (CAS; Merck, USA), fluconazole [(National Institute for Food and Drug Control (NIFDC), China], voriconazole (NIFDC, China), amphotericin B (NIFDC, China), and flucytosine (NIFDC, China) were determined using the CLSI broth microdilution method. MICs were determined after 36 h of culture. *Candida krusei* ATCC 6258 and *C. parapsilosis* ATCC 22019 were used as quality control strains. When the MIC obtained by the two methods fell within a twofold dilution gradient, the essential agreement (EA) between Sensititre™ YeastOne™ and CLSI was considered for *D. catenulata*. The clinical breakpoints of antifungals against *D. catenulata in vitro* have not yet been established by the Clinical and Laboratory Standards Institute (CLSI) or the European Committee on Antimicrobial Susceptibility Testing (EUCAST). Consequently, the interpretative criteria were followed to test the *in vitro* susceptibility of *Candida* spp. according to the CLSI M59 guidelines (CLSI, 2017).

DNA Extraction and Sequencing of *ERG11* and *FKS1*

On comparing published amino acid sequences of *ERG11* (3641571, 1466526) and *FKS1* (3639844, 856398) with *D. catenulata* CBS 565 whole-genome sequences (PJEZ00000000.1) and conducting gene annotation, we identified the *ERG11* and *FKS1* homologous proteins in *C. catenulata*. Amino acid alignment of Erg11p and Fks1p from published data and whole-genome sequencing of analyzed data is shown in **Supplementary Figures 1**, **2**.

ERG11 and *FKS1* Sequencing

Genomic *ERG11* and *FKS1* were amplified by PCR using specific primers and sequenced as previously described. The forward (5′- ACATTATTTATTGCCCCATG-3′) and reverse primers (5′-GCAAGTATCCCGCTTTTCCC-3′) for *ERG11* and those for *FKS1* are shown in **Supplementary Table 1**.

Nucleotide Sequence Accession Numbers

The ITS region sequences of strains found in this study were deposited in GenBank with accession numbers MW624477 to MW624482.

Literature Review

This literature review considered the available data regarding the susceptibility of the *D. catenulata* species to antifungals. The literature search was performed on September 3, 2021, using the following three databases: PubMed (https://pubmed.ncbi.nlm.nih.gov), Web of Science (https://webofknowledge.com), and Embase (https://www.embase.com). The terms "*Diutina catenulates*" or "*Candida catenulate*" or "*Candida ravautii*" were entered in the category of "Title/Abstract" in the PubMed Advanced Search Builder, and "TS=(*Diutina catenulata*)" or "TS=(*Candida catenulata*)" or "TS=(*Candida ravautii*)" was entered in the Web of Science databases. The search in Embase was conducted in the advanced search area, including the terms "'diutina catenulate':ti,ab,kw" or "'candida catenulata':ti,ab,kw" or "'candida ravautii':ti,ab,kw." Studies describing the patients infected with *D. catenulata* were selected and summarized.

RESULTS

Species Identification of *D. catenulata* Using MALDI-TOF and DNA Sequencing

All 11 clinical isolates were identified as *D. catenulata* by the Autof MS 1000 and Vitek MS. The ITS sequences of the study isolates exhibited 100% sequence identity to the corresponding ITS sequences from the reference *D. catenulata* isolates in GenBank (*C. catenulata* CBS 565). We performed a phylogenetic analysis using ITS sequences (**Figure 1**).

This study comprised 72.7% (8/11) males and 27.3% (3/11) females, with an average age of 58 years. Among the specimens,

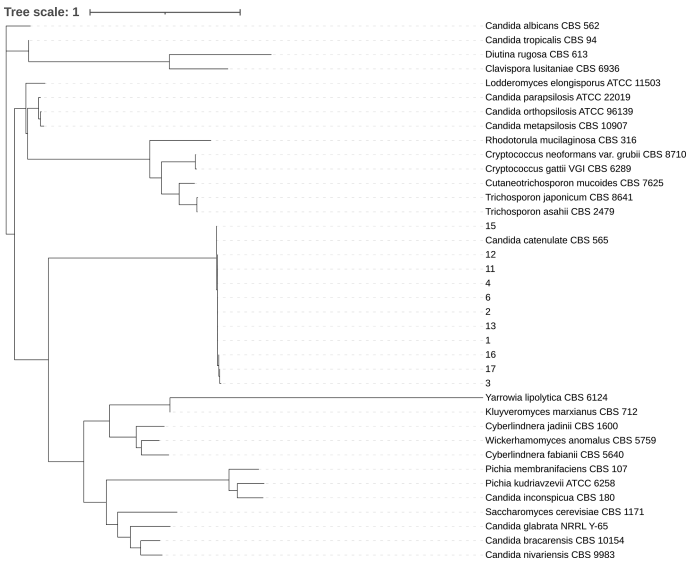

FIGURE 1 | Phylogenetic tree. Internal transcribed spacer (ITS) sequences of nuclear rDNA of *Candida* spp. were used. The ITS sequence of the model strain was obtained from NCBI gene bank. CLC sequence viewer software was used for sequence alignment and IQ-Tree ultrafast bootstrap with 1,000 replicates was used for tree construction.

blood accounted for 45.5% (5/11), urine for 27.3% (3/11), ascites for 18.2% (2/11), and cerebrospinal fluid for 9.1% (1/11). The patients belonged to the following departments: intensive care unit (ICU) 45.5% (5/11), organ transplant department 18.2% (2/11), neurosurgery department 18.2% (2/11), hematology department 9.1% (1/11), and healthcare department 9.1% (1/11).

Antifungal Susceptibility

The quality control strains (*C. krusei* ATCC 6258 and *C. parapsilosis* ATCC 22019) showed MICs within the expected ranges. Aggregated MIC distributions of the nine antifungal agents tested against *D. catenulata* isolates by YeastOne™ are shown in **Table 2**. For all 11 *D. catenulata* isolates, the MICs of itraconazole and posaconazole were in the range of 0.06 to 0.12 μg/ml. In addition, 63.6% (7/11) of *D. catenulata* isolates exhibited high MIC values for fluconazole (MIC >8 μg/ml) and 81.8% (9/11) showed high MIC values (MIC ≥4 μg/ml) for caspofungin. A total of 54.5% (6/11) of *D. catenulata* isolates showed MICs of ≥1 μg/ml for anidulafungin. A total of 36.4% (4/11) of *D. catenulata* isolates showed high MICs for micafungin (MIC ≥1 μg/ml). The MICs of amphotericin B and 5-flucytosine against all *D. catenulata* isolates ranged from 0.25 to 1 and <0.06 to 0.12 μg/ml, respectively. Four *D. catenulata* isolates exhibiting increased MICs of ≥1 μg/ml for all three echinocandins were obtained in our study. Furthermore, the MIC values of echinocandins and fluconazole were high for five isolates of *D. catenulata*.

Agreement Between the CLSI Method and Sensititre YeastOne™

The EA values of the MICs between the CLSI method and YeastOne™ for a majority of the antifungal drugs tested were >90%. In triazoles,

TABLE 2 | Epidemiological cutoff values (ECV) of nine antifungal agents based on aggregated minimum inhibitory concentration (MIC) distributions of *Diutina catenulata*.

	MIC (μg/ml)										Range	Mode[a]	ECV (μg/ml)[b] at:		
	<0.06	0.06	0.12	0.25	0.5	1	2	4	8	>8			95%	97.50%	99%
Fluconazole								4		7	4–256	4	256	256	256
Voriconazole		1	3	2	2	2		1			0.12–4	0.12	4	4	4
Itraconazole		5	6								0.06–0.12	0.12	0.12	0.12	0.12
Posaconazole	1	6	4								0.06–0.12	0.06	0.12	0.12	0.12
Caspofungin		1	1		1			2		6	0.06–>8	>8	>8	>8	>8
Micafungin	4		2		1				1	3	0.03–>8	<0.06	>8	>8	>8
Anidulafungin		2	2		1	2		2		2	0.06–>8	0.06, 0.12, 1, 4, >8	>8	>8	>8
5-Flucytosine	10		1								<0.06–0.12	<0.06	0.12	0.12	0.12
Amphotericin B				1	5	5					0.25–1	1	1	1	1

[a]*Most frequent MIC.*

[b]*Calculated ECVs comprising ≥95, ≥97.5, or ≥99% of the statistically modeled MIC population.*

100% EA values were obtained for amphotericin B and 5-flucytosine. EA values for caspofungin and micafungin were 81.9 (9/11) and 91% (10/11), respectively (**Supplementary Table 2**).

Sequence Analysis of the *ERG11* Gene in the Clinical Isolates

The complete open reading frame of *D. catenulata ERG11* gene, predicted using bioinformatics analysis, showed that *ERG11* comprises 1,563 base pairs (**Table 3**). The *ERG11* gene was sequenced for all 11 *D. catenulata* isolates. These isolates displayed amino acid substitutions in Erg11p compared with the sequences in GenBank. The SNP F126L (C378G) and synonymous mutations C681T, C888A, C999T, and C1164T were found in two isolates with high fluconazole MICs (>32 μg/ml). Amino acid substitutions, F126L (C378G) and G417K (L139F), and synonymous mutations, C681T, C888A, C999T, and C1164T, were found in three isolates with fluconazole MICs >64 μg/ml. Additionally, one isolate with K143R (A428G) and synonymous mutations, C681T, C888A, C999T, and C1164T, showed high resistance to fluconazole (MIC >256 μg/ml). Only one resistant strain had the K143R (A428G) mutation. In addition, synonymous mutations G306A and C852T were found in three isolates (**Table 4**). By aligning the amino acid sequences of Erg11P from *C. albicans* and *S. cerevisiae*, we found that Erg11p of *D. catenulata* shared 69.75 and 65.25% identity with that of *C. albicans* and *S. cerevisiae*, respectively. Notably, the *C. catenulata* Erg11p contained residues at three locations (F126, L139, K143) that corresponded with three residues (F126, L139, K143, respectively) in *C. albicans* ERG11 (**Supplementary Figure 1**) whose alterations (F126L, K143R) have been reported to be associated with azole resistance (Berkow and Lockhart, 2017).

TABLE 3 | The variability of *ERG11* and *FKS1* genes in clinical *Diutina catenulata* isolates.

	DNA sequence			Protein sequence	
	Length (nt)	No. of SNPs	No. of allele types	Amino acid changes	No. of protein types
ERG11	1563	10	5	3	3
FKS1	5652	27	9	7	7

Sequence Analysis of *FKS1* Gene in Clinical Isolates

The complete open reading frame of *D. catenulata FKS1*, determined by bioinformatics analysis, showed that *FKS1* comprises 5,652 base pairs (**Table 3**). The *FKS1* gene was sequenced for all 11 *D. catenulata* clinical isolates. We found 27 SNPs (A591G, G732C, T1119C, C1194T, G1203A, C1299T, G1365T, A1554G, T1605C, T1861A, C1874T, T2079C, C2100T, C2682T, C2781G, G2871A, G3036A, C3273T, G3367A, T4043G, T4062G, G4230C, C4462T, C4704T, T4977C, C5006T, and 5088C) (**Supplementary Table 3**). The SNP T4062G was found in an isolate with high aggregated MIC distributions for echinocandin (≥8 μg/ml). By aligning the amino acid sequence of Fks1p of *D. catenulata* with those of the corresponding proteins in *C. albicans* and *S. cerevisiae* (which had 83.51 and 71.29% identities with *D. catenulata*, respectively), we found seven amino acid substitutions in the Fks1p of *D. catenulata* (**Supplementary Table 3**). Amino acid substitution F621I was found in one isolate (Isolate 2) with capofungin MIC >8 μg/ml. Substitution I1348S was found in three isolates with echinocandin MIC ≥4 μg/ml (isolates 15, 16, and 17). Additionally, amino acid substitutions S625L and F1354L were found in one isolate with an MIC ≥8 μg/ml for three types of echinocandins (Isolate 13) (**Table 5**).

Literature Review

Only three of the sourced articles had reported clinical cases of infection with *D. catenulata*, including one case, in which the *D. catenulata* was isolated from the nails and two cases of *D. catenulata* isolated from blood culture (Crozier, 1977; Radosavljevic et al., 1999; Ha et al., 2018). One of the patients was diagnosed with gastric cancer and the other with endocarditis. One of the isolates showed low MICs for amphotericin B, miconazole, econazole, tioconazole, ketoconazole (1 μg/ml), traconazole (0.25 μg/ml), and fluconazole (16 μg/ml). Other isolates showed low MICs for fluconazole and micafungin (2 and 0.06 μg/ml, respectively). In addition, based on the patients' clinical information, we can conclude that broad-

TABLE 4 | The variability of *ERG11* gene in clinical *D. catenulata* isolates.

Isolate	Missense mutation	Synonymous mutation				MICs (μg/ml)			
	Nucleotide mutation (amino acid mutation)					FZ[a]	VOR[a]	PZ[a]	IZ[a]
1	A428G (K143R)	C681T	C888A	C999T	C1164T	256	0.5	0.12	0.12
2	C378G (F126L)	C681T	C888A	C999T	C1164T	64	1	0.12	0.12
3		G306A	C852T			4	0.12	0.06	0.12
4		G306A	C852T			4	0.12	0.06	0.06
6	C378G (F126L)	C681T	C888A	C999T	C1164T	32	0.25	0.06	0.06
11						4	0.12	0.06	0.06
12	A428G (K143R)					64	0.25	0.12	0.12
13		G306A	C852T			4	0.06	0.03	0.06
15	C378G (F126L), G417K (L139F)	C681T	C888A	C999T	C1164T	256	4	0.12	0.12
16	C378G (F126L), G417K (L139F)	C681T	C888A	C999T	C1164T	128	1	0.06	0.12
17	C378G (F126L), G417K (L139F)	C681T	C888A	C999T	C1164T	64	0.5	0.06	0.06

[a]*FZ, Fluconazole; VOR, Voriconazole; PZ, Posaconazole; IZ, Itraconazole.*

TABLE 5 | The variability of *FKS1* gene in the hot spot 1 and near hot spot 2 regions in clinical *D. catenulata* isolates.

Isolate	Missense mutation in *FKS1* hot spot	MICs (μg/ml)		
	Nucleotide mutation (amino acid mutation)	AND[a]	MF[a]	CAS[a]
Hot spot 1				
2	T1861A (F621I), G3367A (G1123S)	1	0.5	>8
6	T1861A (F621I), G3367A (G1123S)	1	0.12	>8
13	C1874T (S625L), T4062G (F1354L)	>8	8	>8
Around hot spot 2				
15	G3367A (G1123S), T4043G (I1348S)	>8	>8	>8
16	G3367A (G1123S), T4043G (I1348S)	4	>8	>8
17	G3367A (G1123S), T4043G (I1348S)	4	>8	>8

[a]*AND, Anidulafungin; MF, Micafungin; CAS, Caspofungin.*

spectrum antibiotic therapy may be a risk factor for infection with *D. catenulata* (**Supplementary Table 4**).

DISCUSSION

With the development of identification technologies, such as MALDI-TOF MS and high-throughput sequencing, many hitherto unknown species of microorganisms have been precisely identified (Qiu et al., 2019). *Diutina catenulata* is a rare yeast that causes infections in humans (Radosavljevic et al., 1999; Ha et al., 2018; Çakır et al., 2019). Therefore, we determined the proportion of *D. catenulata* isolates among clinical strains recovered from patients using CHIF-NET and the CHIF-NET North China Program. DNA sequencing and MALDI-TOF MS can be used to identify *D. catenulata* at the species level, and the proportions of the different species in the sample can be compared. ITS sequencing identified all 11 isolates, and the consistency of these clinical isolates with CBS 565 was 100%. Currently, ITS sequencing is considered a reliable marker for fungal identification (Wang et al., 2012).

Most *Candida* species are pathogens that cause infections in immunocompromised patients (Cernakova et al., 2019). In this study, *D. catenulata* infection mainly occurred in elderly male admitted ICU patients, and nearly half of the infections were bloodstream infections. There are differences in drug resistance rates among *Candida* species (Sanguinetti et al., 2015). *Candida auris* has attracted much attention worldwide due to its high drug resistance and high fatality rates (Lone and Ahmad, 2019). Despite the low frequency of the species, the high MIC values observed for *D. catenulata* potentially could be important. *In vitro* antifungal susceptibility results showed that all *D. catenulata* showed low MICs for itraconazole, posaconazole, amphotericin B, and 5-flucytosine, but four isolates showed high MICs (≥4 μg/ml) for the echinocandins. More than 36.4% of the isolates showed high MIC values for two echinocandins. High MICs of caspofungin may predict high MICs of micafungin and anidulafungin. More than 72.7% of the isolates showed high MICs for fluconazole. Thus, we suggest that *D. catenulata* with high MICs for fluconazole should be evaluated for its susceptibility to other antifungals. Micafungin has excellent effects *in vivo* against *D. catenulata* in infants (Çakır et al., 2019). However, in the present study, our *in vitro* antifungal susceptibility test showed that 36.4% of isolates showed high MICs (≥4 μg/ml) for echinocandins.

To analyze the molecular mechanisms of the antifungal resistance of *D. catenulata*, we sequenced the *ERG11* and *FKS1* genes. In agreement with the azole drug susceptibility profiles, we found three mutations in *ERG11* of *D. catenulata*. Interestingly, F126L and K143R are the most prevalent residue substitutions in *ERG11* (Berkow et al., 2017), but the L139F substitution is an unreported new observation. The mutations in *FKS1* showed polymorphism. We identified two mutations in *FKS1* hot spot 1 [F621I (F641) and S625L (S645)] and one near *FKS1* hot spot 2 [I1348S (I1368)] associated with high MICs of caspofungin (Toutounji et al., 2019). S625L (S645) has been reported to cause failure of micafungin treatment against *C. albicans* (Slater et al., 2011). G3367A was found in isolates showing high and low MIC values against caspofungin and therefore may not be a potential of high MIC values against this antifungal. Of note, caspofungin was found to have a high interlaboratory variation (Espinel-Ingroff et al., 2013) and therefore the high MIC observed for this antifungal may not necessarily be a cause of concern as long as the MIC of the micafungin and anidulafungin are included and remain low. Polymorphisms of *D. catenulata* may also be used as a basis for typing.

Compared with the three articles have been described, we have noticed that the MICs of fluconazole and echinocandin of some of our strains were higher than 64 and 4 μg/mL, respectively, which are significantly higher than previous studies. This obvious difference also shows that there may be some evolutionary differences between Chinese and foreign isolates. In addition, our ICU patients also are treated with antibiotics. Therefore, patients maybe at high risk of *D. catenulata* infection. Similar to the case with most studies, lack of detailed clinical data on antifungal treatment is a major limitation of our study, which precludes us from reaching a conclusive statement about the choice of antifungal treatment and their potential outcome.

In conclusion, because of the low isolation rates, epidemiological knowledge of rare species is critical for clinical treatment. To the best of our knowledge, this study is the first to report the occurrence and distribution of *D. catenulata* in China, and its findings are expected to guide clinical treatment of *D. catenulata* infection in the future.

DATA AVAILABILITY STATEMENT

The datasets presented in this study can be found in online repositories. The names of the repository/repositories and accession number(s) can be found in the article/**Supplementary Material**.

AUTHOR CONTRIBUTIONS

X-FC and WZ conceived and designed the experiment. XF, WK, GZ, HZ, W-HY, J-WW, D-WG, Z-YS, Z-JC, L-GZ, X-FD, Y-HP, BL, and HH contributed reagents/materials/analysis tools. X-FC, X-YL, J-JH, Y-XL, and WZ performed the experiments. X-FC and WZ analyzed the data and wrote the manuscript. Y-CX, XF, XH, and Y-XL revised the manuscript. All authors contributed to the article and approved the submitted version.

FUNDING

This work was supported by the Natural Science Foundation of Beijing, China (Grant No. 7204288), National Natural Science Foundation of China (82002178 and 81971979), Special Foundation for National Science and Technology Basic Research Program of China (2019FY101200), Beijing Municipal Science and Technology Project (Z181100001618015), Beijing Key Clinical Specialty for Laboratory Medicine-Excellent Project (No. ZK201000), and Scientific Research Foundation Project of Hebei Provincial Health Commission (Grant No. 20210702, 20190904, 20180843).

ACKNOWLEDGMENTS

The authors would like to thank all the hospitals involved in the CHIF-NET study and Ms. Yan-Ting Cai (Autobio Labtec Instruments Co., Ltd.) and Ms. Li-Li Wang (Zhuhai Meihua Medical Technology Co., Ltd.) for technical support with MALDI-TOF MS identification of the *Candida* isolates. Dr. Bin Cheng (Beijing Miyun Hospital, Capital Medical University), Ms. Li-Li Wang, Ms. Yan-Ting Cai, Mr. Cheng-Hai Liu (Zhuhai DL Biotech Co., Ltd.), Mr. Wen-Pan Guo (Zhuhai DL Biotech Co., Ltd.), and Ms. Qi Shu (Bioyong Technologies Inc.) took macro and micro photos of the strains. Finally, we would like to thank Shu-Ying Yu, Pei-Yao Jia, Jing-Jia Zhang, and Ya-Ting Ning (Peking Union Medical College Hospital) for their valuable suggestions.

SUPPLEMENTARY MATERIAL

The Supplementary Material for this article can be found online at: https://www.frontiersin.org/articles/10.3389/fcimb.2021.739496/full#supplementary-material

REFERENCES

Arastehfar, A., Daneshnia, F., Hilmioglu-Polat, S., Ilkit, M., Yasar, M., Polat, F., et al. (2021). Genetically Related Micafungin-Resistant *Candida parapsilosis* Blood Isolates Harbouring Novel Mutation R658G in Hotspot 1 of Fks1p: A New Challenge? *J. Antimicrob. Chemother.* 76, 418–422.

Babaei, F., and Habibi, A. (2018). Fast Biodegradation of Diesel Hydrocarbons at High Concentration by the Sophorolipid-Producing Yeast *Candida Catenulata* KP324968. *J. Mol. Microb. Biotech.* 28, 240–253. doi: 10.1159/000496797

Berkow, E. L., and Lockhart, S. R. (2017). Fluconazole Resistance in *Candida* species: A Current Perspective. *Infect. Drug Resist.* 10, 237–245. doi: 10.2147/IDR.S118892

Cafarchia, C., Iatta, R., Danesi, P., Camarda, A., Capelli, G., and Otranto, D. (2019). Yeasts Isolated From Cloacal Swabs, Feces, and Eggs of Laying Hens. *Med. Mycol.* 57, 340–345. doi: 10.1093/mmy/myy026

Çakır, S., Çelebi, S., Özkan, H., Köksal, N., Dorum, B. A., Yeşil, E., et al. (2019). Results of the Use of Micafungin in Newborns. *Mikrobiyol. Bul.* 53, 70–80. doi: 10.5578/mb.67599

Cernakova, L., Light, C., Salehi, B., Rogel-Castillo, C., Victoriano, M., Martorell, M., et al. (2019). Novel Therapies for Biofilm-Based Candida Spp. *Infections Adv. Exp. Med. Biol.* 1214, 93–123. doi: 10.1007/5584_2019_400

Clinical and Laboratory Standards Institute [CLSI] (2020). Epidemiological Cutoff Values for Antifungal Susceptibility Testing. 3nd ed. CLSI supplement M59. Wayne, PA: Clinical and Laboratory Standards Institute.

CLSI (2017). *Performance Standards for Antifungal Susceptibility Testing of Yeasts, CLSI Supplement M60, 1st Edn.*. Wayne, PA: CLSI.

Crozier, W. J. (1977). A Case of Onychomycosis Due to Candida Ravautii. *Aust. J. Dermatol.* 18, 139–140. doi: 10.1111/j.1440-0960.1977.tb00027.x

Espinel-Ingroff, A., Arendrup, M. C., Pfaller, M. A., Bonfietti, L. X., Bustamante, B., Canton, E., et al. (2013). Interlaboratory variability of Caspofungin MICs for Candida spp. Using CLSI and EUCAST methods: should the clinical laboratory be testing this agent? *Antimicrob. Agents Chemother.* 57, 5836–5842.

Glushakova, A. M., Rodionova, E. N., and Kachalkin, A. V. (2021). Yeasts in Feces of Pigeons (Columba Livia) in the City of Moscow. *Curr. Microbiol.* 78, 238–243. doi: 10.1007/s00284-020-02251-5

Ha, M. V., Choy, M. S., McCoy, D., Fernandez, N., and Suh, J. S. (2018). Candida Catenulata Candidaemia and Possible Endocarditis in a Cirrhotic Patient Successfully De-Escalated to Oral Fluconazole. *J. Clin. Pharm. Ther.* 43, 910–913. doi: 10.1111/jcpt.12728

Hou, X., Xiao, M., Chen, S. C., Wang, H., Zhang, L., Fan, X., et al. (2016). Sequencer-Based Capillary Gel Electrophoresis (SCGE) Targeting the rDNA Internal Transcribed Spacer (ITS) Regions for Accurate Identification of Clinically Important Yeast Species. *PloS One* 11, e0154385. doi: 10.1371/journal.pone.0154385

Joo, H. S., Ndegwa, P. M., Shoda, M., and Phae, C. G. (2008). Bioremediation of Oil-Contaminated Soil Using Candida Catenulata and Food Waste. *Environ. Pollut.* 156, 891–896. doi: 10.1016/j.envpol.2008.05.026

Lone, S. A., and Ahmad, A. (2019). Candida Auris-the Growing Menace to Global Health. *Mycoses* 62, 620–637. doi: 10.1111/myc.12904

O'Brien, C. E., McCarthy, C. G. P., Walshe, A. E., Shaw, D. R., Sumski, D. A., Krassowski, T., et al. (2018). Genome Analysis of the Yeast Diutina Catenulata, a Member of the Debaryomycetaceae/Metschnikowiaceae (CTG-Ser) Clade. *PloS One* 13, e0198957. doi: 10.1371/journal.pone.0198957

Pristov, K. E., and Ghannoum, M. A. (2019). Resistance of Candida to Azoles and Echinocandins Worldwide. *Clin. Microbiol. Infect.* 25, 792–798. doi: 10.1016/j.cmi.2019.03.028

Qiu, W., Huang, Y., Zhao, C., Lin, Z., Lin, W., and Wang, Z. (2019). Microflora of Fresh White Button Mushrooms (Agaricus Bisporus) During Cold Storage Revealed by High-Throughput Sequencing and MALDI-TOF Mass Spectrometry Fingerprinting. *J. Sci. Food Agric.* 99, 4498–4503. doi: 10.1002/jsfa.9695

Radosavljevic, M., Koenig, H., Letscher-Bru, V., Waller, J., Maloisel, F., Lioure, B., et al. (1999). Candida Catenulata Fungemia in a Cancer Patient. *J. Clin. Microbiol.* 37, 475–477. doi: 10.1128/JCM.37.2.475-477.1999

Sanguinetti, M., Posteraro, B., and Lass-Florl, C. (2015). Antifungal Drug Resistance Among Candida Species: Mechanisms and Clinical Impact. *Mycoses* 58 (Suppl 2), 2–13. doi: 10.1111/myc.12330

Slater, J. L., Howard, S. J., Sharp, A., Goodwin, J., Gregson, L. M., Alastruey-Izquierdo, A., et al. (2011). Disseminated Candidiasis Caused by Candida Albicans With Amino Acid Substitutions in Fks1 at Position Ser645 Cannot be Successfully Treated With Micafungin. *Antimicrob. Agents Chemother.* 55, 3075–3083. doi: 10.1128/AAC.01686-10

Subramanya, S. H., Sharan, N. K., Baral, B. P., Hamal, D., Nayak, N., Prakash, P. Y., et al. (2017). Diversity, *in-Vitro* Virulence Traits and Antifungal Susceptibility Pattern of Gastrointestinal Yeast Flora of Healthy Poultry, Gallus Gallus Domesticus. *BMC Microbiol.* 17, 113. doi: 10.1186/s12866-017-1024-4

Toutounji, M., Tokajian, S., and Khalaf, R. A. (2019). Genotypic and Phenotypic Characterization of Candida Albicans Lebanese Hospital Isolates Resistant and Sensitive to Caspofungin. *Fungal Genet. Biol.* 127, 12–22. doi: 10.1016/j.fgb.2019.02.008

Trifinopoulos, J., Nguyen, L. T., von Haeseler, A., and Minh, B. Q. (2016). W-IQ-TREE: A Fast Online Phylogenetic Tool for Maximum Likelihood Analysis. *Nucleic Acids Res.* 44, W232–W235. doi: 10.1093/nar/gkw256

Wang, H., Xiao, M., Chen, S. C., Kong, F., Sun, Z. Y., Liao, K., et al. (2012). *In Vitro* Susceptibilities of Yeast Species to Fluconazole and Voriconazole as Determined by the 2010 National China Hospital Invasive Fungal Surveillance Net (CHIF-NET) Study. *J. Clin. Microbiol.* 50, 3952–3959. doi: 10.1128/JCM.01130-12

Zhang, L., Xiao, M., Wang, H., Gao, R., Fan, X., Brown, M., et al. (2014). Yeast Identification Algorithm Based on Use of the Vitek MS System Selectively Supplemented With Ribosomal DNA Sequencing: Proposal of a Reference Assay for Invasive Fungal Surveillance Programs in China. *J. Clin. Microbiol.* 52, 572–577. doi: 10.1128/JCM.02543-13

Conflict of Interest: The authors declare that the research was conducted in the absence of any commercial or financial relationships that could be construed as a potential conflict of interest.

Publisher's Note: All claims expressed in this article are solely those of the authors and do not necessarily represent those of their affiliated organizations, or those of the publisher, the editors and the reviewers. Any product that may be evaluated in this article, or claim that may be made by its manufacturer, is not guaranteed or endorsed by the publisher.

frontiers in Cellular and Infection Microbiology

ORIGINAL RESEARCH
published: 01 November 2021
doi: 10.3389/fcimb.2021.749905

Prevalence of Fungal and Bacterial Co-Infection in Pulmonary Fungal Infections: A Metagenomic Next Generation Sequencing-Based Study

Zhan Zhao[1], Junxiu Song[1], Changqing Yang[1], Lei Yang[1], Jie Chen[3], Xinhui Li[3], Yubao Wang[2] and Jing Feng[1]**

[1] Respiratory Department, Tianjin Medical University General Hospital, Tianjin, China, [2] Institute of Infectious Diseases, The Second Hospital of Tianjin Medical University, Tianjin, China, [3] Guangzhou Sagene Biotechnology Company, Limited, Guangzhou, China

With the widespread use of antibacterial drugs and increasing number of immunocompromised patients, pulmonary fungal infections are becoming more common. However, the incidence of pulmonary fungal and bacterial co-infection is rarely reported. In this study, 119 patients definitively diagnosed with pulmonary fungal infections between July 2018 and March 2020 were assessed using metagenomic next-generation sequencing (mNGS) as well as traditional pathogen detection to gauge the incidence of fungal and bacterial co-infection and evaluate the associated risk factors. We found that of the 119 patients with fungal infections, 48 (40.3%) had pulmonary fungal and bacterial co-infection. We identified immunocompromised status and the presence of one or more pulmonary cavities as risk factors associated with fungal and bacterial co-infection. The most commonly isolated fungi species were *Aspergillus, Pneumocystis*, and *Rhizopus.* The most commonly isolated bacterial species were *Pseudomonas aeruginosa, Acinetobacter baumannii*, and *Stenotrophomonas maltophilia.* Seventy-nine (66.4%) patients had received empirical antibiotic treatment before their pathogenic test results became available, and 41.7% (fungal infection group) and 38.7% (fungal and bacterial co-infection group) of the patients had their antibacterial drug dosage changed accordingly. This mNGS-based study showed that the incidence of fungal and bacterial co-infection is significant. Our research outcomes can, thus, guide the use of antibacterial drugs in the treatment of clinical fungal infections.

Keywords: fungal infection, fungal and bacterial co-infection, risk factor, mNGS, antibacterial treatment

OPEN ACCESS

Edited by:
Abdullah M. S. Al-Hatmi, University of Nizwa, Oman

Reviewed by:
Ci Fu, University of Toronto, Canada
Min Chen, Shanghai Changzheng Hospital, China

***Correspondence:**
Yubao Wang
yubaowang2020@hotmail.com
Jing Feng
zyyhxkfj@126.com

Specialty section:
This article was submitted to Fungal Pathogenesis, a section of the journal Frontiers in Cellular and Infection Microbiology

Received: *30 July 2021*
Accepted: *18 October 2021*
Published: *01 November 2021*

Citation:
Zhao Z, Song J, Yang C, Yang L, Chen J, Li X, Wang Y and Feng J (2021) Prevalence of Fungal and Bacterial Co-Infection in Pulmonary Fungal Infections: A Metagenomic Next Generation Sequencing-Based Study. Front. Cell. Infect. Microbiol. 11:749905. doi: 10.3389/fcimb.2021.749905

INTRODUCTION

The human respiratory tract is exposed to various microorganisms present in the ambient atmosphere including fungi. In most individuals, immune function can prevent fungal growth and invasion, but a growing number of immunocompromised patients and the widespread use of antibiotics has led to an increase in the incidence of pulmonary fungal infections (Limper et al., 2011; Denning and Chakrabarti, 2017; Li et al., 2021). Generally, fungal infections are more common in the elderly. However, one report provided evidence that the incidence of fungal

infections in hospitalized patients aged 14–30 years has shown a clear upward trend from 2013 to 2019 (Li et al., 2021). Invasive fungal infections are associated with high mortality, with mortality rates as high as 67% being reported among patients with acute infections (Chen et al., 2001). Clearly, pulmonary fungal infections represent a significant clinical and financial burden to the medical community.

To date, few studies have reported the incidence of pulmonary co-infection of fungi and bacterium or the species of co-infecting bacteria. One report described fungal and bacterial co-infection in burn wounds (de Macedo and Santos, 2005). Presently, the clinical treatment for pulmonary fungal infections usually consists of combining antifungal and antibacterial drugs (Guan et al., 2020). In the absence of a complete understanding of fungal and bacterial co-infection, empirical addition of antibacterial drugs could enhance the risk of drug resistance. Furthermore, the non-specific symptoms of pulmonary co-infections, the limitation of diagnostic methods, and the long, time-consuming traditional detection methods with poor detection rates have hampered efforts to distinguish fungal and bacterial co-infection from other pathogenic infections.

Given the limitations of current pathogenic diagnosis, a rapid and accurate alternative method is imperative. Metagenomic next-generation sequencing (mNGS), also known as high-throughput sequencing, is a promising technique that can be used for rapid identification of infectious pathogens without the need for culture, and with greater sensitivity than traditional culture methods (Gu et al., 2019; Wang et al., 2019). Moreover, mNGS furthers the concept of "precision diagnosis and treatment," as it can be used for multidisciplinary infection diagnosis. According to one report on peripheral pulmonary infectious lesions, the pathogen detection rate *via* mNGS is nearly 89%, which is significantly higher than that *via* traditional detection methods (Huang et al., 2020). Identifying pathogens at an early stage may change the outcome of the disease, but traditional methods based on microbiological and biochemical features are time-consuming and have low detection rates (Petrucelli et al., 2020). Therefore, herein, we used mNGS technology to identify pathogens from lung biopsy samples of patients with fungal infections, or bacterial and fungal co-infections, comparing results to those obtained by traditional methods, and assessing the type and prevalence of the species found to better understand and treat these infections.

MATERIALS AND METHODS

Patients

We analyzed 119 patients with fungal infections, who were admitted to the Respiratory Department of Tianjin Medical University General Hospital from July 2018 to July 2020. All enrolled patient samples were analyzed using mNGS as well as traditional pathogen detection methods. We ascertained the underlying disease and confirmed the heart and coagulation function of all patients. Informed consent was obtained from all subjects before performing biopsy surgery. Immunocompromised patients (those with hematological malignancies, autoimmune diseases, or taking immunosuppressants) were identified. CT scans were performed on all patients using a procedure in keeping with the technical principle of CT scans. Meanwhile, we noted the patient's anti-fungal or antibiotic treatment for the month prior to receiving the pathogen test. Enrolled patients also underwent relevant examinations according to the condition of the disease, such as galactomannan test, (1,3)-β-D-glucan test, sputum smear microscopy, and culture-based analysis. For traditional pathogen detection methods, normal flora of the skin or respiratory tract was not interpreted as pathogens. All procedures were carried out by trained personnel and the study was approved by the Ethics Review Committee of Tianjin Medical University General Hospital. The study was conducted in accordance with the guidelines outlined in the Declaration of Helsinki.

Specimen Collection and Processing

Specimens were collected by the trained staff at the Respiratory Endoscopy Center according to standard procedures. The virtual bronchoscope navigation system, endobronchial ultrasound system, and CT imaging were used to precisely locate the lesion and the results were further confirmed *via* rapid on-site evaluation of cytology (ROSE). Transbronchial lung biopsy (TBLB) and bronchoalveolar lavage fluid (BALF) analysis were performed by routine bronchoscopy or ultrathin bronchoscopy (Olympus, Tokyo, Japan). Six to ten pieces of lung tissue were taken from the diseased area, each piece weighing approximately 4 to 6 g. A portion of each lung biopsy was sent to the histopathology laboratory for processing with hematoxylin and eosin, Ziehl-Neelsen acid-fast, and hexamine silver staining. The rest of the tissue was used for mNGS analysis. The bronchopulmonary specimen from the diseased site was rinsed four times with sterile saline and recycled to obtain BALF. A portion of each specimen was stored at 4°C for mNGS analysis, while the remaining BALF samples were processed within 2 h. In the microbiology laboratory, BALF was used for culture and smear microscopy to identify pathogens and also assessed by the GeneXpert mycobacterium tuberculosis (MTB) and galactomannan (GM) tests.

Metagenomic Next-Generation Sequencing and Analysis

DNA was extracted from BALF and TBLB tissue samples using the TIANamp Micro DNA Kit (TIANGEN BIOTECH, Beijing, China) according to the manufacturer's instructions. As previously described, DNA libraries were sequenced on the Beijing Genomics Institute sequencer-100 (Miao et al., 2018). High-quality sequencing data were generated by removing low-quality, adapter contamination, duplicated reads and short (length <35 bp) reads, followed by computational subtraction of human host sequences mapped to the human reference genome (hg19) using Burrows–Wheeler Alignment. The remaining data were classified using four microbial reference genomes consisting of bacteria and fungi (NCBI; ftp://ftp.ncbi.nlm.nih.gov/genomes/). The interpretation criteria used to determine the results of the mNGS test were defined *via* reference to previous studies (Petrucelli et al., 2020). 1) For bacteria and fungi, the relative abundance of was greater than

30% at the genus level excluding *Mycobacterium tuberculosis*; 2) *Mycobacterium tuberculosis* was considered positive, once it is satisfied that at least one read was aligned to the reference genome at species or genus level, and 3) When the pathogen was detected by the traditional detection method and the mNGS reads number was more than 50 at the same time, this pathogen can also be considered to be positively detected (Li et al., 2018).

Statistical Analyses

We used the *t*-test or Chi-square test to compare differences between fungal infection and fungal and bacterial co-infection and used univariate and multivariate logistic regression models to explore the risk factors associated with co-infections. All statistics were calculated by SPSS 22.0 software and results with $P < 0.05$ were considered statistically significant.

RESULTS

Characteristics of Pulmonary Fungal Infection

One hundred and nineteen patients with pulmonary fungal infection in Tianjin Medical University General Hospital underwent imaging examinations, traditional pathogenic examinations, and mNGS. Other examinations were also carried out according to clinical needs, such as Xpert and GM tests of BALF, G test, and blood sample tests, among others. According to etiology, 119 patients were divided into a fungal and bacterial co-infection group (n=48) and a fungal infection group (n=71).

The average age for the patients in the fungal and bacterial co-infection group and the fungal infection group was comparable at 43.04 years and 40.77 years, respectively. In the co-infection and fungal infection groups, males accounted for 66.7% and 56.3% patients, respectively. Factors affecting immunity were heavily implicated in fungal infections. We found that 89.6% (n=43) of patients harboring co-infections were immunocompromised, while just 10.4% (n=5) of patients had normal immune function. By comparison, the proportion of immunocompromised patients in the fungal infection group was 74.6% (n=53), while 25.4% (n=18) patients had normal immune function. Results of CT imaging showed that 22 of 119 (18.5%) patients had cavity lesions in the lungs, of whom 13 were accompanied by fungal and bacterial co-infection and the rest (n=9) had only fungal infection. Among the 119 enrolled patients, 21 cases (17.6%) were detected with viruses, of which 10 cases (20.8%) were from the fungal and bacterial co-infection group, and 11 cases (15.5%) were from the fungal infection group (**Table 1**).

Risk Factors Associated With Fungal and Bacterial Co-Infection

We assessed the role of age, sex, immune function, antibacterial treatment, and pulmonary cavities in pulmonary fungal and bacterial co-infections by univariate and multivariate logistic regression methods. Immunocompromised status had an odds ratio (OR) of 2.92 (95% CI 1.00-8.51, $P = 0.043$), pulmonary cavity had an OR of 2.56 (95% CI 0.99-6.59, $P = 0.047$), and both were significantly associated with fungal and bacterial co-infections. In contrast, age, sex, and antibacterial treatment did not play significant roles in pulmonary fungal and bacterial co-infections (P=0.580, 0.258 and 0.732, respectively), as determined by univariate analysis, and therefore, they were excluded from further analysis. We included 119 patients with complete data for immune function and pulmonary cavity (48 co-infections and 71 fungal infections) in the multivariate logistic regression model. Immunocompromised status (OR = 3.20, 95% CI: 1.07-9.62, $P = 0.038$) and pulmonary cavity (OR = 2.56, 95% CI: 1.06-7.49, $P = 0.039$) were found to be risk factors for fungal and bacterial co-infection (**Table 1**). This further confirmed the previous conclusion that immunocompromised status and the presence of pulmonary cavities are substantially related to co-infection of fungi and bacteria.

Distribution of Fungal Species

In the 119 patients with fungal infections, eight species of fungus were detected by mNGS and conventional laboratory-based diagnostic testing (**Table 1**). The most commonly observed fungal species was *Aspergillus*, which accounted for 47/119 infections (39.5%), followed by *Pneumocystis* (30, 25.2%), and *Rhizopus*, which was observed in 21 cases (17.6%). *Cryptococcus* and *Lichtheimia* were isolated from eleven (9.24%) and five (4.2%) samples, respectively. The relatively rare fungal species observed in this study were *Penicillium, Mucor*, and *Scedosporium* (**Table 1** and **Figure 1**).

The top three fungal species, *Aspergillus, Pneumocystis*, and *Rhizopus*, were most commonly isolated from both the co-infection group and the fungal infection group. However, *Scedosporium* was not observed in the co-infection group, while *Mucor* was not present in the fungal infection group. Moreover, we did not find any difference in the distribution of fungal species between the two groups ($P > 0.05$). In conclusion, *Rhizopus* and *Aspergillus* were the most common species to present with bacterial infections in our study, and the overall occurrence of bacterial infections was unaffected by fungal species.

Pathogenic Bacterial Species in Patients With Fungal Infections

Among patients with fungal and bacterial co-infections, 17 species of bacteria were identified from the 69 strains that were isolated. For the 69 strains of bacteria, the detection rate using mNGS was 89.9%, while that of conventional laboratory-based diagnostic testing was only 21.7% with $P < 0.05$. The most frequently detected bacteria were *Pseudomonas aeruginosa* (n=14) followed by *Acinetobacter baumannii* (n=9) and *Stenotrophomonas maltophilia* (n=8), all belonging to gram-negative bacteria (**Figure 2**). These bacteria are three of the main pathogens often seen in hospital infections (Petrucelli et al., 2020). In addition, *Haemophilus parainfluenzae* (n=6) and *Enterococcus faecium* (n=5) co-occurred with fungi. In this study, *Streptococcus pneumoniae*, *Klebsiella pneumoniae*, and *Mycobacterium tuberculosis* appeared at the same frequency in co-infections (n=4). The strains identified less commonly were *Legionella pneumophila*, *Staphylococcus haemolyticus*, *Enterococcus faecalis*,

TABLE 1 | Baseline characteristics and risk factors of pulmonary co-infection.

	Fungal and bacterial co-infection	Fungal infection	Univariable OR[a] (95% CI[b])	*P* value	Multivariable OR (95% CI)	*P* value
Age (years)	43.04 ± 18.2	40.77 ± 18.8	–	0.580	–	–
Sex						
Male	32 (66.7%)	40 (56.3%)	1.55	0.258	–	–
Female	16 (33.3%)	31 (43.7%)	(0.72–3.32)			
Immune function						
Normal	5 (10.4%)	18 (25.4%)	2.92	0.043	3.20	0.038
Defective	43 (89.6%)	53 (74.6%)	(1.00–8.51)		(1.07–9.62)	
Antibacterial treatment	31 (64.6%)	48 (67.6%)	0.874	0.732	–	–
			(0.40–1.89)			
CT image manifestation	13 (27%)	9 (12.7%)	2.56	0.047	2.81	0.039
(Cavity lesions)			(0.99–6.59)		(1.06–7.49)	
Isolated viruses	10 (20.8%)	11 (15.5%)	–	0.453	–	–
Fungus species						
Aspergillus	21 (43.8%)	26 (36.6%)	–	0.591[c]	–	–
Pneumocystis	11 (22.9%)	19 (26.8%)				
Rhizopus	9 (18.8%)	12 (16.9%)				
Cryptococcus	3 (6.3%)	8 (11.3)				
Lichtheimia	2 (4.2%)	3 (4.2%)				
Penicillium	1 (2%)	2 (2.8%)				
Mucor	1 (2%)	0 (0%)				
Scedosporium	0 (0%)	1 (1.4%)				

[a]*OR, odds ratio.*
[b]*CI, confidence interval.*
[c]*Calculated by t-test.*

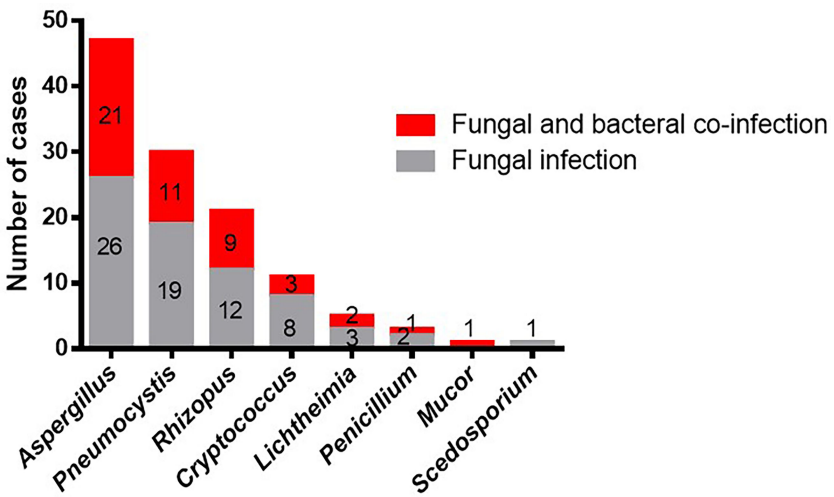

FIGURE 1 | Occurrences of bacterial co-infection with different fungal infections. Red indicates the cases of fungal infections that combine with bacterial infections. Gray indicates the cases of fungal infections. Numbers indicate the number of cases.

Nocardia cyriacigeorgica, *Staphylococcus aureus, Mycobacterium abscessus, Haemophilus influenzae, Enterobacter hormaechei*, and *Acinetobacter junii.* Overall, the frequency of these bacterial species remained the same as in nosocomial infections, with nonfermenting gram-negative bacilli, followed by enterobacteria. For the fungal and bacterial co-infection group, 66.7% (n=32) of patients infected by fungi were co-infected with a single bacterium, 22.9% (n=11) of patients were co-infected with two kinds of bacteria, and 10.4% (n=5) of patients were co-infected with three kinds of bacteria (**Figure 3**). Which bacterial species were found co-infecting with a particular fungal pathogen was shown in **Supplementary Table 1**.

Modification of the Treatment Strategy Due to Etiological Results

We Collected The Clinical Treatment Data Of The 119 Cases, Of Which 66.4% (79 cases: 48 from the fungal infection group and

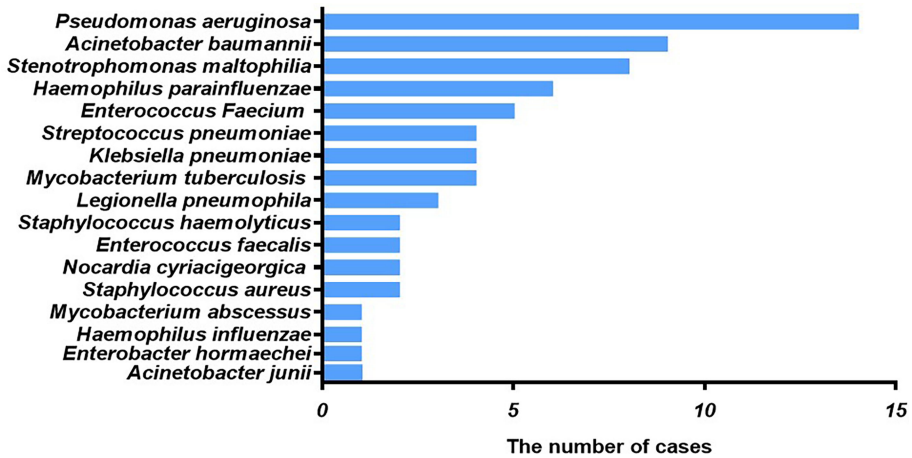

FIGURE 2 | Type of bacteria observed in cases of fungal and bacterial co-infection. The x-axis displays the number of isolates in which the corresponding bacterial species were found.

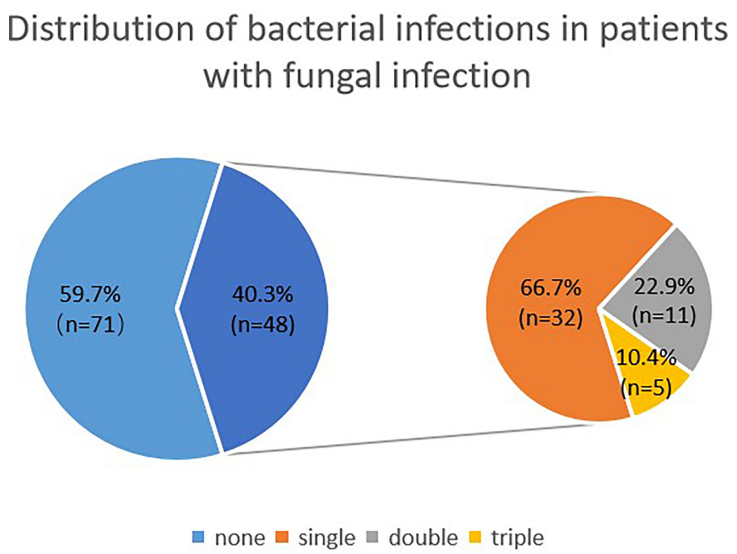

FIGURE 3 | Distribution of bacterial infections in patients with fungal infection. The larger blue pie represents fungal infections *vs* co-infections, and the smaller pie is the distribution of bacterial infections within the co-infection group.

31 from the co-infection group), had received empirical antibiotic treatment before their pathogenic test results became available. Subsequently, the use of antibacterial drugs was appropriately adjusted. The number of patients in the fungal infection group and co-infection group was 14 (29.2%) and 12 (38.7%), respectively. In the fungal infection group, six patients stopped using antibacterial drugs. Treatment adjustments included replacement upgrade and de-escalation of antibiotics. Overall, empirical use of antibacterial drugs was changed in 41.7% of the patients in the fungal infection group and 38.7% of patients in the fungal and bacterial group (**Table 2**).

DISCUSSION

Current evidence on the incidence of pulmonary fungal infections accompanied by other pathogenic infections is sparse, with most studies focusing on the relationship between *Aspergillus* and *Pseudomonas aeruginosa* infection (Briard et al., 2015; Briard et al., 2016). Our results showed that 40.3% of patients with pulmonary fungal infections had fungal and bacterial co-infections. The clinical manifestations of fungal and bacterial co-infections are more serious than those of fungal infections alone. Here, we only studied the co-existence

TABLE 2 | The influence of etiology on clinical antibacterial treatment.

	Fungal infection (case)	Fungal and bacterial infection (case)
Treatment before etiology		
Antibacterial drugs	48	31
Adjustment according with etiology		
Adjusted antibacterial drugs	14 (29.2%)	12 (38.7%)
Stopped antibacterial drugs	6 (12.5%)	–

of bacteria and fungi; however, we do not know which microorganism appeared first in the pulmonary infections. Some studies have reported that *A. fumigatus* colonization is preceded by fungal infection in patients with chronic obstructive pulmonary diseases (COPD) and cystic fibrosis (Borman et al., 2010; Gago et al., 2019).

Microorganisms do not exist alone, and invariably exhibit direct or indirect communication among themselves (Kolwijck and van de Veerdonk, 2014). Compared with a single pathogen infection, a differential immune response is mounted when patients are infected with multiple pathogens, and this may lead to different clinical outcomes. At present, relatively few studies have focused on the interaction between fungi and bacteria, especially in the respiratory system. Prior studies were mostly performed *in vitro* and in animal models, and the results typically demonstrated that bacteria had an inhibitory effect on fungi (Ferreira et al., 2015; Sass et al., 2018). For example, in a murine model of pulmonary disease, immunosuppressed mice with *A. fumigatus* and *P. aeruginosa* co-infection had a higher survival rate than animals infected with *A. fumigatus* alone. However, our result shows that the proportion of patients with bacterial-fungal co-infection is as high as 40.3% among patients with pulmonary fungal infections, which may suggest that interspecies microbial interactions have a positive correlation.

In our study, among the eight types of fungus isolated, *Aspergillus*, *Pneumocystis*, and *Rhizopus* were the most prevalent. However, results of another study analyzed the pathogens in 1,644 in-patients with pulmonary fungal infection and found *Aspergillus*, *Cryptococcus*, and *Talaromyces marneffei* as the three most common fungi (Li et al., 2021). Comparing their study with ours, only the *Aspergillus* was commonly observed in patients with bacterial and fungal co-infections, which may be ascribed to the different geographical distribution and the considerably larger number of cases in the earlier study. For example, *Talaromyces* is epidemic in mountainous/tropical regions in south east Asia, which is likely not present in patients accepted at the location examined in this study presuming no such travel history.

Fungal infections commonly occur in immunocompromised individuals. However, in our study, a large proportion (19.3%) of patients with pulmonary fungal infections had normal immune function. An increasing number of reports show that immunocompetent patients suffer from fungal infections, probably due to environmental exposures, genetic factors, or structural pulmonary risk factors (Denning and Chakrabarti, 2017; Latgé and Chamilos, 2019). Immunocompromised status was nevertheless a significant risk factor for co-infection of bacteria and fungi, which is consistent with previous studies (Zhou et al., 2020). The presence of pulmonary cavity lesions also increased susceptibility to co-infection. Pulmonary cavitation is a relatively serious pulmonary affliction, which may cause massive pulmonary hemorrhage and affect the ability of drugs to reach the diseased site, leading to ineffective treatment (AlShanafey et al., 2019). Antibiotic treatment has been shown to lead to fungal dominance (Jain et al., 2021), however, it is not identified as a risk factor in this study, which is likely due to the patient's short-term treatment. CT cavitary images may be used as the standard for comparing the severity of infection in cases of fungal infection to those with fungal and bacterial co-infection. In our study, the proportion of pulmonary cavitation was significantly higher in the co-infection group than in the fungal infection group. Hence, we concluded that the combined bacterial infection may aggravate the disease, which is consistent with current findings in humans. A retrospective cohort study showed that compared with *P. aeruginosa* infection alone, *A. fumigatus* and *P. aeruginosa* co-infection caused more rapid decline in patients with lung function and worsened clinical outcomes (Amin et al., 2010). Another study suggested that *S. maltophilia* and *P. aeruginosa* infections are associated with a higher probability of concurrent *Aspergillus* infection, which exacerbates clinical manifestations (Granchelli et al., 2018). These findings explain, to some extent, the diversity of interactions and clinical effects observed in fungal and bacterial co-infections. Similarly, the diversity of interactions between microorganisms also partially explains why some clinical treatments against pathogenic bacteria fail. In our study, the appearance of pulmonary cavitation was not common. There are numerous unknown factors surrounding these observations, and further research is required to fully understand the mechanisms at play.

We did not find a difference in the distribution of bacterial species in people with normal and defective immune functions. However, since we only studied the distribution of bacterial species in the short term after the use of antibacterial drugs, we do not know the long-term effects. For fungal and bacterial co-infections, 17 types of bacteria were identified, almost all of which were hospital-associated pathogens. *P. aeruginosa*, the most commonly isolated bacterial species in this study, is a gram-negative opportunistic pathogen existing in diverse environmental settings that harbors multi-drug resistance and poses serious therapeutic challenges (Lister et al., 2009; Leroy et al., 2021). Interestingly, four strains of *Mycobacterium tuberculosis* were isolated in pulmonary bacterial and fungal co-infection, of which three were co-infected with *Aspergillus* and one with *Rhizopus*. A study once reported 8 cases of *Cryptococcus* and *Mycobacterium tuberculosis* co-infections, and most of them occurred in the brain (Chen et al., 2016). Based on statistical analysis and the description of the bacteria likely to co-

infect with fungi in patients with pulmonary fungal infection, our findings will be useful for future clinical management of pulmonary fungal diseases.

The identification of co-infection of fungi and bacteria had a notable impact on clinical treatment. Fungal infections are treated with only antifungal treatment, while antibacterial and antifungal treatment is offered when patients are co-infected. In our study, a large proportion (66.4%) of patients had received empirical antibiotic treatment before their pathogenic test results were available. After the etiological results became known, 40.5% of the previously used empirical antibacterial drugs were discontinued or changed, since patients without bacterial co-infection may have other diseases, necessitating the continued use of antibacterial drugs. Anti-fungal or antibiotic treatment can skew the composition of the species that colonize the host, which consequently show less diversity. It is quite common for immunocompromised patients to be prescribed preventive antibiotic use.

mNGS is an unbiased approach for sequence identification of pathogenic microorganisms. One study revealed that mNGS is advantageous for the evaluation of fungal infections and suggested that mNGS combined with smear analyses should be used as a routine diagnostic tool for identifying invasive fungal infections (Li et al., 2018). We used mNGS combined with conventional laboratory-based diagnostic testing to gain more accurate and comprehensive information related to co-infecting microbes in patients with pulmonary fungal infections. mNGS offers the important advantage of detecting infectious pathogens, since it is less affected by prior antibiotic exposure.

LIMITATIONS

Anti-fungal or antibiotic treatment can change the composition and diversity of the microbial species present in the body. As we only obtained each patient's medication history for one month before diagnosis, we cannot be sure of the impact their earlier medication history might have had on the test results.

CONCLUSIONS

The incidence of fungal and bacterial co-infections is considerable in our mNGS-based study. Our research results should lead to more rational and precise anti-infective treatments, especially for patients who are difficult to diagnose by conventional methods, thereby having a positive impact on assessment of risk and clinical outcomes in these cases.

DATA AVAILABILITY STATEMENT

The data presented in the study are deposited in the NCBI and EMBL-EBI repository, accession number PRJNA773581 and PRJEB48166, respectively.

ETHICS STATEMENT

The studies involving human participants were reviewed and approved by the Ethics Review Committee of Tianjin Medical University General Hospital. The patients/participants provided their written informed consent to participate in this study.

AUTHOR CONTRIBUTIONS

YW and JF contributed to the research design and revision of the manuscript. ZZ drafted the research protocol, analyzed the results, and drafted the manuscript. JS conducted data analysis and assisted in writing the manuscript. CY and LY conducted data acquisition and analysis. JC and XL contributed to the data analysis and data deposition in an acceptable repository. All authors approved the submitted version and agreed to be responsible for all aspects.

FUNDING

This research was supported by grants from National Science and Technology Major Project of China (No.2018ZX10305409-001-001), National Natural Science Foundation of China (81970083, 81270144, 81570084 and 30800507 to JF), and the National Key Technology R&D Program, China (2015BAI12B00 to JF).

ACKNOWLEDGMENTS

We thank the respiratory endoscopy team of Tianjin Medical University General Hospital for technical support and suggestions.

SUPPLEMENTARY MATERIAL

The Supplementary Material for this article can be found online at: https://www.frontiersin.org/articles/10.3389/fcimb.2021.749905/full#supplementary-material

REFERENCES

AlShanafey, S., AlMoosa, N., Hussain, B., and AlHindi, H. (2019). Surgical Management of Pulmonary Aspergillosis in Pediatric Population. *J. Pediatr. Surg.* 54, 1938–1940. doi: 10.1016/j.jpedsurg.2019.01.003

Amin, R., Dupuis, A., Aaron, S. D., and Ratjen, F. (2010). The Effect of Chronic Infection With Aspergillus Fumigatus on Lung Function and Hospitalization in Patients With Cystic Fibrosis. *Chest* 137, 171–176. doi: 10.1378/chest.09-1103

Borman, A. M., Palmer, M. D., Delhaes, L., Carrère, J., Favennec, L., Ranque, S., et al. (2010). Lack of Standardization in the Procedures for Mycological

Examination of Sputum Samples From CF Patients: A Possible Cause for Variations in the Prevalence of Filamentous Fungi. *Med. Mycol.* 48 Suppl;1, S88–S97. doi: 10.3109/13693786.2010.511287

Briard, B., Bomme, P., Lechner, B. E., Mislin, G. L., Lair, V., Prévost, M. C., et al. (2015). Pseudomonas Aeruginosa Manipulates Redox and Iron Homeostasis of Its Microbiota Partner Aspergillus Fumigatus *via* Phenazines. *Sci. Rep.* 5, 8220. doi: 10.1038/srep08220

Briard, B., Heddergott, C., and Latgé, J. P. (2016). Volatile Compounds Emitted by Pseudomonas Aeruginosa Stimulate Growth of the Fungal Pathogen Aspergillus Fumigatus. *mBio* 7, e00219. doi: 10.1128/mBio.00219-16

Chen, M., Al-Hatmi, A. M., Chen, Y., Ying, Y., Fang, W., Xu, J., et al. (2016). Cryptococcosis and Tuberculosis Co-Infection in Mainland China. *Emerg. Microbes Infect.* 5, e98. doi: 10.1038/emi.2016.95

Chen, K. Y., Ko, S. C., Hsueh, P. R., Luh, K. T., and Yang, P. C. (2001). Pulmonary Fungal Infection: Emphasis on Microbiological Spectra, Patient Outcome, and Prognostic Factors. *Chest* 120, 177–184. doi: 10.1378/chest.120.1.177

de Macedo, J. L., and Santos, J. B. (2005). Bacterial and Fungal Colonization of Burn Wounds. *Mem. Inst. Oswaldo Cruz* 100, 535–539. doi: 10.1590/S0074-02762005000500014

Denning, D. W., and Chakrabarti, A. (2017). Pulmonary and Sinus Fungal Diseases in non-Immunocompromised Patients. *Lancet Infect. Dis.* 17, e357–e366. doi: 10.1016/S1473-3099(17)30309-2

Ferreira, J. A., Penner, J. C., Moss, R. B., Haagensen, J. A., Clemons, K. V., Spormann, A. M., et al. (2015). Inhibition of Aspergillus Fumigatus and Its Biofilm by Pseudomonas Aeruginosa Is Dependent on the Source, Phenotype and Growth Conditions of the Bacterium. *PLoS One* 10, e0134692. doi: 10.1371/journal.pone.0134692

Gago, S., Denning, D. W., and Bowyer, P. (2019). Pathophysiological Aspects of Aspergillus Colonization in Disease. *Med. Mycol.* 57, S219–s227. doi: 10.1093/mmy/myy076

Granchelli, A. M., Adler, F. R., Keogh, R. H., Kartsonaki, C., Cox, D. R., and Liou, T. G. (2018). Microbial Interactions in the Cystic Fibrosis Airway. *J. Clin. Microbiol.* 56 (8), e00354–18. doi: 10.1128/JCM.00354-18

Guan, W. J., Ni, Z. Y., Hu, Y., Liang, W. H., Ou, C. Q., He, J. X., et al. (2020). Clinical Characteristics of Coronavirus Disease 2019 in China. *N Engl. J. Med.* 382, 1708–1720. doi: 10.1056/NEJMoa2002032

Gu, W., Miller, S., and Chiu, C. Y. (2019). Clinical Metagenomic Next-Generation Sequencing for Pathogen Detection. *Annu. Rev. Pathol.* 14, 319–338. doi: 10.1146/annurev-pathmechdis-012418-012751

Huang, J., Jiang, E., Yang, D., Wei, J., Zhao, M., Feng, J., et al. (2020). Metagenomic Next-Generation Sequencing *Versus* Traditional Pathogen Detection in the Diagnosis of Peripheral Pulmonary Infectious Lesions. *Infect. Drug Resist.* 13, 567–576. doi: 10.2147/IDR.S235182

Jain, U., Ver Heul, A. M., Xiong, S., Gregory, M. H., Demers, E. G., Kern, J. T., et al. (2021). Debaryomyces is Enriched in Crohn's Disease Intestinal Tissue and Impairs Healing in Mice. *Science* 371, 1154–1159. doi: 10.1126/science.abd0919

Kolwijck, E., and van de Veerdonk, F. L. (2014). The Potential Impact of the Pulmonary Microbiome on Immunopathogenesis of Aspergillus-Related Lung Disease. *Eur. J. Immunol.* 44, 3156–3165. doi: 10.1002/eji.201344404

Latgé, J. P., and Chamilos, G. (2019). Aspergillus Fumigatus and Aspergillosis in 2019. *Clin. Microbiol. Rev.* 33 (1), e00140–18. doi: 10.1128/CMR.00140-18

Leroy, A. G., Caillon, J., Caroff, N., Broquet, A., Corvec, S., Asehnoune, K., et al. (2021). Could Azithromycin Be Part of Pseudomonas Aeruginosa Acute Pneumonia Treatment? *Front. Microbiol.* 12, 642541. doi: 10.3389/fmicb.2021.642541

Li, H., Gao, H., Meng, H., Wang, Q., Li, S., Chen, H., et al. (2018). Detection of Pulmonary Infectious Pathogens From Lung Biopsy Tissues by Metagenomic Next-Generation Sequencing. *Front. Cell Infect. Microbiol.* 8, 205. doi: 10.3389/fcimb.2018.00205

Li, Z., Li, Y., Chen, Y., Li, J., Li, S., Li, C., et al. (2021). Trends of Pulmonary Fungal Infections From 2013 to 2019: An AI-Based Real-World Observational Study in Guangzhou, China. *Emerg. Microbes Infect.* 10, 450–460. doi: 10.1080/22221751.2021.1894902

Limper, A. H., Knox, K. S., Sarosi, G. A., Ampel, N. M., Bennett, J. E., Catanzaro, A., et al. (2011). An Official American Thoracic Society Statement: Treatment of Fungal Infections in Adult Pulmonary and Critical Care Patients. *Am. J. Respir. Crit. Care Med.* 183, 96–128. doi: 10.1164/rccm.2008-740ST

Lister, P. D., Wolter, D. J., and Hanson, N. D. (2009). Antibacterial-Resistant Pseudomonas Aeruginosa: Clinical Impact and Complex Regulation of Chromosomally Encoded Resistance Mechanisms. *Clin. Microbiol. Rev.* 22, 582–610. doi: 10.1128/CMR.00040-09

Miao, Q., Ma, Y., Wang, Q., Pan, J., Zhang, Y., Jin, W., et al. (2018). Microbiological Diagnostic Performance of Metagenomic Next-Generation Sequencing When Applied to Clinical Practice. *Clin. Infect. Dis.* 67, S231–s240. doi: 10.1093/cid/ciy693

Petrucelli, M. F., Abreu, M. H., Cantelli, B. A. M., Segura, G. G., Nishimura, F. G., Bitencourt, T. A., et al. (2020). Epidemiology and Diagnostic Perspectives of Dermatophytoses. *J. Fungi (Basel)* 6 (4), 310. doi: 10.3390/jof6040310

Sass, G., Nazik, H., Penner, J., Shah, H., Ansari, S. R., Clemons, K. V., et al. (2018). Studies of Pseudomonas Aeruginosa Mutants Indicate Pyoverdine as the Central Factor in Inhibition of Aspergillus Fumigatus Biofilm. *J. Bacteriol.* 200, e00345–17. doi: 10.1128/JB.00345-17

Wang, J., Han, Y., and Feng, J. (2019). Metagenomic Next-Generation Sequencing for Mixed Pulmonary Infection Diagnosis. *BMC Pulm. Med.* 19, 252. doi: 10.1186/s12890-019-1022-4

Zhou, P., Liu, Z., Chen, Y., Xiao, Y., Huang, X., and Fan, X. G. (2020). Bacterial and Fungal Infections in COVID-19 Patients: A Matter of Concern. *Infect. Control Hosp. Epidemiol.* 41, 1124–1125. doi: 10.1017/ice.2020.156

Conflict of Interest: Authors JC and XL were employed by company Guangzhou Sagene Biotechnology Company, Limited.

The remaining authors declare that the research was conducted in the absence of any commercial or financial relationships that could be construed as a potential conflict of interest.

Publisher's Note: All claims expressed in this article are solely those of the authors and do not necessarily represent those of their affiliated organizations, or those of the publisher, the editors and the reviewers. Any product that may be evaluated in this article, or claim that may be made by its manufacturer, is not guaranteed or endorsed by the publisher.

frontiers in Cellular and Infection Microbiology

ORIGINAL RESEARCH
published: 01 November 2021
doi: 10.3389/fcimb.2021.723251

High Prevalence of HIV-Related Cryptococcosis and Increased Resistance to Fluconazole of the *Cryptococcus neoformans* Complex in Jiangxi Province, South Central China

Chunxi Yang[1†], Zeyuan Bian[2†], Oliver Blechert[1], Fengyi Deng[1], Hui Chen[1], Yueting Li[1], Yunhong Yang[2], Min Chen[3] and Ping Zhan[1*]*

[1] Jiangxi Provincial People's Hospital Affiliated to Nanchang University, Nanchang, China, [2] Jiangxi Provincial Chest Hospital, Nanchang, China, [3] Department of Dermatology, Shanghai Key Laboratory of Molecular Medical Mycology, Changzheng Hospital, Shanghai, China

OPEN ACCESS

Edited by:
Yong-Sun Bahn,
Yonsei University, South Korea

Reviewed by:
Michael S. Price,
Liberty University, United States
Dee Carter,
The University of Sydney, Australia

***Correspondence:**
Ping Zhan
zhanping1980@163.com
Min Chen
chenmin9611233@163.com

[†]These authors have contributed equally to this work

Specialty section:
This article was submitted to Fungal Pathogenesis, a section of the journal Frontiers in Cellular and Infection Microbiology

Received: 10 June 2021
Accepted: 10 August 2021
Published: 01 November 2021

Citation:
Yang C, Bian Z, Blechert O, Deng F, Chen H, Li Y, Yang Y, Chen M and Zhan P (2021) High Prevalence of HIV-Related Cryptococcosis and Increased Resistance to Fluconazole of the Cryptococcus neoformans Complex in Jiangxi Province, South Central China. Front. Cell. Infect. Microbiol. 11:723251. doi: 10.3389/fcimb.2021.723251

Background: Cryptococcosis is caused by a fungi of the *Cryptococcus neoformans/Cryptococcus gattii* complex and is a severe concern for public health worldwide. *C. neoformans* species are globally distributed, and *C. gattii* species are mostly found in America, Australia, and Sub-Saharan Africa. *Cryptococcus* usually infects an immunocompromised population; however, the majority of cryptococcosis in China has been reported in patients without any recognizable immunosuppression, i.e., HIV infection. To date, very few studies investigated this disease in South Central China.

Methods: The present study recruited 230 clinically suspected cryptococcosis cases in the last 5 years at two hospitals in Jiangxi Province, South Central China. All isolated strains were subjected to multilocus sequence typing (MLST) and phylogenetic analysis. Serotype and mating type were assessed by PCR, *in vitro* antifungal susceptibility was assessed by the CLSI-M27-A3 protocol.

Results: A total of 230 patients were identified as infected by *C. neoformans*, including 12 cases with *Talaromyces marneffei* coinfection. All seven MLST markers were successfully amplified and used to identify the ST genotype in 199 strains. *C. gattii* strains were not detected. In contrast to previous studies, 59.3% of the patients had an immunocompromised status, and 61.9% of these patients were infected with HIV. All isolates manifested serotype A and mating type α. The ST5 genotype was common (89.5%) in the Jiangxi region, and three novel genotypes (ST656, ST657, and ST658 in six isolates) were detected in the present study. A total of 86 of the isolates (43.2%) were not sensitive to fluconazole at a $MIC_{50} \geq 8$ μg/ml, most of the isolates were resistant to amphotericin B, and nearly all isolates were resistant to itraconazole and posaconazole. Resistances to 5-Flucytosine and voriconazole were very rare.

Conclusions: The results of the present study indicated that C. *neoformans* is the predominant species for cryptococcosis in Jiangxi Province, and a large proportion of the strains were not sensitive to fluconazole, which may be related to treatment failure and relapse. A high percentage of HIV-related C. *neoformans* infections was reported in Jiangxi, supporting a previous hypothesis that cryptococcosis is more frequent among the HIV-infected population in China. Continuous monitoring of species distribution and antifungal sensitivity is important for the investigation of this severe disease in the Jiangxi region.

Keywords: *Cryptococcus neoformans*/*Cryptococcus gattii* complex, multilocus sequence typing, antifungal susceptibility, resistance, fluconazole

INTRODUCTION

Cryptococcosis is an invasive fungal infection with high morbidity and mortality. *Cryptococcus neoformans* and *C. gattii* are the main etiological agents of the disease. The pathogens are present in the environment in diverse ecological niches, e.g., eucalyptus trees and the feces of pigeons (Ellis and Pfeiffer, 1990; May et al., 2016).

Based on the pathogenicity and molecular biological characteristics, *C. neoformans*/*C. gattii* is divided in seven distinct taxa (Hagen et al., 2015). The taxon *C. neoformans* (former called *Cryptococcus neoformans* var. *grubii*) has a wide distribution and is the main pathogen of cryptococcosis in China. Strains of this taxon can be identified by PCR-fingerprinting and DNA sequencing (molecular type: VNI, VNII). Strains of *C. neoformans* have the serotype A (Meyer et al., 2003). *C. deneoformans* (synonymy *C. neoformans* var. *neoformans*) is characterized by the molecular type VNIV and having the serotype D. It has a wide distribution but is most commonly found in Europe. *Cryptococcus gatti* s.l. (*sensu lato*, in a broader sense) is now divided in five species: *C. gattii* (with the molecular type VGI), *C. bacillisporus* (VGIII), *C. deuterogattii* (VGII), and *C. tetragattii* (VGIV). These species are characterized by the serotypes B and C. *Cryptococcus gatti* s.l. has a worldwide distribution with hotspots in America, Australia, and Sub-Saharan Africa.

Cryptococcus is mostly found in the haploid form, growing as a yeast, and reproducing asexually; but they are able to mate and have the ability of sexual recombination. Even an interspecific hybridization between *C. neoformans*, *C. deneoformans*, and also *C. gatti* s.l. have been found (Hagen et al., 2015).

Spores or yeast cells of *Cryptococcus* are inhaled from the environment by humans and enter through the respiratory tract (Velagapudi et al., 2009). In immunocompetent hosts, the fungus normally is stopped by the immune system, even though the pathogen sometimes causes a latent and symptomatic infection (Qu et al., 2020). In immunocompromised hosts, *Cryptococcus* can cause pneumonia and can disseminate to other tissues, mainly to the central nervous system (May et al., 2016). In more than 80% of clinical cases with cryptococcal infections, cryptococcal meningitis were diagnosed (Rajasingham et al., 2017). Although the absolute number of cryptococcal deaths has decreased since 2008, the proportion of AIDS-related mortality remains high. An estimated 15% of cryptococcal meningitis are the cause of AIDS-related deaths (Rajasingham et al., 2017).

Although most fatal infections occur in southern Saharan Africa, an increasing number of cases have been reported in other regions, including China (Yuchong et al., 2012). Interestingly, the majority of cryptococcosis in China was reported in non-HIV patients (>80%), and infections were also reported from immunocompetent hosts (Fang et al., 2015; Zhou et al., 2020). A systematic literature review by Zhou et al. noted that cryptococcal meningitis occurred in China in immunocompetent individuals almost twice as often as in patients with AIDS (Zhou et al., 2020). Jiangxi Province is a large agricultural province in South Central China with a population of more than 45 million residents. The subtropical and humid climate is favorable for *C. neoformans* (Li et al., 2012). Occurrence of cryptococcal infections continues to increase; however, large-scale epidemiological data on cryptococcosis from this region are very limited (Chen et al., 2018). The two most important nationwide studies, reviewing the epidemiology of *Cryptococcus* in China, reported the retrieval of only very few strains from Jiangxi Province (Chen et al., 2008; Fang et al., 2015).

Only the study by Chen et al. (2018), about the epidemiology of cryptococcosis in Jiangxi Province, systematically analyzed the cryptococcosis epidemiology in this province, on the basis of 86 cases (Chen et al., 2018). The study included *Cryptococcus* cases occurring in a period of two years. Notably, all *Cryptococcus* strains were sensitive to routine antifungal agents: flucytosine, amphotericin B, itraconazole, voriconazole, and fluconazole. According to the Invasive Fungal Surveillance Net (CHIF-NET), resistance to fluconazole occurred in about 10% of the strains analyzed in China (Xiao et al., 2018). Thus, we increased the number of analyzed *Cryptococcus* strains collected in Jiangxi Province to obtain a more representative database on fluconazole resistance.

All *Cryptococcus* strains isolated in Jiangxi Province belong to the *Cryptococcus neoformans*/*Cryptococcus gattii* complex. The study of Chen et al. identified all 86 isolates as *C. neoformans* serotype A and mating type α (Chen et al., 2018). Recently, Cao et al. reported emerging *C. gattii s.l.* infections in Guangxi Province, south of Jiangxi Province (Huang et al., 2020). By increasing the number of *Cryptococcus* isolates, we aimed to provide a more accurate description of *Cryptococcus* diversity in Jiangxi Province.

Reports of *C. neoformans* meningitis (CM) were almost exclusively from patients of the hospitals associated with Chinese universities, whereas most Chinese HIV-infected patients are treated in specialized infectious disease hospitals. Thus, Chen et al. suggested that CM cases in the HIV-infected population in China may have been severely underreported (Chen et al., 2020). Additionally, Chen et al. (2018) reported that 40% of *Cryptococcus* infections were HIV-related.

Therefore, to obtain additional information about the species distribution in Jiangxi Province, molecular epidemiology, and antifungal-drug susceptibility, we conducted a two-center retrospective study including 230 clinically diagnosed cryptococcosis cases, which were all recorded in the last 5 years. The patients originated from nearly all regions of Jiangxi Province; a combination of MLST genotype analysis and *in vitro* antifungal tests was used for serotype and mating type determination. The aims of the present study were as follows: (1) to describe the species distribution and molecular epidemiology of clinical *Cryptococcus* in Jiangxi Province; (2) to explore the *in vitro* antifungal profiles of *Cryptococcus*, especially potential resistance to fluconazole; and (3) to describe the serotype and mating type loci in the clinical strains in South China.

MATERIALS AND METHODS

Study Population and Geographic Region

The present retrospective study was conducted at two high level general hospitals in Jiangxi Province, Jiangxi Provincial Chest Hospital and Jiangxi People's Provincial Hospital. The data were retrieved from the medical records stored at the hospitals, and all Jiangxi native patients diagnosed with *Cryptococcus* infections from July 2015 to June 2020 were recruited. Approval for the present study was granted by the Ethics Committee of Jiangxi People's Provincial Hospital affiliated with Nanchang University.

The investigated area, Jiangxi, is located in South Central China on the south bank of the middle and lower reaches of the Yangtze River (**Figure 1**). The location is characterized by an annual 77.5% humidity and 18.75°C temperature, which corresponds to a typical subtropical climate. The data were checked by two highly qualified physicians (ZP and CM), including the epidemiological, demographic, clinical, and laboratory examinations. The inclusion criteria were as follows: (1) discharge diagnosis referring to "cryptococcosis"; (2) clinical and radiographic findings consistent with cryptococcosis; (3) positive result of a cryptococcal capsular polysaccharide antigen (CrAg) test; and (4) positive fungal culture and persistence in the microbiology tests (see below).

Strains and Polymerase Chain Reaction Procedure

All clinical strains were stored in 20% glycerol at -80°C and recovered by culture at 35°C in a Sabouraud dextrose agar (SDA; 1% peptone, 4% glucose, and 1.5% agar) medium containing chloramphenicol (100 μg/ml). Genomic DNA was extracted from each isolate according to the instructions of the manufacturer (plant genomic DNA extraction reagents from KangWei Century Co., product no. CW0531M) with minor modifications. Briefly, the strains were incubated on SDA agar plates at 35°C for 24 hours. Half gram of fungal cells was picked and transferred to a 2-ml Eppendorf tube containing 400 μl of LP1 buffer; the tube was shaken three times by a tissue lapping machine. Then, the mixture was removed, and 5 μl of RNase A was added; subsequent steps followed the instructions of the manufacturer. Finally, the DNA was dissolved in 50 μl of sterilized water and stored at -80°C. PCR was performed with the 2×T5 Super PCR Mix (Qingke Biotechnology Company, TSE005) according to the instructions of the manufacturer.

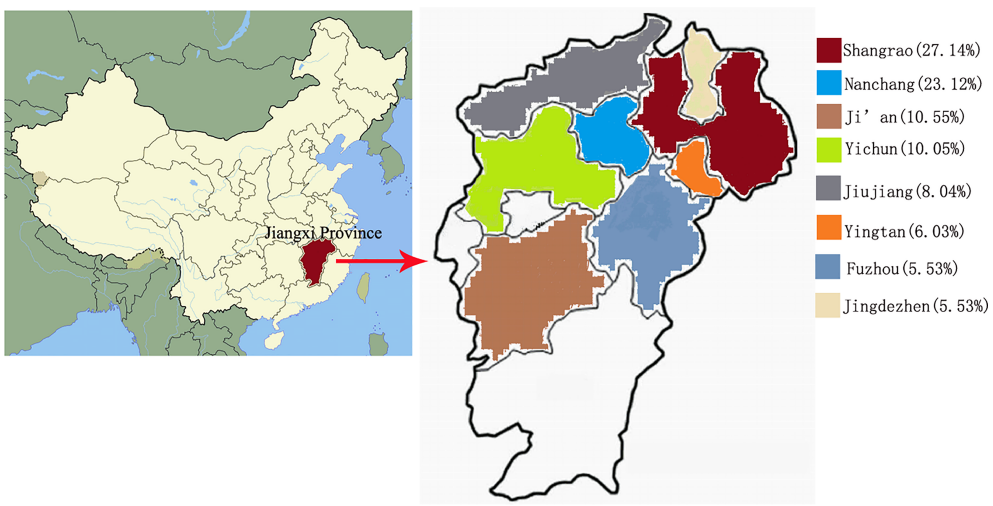

FIGURE 1 | Surveillance point, Jiangxi Province and patient distribution in various cities.

Identification of the Species, Serotypes, and Mating Types

To identify the *Cryptococcus* species, we amplified the IGS1 gene regions of all samples. The PCR products were detected after electrophoresis through 1% agarose gels, and positive products were sequenced by Qingke Biotechnology Company on the ABI 3730xL platform. The sequences were edited by the Seqman software and BLAST'ed in the NCBI database. To determine the serotypes and mating types, we used a previously reported method (Yan et al., 2002). Briefly, serotype- and mating type-specific primers (**Table S1**) of the STE20 gene were amplified and checked on 1% agarose gels together with the samples of the reference strains.

Multiolocus Sequence Typing and Phylogeny Analysis

The present study used seven universal housekeeping genes for the MLST analysis of the *C. neoformans/C. gattii* complex according to the ISHAM consensus criteria (CAP59, GPD1, LAC1, PLB1, SOD1, URA5, and IGS1 regions) (see **Table S1**) (Hiremath et al., 2008; Meyer et al., 2009). Briefly, all genes were amplified according to (Hiremath et al., 2008), sequenced by Qingke Biotechnology Company, and then BLAST'ed in NCBI for confirmation. Then, all sequences were submitted to the NCBI GenBank to acquire the gene accessions and to the *C. neoformans/C. gattii* species complex database (https://mlst.mycologylab.org/page/Home) to obtain the sequence types (ST).

For each ST genotype, we used a single clinical strain for the phylogenetic analysis. The STs reported by Chen et al. (2018) and different from the STs in the present study were downloaded and incorporated into the tree. Each gene was checked by the Mega 6.06 software, and the seven MLST loci were concatenated by Gedit. The phylogenetic tree was constructed by the neighbor-joining algorithm according to the Tamura-Nei model using 500 bootstrap replications with JEC21 as the outgroup (Tamura et al., 2013).

In Vitro Antifungal Susceptibility Testing

According to the antifungal drug sensitivity test protocol CLSI-M27-A3, fluconazole (FLU) drug sensitivity test was performed in a total of 199 C. *neoformans* isolates, and 86 strains with FLU MIC_{50} ≥ 8 μg/ml were tested for antifungal susceptibility to amphotericin B (AMB), flucytosine (5FC), voriconazole (VOR), itraconazole (ITR), and posaconazole (POS). *Candida krusei* ATCC6258 and *Candida parapsilosis* ATCC22019 were used as quality controls. The minimal inhibitory concentrations (MICs) and epidemiological cutoff values (ECVs) were obtained according to the standard manual procedures. The ECV breakpoints for fluconazole and flucytosine were ≥8 μg/ml, as suggested by previous studies (Espinel-Ingroff et al., 2012a; Espinel-Ingroff et al., 2012b), and breakpoints for amphotericin B were ≥1 μg/ml (Espinel-Ingroff et al., 2012b). For ITR, VOR, and POS, we used the value ≥0.25 μg/ml from a previous study (Espinel-Ingroff et al., 2012a).

RESULTS

Demographic Data Relevant to Clinical Isolates

The present study recruited 230 cryptococcosis cases based on the clinical records in the last 5 years in Jiangxi Province, South China. A total of 5.2% (12/230) of the patients had a coinfection with *Talaromyces marneffei*. Therefore, 218 samples were used for the subsequent molecular and epidemiological analysis. Amplifications based on all seven MLST primer sets identified the genotypes in 199 samples (see below). Most of the isolates were obtained from cerebrospinal fluid (n = 141; 70.9%), followed by blood (n = 56; 28.1%), and single isolate was obtained from the bone marrow and pleural fluid (n = 1; 0.5%). The isolates were obtained from patients in 11 cities in Jiangxi Province (**Table 1** and **Figure 1**). A total of 54 (27.1%) samples were from Shangrao City, 46 (23.1%) samples from Nanchang City, 21 (10.6%) samples from Ji'an, 20 (10.1%) samples from Yichun, 16 (8%) samples from Jiujiang, 12 (6%) samples from Yingtan, 11 (5.5%) samples from Fuzhou, and 11 (5.5%) samples from Jingdezhen. The remaining 8 (4%) samples were obtained from smaller cities or villages. More than 50% of the patients were from the two main cities, Shangrao and Nanchang; Nanchang harbors the central surveillance station

TABLE 1 | Clinical information of 199 cryptococcus neoformans infections.

Location	Shangrao		54 (27.1%)
	Nanchang		46 (23.1%)
	Ji'an		21 (10.6%)
	Yichun		20 (10.1%)
	Jiujiang		16 (8%)
	Yingtan		12 (6%)
	Fuzhou		11 (5.5%)
	Jingdezhen		11 (5.5%)
	Xinyu		4 (2%)
	Ganzhou		3 (1.5%)
	Pingxiang		1 (0.5%)
Gender	Male		128 (64.3%)
	Female		71 (35.7%)
Specimen	Cerebrospinal fluid (CSF)		141 (70.9%)
	Blood		56 (28.1%)
	Hydrothorax		1 (0.5%)
	Bone marrow		1 (0.5%)
Immune status	Immunocompromised 59.30% (118/199)	HIV	61.9% (73/118)
		Other opportunistic infections	40.7% (48/118)
		Diabetes	22% (26/118)
		Autoimmune systemic diseases	7.6% (9/118)
		Others	9.3% (11/118)
	Immunocompetent	40.7% (81/199)	

for fungal infections in Jiangxi Province. Fewer cases were from Ganzhou, which is 400 km away from Nanchang and has its own large general hospital.

A total of 199 isolates included 128 (64.3%) isolates from male patients and 71 (35.7%) isolates from female patients. The age of the patients ranged from 4 to 79 years, with a mean age of 48.8 ± 17 (M ± SD) years. The following age distribution was detected: 3 patients younger than 18 years, 79 aged 19–45 years, 94 aged 46–70 years, and 23 older than 70 years.

In total, 59.3% (118/199) of the patients had a deficient or suppressed immune status, and 40.7% (81/199) were apparently immunocompetent. A total of 36.7% (73/199) of the patients had an HIV-related pathology, 13.1% (26/199) had diabetes, 24.1% (48/199) had other opportunistic infections, i.e., cytomegalovirus infection and *Mycobacterium tuberculosis*, 4.5% (9/199) had a systemic autoimmune disease, and the remaining 5.5% (11/199) were immunosuppressed with other diseases, including malignant cancer and leukopenia. All patients received timely antifungal treatment in combination with supportive therapy after the diagnosis of cryptococcosis; however, 8 patients died due to severe organ damage.

Identification and Analysis of the Serotype, Mating Type, and Multilocus Sequence Typing

Initially, genomic DNA of the strains was extracted, and the IGS1 gene was amplified. BLASTn search against the NCBI database identified 218 isolates as *C. neoformans* species. A total of 199 strains were identified at the level of the genotypes by MLST analysis. The 12 isolates, coinfected with *Talaromyces marneffei*, were not further explored. *C. gattii* strains were not detected. The serotype and mating type of all these isolates were determined by the methods described by Yan et al. (2002). The primer sequences are listed in **Table S1**. A 588-bp fragment of all 199 strains was amplified by using the STE20Aα primer pair. All tests with the STE20Aa, STE20Da, and STE20Dα primer pairs were negative. All strains were determined to be serotype A and mating type α.

MLST analysis identified eight different sequence types (STs). A total of 178 (89.5%) isolates belonged to ST5, 9 to ST359, 4 to ST6, 1 to ST31, and 1 to ST81. Three novel sequence types were detected in six isolates with previously unknown sequence variations. The new sequence variations matched the ST656, ST657, and ST658 designations from the Fungal MLST Database (https://mlst.mycologylab.org).

Allelic assignments of the gene sequences in the MLST database for eight multilocus sequence types are listed in **Table 2**. The ST5 genotype was predominant and widely distributed in Jiangxi Province. Nine ST359 strains originated from Ji'an (3), Shangrao (2), Nanchang (2), Jiujiang (1), and Xinyu (1). All four ST6 strains originated from Shangrao; a single ST81 strain originated from Yichun, and a single ST31 strain originated from Ganzhou. Three ST657 strains with novel genotypes were from Shangrao; two ST658 strains from Yichun, and the ST656 strain from Nanchang.

Phylogenetic Analysis

A combination with the data reported in a study of Chen et al. (2018) indicated that 13 ST types were present in Jiangxi Province, including ST5, ST6, ST31, ST32, ST81, ST139, ST186, ST226, ST319, ST359, ST656, ST657, and ST658. The results of the present study indicated that ST31, ST32, and ST319 were genetically similar and clustered into a clade separate from the other strains. The other strains were more similar to each other, having only a few nucleotide polymorphisms (**Figure 2**).

Details of a New Sequence Type Genotype

The present study detected three novel genotypes (ST656, ST657, and ST658), which were different from the previously known STs in the loci SOD1, PLB1, and IGS1. Detailed allelic assignment of each new sequence type was as follows: SOD1: allele #68 was detected in ST656; PLB1: allele #44 in ST657; and IGS1: allele #98 in ST658. The three new genotypes were scattered in various regions, and the patients had different underlying diseases. The ST656 strain originated from the CSF of a 79-year-old male patient who lived in Nanchang and had concomitant complications, including pulmonary tuberculosis, hypertension, gout disease, and chronic hepatitis B infection. Five other patients were immunocompromised and had HIV infection, diabetes, cancer, or surgery. However, none of these patients reported a history of travel or close contact with pigeons.

In Vitro Antifungal Susceptibility

The drug sensitivity test to fluconazole (FLU) was performed using 199 C. *neoformans* isolates, including 113 (56.8%) isolates that had an MIC_{50} < 8 μg/ml, 64 (32.2%) that had an MIC_{50} of 8 μg/ml, and 22 (11.1%) that had an MIC_{50} ≥ 16 μg/ml (**Table 3**). Recommended breakpoints for *Cryptococcus* sensitivity to FLU

TABLE 2 | Allelic assignments of eight multilocus sequence types in the present study.

Sequence Type	CAP59	GPD1	IGS1	LAC1	PLB1	SOD1	URA5	Isolates amount
ST5	1	3	1	5	2	1	1	178
ST6	1	1	1	3	2	1	5	4
ST31	1	1	10	3	2	1	1	1
ST81	1	1	1	5	2	1	1	1
ST359	1	25	1	5	2	1	1	9
ST656	1	25	1	5	2	68	1	1
ST657	1	25	1	5	44	1	1	3
ST658	1	3	98	5	2	1	1	2

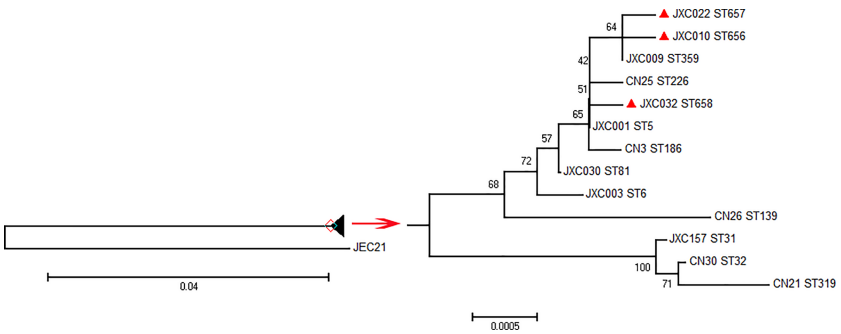

FIGURE 2 | Phylogenetic tree constructed using the neighbor-joining method with a bootstrap of 500 based on the concatenated sequences at seven MLST loci using JEC21 as the outgroup.

are undefined; thus, we regarded 86 strains (43.2%) with an MIC_{50} 0 ≥8 μg/ml as resistant strains and tested their susceptibility to other commonly used antifungal drugs, including amphotericin B (AMB), flucytosine (5-FC), voriconazole (VOR), itraconazole (ITR), and posaconazole (POS).

MIC_{50} for FLU ranged from 0.25 to 64 μg/ml (GM 5.1 μg/ml). The percentages of resistant strains in each location were as follows: 40.7% (22/54) in Shangrao, 45.7% (21/46) in Nanchang, 38.1% (8/21) in Ji'an, 55% (11/20) in Yichun, 50% (8/16) in Jiujiang, 50% (6/12) in Yingtan, 54.6% (6/11) in Jingdezhen, 66.7% (2/3) in Ganzhou, 9.1% (1/11) in Fuzhou, and 25% (1/4) in Xinyu. These FLU-resistant strains had a highly variable ST genotype distribution: 39.9% (71/178) of ST5, 75% (3/4) of ST6, 66.7% (6/9) of ST359, 33% (1/3) of ST657, 50% (1/2) of ST658, and 100% of ST81 (1/1) and ST656 (1/1). Considering the high variability in the ST strain percentages, it is difficult to define the relationship between FLU resistance and the ST genotypes.

Our data indicated that nearly all 86 fluconazole-resistant *Cryptococcus* isolates were also resistant to ITR and POS, most of the 86 fluconazole-resistant *Cryptococcus* isolates were resistant to AMB. Only three strains (JXC070, JXC010, and JXC136) were susceptible to POS; a single strain (JXC136) was susceptible to ITR (**Table 3**).

These 86 strains included 18 strains that were not susceptible to 5-FC (JXC008, JXC013, JXC016, JXC017, JXC019, JXC032, JXC038, JXC054, JXC070, JXC081, JXC096, JXC113, JXC145, JXC146, JXC181, JXC254, JXC260, and JXC278), and 6 strains were not sensitive to VOR (JXC001, JXC003, JXC038, JXC054, JXC143, and JXC191). A total of 22 strains with an FLU MIC_{50} ≥ 16 μg/ml included 7 isolates (JXC017, JXC019, JXC038, JXC054, JXC081, JXC113, and JXC145) resistant to 5-FC and 5 isolates (JXC003, JXC038, JXC054, JXC143, and JXC191) to VOR (**Table 3**).

DISCUSSION

An increasing number of studies on the epidemiology of cryptococcosis in China have been published; however, only a very few reports described the situation in Jiangxi Province, which is a large agricultural province with a population of more than 45 million people in South Central China (Chen et al., 2008). Only a single molecular epidemiology study on cryptococcosis was reported in 2018, in which Chen et al. (2018) analyzed 86 clinical cryptococcosis cases in this region. *C. gattii* was not detected, and all strains were sensitive to flucytosine, amphotericin B, fluconazole, itraconazole, and voriconazole (Chen et al., 2018). The study has been the first to report the profiles of *Cryptococcus* infections in the Jiangxi region; however, some questions remained and needed to be confirmed using large-scale data.

The present study recruited 230 cases of cryptococcosis over 5 years at two hospitals. One of the hospitals was a large general hospital (Jiangxi Provincial People's Hospital with more than 3,500 ward beds), and another hospital was a specialized hospital (Jiangxi Provincial Chest Hospital), which is famous for treating cryptococcosis and registered the highest number of *Cryptococcus* cases in Jiangxi Province. To a certain extent, these data can reveal the general distribution of this disease.

TABLE 3 | The results of the *in vitro* tests of six antifungal drugs in 86 fluconazole-resistant isolates.

Drugs	Break points (μg/ml)	Isolates amount		Genotype
FLU	≥16	22	–	ST5 (15), ST6 (3), ST359 (2)
	8	–	64	ST5(56), ST81(1), ST359 (4), ST656(1), ST657(1), ST658 (1)
ITR	≥0.25	85		ST5(73), ST6(3), ST81(1), ST359(5), ST656(1), ST657(1), ST658 (1)
AMB	≥1	69		ST5(59), ST6(2), ST81(1), ST359(5), ST657(1), ST658 (1)
POS	≥0.25	83		ST5(72), ST6(3), ST81(1), ST359(5), ST657(1), ST658(1)
VOR	≥0.25	6		ST5(4), ST6(2)
5FC	≥8	18		ST5(14), ST6(1), ST359(2), ST658(1)

C. neoformans s.l. is globally distributed, and *Cryptococcus gattii* s.l. has a wide distribution with hot spots in America, Australia, and Sub-Saharan Africa. Recently, Cao et al. reported an emergence of *C. gattii* s.l. infections in Guangxi in South China (Huang et al., 2020) However, the present study and the study of Chen et al. (2018) did not detect the strains of *C. gattii* s.l. in Jiangxi. All 199 strains belonged to the serotype A and MATα. Monitoring should be continued to prevent the invasion and spreading of *C. gattii* s.l.

Usually, cryptococcosis is an opportunistic fungal disease that mainly infects immunocompromised populations, particularly HIV-infected patients. However, the situation seems to be rather different in China. A review by Chen et al. published in 2020 pointed out that the proportion of HIV-related cryptococcosis meningitis (CM) is 80% in the United States, 95% in Brazil, 77% in Europe, and only 16% in China (Viviani et al., 2006; Leal et al., 2008; Pyrgos et al., 2013; Chen et al., 2020). The authors speculated that the reported differences are likely due to a biased reporting in China, and most cases have been reported by university-affiliated hospitals, which are not officially designated specialized hospitals that treat highly infectious diseases, i.e., HIV and tuberculosis. Therefore, the authors suggested that occurrence of CM in HIV-infected population in China has been severely underreported (Chen et al., 2020). The results of the present study indicated that HIV-positive patients accounted for 36.7% of all cases, and approximately 60% of the patients had an underlying deficiency or suppressed immune system; these numbers were considerably higher than the numbers reported previously. Considering that most of the cases of the present study originated from Jiangxi Provincial Chest Hospital, which is famous for treating cryptococcosis and, therefore, attracts the highest number of cases of this disease, the results of the present study confirmed the suggestion of Chen on the enormous underreporting of HIV-related cryptococcosis infections.

To date, a total of 17 ST genotypes have been reported in China, including 15 sequence types (ST5, ST31, ST38, ST53, ST57, ST63, ST93, ST186, ST191, ST194, ST195, ST295, ST296, ST359, and ST360) in mainland China and another two types (ST4 and ST6) from Hong Kong, China (Khayhan et al., 2013; Dou et al., 2015; Fan et al., 2016; Dou et al., 2017). Here, we reported three new STs (ST356, ST357, ST358), but according to the phylogenetic analysis, they are very similar to the existing genotypes and only one nucleotide differentiated in each new ST. Cryptococcosis in China is mainly caused by *C. neoformans*, and >90% of the strains belong to ST5 (Fan et al., 2016). Combined analysis of the sequences reported by Chen et al. (2018) indicated that 13 STs were identified in Jiangxi by a consensus multilocus sequence typing protocol, and three novel ST genotypes (ST656, ST657, and ST658) were detected in the present study and acquired from the Fungal MLST Database (https://mlst.mycologylab.org). Similar to a report of Chen et al. (2018), 90% of the strains in the present study belonged to ST5 (molecular type VNI), serotype A, and mating type α (MAT α). Therefore, these data indicated that serotype A and MAT α strains of the ST5 genotype are predominant in Jiangxi Province. *C. neoformans* is very successful at long-distance and short-distance dispersal, and abundant genetic mutant strains may be present in Jiangxi and may have unique genes. The spread of the genotypes between various geographical locations may be caused by wind, pigeons and other animals, plants, and human activities. Genetic mutations may be a reason for the presence of new sequence types in Jiangxi.

Mainly three classes of agents are used to treat *Cryptococcus* infections: polyenes (mainly amphotericin B), azoles (mainly fluconazole), and nucleoside analog (mainly 5-flucytosine). Amphotericin B preparations plus 5-flucytosine is often used as the initial treatment of meningitis, disseminated infection, or moderate-to-severe pulmonary infection followed by fluconazole as a consolidation therapy. Resistance against these substances have been detected in several *Cryptococcus* strains. The general molecular mechanisms of resistance are conserved among fungal species but have been acquired independently in several fungal strains and taxa. The most prevalent mechanism of resistance involves increased drug efflux pump activity and alterations in antifungal drug targets, due to increased target expression or mutations within the target protein sequence (Berman and Krysan, 2020).

Fluconazole is the most commonly used antifungal agent for the treatment and prophylaxis of cryptococcosis. Over the years, resistance of the clinical isolates of *C. neoformans* to FLU has gradually increased, and current resistance is a relatively common event in relapse episodes of cryptococcal meningitis (Bongomin et al., 2018). In contrast to the report of Chen et al. (2018), which demonstrated that all isolates were sensitive to routine antifungal agents, antifungal susceptibility tests in the present study indicated that 43.2% of the strains had MICs ≥ 8 μg/ml for fluconazole and 11.1% of the strains had MICs higher than ≥16 μg/ml. Most of the strains with MICs ≥ 8 μg/ml were also resistant to ITR, AMB, and POSA, and a few of these strains were resistant to VRC and 5FC. Fluconazole resistance has been reported by a CHIF-NET study in 2018 in China, in which fluconazole-resistant isolates of *C. neoformans* were detected in 9.7% of the strains.

We observed variations in MICs between various ST genotype strains. Approximately 40% of ST5 isolates were not sensitive to FLU with MIC_{50} ≥ 8 μg/ml; for ST6, ST81, ST359, ST656, and ST658 this was 75%, 100%, 66.7%, 100%, and 50%, respectively. Considering the limited data on these ST strains, we cannot determine a relationship between these genotypes and antifungal sensitivity.

In conclusion, the present study on 199 clinical cryptococcosis cases identified ST5 (molecular type VNI) belonging to serotype A and mating type α (MAT α) as the predominant *C. neoformans* in Jiangxi Province, South Central China. High prevalence of immunocompromised-related infections, particularly in the HIV-infected populations, was reported in Jiangxi Province. Additionally, an increased resistance of *C. neoformans* species to fluconazole was detected in this region. Therefore, a close and continuous monitoring of the epidemiology of this severe fungal disease is necessary for public surveillance and precise treatment.

DATA AVAILABILITY STATEMENT

The original contributions presented in the study are included in the article/**Supplementary Material**. Further inquiries can be directed to the corresponding authors.

AUTHOR CONTRIBUTIONS

PZ and MC designed the research. CY, ZB, and FD performed the research. CY, ZB, OB, HC, YL, and YY analyzed the data CY, OB, and PZ wrote the paper. All authors contributed to the article and approved the submitted version.

FUNDING

This work was supported by the National Natural Science Foundation of China [81960367], Project of Health Commission of Jiangxi Province (202130956), and Key R&D Project of Science and Technology Department of Jiangxi Province (20203BBG73040).

SUPPLEMENTARY MATERIAL

The Supplementary Material for this article can be found online at: https://www.frontiersin.org/articles/10.3389/fcimb.2021.723251/full#supplementary-material

Supplementary Table 1 | PCR primers used in the present study.

Supplementary Table 2 | Detailed information of the 199 clinical isolates of *Cryptococcus neoformans* from Jiangxi Province, China.

Supplementary Table 3 | Susceptibilities of the 86 C. *neoformans* isolates from Jiangxi Province against six common antifungal drugs.

Supplementary Table 4 | The list of gene bank accession numbers for seven genes of 199 isolates.

REFERENCES

Berman, J., and Krysan, D. J. (2020). Drug Resistance and Tolerance in Fungi. *Nat. Rev. Microbiol.* 18 (6), 319–331. doi: 10.1038/s41579-019-0322-2

Bongomin, F., Oladele, R. O., Gago, S., Moore, C. B., and Richardson, M. D. (2018). A Systematic Review of Fluconazole Resistance in Clinical Isolates of Cryptococcus Species. *Mycoses* 61 (5), 290–297. doi: 10.1111/myc.12747

Chen, J., Varma, A., Diaz, M. R., Litvintseva, A. P., Wollenberg, K. K., and Kwon-Chung, K. J. (2008). Cryptococcus Neoformans Strains and Infection in Apparently Immunocompetent Patients, China. *Emerging. Infect. Dis.* 14 (5), 755–762. doi: 10.3201/eid1405.071312

Chen, M., Xu, N., and Xu, J. (2020). Cryptococcus Neoformans Meningitis Cases Among China's HIV-Infected Population May Have Been Severely Under-Reported. *Mycopathologia* 185 (6), 971–974. doi: 10.1007/s11046-020-00491-4

Chen, Y. H., Yu, F., Bian, Z. Y., Hong, J. M., Zhang, N., Zhong, Q. S., et al. (2018). Multilocus Sequence Typing Reveals Both Shared and Unique Genotypes of Cryptococcus Neoformans in Jiangxi Province, China. *Sci. Rep.* 8 (1), 1495. doi: 10.1038/s41598-018-20054-4

Dou, H., Wang, H., Xie, S., Chen, X., Xu, Z., and Xu, Y. (2017). Molecular Characterization of Cryptococcus Neoformans Isolated From the Environment in Beijing, China. *Med. Mycol.* 55 (7), 737–747. doi: 10.1093/mmy/myx026

Dou, H. T., Xu, Y. C., Wang, H. Z., and Li, T. S. (2015). Molecular Epidemiology of Cryptococcus Neoformans and Cryptococcus Gattii in China Between 2007 and 2013 Using Multilocus Sequence Typing and the DiversiLab System. *Eur. J. Clin. Microbiol. Infect. Dis.* 34 (4), 753–762. doi: 10.1007/s10096-014-2289-2

Ellis, D. H., and Pfeiffer, T. J. (1990). Natural Habitat of Cryptococcus Neoformans Var. Gattii. *J. Clin. Microbiol.* 28 (7), 1642–1644. doi: 10.1128/jcm.28.7.1642-1644.1990

Espinel-Ingroff, A., Aller, A. I., Canton, E., Castañón-Olivares, L. R., Chowdhary, A., Cordoba, S., et al. (2012a). Cryptococcus Neoformans-Cryptococcus Gattii Species Complex: An International Study of Wild-Type Susceptibility Endpoint Distributions and Epidemiological Cutoff Values for Fluconazole, Itraconazole, Posaconazole, and Voriconazole. *Antimicrob. Agents Chemother.* 56 (11), 5898–5906. doi: 10.1128/AAC.01115-12

Espinel-Ingroff, A., Chowdhary, A., Cuenca-Estrella, M., Fothergill, A., Fuller, J., Hagen, F., et al. (2012b). Cryptococcus Neoformans-Cryptococcus Gattii Species Complex: An International Study of Wild-Type Susceptibility Endpoint Distributions and Epidemiological Cutoff Values for Amphotericin B and Flucytosine. *Antimicrob. Agents Chemother.* 56 (6), 3107–3113. doi: 10.1128/AAC.06252-11

Fang, W., Fa, Z., and Liao, W. (2015). Epidemiology of Cryptococcus and Cryptococcosis in China. *Fungal Genet. Biol.* 78, 7–15. doi: 10.1016/j.fgb.2014.10.017

Fan, X., Xiao, M., Chen, S., Kong, F., Dou, H. T., Wang, H., et al. (2016). Predominance of Cryptococcus Neoformans Var. Grubii Multilocus Sequence Type 5 and Emergence of Isolates With Non-Wild-Type Minimum Inhibitory Concentrations to Fluconazole: A Multi-Centre Study in China. *Clin. Microbiol. Infect.* 22 (10), 881–887. doi: 10.1016/j.cmi.2016.07.008

Hagen, F., Khayhan, K., Theelen, B., Kolecka, A., Polacheck, I., Sionov, E., et al. (2015). Recognition of Seven Species in the Cryptococcus Gattii/Cryptococcus Neoformans Species Complex. *Fungal Genet. Biol.: FG. B.* 78, 16–48. doi: 10.1016/j.fgb.2015.02.009

Hiremath, S. S., Chowdhary, A., Kowshik, T., Randhawa, H. S., Sun, S., and Xu, J. (2008). Long-Distance Dispersal and Recombination in Environmental Populations of Cryptococcus Neoformans Var. Grubii From India. *Microbiol. (Reading England)* 154 (Pt 5), 1513–1524. doi: 10.1099/mic.0.2007/015594-0

Huang, C., Tsui, C. K. M., Chen, M., Pan, K., Li, X., Wang, L., et al. (2020). Emerging Cryptococcus Gattii Species Complex Infections in Guangxi, Southern China. *PloS Neglect. Trop. D.* 14 (8), e8493. doi: 10.1371/journal.pntd.0008493

Khayhan, K., Hagen, F., Pan, W., Simwami, S., Fisher, M. C., Wahyuningsih, R., et al. (2013). Geographically Structured Populations of Cryptococcus Neoformans Variety Grubii in Asia Correlate With HIV Status and Show a Clonal Population Structure. *PloS One* 8 (9), e72222. doi: 10.1371/journal.pone.0072222

Leal, A. L., Faganello, J., Fuentefria, A. M., Boldo, J. T., Bassanesi, M. C., and Vainstein, M. H. (2008). Epidemiological Profile of Cryptococcal Meningitis Patients in Rio Grande do Sul, Brazil. *Mycopathologia* 166 (2), 71–75. doi: 10.1007/s11046-008-9123-2

Li, A., Pan, W., Wu, S., Hideaki, T., Guo, N., Shen, Y., et al. (2012). Ecological Surveys of the Cryptococcus Species Complex in China. *Chin. Med. J.-Peking.* 125 (3), 511–516. doi: 10.3760/cma.j.issn.0366-6999.2012.03.020

May, R. C., Stone, N. R., Wiesner, D. L., Bicanic, T., and Nielsen, K. (2016). Cryptococcus: From Environmental Saprophyte to Global Pathogen. *Nat. Rev. Microbiol.* 14 (2), 106–117. doi: 10.1038/nrmicro.2015.6

Meyer, W., Aanensen, D. M., Boekhout, T., Cogliati, M., Diaz, M. R., Esposto, M. C., et al. (2009). Consensus Multi-Locus Sequence Typing Scheme for Cryptococcus Neoformans and Cryptococcus Gattii. *Med. Mycol.* 47 (6), 561–570. doi: 10.1080/13693780902953886

Meyer, W., Castañeda, A., Jackson, S., Huynh, M., Castañeda, E.IberoAmerican Cryptococcal Study Group (2003). Molecular Typing of IberoAmerican Cryptococcus Neoformans Isolates. *Emerging. Infect. Dis.* 9 (2), 189–195. doi: 10.3201/eid0902.020246

Pyrgos, V., Seitz, A. E., Steiner, C. A., Prevots, D. R., and Williamson, P. R. (2013). Epidemiology of Cryptococcal Meningitis in the US: 1997-2009. *PloS One* 8 (2), e56269. doi: 10.1371/journal.pone.0056269

Qu, J., Zhang, X., Lu, Y., Liu, X., and Lv, X. (2020). Clinical Analysis in Immunocompetent and Immunocompromised Patients With Pulmonary

Cryptococcosis in Western China. *Sci. Rep.-UK.* 10 (1), 9387. doi: 10.1038/s41598-020-66094-7

Rajasingham, R., Smith, R. M., Park, B. J., Jarvis, J. N., Govender, N. P., Chiller, T. M., et al. (2017). Global Burden of Disease of HIV-Associated Cryptococcal Meningitis: An Updated Analysis. *Lancet Infect. Dis.* 17 (8), 873–881. doi: 10.1016/S1473-3099(17)30243-8

Tamura, K., Stecher, G., Peterson, D., Filipski, A., and Kumar, S. (2013). MEGA6: Molecular Evolutionary Genetics Analysis Version 6.0. *Mol. Biol. Evol.* 30 (12), 2725–2729. doi: 10.1093/molbev/mst197

Velagapudi, R., Hsueh, Y., Geunes-Boyer, S., Wright, J. R., and Heitman, J. (2009). Spores as Infectious Propagules of Cryptococcus Neoformans. *Infect. Immun.* 77 (10), 4345–4355. doi: 10.1128/IAI.00542-09

Viviani, M. A., Cogliati, M., Esposto, M. C., Lemmer, K., Tintelnot, K., Colom, V. M., et al. (2006). Molecular Analysis of 311 Cryptococcus Neoformans Isolates From a 30-Month ECMM Survey of Cryptococcosis in Europe. *FEMS Yeast, Res.* 6 (4), 614–619. doi: 10.1111/j.1567-1364.2006.00081.x

Xiao, M., Chen, S. C., Kong, F., Fan, X., Cheng, J. W., Hou, X., et al. (2018). Five-Year China Hospital Invasive Fungal Surveillance Net (CHIF-NET) Study of Invasive Fungal Infections Caused by Noncandidal Yeasts: Species Distribution and Azole Susceptibility. *Infect. Drug Resist.* 11, 1659–1667. doi: 10.2147/IDR.S173805

Yan, Z., Li, X., and Xu, J. (2002). Geographic Distribution of Mating Type Alleles of Cryptococcus Neoformans in Four Areas of the United States. *J. Clin. Microbiol.* 40 (3), 965–972. doi: 10.1128/JCM.40.3.965-972.2002

Yuchong, C., Fubin, C., Jianghan, C., Fenglian, W., Nan, X., Minghui, Y., et al. (2012). Cryptococcosis in Chin-2010): Review of Cases From Chinese Database. *Mycopathologia* 173 (5-6), 329–335. doi: 10.1007/s11046-011-9471-1

Zhou, L. H., Jiang, Y. K., Li, R. Y., Huang, L. P., Yip, C. W., Denning, D. W., et al. (2020). Risk-Based Estimate of Human Fungal Disease Burden, China. *Emerging. Infect. Dis.* 26 (9), 2137–2147. doi: 10.3201/eid2609.200016

Conflict of Interest: The authors declare that the research was conducted in the absence of any commercial or financial relationships that could be construed as a potential conflict of interest.

Publisher's Note: All claims expressed in this article are solely those of the authors and do not necessarily represent those of their affiliated organizations, or those of the publisher, the editors and the reviewers. Any product that may be evaluated in this article, or claim that may be made by its manufacturer, is not guaranteed or endorsed by the publisher.

frontiers in Cellular and Infection Microbiology

ORIGINAL RESEARCH
published: 02 November 2021
doi: 10.3389/fcimb.2021.711768

First Case of Subcutaneous Mycoses Caused by *Dirkmeia churashimaensis* and a Literature Review of Human *Ustilaginales* Infections

*Fengming Hu[1], Chong Wang[2], Peng Wang[1], Lei Zhang[1,3], Qing Jiang[1], Abdullah M. S. Al-Hatmi[4,5,6], Oliver Blechert[7] and Ping Zhan[7]**

[1] Department of Integrated Chinese and Western Medicine, Dermatology Hospital of Jiangxi Province and Jiangxi Dermatology Institute, Nanchang, China, [2] Dermatology Department, Liaocheng People's Hospital, Liaocheng, China, [3] Dermatology Department, The Second People's Hospital of Guiyang, Guiyang, China, [4] Natural & Medical Sciences Research Center, University of Nizwa, Nizwa, Oman, [5] Department of Biological Sciences & Chemistry, College of Arts and Sciences, University of Nizwa, Nizwa, Oman, [6] Centre of Expertise in Mycology Radboudumc/CWZ, Nijmegen, Netherlands, [7] The Institute of Clinical Medicine & Dermatology Department, Jiangxi Provincial People's Hospital Affiliated to Nanchang University, Nanchang, China

OPEN ACCESS

Edited by:
Anuradha Chowdhary, University of Delhi, India

Reviewed by:
Marie Desnos-Ollivier, Institut Pasteur, France
Soo Chan Lee, University of Texas at San Antonio, United States

***Correspondence:**
Ping Zhan
zhanping1980@163.com

Specialty section:
This article was submitted to Fungal Pathogenesis, a section of the journal Frontiers in Cellular and Infection Microbiology

Received: *19 May 2021*
Accepted: *10 August 2021*
Published: *02 November 2021*

Citation:
Hu F, Wang C, Wang P, Zhang L, Jiang Q, Al-Hatmi AMS, Blechert O and Zhan P (2021) First Case of Subcutaneous Mycoses Caused by Dirkmeia churashimaensis and a Literature Review of Human Ustilaginales Infections. Front. Cell. Infect. Microbiol. 11:711768. doi: 10.3389/fcimb.2021.711768

Objective: *Dirkmeia churashimaensis*, belonging to Ustilaginales fungi, has never been reported as clinical pathogenic until very recently. In this study, we report an unusual subcutaneous infection with *Dirkmeia churashimaensis* and reviewed all human Ustilaginales infections. The aim is to better understand their epidemiology, infection type, risk factors, and the sensitivity to antifungal agents.

Methods: An 80-year-old female farmer developed extensive plaques and nodules on her left arm within 2 years. Pathological and microbiological examinations identified a new pathological agent, *Dirkmeia churashimaensis*, as the cause of this infection. The patient was successfully cured by oral itraconazole. We reviewed a total of 31 cases of Ustilaginales cases, among of which only three were skin infections.

Results: Local barrier damage (i.e., surgery, trauma, and basic dermatosis) and systemic immunodeficiency (i.e., preterm and low birthweight, Crohn's disease, malignant cancer, and chemotherapy) are risk factors for Ustilaginales infection. The D1/D2 and ITS regions are the frequently used loci for identifying the pathogens together with phenotype. Most patients could survive due to antifungal treatment, whereas seven patients died. Amphotericin B, posaconazole, itraconazole, and voriconazole showed good activity against these reported strains, whereas fluconazole, 5-flucytosine, and echinocandins usually showed low susceptibility. Itraconazole had good efficiency for subcutaneous infections.

Conclusions: The present case study and literature review reveal that Ustilaginales can be opportunistic pathogenic normally in immunocompromised and barrier damage people. A proper identification of fungi can be crucial for clinical treatment, and more data of antifungal are needed for choice of medication against this kind of infections.

Keywords: *Dirkmeia*, *Pseudozyma*, *Moesziomyces*, Ustilaginales, infection, subcutaneous

INTRODUCTION

Ustilaginales is a large order within the smut fungi (Ustilaginomycetes) including many species forming blackish to brownish powdery spore mass in different organs of plants (Kruse et al., 2017). Most of them are typically parasitic and some species are important pathogens of plants, such as corn smut (*Pseudozyma prolifica*) and wheat smut (*Ustilago nuda*) (Kruse et al., 2017) (Morita et al., 2011). Ustilaginales were occasionally isolated from clinical context, mainly consisting of species within *Pseudozyma* and *Moesziomyces* (Telles et al., 2020), (Liu et al., 2019). The first report of human infection was reported from Japan in 2003 (Sugita et al., 2003). Since then, several species, including *M. antarcticus*, *M. parantarctica*, *P. thailandica*, *M. aphidis*, *M. bullatus*, *P. crassa*, and *P. siamensis*, were reported for human infections (Liu et al., 2019). Up to now, a total of 31 cases of patients with Ustilaginales invasion were reported indicating the infectious potential of these plant-pathogenic fungal species (**Table 1**). The species *D. churashimaensis* (previously *Pseudozyma churashimaensis*) was first isolated from leaves of sugarcane in Okinawa, Japan, and described as a new species in 2011 with its host ranging from rice, corn, and sugarcane (Morita et al., 2011). In 2015, by multiloci phylogeny analysis, Wang et al. proposed this fungus to be a new genus *Dirkmeia gen. nov* which only having this species up to now (Wang et al., 2015). In 2020, Anuradha et al. reported 12 cases due to an outbreak of *D. churashimaensis* fungemia in a Neonatal Intensive Care Unit, India, which revealed its pathogenicity in immune suppressed population (Chowdhary et al., 2020). Here, we describe a case of rare subcutaneous infection caused by *D. churashimaensis*. Further, we successfully cured the infection by oral itraconazole treatment.

MATERIALS AND METHODS

Case Presentation

An 80-year-old female farmer was firstly admitted to our clinic on March 7, 2017 (Dermatology Hospital of Jiangxi Province and Jiangxi Dermatology Institute, Nanchang, South China). Two years prior to her visit, an egg-sized plaque appeared on the extensor side of her left forearm with slight pain, near the wrist joint. The lesion was given no medical attention and slowly spread to the surrounding region. Papules, plaques, and nodules developed successively, with exudation and ulcers appearing on the lesion surface. There was no severe suppuration and sinus tract. Generally, the patient was in a good condition without fever, cough, or fatigue. History of trauma was not recorded, and she had no accompanying systemic diseases or special drug use. She usually works in a farm and get in contact with crops, such as rice and wheat.

No abnormality was found by biochemical and routine blood examination. CD4+ and CD8+ cell counts were within the normal ranges. The dermatological examination showed a 14 cm × 9 cm irregular infiltrated erythematous plaque on her extensor side of left forearm with distinct margin. Varisized nodes, superficial ulcers, and scales could be observed within the involved region (**Figure 1A**). Moderate to severe pain was reported. Neighboring lymphadenectasis was not discerned.

A skin biopsy was taken from the lesion, and direct examination (KOH 10%) showed fungal spores and conidia. In addition, Periodic acid–Schiff (PAS) and Gomori-Grocott methenamine silver (GM) stains showed a type of infectious granuloma and abundant blastoconidia (**Figure 1B**). Culture of skin biopsy on Sabouraud's glucose agar (SGA) showed yeast like colonies (**Figure 1D**). Further identification of the fungus was undertaken using ITS sequences using standard primer-pair ITS1 and ITS4. For the identification, a similarity searches with the sequences of ITS regions were done using the BLAST tool against the NCBI database and against the MLST database hosted by Westerdijk Institute, Utrecht, The Netherlands. These BLAST searches revealed that the fungus matched with *Dirkmeia churashimaensis* with 100% similarities (MN515013 and MN515015). The ITS1/2 sequence of the fungus was deposited at GenBank with accession number MK463929.

The *in vitro* antifungal-drug susceptibility test, by the EUCAST. DEF.7.3.1 method, gave a minimum inhibitory concentration (MIC) for fluconazole and 5-flucytocine of 64 mg/L, for ketoconazole and amphotericin B of 0.5 mg/L, for Posaconazole and voriconazole of 2 mg/L, for itraconazole of 1 mg/L, and for terbinafine of 4 mg/L. The case was diagnosed as subcutaneous fungal granuloma by the attending physician, and oral itraconazole (Sporanox) was prescribed with a dosage of 0.2 mg twice a day. Hepatorenal function and whole blood cell analysis were monitored every 2 weeks.

The lesion was healing in the first 2 months of the treatment and dispelled constantly since then. Three months later, all ulcers were cured completely and no new lesions were seen. Consequently, the itraconazole dose was reduced to 0.2 mg per day. The lesion improved continuously and became flattened in the following months. The itraconazole doses was reduced to 0.1 mg each day at 5 months and ended after 6 months of treatment due to the complete relief (**Figure 1C**). The patient tolerated the itraconazole treatment, and no side-effect was reported neither by the patient nor was seen by the physicians. In the 1-year follow-up examination, the patient was free of symptoms.

Literature Review

For the literature review of clinical reports, we searched in Pubmed, with Google, and in the English language version of the Web of Science database. *Pseudozyma*, *Moesziomyces*, *Dirkmeia*, and *Ustilaginales* were used as keywords, and all reports before April 1, 2021 were included. The etiological agents were undoubtedly identified by morphology and molecular methods. The details of clinical and strain information were retrieved.

RESULTS

A total of 15 publications including 30 cases were obtained by the search and included, together with the case of this study, in the

Abbreviations: SGA, Sabouraud's glucose agar; CD4, cluster of differentiation 4; CD8, cluster of differentiation 8; MIC, Minimum inhibitory concentration; KOH, Potassium Hydroxide; PAS, Periodic acid–Schiff; GM, Gomori-Grocott methenamine.

TABLE 1 | Clinical information of Ustilaginales infections in human.

Author, year	Species/ Identification	Region	Infection Type/ Source	Age/ Gender*	Underlying Disease[&]	Clinical Presentation	Treatment[#]	Prognosis
Sugita et al., 2003	*M. antarcticus* *P. thailandica* *M. aphidis*	Northern Thailand	Blood/N/A	NA/M 52/F 21/F	Spontaneous pneumothorax Asthmatic and respiratory failure leptospirosis and aseptic meningitis	N/A	N/A	N/A
Lin et al., 2008	*M. aphidis*	NC USA	Blood/CVC	7/F	Short gut syndrome	Fever, chill, malaise and fatigue	FLC failed→CVC Removal+ oral ITC	Survived
Hwang et al., 2010	*Pseudozyma spp*	Seoul South Korea	Brain Abscess/ surgery	78/M	Astrocytoma, MRSA infection	Fever	No AFT	Died
Chen et al., 2011	*M. aphidis*	Wenzhou China	Leg/secondary	51/M	Mycetoma and nocardiosis of leg,	Swollen, discharging sinuses	Oral ITC	Survived
de Carvalho Parahym et al., 2013	*M. aphidis*	Recife Brazil	Pleural fluid/ inhalation	17/M	Burkitt lymphoma, chemotherapy	Fever, lung infiltrates	LAMB→VRC	Survived
Prakash et al., 2014	*M. aphidis*	New Delhi India	Blood/N/A	0/M	Hemolytic jaundice	Lethargy, fever, chill	AMB→VRC	Survived
Orecchini et al., 2015	*M. aphidis*	Argentina	Blood/CVC	6/F	Osteosarcoma with lung metastasis, chemotherapy	Fever	LAMB, CVC Removal	Survived
Mekha, 2014	*P. alboarmeniaca* *P. crassa* *P. siamensis*	Nonthaburi Thailand	Blood/N/A	N/A	N/A	N/A	N/A	N/A
Siddiqui, 2014	*Pseudozyma spp*	Georgia USA	Blood/CVC	52/F	Crohn's disease, colectomy	Fever, headache and weakness	FLC failed→VRC	Survived
Okolo et al., 2015	*M. bullatus*	Córdoba Negeria	Blood/CVC	0/F	Preterm low birth weight	Hypothermia	FLC	Died
Herb et al., 2015	*M. aphidis*	Strasbourg France	Blood/CVC	68/F	Adenocarcinoma of ampulla of Vater, surgery	Fever, chill	LAMB +CVC Removal	Survived
Joo et al, 2016	*M. aphidis*	South Korea	Blood/CVC	51/M	AML, chemotherapy	Fever, lung infiltrate	LAMB+CVC Removal→VRC	Survived
Pande et al., 2017	*Pseudozyma* spp.	Missouri USA	Blood and skin/ CVC	44/M	HSCT recipient	High fever	CVC Removal +AmB→VRC	Survived
Liu et al., 2019	*M. antarcticus*	Chengdu, China	Blood	93/M	hypertension, chronic renal insufficiency, Alzheimer's disease, cerebral infarction, COPD	Fever	CAS(failed)→AMB	Survived
Chowdhary, 2020	*D.churashimaensis* (12 cases)	Delhi, India	blood	neonate	Preterm, low birthweight	N/A	FLU	7 survived, 5 died
This study	*D.churashimaensis* (this study)	Nanchang China	Skin	80/F	No underlying disease	Erythema plaques and nodules	oral ITC	survived

P, pesudozyma; M. Moesziomyces; D. Dirkmiea; USA, the United States.

**In this column, M means male and F means female.*

[&]In this column, MRSA means methicillin-resistant Staphylococcus aureus; AML, acute myeloid leukemia; HSCT, haematopoietic stem cell transplantation; COPD, chronic obstructive pulmonary disease.

[#]In this column, → means changing to a new therapy, + means combined therapy. CVC, central venous catheter-related; N/A, not available.; AFT, antifungal treatment; TMP/SMX, trimethoprim/sulfamethoxazole; FLC, fluconazole; AMB, amphotericin B; LAMB, liposomal amphotericin B; VRC, voriconazole; ITC, itraconazole.

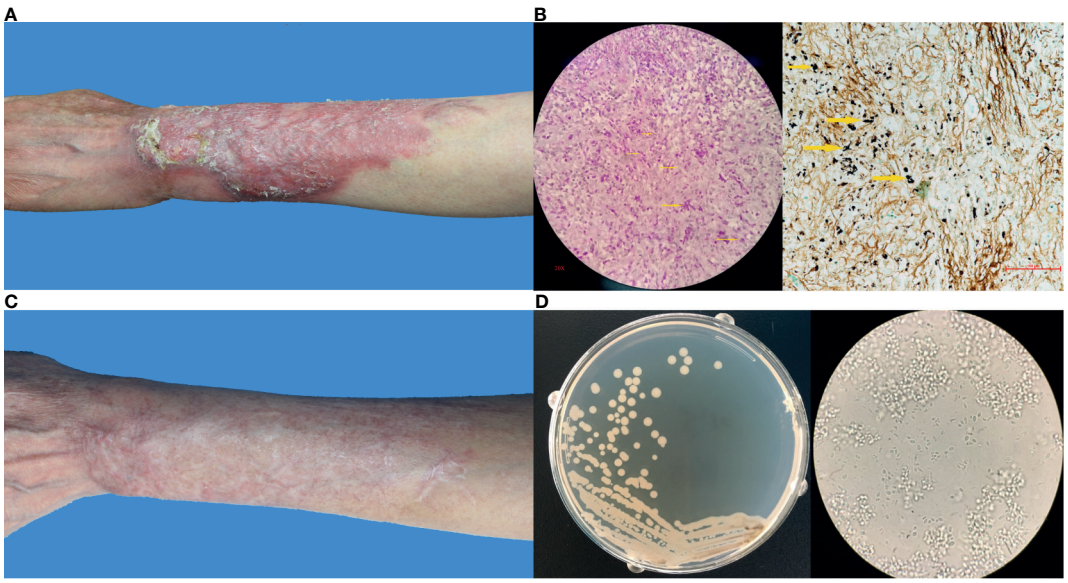

FIGURE 1 | **(A)** Clinical image of this patient before treatment; **(B)** Histopathological examination by Periodic acid–Schiff stain and Methenamine silver stain showing a type of infectious granuloma, abundant blastoconidia, and hyphae elements (yellow arrows indicated); **(C)** Clinical image of this patient after treatment; **(D)** Fungal culture showing yeast-like colonies and budding spores under microscope.

data analysis. The clinical data were shown in **Table 1**. The information about the strains, including the available antifungal drug resistances data, was summarized in **Table 2**.

The first case of human infection with Ustilaginales species was reported by Sugita et al. in 2003, and three strains were isolated from North Thailand in the year of 2001 which were identified as *M. antarcticus*, *P. thailandica*, and *M. aphidi* (Sugita et al., 2003). We analyzed the 31 cases, including 30 cases from the literature and the case from this study, for the geographic distribution, temporal distribution, species identification, site of infection, clinical manifestation, treatment, and antifungal drug resistance.

Most cases of Ustilaginales infections were reported from Asian countries with 24 cases (77%), 13 from India, 6 from Thailand, 3 from China, 2 from South Korea. There were three cases from the USA and two cases from Africa, one from Argentina, and the other one from Nigeria. Only one case was reported from Europe, from Strasbourg, France. Most of the cases appeared after the year of 2010, taking a percentage of 90% of the reported cases. In the recent 6-year period, 18 cases were reported, which accounts for more than 50% of the reported cases. Fourteen newborns were reported to get infections with Ustilaginales fungi, and the oldest patient was 93 years old (Liu et al., 2019).

Of the 31 isolates, all strains were identified by both phenotype and molecular methods, whereby the sequence of the internal transcribed spacer region (ITS1/2) and D1/D2 region is routinely used for molecular biological species identification. Twenty-eight of the strains were identified to species level, whereas the other 3 were reported as *Pseudozyma* spp. without accession information.

Dirkmeia churashimanesis was the predominant clinical species with a percentage of 46% (13/28), and *Moesimyces aphidis* was the second common with 28.6% (8/28) among the identified strains. Additionally, *M. antarctica* two cases were reported and of the other species *M. bullatus*, *P. alboarmeniaca*, *P. crassa*, *P. siamensis*, and *P. thailandica* each one case.

The majority of patients had blood disseminated infections (29/31). Notedly, two of these patients had breaking through infections, with prophylactic treatment of fluconazole and echinocandins (de Carvalho Parahym et al., 2013) (Joo et al., 2016). Two patients in literature had skin infections: one had a secondary to chronic mycetoma and one had a papular eruption over the body with a concurrent blood infection (Chen et al., 2011) (Pande et al., 2017). In this study, we reported the third case of a skin disease caused by *Dirkmeia churashimaensis*. Parahym et al. reported a pulmonary infection of *M. aphidis* from a patient, with a Burkitt lymphoma, during chemotherapy (de Carvalho Parahym et al., 2013). The infection resulted from environmental inhalation. Before the infection occurred, the 17-year-old boy received broad-spectrum antibiotics and antifungal prophylaxis with fluconazole and caspofungin. The blood cultures were negative but the pleural fluid was positive in the fungal examination, and the pathogen was identified as *M. aphidis*. Hwang et al. reported a strain of *Pseudozyma* species isolated from barin abscess (Hwang et al., 2010).

The therapy process for 25 patients was described in the literature as well our study; for six cases, no clinical details were available (Sugita et al., 2003) (Mekha et al., 2014). Eighteen of the 25 patients recovered, and 7 died. Seven patients were prescribed systemic amphotericin B or voriconazole, and all of them

TABLE 2 | Strain information of Ustilaginales infections in human.

No.	Species/Identification	Gene Accession	MIC									AFST Method
			FLC	ITC	VRC	AMB	CAS	5FC	Ani	Pos	Others	
1	*M. antarcticus*	AB089375(26S) AB089374(ITS)	0.5	0.06	N/A	0.125	N/A	>64	N/A	N/A	N/A	EIKEN kit (Eiken Chemical, Tokyo)
2	*P. thailandica*	AB089355(26S) AB089354(ITS)	2	0.25	N/A	0.25	N/A	>64	N/A	N/A	N/A	EIKEN kit (Eiken Chemical, Tokyo)
3	*M. aphidis*	AB089357(26S) AB089356(ITS)	>64	>8	N/A	0.25	N/A	>64	N/A	N/A	N/A	EIKEN kit (Eiken Chemical, Tokyo)
4	*M. aphidis*	Bankit1010363(ITS)	4	0.125	N/A	0.25	N/A	N/A	N/A	N/A	N/A	YeastOne system (Trek Diagnostic)
5	*Pseudozyma spp*	N/A	N/A	N/A	N/A	N/A	N/A	N/A	N/A	N/A	N/A	N/A
6	*M. aphidis*	N/A	N/A	N/A	N/A	N/A	N/A	N/A	N/A	N/A	N/A	N/A
7	*M. aphidis*	JQ743064(ITS)	4	0.25	0.03	0.25	4	N/A	4	N/A	N/A	CLSI M27-A3
8	*M. aphidis*	KC812275(D1/D2)	8	0.03	0.06	0.03	8	>64	8	0.03	**Isa** 0.25	CLSI M27-A3
9	*M. aphidis*	KM610219(ITS) KM610218(D1/D2)	2	0.03	0.03	0.13	N/A	128	N/A	0.015	N/A	EUCAST E.Def 7.2
10	*P. alboarmeniaca*	AB117961(ITS)	32	4	2	0.25	>16	>64	N/A	N/A	Mica>16	EIKEN kit (Eiken Chemical, Tokyo)
11	*P. crassa*	AB117962(ITS)	>64	>8	2	0.25	>16	>64	N/A	N/A	Mica>16	EIKEN kit (Eiken Chemical, Tokyo)
12	*P. siamensis*	AB117963(ITS)	32	4	2	0.125	>16	>64	N/A	N/A	Mica>16	EIKEN kit (Eiken Chemical, Tokyo)
13	*Pseudozyma spp*	N/A	N/A	N/A	N/A	N/A	N/A	N/A	N/A	N/A	N/A	N/A
14	*M. bullatus*	N/A	128	0.12	0.03	1	8	64	N/A	N/A	N/A	YeastOne Y010
15	*M. aphidis*	N/A	16	0.19	0.03	0.19	>32	>32	N/A	N/A	N/A	EUCAST E.Def 7.2
16	*M. aphidis*	KF443199(ITS) KF443201(D1/D2)	N/A	N/A	N/A	N/A	N/A	N/A	N/A	N/A	N/A	N/A
17	*Pseudozyma* spp.	N/A	N/A	N/A	N/A	N/A	N/A	N/A	N/A	N/A	N/A	N/A
18	*M. antarcticus*	MH185803	128	4	8	<0.5	N/A	>16	N/A	N/A	N/A	ATB FUNGUS 3 (bioMérieux)
19-30	*D. churashimaensis*	N/A	0.157	0.03-0.25	0.03-0.125	0.198	>8	0.157	>8	0.03-0.25	Isa 0.03-0.125	CLSI M27 M60
31	*D. churashimaensis*	MK463929	64	4	2	0.5	N/A	64	N/A	2	KET 0.5	CLSI M27 M60

P, Pesudozyma; M. Moesziomyces; D. Dirkmiea; FLC, fluconazole; ITC, itraconazole; VRC, voriconazole; AMB, amphotericin B; CAS, caspofungin; 5FC, flucytosine; Mica, micafungin; Ani, anidulafungin; Pos, posaconazole; Isa, isavuconazole; KET, ketoconazole; N/A, not available.

recovered finally with good results, among of which three patients were combined with the removal contaminated catheter. Three patients with localized skin and subcutaneous infection completely were cured with oral itraconazole for 2 weeks to 6 months (Chen et al., 2011) (Pande et al., 2017). The therapy of three patients failed with fluconazole (2 cases) or caspofungin (1 case) until changing to the efficient medicines itraconazole, amphotericin B, or voriconazole (Lin et al., 2008) (Siddiqui et al., 2014) (Liu et al., 2019). Furthermore, Chowdhary reported an outbreak of 12 case infections due to *D. churashimanesis* in a neonatal intensive care unit in Delhi India; all patients were treated with fluconazole at a loading dose of 12 mg/kg bodyweight and then 6 mg/kg for 10–14 days; 5 patients died, a case-fatality rate of 42% (Chowdhary et al., 2020). In 2015, Orecchini et al. reported a similar fatal neonate baby as the etiological agent is *M. bullatus* with blood invasion (Orecchini et al., 2015).

Except for these six above deaths, Hwang et al. reported another fatal case. A 78-year-old patient got a brain abscess due to a *Pseudozyma* species in combination with a methicillin-resistant *Staphylococcus aureus* (MRSA) infection after a needle biopsy of brain astrocytoma. The fungal pathogen was identified as *Pseudozyma* strain CBS 10103 (Hwang et al., 2010). The other six dead cases were all preterm, low weight babies who got neonatal sepsis due to *D. churashimanesis* (five cases) (Chowdhary et al., 2020) and *M. bullatus* (one case) (Orecchini et al., 2015). These babies died despite fluconazole treatment. For 26 of the strains, antifungal drug resistances data were available (**Table 2**). Most strains had low MICs to itroconazole, voriconazole, and amphotericin B, whereas high MICs to fluconazole (0.5–128 mg/L), flucytosine (>64 mg/L), caspofungin (4–32 mg/L), and micafungin (>16 mg/L). However, in Chowdhary's report (Chowdhary et al., 2020), all the 12 *D. churashimanesis* strains showed sensitive to azoles, including itraconazole, fluconazole, voriconazole, Posaconazole, and isavuconazole, with low MICs. Amphotericin B and 5-flucytosine also had potent activity. The resistance to echinocandins, including caspofungin, anidulafungin, and micafungin (MICs > 8 mg/L), is coincident with other strains.

DISCUSSION

In this paper, we reported a severe subcutaneous infection caused by *D. churashimaensis* and performed a literature review of human disease caused by Ustilaginales fungi. By analyzing the demographic, clinical, and strain information, we got a better understanding of their geographical distribution, susceptible population, and susceptibility to routine antifungal drugs. Our patient presented an extensive granuloma on her forearm, and the pathogenic agent was identified as *D. churashimaensis* by morphology and molecular methods. After long-term treatment with itraconazole for 6 months with a total dose of 49.5 grams, the patient recovered completely.

The species *D. churashimaensis* (previously *Pseudozyma churashimaensis*) was first described in 2011 from the leaves of sugarcane in Japan. By multigene phylogeny analysis combined ITS and LSU rRNA gene, Wang et al. proposed it to be a new genus, *Dirkmeia* which belongs to an isolated branch in the Ustilaginales (Wang et al., 2015). In our case, the yeast form of this fungus was highly virulent and invaded the epidermis and dermis layers, which lead to a very extensive damage within 2 years. However, our strains presented as cream-colored yeast colony without blackish to brownish powdery spores whose synthesis perhaps was blocked by unappropriated environment in skin tissue. Chowdhary et al. reported an outbreak of 12 cases due to this fungus in NICU, in India last year (Chowdhary et al., 2020). All the patients were preterm neonates with other risk factors, including central venous catheter, persistent hypoglycemia, severe asphyxia, sepsis, and mechanical ventilation. All samples were isolated from blood and grew as yeast-like cream to pale yellow. In our case, the patient had no obvious immunocompromised status. Considering she usually works in gardens and farms, we speculate that chronic damage of the skin was due to farm work in combination with chronic exposure to the opportunist which cause the infection. Our study together with Chowdhary et al. reported the significance of the *D. churashimaensis* as opportunistic fungi in human hosts.

We also reviewed 31 clinical cases caused by the following fungi including *D. churashimaensis* and *M. aphidis* (synonym to *P. aphidis*) which were the most common agents, responsible for 75% of all strains identified to species level. In addition, some other species were also reported including *M. antarcticus*, *P. thailandica*, *M. parantarctica*, *P. alboarmeniaca*, *P. crassa*, *P. siamensis*, and *M. bullatus*.

Smut fungi are usually found in the environment and can be transferred to human by direct and indirect contact. Catheter-related infections were common invasive route and could lead to blood dissemination for invasive yeast infections (Pappas et al., 2015). Removals of the contaminated catheter were strongly suggested for catheter-related infections of candidemia (Pappas et al., 2015). In our review, catheter removal was explored to three cases with proper antifungal therapy and the infection vanished. In three of these patients, locally skin irritations and in one patient cutaneous rash were diagnosed and were related to the blood infection. Infections by inhalation were not common and, in this review, only one case got pulmonary invasion during chemotherapy (de Carvalho Parahym et al., 2013). Furthermore, one brain abscess occurred after traumatic examination (Hwang et al., 2010).

Generally, underlying immune deficiency was high-risk factor for invasive fungal infections. Among those with detailed clinical information, 29 of 31 patients had a local barrier damage (including pneumothorax, surgery, and basic dermatosis) or systemic immunodeficiency including preterm, low birth weight, Crohn's disease, short gut syndrome, malignant cancer, and chemotherapy. With the rise of the immunocompromised population, the overuse of antibiotics and increase of invasive operations, clinical cases due to unusual saprophytic fungi have increased during the last few years (Skiada et al., 2017). Especially in immunocompromised patient, saprophytic fungal species take the opportunity to invade the host and as the boundary between

saprophytic and pathogenic are less clear in these cases. Diagnosis of unusual fungal infections should be done regularly, and drug susceptibility test should be performed for all of this these strains.

For these strains within the genus *Dirkmeia*, *Pseudozyma*, and *Moesziomyces*, amphotericin B and azoles (ketoconazole, posaconazole, itraconazole and voriconazole) have a good antifungal activity. Doing antifungal susceptibility testing might help in choosing proper therapy for these kinds of infections. All *Dirkmeia* isolates from Chowdhary's study showed potent activity of fluconazole (MIC 1–4 μg/ml; GM 2.37 μg/ml) and 5-flucytosine (GM MIC: 0.157 μg/ml). Although, in the other studies, the MICs of fluconazole and 5-flucytosine show high MICs, the former with a range of 2–128 mg/L and the latter higher than 32 mg/L (Chowdhary et al., 2020). Considering the high percentage of death especially from those who received fluconazole therapy and there were two breakthrough infections occurred with prophylactic use of fluconazole as fluconazole seems not efficient for these kinds of infections. Therefore, *in vitro* antifungal test with more clinical strains of Ustiginales is needed in future. Caspofungin, micafungin, and anidufungin had high MICs for all species and always failed as therapeutic against Ustilaginales infection. Considering that echinocandins are commonly used for treating of invasive *Candida* infection, the attending physician should be aware of the possibility of a Ustilaginales infections.

Itraconazole is a broad-spectrum antifungal agent commonly used for subcutaneous fungal infection and applied with an empirical dose of 0.4 mg/day. In our case, the *in vitro* and *in vivo* efficiency of itraconazole correlations and our results is in agreement with previous published guidelines of subcutaneous fungal infections (Kauffman et al., 2007). Most of cases from the literature especially with local skin infection were successfully treated with oral itraconazole. A high dose at the beginning of the therapy increases quickly the concentration in the blood and inhibits the fungal growth. When the lesion is under controlled, the dosage can be adjusted according to the clinical prognosis and adverse reactions. Our patient treated with itraconazole lasted for 6 months, and no relapse was seen in the 1 year follow up control examination.

In conclusion, we report a case of human infection due to *D. churashimaensis*. The patient, an 80-year-old woman, developed plaques and nodules on her left arm. Oral treatment with itraconazole was successful against the infection. An antifungal drug susceptibility test of *D. churashimaensis* and a literature review indicates that itraconazole could be the first choice for the therapy against skin/subcutaneous *D. churashimaensis* infections. Since some of the common antifungal drugs, for example; fluconazole and echinocandins, are ineffective against *Dirkmeia* species, we here highlight the importance of proper identification of the causative agents. Furthermore, antifungal susceptibility tests should be done regularly.

DATA AVAILABILITY STATEMENT

The datasets presented in this study can be found in online repositories. The names of the repository/repositories and accession number(s) can be found in the article/supplementary material.

ETHICS STATEMENT

Written informed consent was obtained from the individual(s) for the publication of any potentially identifiable images or data included in this article.

AUTHOR CONTRIBUTIONS

FH and PW contributed to diagnosing, deciding treatment, and follow-up. LZ contributed to the pathological examinations. QJ contributed to the fungal identification. CW, AA-H, OB, and PZ contributed to manuscript writing and revisions and approved the final manuscript. All authors contributed to the article and approved the submitted version.

FUNDING

This work was supported by National Natural Science Foundation of China (81960367) and the Natural Science Foundation of Shandong Province of China (ZR2017MH121).

REFERENCES

Chen, B., Zhu, L. Y., Xuan, X., Wu, L. J., Zhou, T. L., Zhang, X. Q., et al. (2011). Isolation of Both Pseudozyma Aphidis and Nocardia Otitidiscaviarum From a Mycetoma on the Leg. *Int. J. Dermatol.* 50, 714–719. doi: 10.1111/j.1365-4632.2010.04814.x

Chowdhary, A., Sharada, K., Singh, P. K., Bhagwani, D. K., Kumar, N., de Groot, T., et al. (2020). Outbreak of Dirkmeia Churashimaensis Fungemia in a Neonatal Intensive Care Unit, India. *Emerg. Infect. Dis.* 26, 764–768. doi: 10.3201/eid2604.190847

de Carvalho Parahym, A. M. R., da Silva, C. M., de Farias Domingos, I., Gonçalves, S. S., de Melo Rodrigues, M., de Morais, V. L. L., et al. (2013). Pulmonary Infection Due to Pseudozyma Aphidis in a Patient With Burkitt Lymphoma: First Case Report. *Diagn Microbiol. Infect. Dis.* 75, 104–106. doi: 10.1016/j.diagmicrobio.2012.09.010

Herb, A., Sabou, M., Delhorme, J. B., Pessaux, P., Mutter, D., Candolfi, E., et al. (2015). Pseudozyma Aphidis Fungemia After Abdominal Surgery: First Adult Case. *Med. Mycol. Case Rep.* 8, 37–39. doi: 10.1016/j.mmcr.2015.03.001

Hwang, S., Kim, J., Yoon, S., Cha, Y., Kim, M., Yong, D., et al. (2010). First Report of Brain Abscess Associated With Pseudozyma Species in a Patient With Astrocytoma. *Korean J. Lab. Med.* 30, 284–288. doi: 10.3343/kjlm.2010.30.3.284

Joo, H., Choi, Y. G., Cho, S. Y., Choi, J. K., Lee, D. G., Kim, H. J., et al. (2016). Pseudozyma Aphidis Fungaemia With Invasive Fungal Pneumonia in a Patient With Acute Myeloid Leukaemia: Case Report and Literature Review. *Mycoses* 59, 56–61. doi: 10.1111/myc.12435

Kauffman, C. A., Bustamante, B., Chapman, S. W., and Pappas, P. G. (2007). Clinical Practice Guidelines for the Management of Sporotrichosis: 2007 Update by the Infectious Diseases Society of America. *Clin. Infect. Dis.* 45, 1255–1265. doi: 10.1086/522765

Kruse, J., Doehlemann, G., Kemen, E., and Thines, M. (2017). Asexual and Sexual Morphs of Moesziomyces Revisited. *IMA Fungus* 8, 117–129. doi: 10.5598/imafungus.2017.08.01.09

Lin, S. S., Pranikoff, T., Smith, S. F., Brandt, M. E., Gilbert, K., Palavecino, E. L., et al. (2008). Central Venous Catheter Infection Associated With Pseudozyma Aphidis in a Child With Short Gut Syndrome. *J. Med. Microbiol.* 57, 516–518. doi: 10.1099/jmm.0.47563-0

Liu, Y., Zou, Z., Hu, Z., Wang, W., and Xiong, J. (2019). Morphology and Molecular Analysis of Moesziomyces Antarcticus Isolated From the Blood Samples of a Chinese Patient. *Front. Microbiol.* 10, 254. doi: 10.3389/fmicb.2019.00254

Mekha, N., Takashima, M., Boon-long, J., Cho, O., and Sugita, T. (2014). Three New Basidiomycetous Yeasts, Pseudozyma Alboarmeniaca Sp. Nov., Pseudozyma Crassa Sp. Nov. And Pseudozyma Siamensis Sp. Nov. Isolated From Thai Patients. *Microbiol. Immunol.* 58, 9–14. doi: 10.1111/1348-0421.12111

Morita, T., Ogura, Y., Takashima, M., Hirose, N., Fukuoka, T., Imura, T., et al. (2011). Isolation of Pseudozyma Churashimaensis Sp. Nov., a Novel Ustilaginomycetous Yeast Species as a Producer of Glycolipid Biosurfactants, Mannosylerythritol Lipids. *J. Biosci. Bioeng* 112, 137–144. doi: 10.1016/j.jbiosc.2011.04.008

Ojogba, M. O., Anne, D., Bose, T., Nnaemeka, E. N., Mebi, G. A., Ikenna, K. O., et al. (2015). First Report of Neonatal Sepsis due to Moesziomyces bullatus in a Preterm Low-Birth-Weight Infant. *JMM Case Rep.* 2015, 1–4. doi: 10.1099/ jmmcr.0.000011

Okolo, O. M., Van Diepeningen, A. D., Toma, B., Nnadi, N. E., Ayanbimpe, M. G., Onyedibe, I. K., et al. (2015). First Report of Neonatal Sepsis Due to Moesziomyces bullatus in a Preterm Low-Birth-Weight Infant. *JMM Case Reports*. 2 (2). doi: 10.1099/jmmcr.0.000011

Orecchini, L. A., Olmos, E., Taverna, C. G., Murisengo, O. A., Szuzs, W., Vivot, W., et al. (2015). First Case of Fungemia Due to Pseudozyma Aphidis in a Pediatric Patient With Osteosarcoma in Latin America. *J. Clin. Microbiol.* 53, 3691–3694. doi: 10.1128/JCM.01095-15

Pande, A., Non, L. R., Romee, R., and Santos, C. A. Q. (2017). Pseudozyma and Other non- Candida Opportunistic Yeast Bloodstream Infections in a Large Stem Cell Transplant Center. *Transpl Infect. Dis.* 19, e12664. doi: 10.1111/tid.12664

Pappas, P. G., Kauffman, C. A., Andes, D. R., Clancy, C. J., Marr, K. A., Ostrosky-Zeichner, L., et al. (2015). Clinical Practice Guideline for the Management of Candidiasis: 2016 Update by the Infectious Diseases Society of America. *Clin. Infect. Dis.* 62, e1–e50. doi: 10.1093/cid/civ933

Prakash, A., Wankhede, S., Singh, P. K., Agarwal, K., Kathuria, S., Sengupta, S., et al. (2014). First Neonatal Case of Fungaemia Due to Pseudozyma Aphidis and a Global Literature Review. *Mycoses* 57, 64–68. doi: 10.1111/myc.12098

Siddiqui, W., Ahmed, Y., Albrecht, H., and Weissman, S. (2014). Pseudozyma Spp Catheter-Associated Blood Stream Infection, an Emerging Pathogen and Brief Literature Review. *BMJ Case Rep.* 2014, 10–12. doi: 10.1136/bcr-2014-206369

Skiada, A., Pavleas, I., and Drogari-Apiranthitou, M. (2017). Rare Fungal Infectious Agents: A Lurking Enemy. *F1000Research* 6, 1–17. doi: 10.12688/f1000research.11124.1

Sugita, T., Takashima, M., Poonwan, N., Mekha, N., Malaithao, K., Thungmuthasawat, B., et al. (2003). The First Isolation of Ustilaginomycetous Anamorphic Yeasts, Pseudozyma Species, From Patients' Blood and a Description of Two New Species: P. Parantarctica and P. Thailandica. *Microbiol. Immunol.* 47, 183–190. doi: 10.1111/j.1348-0421.2003.tb03385.x

Telles, J. P., Ribeiro, V. S. T., Kraft, L., and Tuon, F. F. (2020). Pseudozyma Spp. Human Infections: A Systematic Review. *Med. Mycol* 59, 1–6. doi: 10.1093/mmy/myaa025

Wang, Q. M., Begerow, D., Groenewald, M., Liu, X. Z., Theelen, B., Bai, F. Y., et al. (2015). Multigene Phylogeny and Taxonomic Revision of Yeasts and Related Fungi in the Ustilaginomycotina. *Stud. Mycol.* 81, 55–83. doi: 10.1016/j.simyco.2015.10.004

Conflict of Interest: The authors declare that the research was conducted in the absence of any commercial or financial relationships that could be construed as a potential conflict of interest.

Publisher's Note: All claims expressed in this article are solely those of the authors and do not necessarily represent those of their affiliated organizations, or those of the publisher, the editors and the reviewers. Any product that may be evaluated in this article, or claim that may be made by its manufacturer, is not guaranteed or endorsed by the publisher.

frontiers in Cellular and Infection Microbiology

ORIGINAL RESEARCH
published: 27 December 2021
doi: 10.3389/fcimb.2021.761596

OPEN ACCESS

Edited by:
Jianping Xu,
McMaster University, Canada

Reviewed by:
Himeshi Samarasinghe,
McMaster University, Canada
Min Chen,
Shanghai Changzheng Hospital, China

***Correspondence:**
Wieland Meyer
wieland.meyer@sydney.edu.au;
wieland.meyer@curtin.edu.au

†Present address:
Katharina Schwabenbauer, A.M.I. GmbH, Feldkirch, Austria;
Carolina Firacative, Translational Microbiology and Emerging Diseases (MICROS) Research Group, School of Medicine and Health Sciences, Universidad del Rosario, Bogota, Colombia;
Wieland Meyer, Curtin Medical School, Curtin University, Perth, WA, Australia

Specialty section:
This article was submitted to Fungal Pathogenesis, a section of the journal Frontiers in Cellular and Infection Microbiology

Received: *20 August 2021*
Accepted: *26 November 2021*
Published: *27 December 2021*

Citation:
Harun A, Kan A, Schwabenbauer K, Gilgado F, Perdomo H, Firacative C, Losert H, Abdullah S, Giraud S, Kaltseis J, Fraser M, Buzina W, Lackner M, Blyth CC, Arthur I, Rainer J, Lira JFC, Artigas JG, Tintelnot K, Slavin MA, Heath CH, Bouchara J-P, Chen SCA and Meyer W (2021) Multilocus Sequence Typing Reveals Extensive Genetic Diversity of the Emerging Fungal Pathogen Scedosporium aurantiacum. Front. Cell. Infect. Microbiol. 11:761596. doi: 10.3389/fcimb.2021.761596

Multilocus Sequence Typing Reveals Extensive Genetic Diversity of the Emerging Fungal Pathogen *Scedosporium aurantiacum*

***Azian Harun*[1,2], *Alex Kan*[1], *Katharina Schwabenbauer*[1†], *Felix Gilgado*[1], *Haybrig Perdomo*[3], *Carolina Firacative*[1†], *Heidemarie Losert*[4], *Sarimah Abdullah*[2], *Sandrine Giraud*[5], *Josef Kaltseis*[6], *Mark Fraser*[7], *Walter Buzina*[8], *Michaela Lackner*[6], *Christopher C. Blyth*[1,9], *Ian Arthur*[10], *Johannes Rainer*[11], *José F. Cano Lira*[3], *Josep Guarro Artigas*[3], *Kathrin Tintelnot*[4], *Monica A. Slavin*[12], *Christopher H. Heath*[13], *Jean-Philippe Bouchara*[5], *Sharon C. A. Chen*[1,14] *and Wieland Meyer*[1*†]

[1] *Molecular Mycology Research Laboratory, Centre for Infectious Diseases and Microbiology, Faculty of Medicine and Health, Sydney Medical School, Westmead Clinical School, Sydney Institute for Infectious Diseases, Westmead Hospital-Research and Education Network, Westmead Institute for Medical Research, University of Sydney, Sydney, NSW, Australia,* [2] *School of Medical Sciences, Universiti Sains Malaysia, Kota Bharu, Malaysia,* [3] *Unitat de Microbiologia, Facultat de Medicina i Ciencies de la Salut, Universitat Rovira i Virgili, Reus, Spain,* [4] *FG 16 Mycology, Robert Koch Institute, Berlin, Germany,* [5] *UNIV Angers, Université de Bretagne Occidentale, Centre Hospitalier Universitaire (CHU) d'Angers, Groupe d'Etude des Interactions Hôte-Pathogène (GEIHP), EA3142, Structure Fédérative de Recherche "Interactions Cellulaires et Applications Thérapeutiques (SFR ICAT), Angers, France,* [6] *Institute of Hygiene and Microbiology, Medical University Innsbruck, Innsbruck, Austria,* [7] *UK National Mycology Reference Laboratory, National Infection Service, Public Health England South-West, Bristol, United Kingdom,* [8] *Institute of Hygiene, Microbiology and Environmental Medicine, Medical University, Graz, Austria,* [9] *Telethon Kids Institute and Medical School, University of Western Australia, Perth, WA, Australia,* [10] *Mycology Laboratory, Division of Microbiology and Infectious Diseases, PathWest Laboratory Medicine Western Australia, Perth, WA, Australia,* [11] *Institute of Microbiology, Leopold Franzens University Innsbruck, Innsbruck, Austria,* [12] *Peter MacCallum Cancer Centre and Sir Peter MacCallum Department of Oncology, Melbourne, VIC, Australia,* [13] *Department of Microbiology, PathWest Laboratory Medicine, Fiona Stanley Hospital, Murdoch; & Infectious Diseases Department, Fiona Stanley Hospital, Murdoch; Department of Microbiology & Infectious Diseases, Royal Perth Hospital, Perth; & the University of Western Australia, Perth, WA, Australia,* [14] *Center for Infectious Diseases and Microbiology Laboratory Services, Institute of Clinical Pathology and Medical Research, New South Wales Health Pathology, Sydney, NSW, Australia*

Scedosporium spp. are the second most prevalent filamentous fungi after *Aspergillus* spp. recovered from cystic fibrosis (CF) patients in various regions of the world. Although invasive infection is uncommon prior to lung transplantation, fungal colonization may be a risk factor for invasive disease with attendant high mortality post-transplantation. Abundant in the environment, *Scedosporium aurantiacum* has emerged as an important fungal pathogen in a range of clinical settings. To investigate the population genetic structure of *S. aurantiacum*, a MultiLocus Sequence Typing (MLST) scheme was developed, screening 24 genetic loci for polymorphisms on a tester strain set. The six most polymorphic loci were selected to form the *S. aurantiacum* MLST scheme: actin (*ACT*), calmodulin (*CAL*), elongation factor-1α (*EF1α*), RNA polymerase subunit II (*RPB2*), manganese superoxide dismutase (*SOD2*), and β-tubulin (*TUB*). Among 188 global

clinical, veterinary, and environmental strains, 5 to 18 variable sites per locus were revealed, resulting in 8 to 23 alleles per locus. MLST analysis observed a markedly high genetic diversity, reflected by 159 unique sequence types. Network analysis revealed a separation between Australian and non-Australian strains. Phylogenetic analysis showed two major clusters, indicating correlation with geographic origin. Linkage disequilibrium analysis revealed evidence of recombination. There was no clustering according to the source of the strains: clinical, veterinary, or environmental. The high diversity, especially amongst the Australian strains, suggests that *S. aurantiacum* may have originated within the Australian continent and was subsequently dispersed to other regions, as shown by the close phylogenetic relationships between some of the Australian sequence types and those found in other parts of the world. The MLST data are accessible at http://mlst.mycologylab.org. This is a joined publication of the ISHAM/ECMM working groups on "*Scedosporium/Pseudallescheria* Infections" and "Fungal Respiratory Infections in Cystic Fibrosis".

Keywords: *Scedosporium aurantiacum*, MLST (multilocus sequence typing), genotyping, geographical origins, ecological context, clinical association

INTRODUCTION

Fungi of the genera *Scedosporium* and *Lomentospora* are increasingly encountered as causes of invasive fungal infections (Cortez et al., 2008; Heath et al., 2009; Nakamura et al., 2013; Lass-Flörl and Cuenca-Estrella, 2017; Kondo et al., 2018; Ramirez-Garcia et al., 2018; Chen et al., 2021; Mizusawa et al., 2021). Moreover, these fungi are frequently associated with airway colonization, particularly in the context of abnormal airway function in chronic respiratory disease (Cortez et al., 2008; Pihet et al., 2009; Blyth et al., 2010; Zouhair et al., 2013; Schwarz et al., 2018). Infections due to *Scedosporium/Lomentospora* spp. are noteworthy due to their inherent resistance to most available antifungal agents (Gilgado et al., 2006; Troke et al., 2008; Lackner et al., 2014a; Rivero-Menendez et al., 2020). Recent taxonomic reassignments within these genera and the identification of new *Scedosporium* species/species complex (Guarro et al., 1999; Gilgado et al., 2005; Gilgado et al., 2008; Lackner et al., 2014b; Chen et al., 2016; Chen et al., 2021) have raised the need to gain better insight into the epidemiology of clinically relevant species.

Scedosporium aurantiacum has emerged as a pathogen with a relatively high prevalence in Australia and is often associated with chronic lung disease (Delhaes et al., 2008; Heath et al., 2009). *In vivo* experiments in mice showed that *S. aurantiacum* is as virulent as *Lomentospora prolificans* (former *Scedosporium prolificans*) (Harun et al., 2010b), and more virulent than the other members of the genus (Gilgado et al., 2009; Rodriguez et al., 2010). Further, *S. aurantiacum* was found to be highly abundant in the Australian environment (Harun et al., 2010a), although a specific association between its occurrence in the environment and the relatively high clinical incidence has not yet been explored. Given the emerging nature and the poor clinical outcomes generally associated with *Scedosporium/Lomentospora* spp. infections, a better understanding of the epidemiology and transmission is necessary to ensure effective therapeutic and preventative measures. Therefore, an investigation of the population genetic structure of this pathogen is crucial to enable a correlation between the observed genotype, source of isolation (clinical and environmental), virulence, antifungal susceptibility, and clinical outcome.

Several molecular typing techniques have been applied to isolates of the genera *Scedosporium* and *Lomentospora*, to detect genetic variation over time, to discriminate between strains and to identify possible sources of infection. Among those methods are: Random Amplified Polymorphic DNA (RAPD) analysis (Zouhair et al., 2001; Defontaine et al., 2002), Multi-Locus isoEnzyme Electrophoresis (MLEE) (Zouhair et al., 2001), Amplified Fragment Length Polymorphism (AFLP) (Delhaes et al., 2008), PCR fingerprinting (Rainer et al., 2000; Delhaes et al., 2008) and MultiLocus Sequence Typing (MLST) (Bernhard et al., 2013). However, many of these studies were conducted prior to the taxonomical resolution of the *Scedosporium boydii* species complex, with few data, if any, describing the genetic diversity within *S. aurantiacum*. MLST has been successfully applied to study the genetic diversity of medically important fungi, including *Candida albicans* (Bougnoux et al., 2002), *Candida glabrata* (Dodgson et al., 2003; Lott et al., 2010), *Candida tropicalis* (Tavanti et al., 2005), *Candida krusei* (Jacobsen et al., 2007), *Cryptococcus gattii* (Feng et al., 2008; Meyer et al., 2009; Carriconde et al., 2011), *Cryptococcus neoformans* var. *grubii* (Litvinseva et al., 2006), *Aspergillus fumigatus* (Bain et al., 2007), and *Fusarium solani* species complex (Debourgogne et al., 2010), but has only been applied to *Scedosporium apiospermum* and *S. boydii* (formerly *Pseudallescheria boydii*) within the genus *Scedosporium* (Bernhard et al., 2013). It has a strong advantage over other typing techniques, as it provides unambiguous data, allowing for inter-laboratory data comparisons, construction of large international, internet-accessible databases (www.mlst.net or http://mlst.mycologylab.org) (Maiden et al., 1998; Odds and

Jacobsen, 2008; Carriconde et al., 2011), and is only exceeded in its discriminatory power by whole genome sequencing, which is not yet feasible in most clinical mycology laboratories.

The current study describes the development of an MLST scheme specific for *S. aurantiacum* and its application to a global set of *S. aurantiacum* isolates. Partial sequences from six genetic loci, including: actin (*ACT*), calmodulin (*CAL*), elongation factor 1 alpha (*EF1α*), RNA polymerase II subunit (*RPB2*), superoxide dismutase (*SOD2*) and beta tubulin (*TUB*), were obtained from a population of 188 *S. aurantiacum* strains. Genetic relatedness between strains from different geographical origins, ecological contexts, and clinical associations were examined.

MATERIAL AND METHODS

Isolates

During the development phase, 12 *S. aurantiacum* strains were selected as tester strains from the Molecular Mycology Research Laboratory Culture Collection at Sydney Medical School - Westmead Hospital (as indicated by the strain numbers in bold and italics in **Supplementary Table S2**). These strains were selected to represent diverse geographic regions, had known clinical associations, and known genetic characteristics (identical and diverse genotypes) as established by PCR fingerprinting and AFLP analysis (Delhaes et al., 2008). In the application phase, the developed scheme was applied to a total of 188 strains that comprised 106 clinical, 1 veterinary and 81 environmental strains. Details of these strains are provided in **Supplementary Table S2**. Most of strains originated from Australia (n = 84), followed by France (n = 48), Austria (n = 15), Germany (n = 13), Spain (n = 5), New Zealand (n = 4), the UK (n = 3), Nepal (n = 2), Thailand (n = 2), Ireland (n = 1), and the USA (n = 1). All isolates were grown on Sabouraud dextrose agar (Oxoid, Hampshire, UK) and incubated at 30°C for 5 to 7 days before DNA extraction.

DNA Extraction

Extraction of genomic DNA was performed according to a previously published protocol (Ferrer et al., 2001), with minor modification. The mycelia from 5-day-old cultures were harvested and placed in 1.5 ml tubes. After washing in deionized water, mycelia were frozen in liquid nitrogen. Using a sterile miniature pestle, frozen mycelia were finely ground to disrupt the fungal cell walls; 500 µl of SDS lysis buffer and 5 µl of 2-mercaptoethanol were then added and the mixture was mixed vigorously by vortexing. After incubation at 65°C for 1 hour, with 2-3 times vortexing in between, 500 µl of phenol:chloroform: isoamyl alcohol (25:24:1) (Sigma, St. Louis, USA) were added. The tubes were flipped for 2 minutes to ensure thorough mixing, followed by centrifugation at 14,000 rpm for 15 minutes. DNA from the aqueous phase was transferred to a fresh 1.5 ml tube. An equal amount of isopropanol (Merck, Kilsyth, Australia) was then added to precipitate the DNA. The tubes were then incubated at - 20°C for a minimum of 1 hour but usually overnight to increase DNA yield. The precipitated DNA was pelleted by centrifugation at 14,000 rpm for 15 minutes. After washing with 500 µl 70% ethanol (Merck) and centrifugation, the DNA pellet was dried at room temperature and reconstituted in 100 µl of sterile distilled water. DNA concentration was determined spectrophotometrically.

Selection of Candidate Loci

In the preliminary development stage, 24 gene loci, namely *AAT, ACT, ANXC4, ATP6, BGT, BT2, EF1a, CAL, CAT, CHS, D1D2, FKS, LIP, GLN, IGS, MDH1, mtSSU, MP1, RPB1, RPB2, SOD2, TUB, VPS13* and *ZRF*, were amplified from the 12 tester strains (see above) to identify the most polymorphic loci. These loci had been previously utilized in either phylogenetic and/or genotyping studies of other Scedosporium species and/or other fungi, such as Candida, Aspergillus and Penicillium species (O'Donnell et al., 1998; Liu et al., 1999; Bougnoux et al., 2002; Cruse et al., 2002; Dodgson et al., 2003; Gilgado et al., 2005; Bain et al., 2007; Hoffman et al., 2007). For each genetic locus, the 12 sequences obtained from the tester strains were aligned using BioEdit™ Sequence Alignment Editor (Tom Hall, Carlsbad, USA) to determine the sequence variation. The genetic loci, which demonstrated a high polymorphism and yielded the largest number of sequence types in combination, were selected to form the new S. aurantiacum MLST scheme.

Primer Design

Twenty-four loci were selected for initial screening of genetic polymorphisms (see above). For the PCR amplification of these loci, primers were used as previously published except for *SOD2* for which primers were specifically designed in the current study (O'Donnell et al., 1998; Liu et al., 1999; Bougnoux et al., 2002; Cruse et al., 2002; Dodgson et al., 2003; Gilgado et al., 2005; Bain et al., 2007; Hoffman et al., 2007) (**Supplementary Table S1**). Partial or full *SOD2* gene sequences were obtained from the GenBank database (http://www.ncbi.nlm.nih.gov). Sequences from as many fungal genera as possible for *SOD2* were downloaded and then aligned using the program BioEdit™ Sequence Alignment Editor. Initial primers for *SOD2* were designed based on the aligned sequences. Following the initial amplification and selection of the six most polymorphic loci, *S. aurantiacum* specific primers were subsequently designed for those loci (**Table 1**) based on the obtained sequences and on the nucleotide sequence of these loci identified *via* BLAST searches in the draft genome of *S. aurantiacum* strain WM 09.24 (available in the DDBJ/EMBL/GenBank under the accession number JUDQ00000000) (Pérez-Bercoff et al., 2015).

Amplification and DNA Sequencing

PCR amplifications were performed in a total volume of 50 µl. Generally, each reaction mixture contained: 1x PCR buffer (20 mM Tris-HCl, 50 mM KCl), 1.5-2.5 mM $MgCl_2$, 100-200 µM of each deoxyribonucleotide triphosphate (dATP, dCTP, dGTP, dTTP) (Invitrogen, Carlsbad, USA), 0.2-0.4 mM each of forward and reverse primer, and 1.25 U of DNA polymerase (Bioline™, London, UK). 20-60 ng of template DNA was added to the reaction mixture. Sterile distilled water in place of DNA was used as a negative control. The primer sequences used in the

TABLE 1 | Selected gene loci, primer sequences and annealing temperatures used in the consensus MLST scheme for *Scedosporium aurantiacum* strain typing.

Locus	Coded protein	Sequence 5'-3'	Annealing temperature (°C)	Product length (bp)	Targeted allele length (bp)
ACT	Actin	ACT-Sau-F: CTCCTGCTTGGAGATCCACAT ACT-Sau-R: TCTCCGCTACCCTATCGAGC	60	998	830
CAL	Calmodulin	CAL-Sau-F: TCTACGTTCGCACGCTAAACT CAL-Sau-R: GGAGGAGGGACGCTACTTTTG	58	837	689
EF1	Elongation factor 1-alpha	EF1-Sau-F: CAGCCTGGGAGGTACCAGTAAT EF1-Sau-R: AGCGCCTGGATGAGCCAATG	62	859	715
RPB2	RNA polymerase II subunit	RPB2-Sau-F: AGTGTTACGCGGGGACTAAA RPB2-Sau-R: TGATCGTGATCACTTCGGCAA	62	1214	952
SOD2	Manganese superoxide dismutase	SOD2-Sau-F: GCCCTACATTAGCGCCAAGA SOD2-Sau-R: TTGCGGTTCTCGTACTGGAG	60	584	437
TUB	Beta-tubulin	TUB-Sau-F: CTGTCTCACCCCTCGTACGGTGACCTCAAC TUB-Sau-R: GCCCTCGCTAGTGTACCAATGCAAGAAAGC	68	676	401

development phase are listed in **Supplementary Table S1** and for the final consensus MLST scheme in **Table 1**. Initial PCR amplifications were performed in a thermal cycler (Perkin Elmer Cetus, Norwalk, USA) under the following conditions: an initial denaturation at 94°C for 5-10 minutes, followed by 35 cycles of 94°C for 45 seconds at a temperature ranging from 50-60°C for annealing depending on the amplified genetic loci (see **Supplementary Table S1**), followed by an extension step 1 min at 72°C and a denaturation step of 45 seconds at 94°C, with a final extension step at 72°C for 10 min. Optimized annealing temperatures for the primer sets used in the final MLST scheme are as listed in **Table 1**. PCR products were separated on 1.4% agarose gels in Tris-borate-EDTA (TBE) buffer, stained with ethidium bromide (Sigma) and visualized by UV transillumination. The products were purified using PureLink™ PCR Purification Kit (Invitrogen) following the manufacturers protocol and the concentration of purified DNA was measured spectrophotometrically. DNA sequencing was performed by Macrogen Inc., Seoul, Korea (http://www.macrogen.co.kr/eng/sequencing), and the Australian Genome Research Facility (AGRF) Pty. Ltd., St. Lucia, Queensland, Australia (http://www.agrf.org.au). The quality of nucleotide sequences was verified by aligning both forward and reverse strands using the software Sequencher™ 5.4 (Gene Codes Corp., Ann Arbor, USA).

Sequence Data Analysis

During the development phase, the consensus sequences of the 12 selected strains were aligned for each genetic locus. The genetic loci that were most polymorphic were selected for inclusion in the final *S. aurantiacum* MLST scheme. In the application phase, all obtained sequences from the 188 strains were aligned and analyzed. Sequence alignments were performed using BioEdit™ Sequence Alignment Editor. For each locus, numbers were assigned to designate unique allelic variants, with a single bp difference resulting in a new allele type. These numbers were subsequently combined to yield unique sequence types (see **Supplementary Table S2**). A *S. aurantiacum* MLST database using the BioloMICS software version 21.07.9.324 (BioAware, Hannut, Belgium) was constructed for the six loci at the Molecular Mycology Research Laboratory and can be accessed at http://mlst.mycologylab.org. GenBank accession numbers for all MLST sequences generated in this study are listed in **Supplementary Table S3**. All allele and sequence types can be accessed *via* the specific MLST *S. aurantiacum* website at http://mlst.mycologylab.org. Phylogenetic trees were constructed using the software MEGA version 11 (The Biodesign Institute, Tempe, USA) (Tamura et al., 2021). To further investigate the geographical relationship between genotypes, a goeBURST minimum spanning tree was generated from the aligned concatenated sequences of the strains studied using the PHYLOViZ 2.0 analysis software (http://www.phyloviz.net/).

Test for Selective Pressure, Variability, and Neutrality

Assessment of the likelihood of selective pressure at each locus was estimated by the ratio of non-synonymous to synonymous nucleotide substitutions (d_N/d_S) (Nei and Gojobori, 1986). To test for purifying selection the codon-based Z-test using evolutionary pathway by Nei and Gojobori was performed (Nei and Gojobori, 1986) using MEGA version 11 (Tamura et al., 2021). To evaluate the variability of the selected loci, the haplotype diversity (*Hd*), nucleotide diversity (π) and the average number of nucleotide differences (k) were determined using the software DNA Sequence Polymorphism DnaSP version 6.12.03 (Rozas et al., 2017). Testing for neutrality utilizing the Tajima's D test (equal to zero at neutral equilibrium) (Tajima, 1989) was performed in MEGA version 11 (Tamura et al., 2021).

Test for Recombination and Linkage Disequilibrium

Intragenic linkage disequilibrium (LD), and intragenic recombination rates were calculated by using DNA Sequence Polymorphism DnaSP version 6.12.03 (Rozas et al., 2017). Evidence of recombination was shown using the 4-gamete test to infer the minimum number of recombination events (Rm).

Associations of Clinical Variables With Sequence Type or Clusters

Patients' demographic and clinical data were recorded. Associations between genotypes and clinical variables were

explored. The variables examined included age, sex, and geographical origin, source of isolates, infection status and predisposing factors (**Supplementary Table S2**). We investigated potential associations between sequence type and the variables using Pearson Chi Square test. Statistical analysis was performed using PASW Statistics 18 (SPSS Inc., Chicago, IL, USA) and STATA 15 (StataCorp LP, College Station, USA). *P*-values of <0.05 were considered statistically significant.

Virulence Study

Virulence studies based upon *in vivo* survival in a murine model (Harun et al., 2010b) were performed. Eighteen strains listed in **Supplementary Table S2** (indicated by underlined strain numbers) and in **Figure 4** were selected to represent a wide global spectrum. Five seven-week-old female Balb/C mice were used, in which 0.2 ml of a conidial suspension (10^6 conidia/ml) was inoculated intravenously *via* the lateral tail vein. The mice were monitored daily till 30 days post-inoculation for signs of infection, including ruffling of fur, inactivity, loss of weight, difficulty in breathing, and neurological signs such as ataxia. In accordance with the protocol approved by Western Sydney Local Health District Animal Ethics Committee (WSLHD AEC), mice that were deteriorating prior to that end point were sacrificed. Mean survival time (MST), estimated by Kaplan-Meier method, was used as a parameter to compare the relative pathogenicity among the selected strains. Comparison between each group was performed by the log-rank test as part of the software package PASW Statistics 18. Graphs were plotted using GraphPad Prism version 5.0b (GraphPad Software Inc., San Diego, USA). *P*-values of < 0.05 was considered as statistically significant.

RESULTS

Selection of Genes for the *S. aurantiacum* MLST Scheme

DNA sequences of 24 genetic loci (*AAT, ACT, ANXC4, ATP6, BGT, BT2, EF1a, CAL, CAT, CHS, D1D2, FKS, LIP, GLN, IGS, MDH1, mtSSU, MP1, RPB1, RPB2, SOD2, TUB, VPS13*, and *ZRF*,) (**Supplementary Table S1**) were screened to assess their polymorphisms and hence suitability as candidate genetic loci for the S. aurantiacum MLST scheme. Following analysis of the DNA sequences obtained from 12 tester strains, the following six loci, actin (*ACT*), calmodulin (*CAL*), elongation factor 1-alpha (*EF1a*), RNA polymerase II subunit (*RPB2*), manganese superoxide dismutase (*SOD2*) and beta tubulin (*TUB*), were found to be the most variable, and were therefore selected to form the S. aurantiacum MLST scheme (http://mlst.mycologylab.org) (**Table 1**), and to identify the allele and sequence types of S. aurantiacum strains.

Sequence Variability

The sizes of the six MLST gene fragments obtained including all gaps were: 830 bp for the *ACT* locus, 689 bp for the *CAL* locus, 715 bp for the *EF1α* locus, 952 bp for the *RPB2* locus, 437 bp for the *SOD2* locus and 401 bp for the *TUB* locus (**Table 2**). Seventy-seven (1.89%) polymorphic sites were identified across all six genes combined, which represents a total of 4,024 bp. The number of variable nucleotide sites per locus ranged between 5 (0.73%, *CAL*) and 18 (4.12%, *SOD2*). The variability among loci is shown in **Table 2**.

Test for Selective Pressure, Variability, and Neutrality

The ratio of non-synonymous to synonymous nucleotide substitutions (d_N/d_S) was < 1 for five of the six MLST loci studied (**Table 2**). In all loci, the probability (p value was > 0.05 and therefore the null hypothesis of strict neutrality (*dN=dS*) was not rejected. All but one locus showed an *dN-dS* of negative value (*dN<dS*, *dN/dS* ratio of <1), thus indicating that with exception to *SOD2* none of the studied loci were under positive selective pressure (**Table 2**). The nucleotide diversity (π) ranged from 0.00196 for *CAL* to 0.01335 for *SOD2*, the haplotype diversity (*Hd*) ranged from 0.582 for *TUB* to 0.864 for *RPB2*, and the average number of nucleotide differences (k) ranged from 1.35305 for *CAL* to 5.78177 for *SOD2*, indicating an equal range for all loci, except for *SOD2* (**Table 2**). In the neutrality test, none of the Tajima's D values obtained for the studied loci deviated significantly from zero, except for *SOD2*, suggesting the occurrence of balancing selection (Tajima, 1989) (**Table 2**).

TABLE 2 | Neutrality and genetic variability tests performed on each MLST locus.

Locus	No. of alleles	Length (bp)	Total Number of Sites[1]	No. of polymorphic sites (SNP)	No. of Haplotypes	*dN-dS*	d_N/d_S[2]	Nucleotide Diversity (π)	Haplotype Diversity (*Hd*)	Average no. of nucleotide differences (k)	Tajima's D[3]	Tajima's D (P-value)
ACT	22	830	824	12	12	-0.98	<1	0.00367	0.853	3.02401	0.87646	>0.10
CAL	8	689	689	5	8	-0.39	<1	0.00196	0.702	1.35305	0.63566	>0.10
EF1a	23	715	681	13	12	-0.12	<1	0.00277	0.695	1.88838	-0.54682	>0.10
RPB2	15	952	952	18	15	-3.62	<1	0.00518	0.864	4.93145	1.56775	>0.10
SOD2	18	437	433	18	16	0.81	>1	0.01335	0.770	5.78177	2.29468	<0.05
TUB	12	401	393	11	11	-0.93	<1	0.00517	0.582	2.03089	0.17512	>0.10
Concatenated	159 (ST)	4024	3972	77	149			0.00471	0.9965	18.67192	1.31347	>0.10

[1]*Excluding sites with gaps/missing data.*

[2]*Non synonymous-synonymous substitutions ratio determined as described by Nei and Gojobori (1986) in MEGA version 11 (Tamura et al., 2021).*

[3]*Tajima's test for neutrality (Tajima, 1989).*

Recombination and Linkage Disequilibrium

The intragenic recombination test identified 1-4 recombination events (Rm) at the *ACT, EF1a, RPB2, SOD2*, and *TUB* loci, but no recombination at the *CAL* locus (**Table 3**). Based on the concatenated multilocus sequence data, the interlocus LD was assessed over all segregating sites using pairwise comparisons. The LD (|D′| Y = 0.8257–0.0970X) was detected with a negative slope, indicating a decrease in linkage with increased nucleotide distance. Of the 2556 pairwise comparisons, 798 were significant by the Fisher exact test, and 229 were significant after Bonferroni correction (**Table 3**).

Alleles and Sequence Type Distributions

The sequence alignments showed polymorphisms in all six loci denoting the presence of different alleles (**Table 2**). Each specific sequence was considered a unique allele type, which was then assigned a unique allele type number. For example, 22 alleles were defined for the *ACT* locus, which were assigned as allele types AT1 to AT22, accordingly. The *CAL* locus showed 8 alleles, the *EF1α* locus 23 alleles, the *RPB2* locus 15 alleles, the *SOD2* locus 18 alleles and the *TUB* locus 12 alleles (**Table 2**). A total of 159 sequence types were obtained by combining the allele types of the six MLST loci studied (**Supplementary Table S2**). Most of the strains exhibited unique sequence types (**Supplementary Table S2** and **Figures 2**, **3**). Only a few strains shared the same sequence type, but most of them originated from the same patient or from closely linked soil samples. For example, strains IHEM 23081 and IHEM 23092, which both exhibited the sequence type ST140, were recovered from respiratory secretions of the same patient at a one-year interval; likewise, six strains shared the sequence type ST108, *i.e.* 110349103-01/1, 110349103-01/2 and 110349103-01/3, as well as 110349211-01/1, 110349103-01/2 and 110349103/3, but they were recovered from two soil samples collected at the same location on the banks of the Loire river, in France. On the contrary, strains IHEM 23080 and IHEM 23081, which were recovered from the same clinical sample, exhibited distinct sequence types (ST 139 and ST140, respectively).

Distribution of Sequence Types According to Geographical Origin

Figure 1 shows the distribution of sequence types according to the geographical origin. 69 of the 159 (43%) sequence types were only found in Australia, but none of them were predominant. Most of the Australian strains were obtained from New South Wales (NSW), suggesting a possible study bias. Among the 61 studied strains from NSW, 49 different sequence types were identified, most being specifically identified from this state since only two of these sequence types were also found outside NSW (ST12 and ST15, which were also found in Western Australia (WA)). Twenty strains collected in WA were studied, which revealed 19 sequence types, 17 of them being specifically identified from WA. ST26 and ST27 were found only in South Australia (SA), and ST28 was found only in Queensland (QLD) (**Figure 1** and **Supplementary Table S2**). The sequence types ST39, ST40, ST41 and ST42 were found exclusively in New Zealand.

Ninety-five strains collected in Europe were analyzed in this study. MLST analysis of these strains revealed a total number of 81 sequence types. Almost all of them were country specific, with the highest number of sequence types (39 STs) being found in France (**Figure 1** and **Supplementary Table S2**). A unique sequence type was identified from two distinct countries, *i.e.* the sequence type ST82, which was isolated from both Germany and Austria, with no obvious connection of the patients to each other.

Other sequence types obtained in this study include ST55, which was unique to the United States, ST99 and ST100, which were specific to Thailand, and ST105 and ST106, which were found in Nepal (**Figure 1** and **Supplementary Table S2**).

Phylogenetic Relationships Among *S. aurantiacum* Strains

Parsimonious trees were constructed for each MLST locus (**Supplementary Figures S1**–**S6**). These analyses resulted in

TABLE 3 | Pairwise interlocus linkage disequilibrium and recombination analysis of concatenated multilocus sequences from 188 *Scedosporium aurantiacum* strains.

Population	No. segregating sites analysed	No. pairwise comparisons	No. of pairs of sites with four gametic types	No. of significant pairwise comparisons†	Z_nS*	Linkage disequilibrium (LD) value|D'|	Estimate of R/gene	Minimum no. recombination events (Rm)
All**	74	2556	1181	798 (229)	0.0505	Y = 0.8257 - 0.0970X	59.4	17
ACT	12	55	3	35 (23)	0.1585	Y = 1.0310 - 0.2161X	16	1
CAL	5	6	0	2 (2)	0.0337	Y = 1.0000 - 0.0000X	117	0
EF1a	13	66	6	18 (10)	0.0772	Y = 0.9131 + 0.2146X	4.6	2
RPB2	18	153	19	99 (71)	0.1571	Y = 0.9738 - 0.0082X	22.3	3
SOD2	18	153	30	97 (67)	0.2231	Y = 1.0359 - 0.5977X	5.5	4
TUB	11	55	4	12 (9)	0.1318	Y = 1.0016 - 0.1617X	0.8	1

†*By Fisher's exact test (after Bonferroni correction).*

**Z_nS, interlocus genetic association; |D'|, linkage disequilibrium (LD) value, where Y is LD value and X is nucleotide distance in kilobases.*

***Based on concatenated multilocus gene sequence of all loci.*

different tree topologies, indicating variable rates of gene evolution for each genetic locus (**Supplementary Figures S1–S6**).

Maximum parsimony analysis of the combined gene sequences obtained from the six loci studied revealed a high genetic diversity amongst the 188 *S. aurantiacum* strains investigated (**Figure 2**), with most strains forming unique sequence types, which resulted in the widespread topology of the combined tree (**Figure 2** and **Supplementary Table S2**). Sequence types of the strains from different Australian states demonstrated no tendency to group with each other. When comparing the two major clusters (**Figure 2**), there was a significant difference according to the geographic origin of the strains ($p < 0.0005$). Most Australian strains belonged to cluster 2, while almost all European strains, except one German strain RKI94-0197, were grouped together in cluster 1 (**Figure 2**). The four isolates from New Zealand grouped either basal to cluster 1, which may be called 'global cluster' (WM 07.96, WM 07.97) or to cluster 2, the 'Australian cluster' (WM 07.101, WM 07.108) (**Figure 2**). In between the two major clusters the central basal group contains strains from Australia, Austria, France, Germany, Ireland, Netherlands, Spain, and the United Kingdom.

The goeBURST analysis of the obtained MLST data confirmed the high genetic diversity seen in the Australian *S. aurantiacum* population, as well as in the non-Australian population (**Figure 3**). Most of the Australian strains grouped separate to the European strains, forming a closely connected gene network. However, a subset of Australian strains was intermixed with and are closely related to the global strains, indicating certain genetic links between Australian and non-Australian strains (**Figure 3**). The results of the goeBURST analysis (**Figure 3**) confirmed the genetic relationships identified in the phylogenetic analysis of the combined genes as reflected in the concatenated gene tree (**Figures 2**, **3**).

Both clinical and environmental strains were widely distributed throughout the tree showing no sequence types to be indicative of a human clinical, veterinary, or environmental origin. Similar findings were found for the distribution of strains recovered from patients with either "invasive" disease or "colonization" (hereafter referred to as "invasive" or "colonizing" strains) (**Figure 2**).

Association Between Genotype and Clinical Variables

Overall, the statistical analyses (PASW Statistics and STATA II) performed showed no significant associations between the different sequence types, which occurred largely as singletons, and clinical variables. In addition, there were no significant

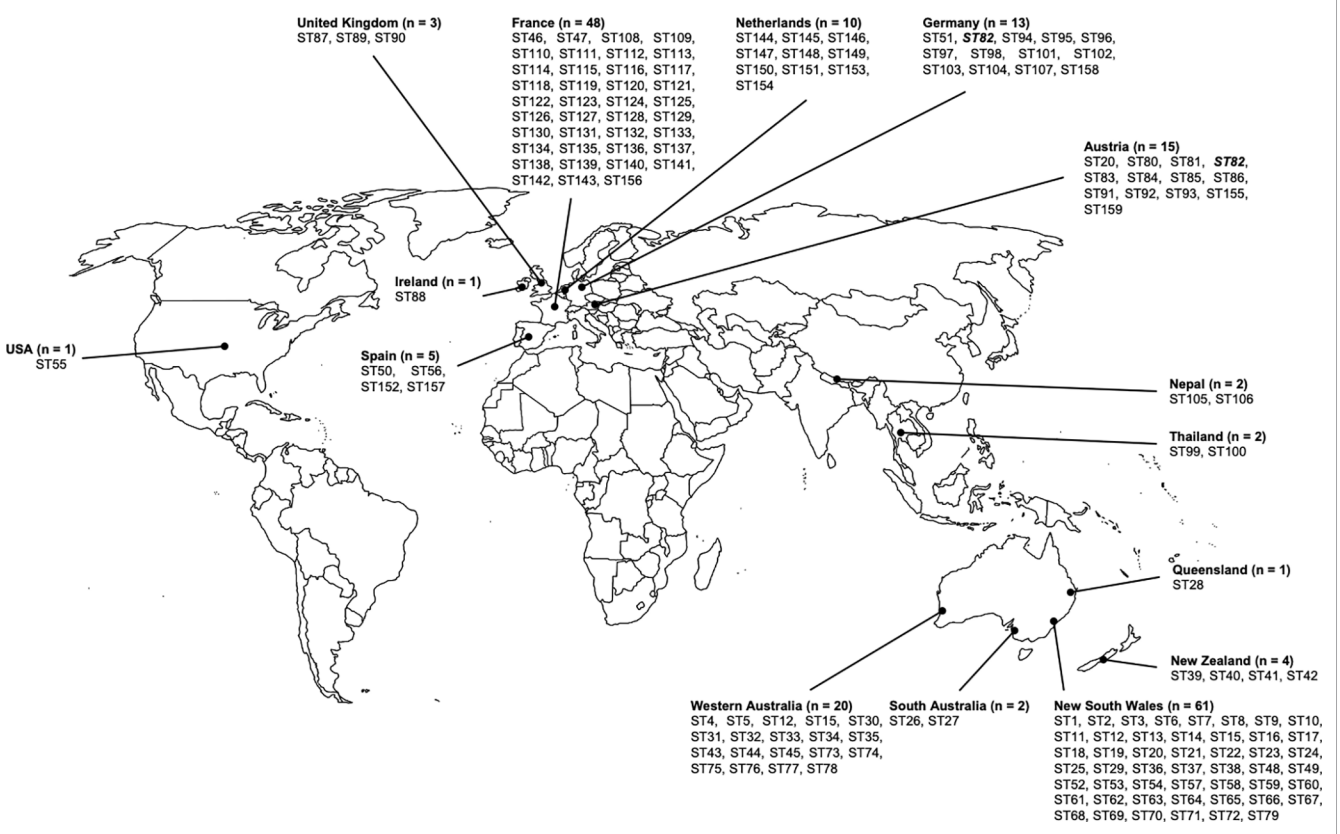

FIGURE 1 | Geographic distribution of *Scedoporium aurantiacum* isolates. Distribution of studied *Scedosporium aurantiacum* isolates and their identified sequence types within Australia, New Zealand, Asia, Europe, and United States. ST's in bold and italics are the only ST shared between two countries.

associations between a particular cluster and patient age (p = 0.078), sex (p = 0.076) or infection site (p > 0.05). Most analyzed strains were recovered from respiratory secretions from patients with chronic lung disease, such as cystic fibrosis; these strains that colonized the airways, were distributed throughout both clusters. There was only a single sequence type which was shared between colonizing and invasive strains, ST15, with WM 06.476 and WM 07.555 being colonizing strains, and WM 07.452 being an invasive strain.

When the two major clusters were compared with the patients predisposing factors (e.g., chronic lung disease, malignancy, diabetes, corticosteroid administration, chemotherapy, trauma, and drowning), there was no association between predisposing factors and any particular cluster (p > 0.05). An exception was a correlation of certain clusters and chronic lung disease, which was noted to show a significant difference (p = 0.005). In the "global cluster" there was a group of colonizing strains including WM 08.2114 and WM 08.215 (both ST53), WM 06.571 (ST37), 10-03-12 (ST149) and 10.03.10.92 (ST154), whereas the "Australian cluster" comprised another group of colonizing strains composed of WM 06.481, WM 08.209, and WM 06.480 (all ST17), WM 06.546, WM 08.210, and WM 08.211 (all ST52), WM 06.492 (ST21) and WM 06.479 (ST16) (**Figure 2**).

Association Between Genotypes and Virulence in a Mouse Model

The results of the survival analysis in mice, expressed as percent survival, for 18 *S. aurantiacum* strains are shown in **Figure 4**. All infected mice showed evidence of active infection (ruffling of fur, severe weight loss and neurological abnormalities, such as ataxia), as early as day 3 post-inoculation (**Figure 4**). An overall comparison between survival curves showed a significant difference (p = 0.007), with WM 06.482 being the most virulent strains followed by WM 09.24 and WM 08.52, and strains WM 08.269 and WM 08.202 being the least virulent strains. Of note, pairwise comparisons among all tested strains showed variable results. Pairwise comparison between invasive and colonizing strains, and between clinical and environmental strains revealed no significant difference.

DISCUSSION

MLST analysis, which allows for the accurate identification of discrete alleles for each analyzed locus, is a highly discriminatory tool for determining genetic variability between microbial strains (Bougnoux et al., 2002; Dodgson et al., 2003; Tavanti et al., 2005; Litvinseva et al., 2006; Bain et al., 2007; Jacobsen et al., 2007; Feng et al., 2008; Meyer et al., 2009; Debourgogne et al., 2010; Carriconde et al., 2011; Bernhard et al., 2013). The developed MLST scheme mirrors many MLST schemes for bacteria and fungi, which employed similar numbers of genetic loci (Maiden et al., 1998; Bougnoux et al., 2002; Dodgson et al., 2003; Tavanti et al., 2005; Litvinseva et al., 2006; Bain et al., 2007; Jacobsen et al., 2007; Feng et al., 2008; Odds and Jacobsen, 2008; Meyer et al., 2009; Debourgogne et al., 2010; Carriconde et al., 2011). In the

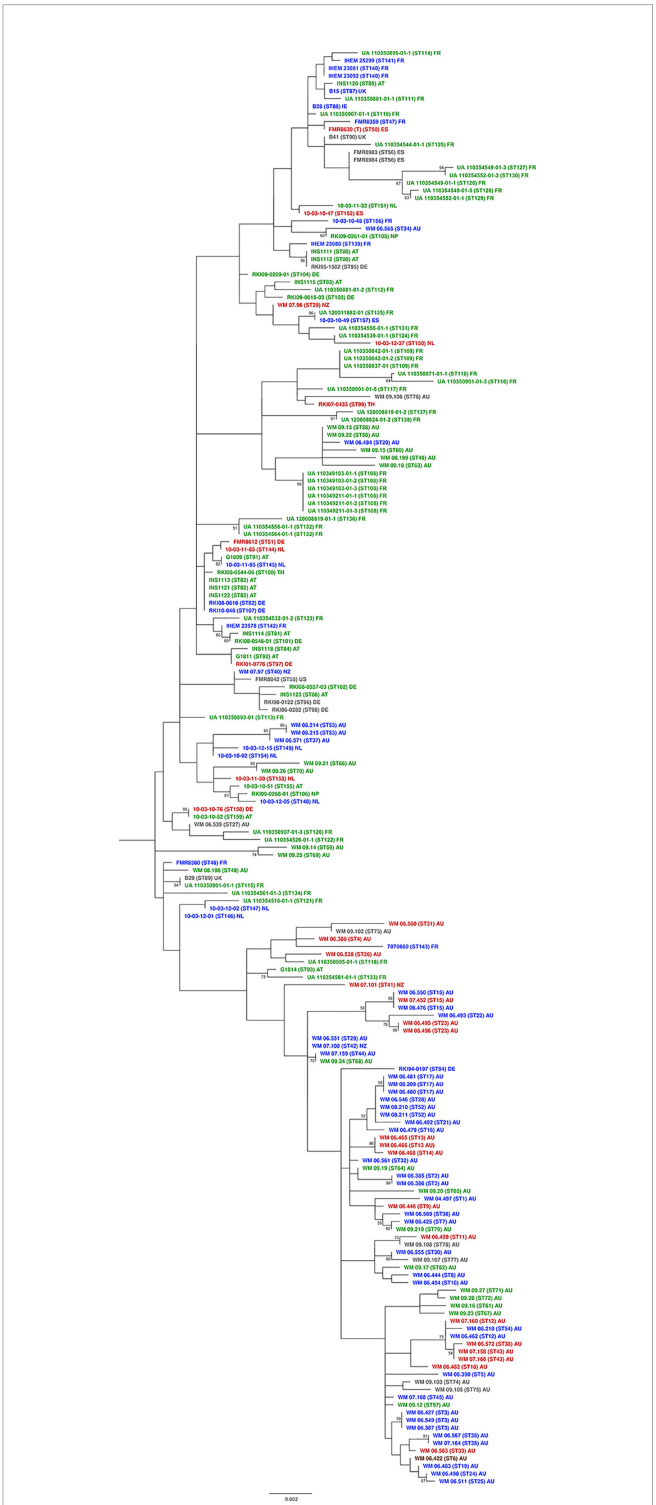

FIGURE 2 | MLST maximum parsimony tree. Combined maximum parsimony tree for the six MLST loci (*ACT*, *CAL*, *EF1α*, *RPB2*, *SOD2* and *TUB*) generated from all obtained *Scedosporium aurantiacum* sequences using the program MEGA version 11. Environmental isolates (green), clinical invasive isolates (red), clinical colonizing isolates (blue), clinical isolates without information (grey), and veterinary isolates (brown). AT, Austria; AU, Australia; DE, Germany; ES, Spain; FR, France; UK, United Kingdom; IE, Ireland; NL, The Netherlands; NP, Nepal; NZ, New Zealand; TH, Thailand; and US, USA.

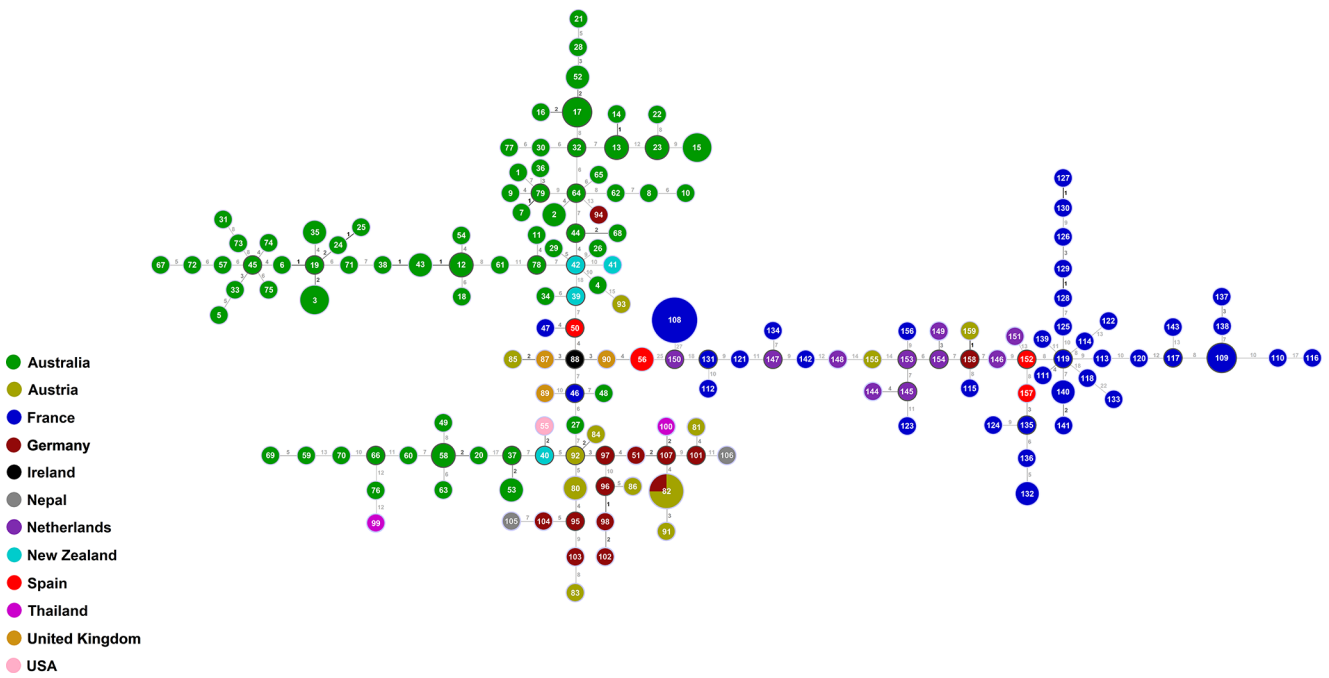

FIGURE 3 | goeBURST minimum spanning tree for all 159 sequence types obtained from the combination of all allele types of the six MLST loci (*ACT*, *CAL*, *EF1α*, *RPB2*, *SOD2* and *TUB*) using the PHYLOViZ 2.0 analysis software, indicating the genetic relationships between all Australian and non-Australian *S. aurantiacum* isolates studied.

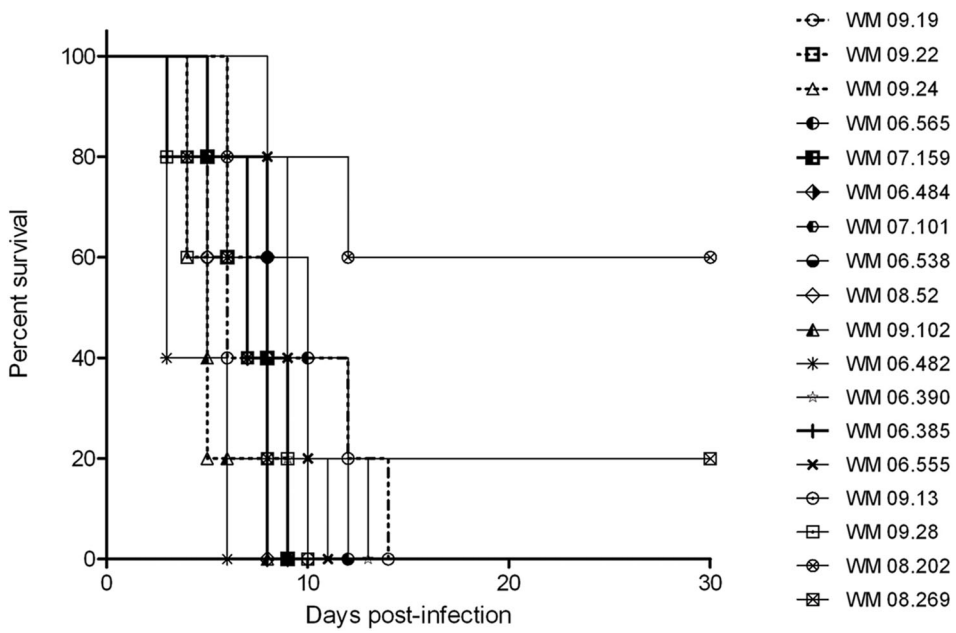

FIGURE 4 | Animal virulence study. Survival plots of mice infected with selected *Scedosporium aurantiacum* strains. Environmental strains: WM 09.13 WM 09.19, WM 09.22, WM 09.24, and WM 09.28; Invasive clinical strains: WM 06.482, WM 06.538, WM 07.101, WM 08.202; Colonizing clinical strains: WM 06.385, WM 06.390, WM 06.484, WM 06.555, WM 06.565, WM 07.159, WM 08.52; and clinical strains without information on infection status: WM 08.269, WM 09.102.

present study, we applied a six-locus MLST approach to differentiate between *S. aurantiacum* strains with a high discrimination rate and for the first time to delineate the genetic variation amongst Australian *S. aurantiacum* strains in the context of a global strain population. Contrary to previous studies (Maiden et al., 1998; Odds and Jacobsen, 2008), the use of additional loci did not improve the resolution.

The herein newly developed MLST scheme, using six unrelated housekeeping genes (*ACT, CAL, EF1a, RPB2, SOD2* and *TUB*), was applied to investigate the population genetic structure of 188 environmental, clinical, and veterinary *S. aurantiacum* strains, mainly originating from Australia and Europe, together with a small number of North American, New Zealand and Asian strains. The MLST analysis revealed between 5-18 variable sites and 8-23 defined alleles per locus studied. Statistical analysis of the obtained dataset showed that the selected loci are suitable for a discriminatory *S. aurantiacum* MLST scheme (**Tables 2**, **3**). The ratio of non-synonymous to synonymous substitutions (d_N/d_S) was shown to be < 1 for five of the six loci, *i.e. ACT, CAL, EF1α*, *RPB2*, and *TUB*, indicating that these loci are not evolving under positive selection pressure (**Table 2**). Whilst a d_N/d_S value of > 1 was calculated for the *SOD2* locus, suggesting a positive selection pressure (**Table 2**), but the high number of polymorphic sites still warrants its inclusion in the new MLST scheme. The Tajima's neutrality test demonstrated that five of the six genetic loci are not undergoing positive selection, except *SOD2*, suggesting that it is maybe going through balancing selection. The purpose of this test is to distinguish between a DNA sequence evolving randomly ("neutrally") and a sequence evolving under non-random processes, including directional selection, or balancing selection, demographic expansion or contraction, genetic hitchhiking, or introgression. Randomly evolving DNA sequences contain mutations with no effect on the fitness and survival of an organism. The randomly evolving mutations are called "neutral", while mutations under selection are "non-neutral" (Perez-Losada et al., 2006). Indeed, the obtained statistical result is an important finding since genes that are under selective pressure or diversifying selection, may exhibit highly polymorphic nucleotides and hence genetic variability that may possibly result in a false inference of the population structure of the organism studied. However, the nucleotide diversity (π) and the haplotype diversity (*Hd*) obtained for *SOD2*, as well as the obtained number of haplotypes, do still lay within the range of the other loci, warranting the inclusion of this locus in the new MLST scheme. The statistical values obtained for the five other MLST loci and the combined analysis of the concatenated sequences of all six loci, confirmed that the polymorphism identified for each of the loci included in the *S. aurantiacum* MLST scheme, resulting in a very high genetic diversity among the investigated strains, is not attributable to inappropriately selected MLST loci. The minimum number of recombination events and LD decay support evidence of genetic recombination, rather than clonal reproduction amongst the investigated strains. This is further supported by the nucleotide diversity (π), the relative high haplotype diversity (*Hd*), and the average number of nucleotide differences (k), showing that all loci contribute to the detection of the large number of polymorphic sites, 77 amongst the concatenated sequences of all six loci, manifested in the high genetic diversity of the studied *S. aurantiacum* population (**Table 2**). This is further supported by the derivation of 149 unique sequence types amongst 159 of the 188 strains. A similar method has been applied to evaluate recombination and linkage disequilibrium in other multilocus studies (Brown et al., 2004; Uraiwan et al., 2007).

In general, individual sequence analysis of each locus revealed a relatively low number of different allele types, and individual analysis of the selected loci resulted in contradicting gene topologies (**Supplementary Figures S1–S6**). This is not uncommon, as each of the genes evolves at different evolutionary rates (Rokas et al., 2003a; Rokas et al., 2003b; Planet, 2005). Datasets composed of multiple genes may have different histories and incongruence can be explained by genuine differences in the evolutionary process (Planet, 2005). As observed in the current study, the genetic variability may differ from one locus to another, with some loci demonstrating a higher polymorphism than others. Data presented show clearly, that the allele types for most of the genetic loci differ according to their geographic origin. Most allele types seen in Europe were rarely seen in Australia (**Supplementary Table S2**).

The combination of all six MLST loci resulted in a high discriminatory power, and consequently nearly all isolates investigated showed an individual sequence type. The phylogenetic analysis of the obtained sequences showed a very high genetic diversity in the Australian and non-Australian *S. aurantiacum* populations (**Figures 2**, **3**), with a total of 159 sequence types being derived from 188 strains studied (**Supplementary Table S2**). Further, strains originating from the same country likewise demonstrated substantial genetic variability (**Figures 1–3** and **Supplementary Table S2**). Possible explanations for this observation are, that the *S. aurantiacum* population is still undergoing active recombination as indicated by the incongruent topologies of the obtained individual gene trees (**Supplementary Figures S1–S6**), along with recombination tests and linkage disequilibrium analysis. Similar evidence has been shown in other genotyping studies, e.g., in *C. glabrata* (Dodgson et al., 2005; Lott et al., 2010), *C. neoformans* var. *grubii* (Litvinseva et al., 2006) and *C. gattii* (Carriconde et al., 2011), in which recombination and/or clonal expansion were demonstrated.

The clustering of the Australian versus the European strains/sequence types obtained from the available strains, the higher genetic diversity among the 84 Australian strains compared to the 95 European strains (**Table 4**), and the mix of some of the Australian strains within the "global cluster" suggest that the species *S. aurantiacum* maybe originated within the Australian continent and was subsequently dispersed to other parts of the world, as also indicated by the close genetic relationships between some of the Australian

TABLE 4 | Comparison of neutrality and genetic variability of concatenated MLST sequences from Australia and Europe.

Geographic origin	No. of strains	No. of sequence types (ST)	Length (bp)	Total number of sites[1]	No. of polymorphic sites (SNP)	No. of haplotypes	Nucleotide diversity (π)	Haplotype diversity (*Hd*)	Average no. of nucleotide differences (k)	Tajima's D[2]	Tajima's D (P-value)
Australia	84	69	3994	3971	59	65	0.00381	0.993	15.12220	0.85368	>0.10
Europe	95	81	4022	3971	58	74	0.00365	0.991	14.47436	0.83132	>0.10

[1]*Excluding sites with gaps/missing data*
[2]*Tajima's test for neutrality (Tajima, 1989).*

sequence types and those from other parts of the world revealed in the goeBURST analysis, while non-Australian sequence types are not interspaced within the main Australian sequence types clusters, except for the single German sequence type 94 (strain RKI95-0197) (**Figure 3**). However, to definitely identify the origin of this species, additional studies further expanding the number of *S. aurantiacum* strains from Africa, America and Asia are warranted.

A key finding of this study is that clinical isolates were not genetically separated from the environmental isolates, whereby clinical isolates were present in all branches of the two major clusters, with some branches containing both clinical and environmental isolates. This infers that isolates from both sources are closely related, indicating that the environment may be the most likely source of colonization and subsequent infection. *Scedosporium* species have been reported globally (Rougeron et al., 2018), with *S. aurantiacum* being mainly reported from the environment in Australia (Harun et al., 2010a), Austria (Kaltseis et al., 2009), France (Rougeron et al., 2015), Morocco (Mouhajir et al., 2020) and Thailand (Luplertlop et al., 2016). However, the current analysis did not reveal any sequence type shared by environmental and clinical strains. Hence, it cannot be postulated that either infection or colonization is directly associated with a certain genotype of *S. aurantiacum* present in the environment.

Similarly, the current study did not show any clustering of either colonizing or invasive strains. However, some association was noted with some branches in the two main clusters harboring either mainly invasive strains or containing mainly colonizing strains. There were no genotypes which were identical or closely related between colonizing and invasive strains, except ST15 (colonizing strains WM 06.476, WM 07.555, and invasive strain WM 07.452). However, they are not directly related, as they have been isolated in 2004, 2005 and 2007, respectively (**Figure 2** and **Supplementary Table S2**). Both groups of strains can co-exist and have an equal possibility of colonizing the human host and subsequently causing invasive infection. Similar findings were made when the ability to degrade key elements of the complement cascade in the cerebrospinal fluid was investigated in correlation with the phylogenetic background, finding no phylogenetic grouping with the ability of a strain to degrade either the complement factors C3 or C1 (Rainer et al., 2011). Further studies are needed, on a wider range of clinical isolates systematically collected as part of a longitudinal clinical study to characterize the relatedness of colonizing and invasive isolates during progression to disease.

The lack of association between MLST genotype and infection sites in this study has also been noted in MLST studies of bacterial pathogens, such as *Streptococcus agalactiae* (Van der Mee-Marquet et al., 2008) and *Acinetobacter baumannii* (Sahl et al., 2011). In *C. albicans*, multi-locus sequence types were not associated with mating type, anatomical origin, or antifungal resistance (Chen et al., 2006). Apart from chronic lung disease, no significant association was seen for the other predisposing factors within specific branches of the two major clusters or with individual sequence types. However, interpretation of this study might be affected by missing data that resulted in a small sample analysis for both PASW Statistics and STATA II.

This study also attempted to find an association between different genotypes and virulence using a murine model. The major difference between the survival curves was obtained for the two clinical strains WM 08.202 and WM 08.269, for which end point survival rates were 20% and 40%, respectively. The other strains tested caused 100% mortality, with the clinical strain WM 06.482 inducing the highest mortality rate, followed by the environmental strain WM 09.24 and clinical strain WM 08.52, showing that highly virulent strains can circulate in the environment representing a potential risk of infections to humans. The lack of differences among the remaining strains suggests that most tested genotypes, regardless of their origin and clinical status, have a comparable degree of pathogenicity, and that genotype is not indicative of the virulence of a fungal strain as it has been shown for the molecular type VGII of the human pathogenic fungus *Cryptococcus gattii* (Ngamskulrungroj et al., 2011).

CONCLUSIONS

The MLST typing scheme for *S. aurantiacum* developed as part of this study, is the first of its kind for *S. aurantiacum*. When applied to Australian and non-Australian strains it showed that this species is highly polymorphic. This MLST scheme offers a robust, reliable, and highly discriminatory molecular typing tool for *S. aurantiacum*. Together with the established database at http://mlst.mycology.org, it will enable data sharing and foster even greater international collaboration to enable an improved understanding of the *S. aurantiacum* population structure and to define the ultimate origin of the species. This will form the basis for further studies investigating the associations between genotypes and virulence or antifungal resistance, to facilitate more effective and tailored prevention and

management strategies for patients at risk for infections by this emerging pathogen.

AUTHORS CONTRIBUTIONS

WM, AH, J-PB, and SC conceived and designed the study. AH, AK, KS, FG, CF, and HL performed the experiments and data analysis. AH, HP, HL, SG, JK, MF, WB, ML, CB, IA, JR, JL, JA, KT, MS, CH, J-PB, SC, and WM collected, contributed strains and metadata to this study. AH, CH, J-PB, SC, and WM wrote the manuscript, with contributions and comments from all authors. All authors contributed to the article and approved the submitted version.

DATA AVAILABILITY STATEMENT

The datasets presented in this study can be found in online repositories. The names of the repository/repositories and accession number(s) can be found in the article/**Supplementary Material**.

ETHICS STATEMENT

The animal study was reviewed and approved by Western Sydney Local Health District Animal Ethics Committee (#4194.06.012).

FUNDING

The work was funded by an NHMRC project grant (APP1031943) to WM.

ACKNOWLEDGMENT

The authors thank Francoise Symoens (Science Institute of Public Health, Brussels, Belgium), Karen Rogers (Auckland City Hospital, Auckland, New Zealand), and the members of the Australian *Scedosporium* Study Group (AUSCEDO) for collecting and submitting strains for this study. Members of the Australian Scedosporium Study Group of the Australasian Society for Infectious Diseases (AUSCEDO): ACT: Peter Collignon (The Canberra Hospital); NSW: Richard Benn (Royal Prince Alfred Hospital), Ian Chambers (Douglass Hanly Moir Pathology), Sharon Chen (Westmead Hospital), Nelson Dennis (Wollongong Hospital), Deo DeWit (Gosford Hospital), John Ferguson (John Hunter Hospital), Iain Gosbell (Liverpool Hospital), Thomas Gottlieb (Concord Hospital), Catriona Halliday (Westmead Hospital), Juliette Holland (Mayne Laverty Pathology), Alison Kesson (New Children's Hospital, Westmead), Richard Lawrence (St. George Hospital), Deborah Marriott (St. Vincent's Hospital, Sydney), Wieland Meyer (Westmead Hospital), Peter Newton (Wollongong Hospital), Quoc Nguyen (St. Vincent's Hospital, Sydney), Pamela Palasanthrian (Sydney Children's Hospital), Robert Pickles (Taree), Robert Pritchard (Royal North Shore Hospital), Tania Sorrell (Westmead Hospital), Lex Tierney (John Hunter Hospital); Voula Tomasotos (Liverpool Hospital), Robert Vaz (Orange Base Hospital); Kerry Weeks (Royal North Shore Hospital). QLD: Anthony Allworth (Royal Brisbane Hospital), Christopher Coulter (The Prince Charles Hospital), Joan Faoagali (Royal Brisbane Hospital), Barbara Johnson (Princess Alexandra Hospital), David Looke (Princess Alexandra Hospital), Joseph McCormack (The Mater Adult Hospital), Graeme Nimmo (Princess Alexandra Hospital), Gabrielle O'Kane (The Prince Charles Hospital), E. Geoffrey Playford (Princess Alexandra Hospital); Jennifer Robson (Sullivan and Nicolaides Pathology); SA: David Ellis (Women's and Children's Hospital), Rosemary Handke (Women's and Children's Hospital), Karen Rowlands (Royal Adelaide Hospital); David Shaw (Royal Adelaide Hospital); TAS: Louise Cooley (Royal Hobart Hospital), Erica Cox (Launceston General Hospital), Alistair McGregor (Royal Hobart Hospital); VIC: Clare Franklin (Alfred Hospital), Cathy Joseph (St Vincent's Hospital, Melbourne), Tony Korman (Monash Medical Centre), Orla Morrissey (Alfred Hospital), Monica Slavin (Peter MacCallum Cancer Centre), Denis Spelman (Alfred Hospital), Bryan Speed (Austin and Repatriation Hospitals), Harsha Sheorey (St. Vincent's Hospital, Melbourne); WA: Western Australia: Peter Boan (Fiona Stanley Hospital (FSH); PathWest Laboratory Medicine, FSH), John Dyer (Fiona Stanley Hospital), Christopher Heath (Fiona Stanley Hospital; PathWest Laboratory Medicine, FSH; & Royal Perth Hospital), Dianne Gardam (PathWest Laboratory Medicine, FSH), Duncan McLennan (Fiona Stanley Hospital), Ronan Murray (Sir Charles Gairdner Hospital, & PathWest Laboratory Medicine, QEII), Todd Pryce (PathWest Laboratory Medicine, FSH), Ian Arthur (PathWest Laboratory Medicine, QEII We thank Krystyna Maszewska for handling the *Scedosporium* culture collection in the Molecular Mycology Research Laboratory.

SUPPLEMENTARY MATERIAL

The Supplementary Material for this article can be found online at: https://www.frontiersin.org/articles/10.3389/fcimb.2021.761596/full#supplementary-material

Supplementary Figure 1 | *ACT* locus tree. Most parsimonious tree for the *ACT* locus for the 188 investigated *Scedosporium aurantiacum* isolates obtained with the program MEGA version 11 (numbers on the branches indicate bootstraps values above 50).

Supplementary Figure 2 | *CAL* locus tree. Most parsimonious tree for the *CAL* locus for the 188 investigated *Scedosporium aurantiacum* isolates obtained with the program MEGA version 11 (numbers on the branches indicate bootstraps values above 50).

Supplementary Figure 3 | *EF1α* locus tree. Most parsimonious tree for the *EF1α* locus for the 188 investigated *Scedosporium aurantiacum* isolates obtained with the program MEGA version 11 (numbers on the branches indicate bootstraps values above 50).

Supplementary Figure 4 | *RPB2* locus tree. Most parsimonious tree for the *RPB2* locus for the 188 investigated *Scedosporium aurantiacum* isolates obtained with the program MEGA version 11 (numbers on the branches indicate bootstraps values above 50).

Supplementary Figure 5 | *SOD2* locus tree. Most parsimonious tree for the *SOD2* locus for the 188 investigated *Scedosporium aurantiacum* isolates obtained with the program MEGA version 11 (numbers on the branches indicate bootstraps values above 50).

Supplementary Figure 6 | *TUB* locus tree. Most parsimonious tree for the *TUB* locus for the 188 investigated *Scedosporium aurantiacum* isolates obtained with the program MEGA version 11 (numbers on the branches indicate bootstraps values above 50).

Supplementary Table 1 | List of primers used in the MLST scheme development.

Supplementary Table 2 | List of the studied *Scedosporium aurantiacum* strains, including strain number, strain information, origin, source of isolation, clinical data, MLST allele types (AT) of the six loci studied, sequence type (ST), and supplier.

Supplementary Table 3 | GenBank accession numbers for all six genetic loci included in the *S. aurantiacum* MLST scheme for all investigated strains.

REFERENCES

Bain, J. M., Tavanti, A., Davidson, A. D., Jacobsen, M. D., Shaw, D., Gow, N. A. R., et al. (2007). Multilocus Sequence Typing of the Pathogenic Fungus Aspergillus Fumigatus. *J. Clin. Microbiol.* 45, 1469–1477. doi: 10.1128/JCM.00064-07

Bernhard, A., Sedlacek, L., Wagner, S., Schwarz, C., Würstl, B., and Tintelnot, K. (2013). Multilocus Sequence Typing of Scedosporium Apiospermum and Pseudallescheria Boydii Isolates From Cystic Fibroses Patients. *J. Cyst Fibros* 12 (6), 592–598. doi: 10.1016/j.jcf.2013.05.007

Blyth, C. C., Middleton, P., Harun, A., Sorrell, T. C., Meyer, W., and Chen, S. C. A. (2010). Clinical Associations and Prevalence of *Scedosporium* Spp.in Australian Cystic Fibrosis Patients: Identification of Novel Risk Factors? *Med. Mycol.* 48, S37–S44. doi: 10.3109/13693786.2010.500627

Bougnoux, M.-E., Morand, S., and d'Enfert, C. (2002). Usefulness of Multilocus Sequence Typing for Characterization of Clinical Isolates of Candida Albicans. *J. Clin. Microbiol.* 40, 1290–1297. doi: 10.1128/JCM.40.4.1290-1297.2002

Brown, G. R., Gill, G. P., Kuntz, R. J., Langley, C. H., and Neale, D. B. (2004). Nucleotide Diversity and Linkage Disequilibrium in Loblolly Pine. *Acad. Sci. U. S. A.* 101, 15255–15260. doi: 10.1073/pnas.0404231101

Carriconde, F., Gilgado, F., Arthur, I., Ellis, D., Malik, R., van de Wiele, N., et al. (2011). Clonality and α-a Recombination in the Australian Cryptococcus Gattii VGII Population – An Emerging Outbreak in Australia. *PloS One* 6, e16936. doi: 10.1371/journal.pone.0016936

Chen, K. -W., Chen, Y. C., Lo, H. -J., Odds, F. C., Wang, T. -H., Lin, C. -Y., et al. (2006). Mutilocus Sequence Typing for Analyses of Candida albicans strains in Taiwan. *J. Clin. Micro*. 44 (6), 2172–2178.

Chen, S. C. A., Halliday, C. L., Hoenigl, M., Cornely, O. A., and Meyer, W. (2021). Scedosporium and *Lomentospora* Infections: Contemporary Microbiological Tools for the Diagnosis of Invasive Disease. *J. Fungi* 7 (1):23. doi: 10.3390/jof7010023

Chen, M., Zeng, J., de Hoog, G. S., Stielow, B., Gerrits Van Den Ende, A. H., Liao, W., et al. (2016). The 'Species Complex' Issue in Clinically Relevant Fungi: A Case Study in Scedosporium Apiospermum. *Fungal Biol.* 120 (2), 137–146. doi: 10.1016/j.funbio.2015.09.003

Cortez, K. J., Roilides, E., Quiroz-Telles, F., Meletiadis, J., Antachopoulos, C., Knudsen, T., et al. (2008). Infections Caused by Scedosporium Spp. *Clin. Microbiol. Rev.* 21, 157–197. doi: 10.1128/CMR.00039-07

Cruse, M., Telerant, R., Gallagher, T., Lee, T., and Taylor, J. W. (2002). Cryptic Species in *Stachybotrys Chartarum*. *Mycologia* 94, 814–822. doi: 10.2307/3761696

Debourgogne, A., Gueidan, C., Hennequin, C., Contet-Audonneau, N., de Hoog, S., and Machouart, M. (2010). Development of a New MLST Scheme for Differentiation of Fusarium Solani Species Complex (FSSC) Isolates. *J. Microbiol. Methods* 82, 319–323. doi: 10.1016/j.mimet.2010.07.008

Defontaine, A., Zouhair, R., Cimon, B., Carrère, J., Bailly, E., Symoens, F., et al. (2002). Genotyping Study of Scedosporium Apiospermum Isolates in Patients With Cystic Fibrosis. *J. Clin. Microbiol.* 40, 2108–2114. doi: 10.1128/JCM.40.6.2108-2114.2002

Delhaes, L., Harun, A., Chen, S. C. A., Nguyen, Q., Slavin, M., Heath, C. H., et al. (2008). Molecular Typing of Australian Scedosporium Isolates Showing Genetic Variability and Numerous S. Aurantiacum. *Emerg. Infect. Dis.* 14, 282–290. doi: 10.3201/eid1402.070920

Dodgson, A. R., Pujol, C., Denning, D. W., Soll, D. R., and Fox, A. J. (2003). Multilocus Sequence Typing of *Candida Glabrata* Reveals Geographically Enriched Clades. *J. Clin. Microbiol.* 41, 5709–5717. doi: 10.1128/JCM.41.12.5709-5717.2003

Dodgson, A. R., Pujol, C., Pfaller, M. A., Denning, D. W., and Soll, D. R. (2005). Evidence for Recombination in *Candida Glabrata*. *Fungal Gen. Biol.* 42, 233–243. doi: 10.1016/j.fgb.2004.11.010

Feng, X., Yao, Z., Ren, D., Liao, W., and Wu, J. (2008). Genotype and Mating Type Analysis of Cryptococcus Neoformans and Cryptococcus Gattii Isolates From China That Mainly Originated From non-HIV-Infected-Patients. *FEMS Yeast Res.* 8, 930–938. doi: 10.1111/j.1567-1364.2008.00422.x

Ferrer, C., Colom, F., Frasés, S., Mulet, E., Abad, J. L., and Alió, J. L. (2001). Detection and Identification of Fungal Pathogens by PCR and by ITS2 and 5.8S Ribosomal DNA Typing in Ocular Infections. *J. Clin. Microbiol.* 39, 2873–2879. doi: 10.1128/JCM.39.8.2873-2879.2001

Gilgado, F., Cano, J., Gene, J., and Guarro, J. (2005). Molecular Phylogeny of the Pseudallescheria Boydii Species Complex: Proposal of Two New Species. *J. Clin. Microbiol.* 43, 4930–4942. doi: 10.1128/JCM.43.10.4930-4942.2005

Gilgado, F., Cano, J., Gene, J., Serena, C., and Guarro, J. (2009). Different Virulence of the Species of the Pseudallescheria Boydii Complex. *Med. Mycol.* 47, 371–374. doi: 10.1080/13693780802256539

Gilgado, F., Cano, J., Gene, J., Sutton, D. A., and Guarro, J. (2008). Molecular and Phenotypic Data Supporting Species Statuses for Scedosporium Apiospermum and Pseudallescheria Boydii and the Proposed New Species *Scedosporium Dehoogii*. *J. Clin. Microbiol.* 46, 766–771. doi: 10.1128/JCM.01122-07

Gilgado, F., Serena, C., Cano, J., and Gene, J. (2006). Antifungal Susceptibility of the Species of the Pseudallescheria Boydii Complex. *Antimicrob. Agents Chemother.* 50, 4211–4213. doi: 10.1128/AAC.00981-06

Guarro, J., Gene, J., and Stchigel, A. M. (1999). Developments in Fungal Taxonomy. *Clin. Microbiol. Rev.* 12, 454–500. doi: 10.1128/CMR.12.3.454

Harun, A., Gilgado, F., Chen, S. C. A., and Meyer, W. (2010a). Abundance of Pseudallescheria/Scedosporium Species in the Australian Urban Environment Suggests a Possible Source for Scedosporiosis Including the Colonization of Airways in Cystic Fibrosis. *Med. Mycol.* 48, S70–S76. doi: 10.3109/13693786.2010.515254

Harun, A., Serena, C., Gilgado, F., Chen, S. C. A., and Meyer, W. (2010b). *Scedosporium Aurantiacum* is as Virulent as *S. Prolificans*, and Shows Strain-Specific Virulence Differences, in a Mouse Model. *Med. Mycol.* 48, S45–S51. doi: 10.3109/13693786.2010.517224

Heath, C. H., Slavin, M. A., Sorrell, T. C., Handke, R., Harun, A., Phillips, M., et al. (2009). Population-Based Surveillance for Scedosporiosis in Australia: Epidemiology, Disease Manifestations and Emergence of Scedosporium Aurantiacum Infection. *Clin. Microbiol. Infect.* 15, 680–693. doi: 10.1111/j.1469-0691.2009.02802.x

Hoffmann, K., Discher, S., and Voigt, K. (2007). Revision of the Genus Absidia (Mucorales, Zygomycetes) Based on Physiological, Phylogenetic, and Morphological Characters; Thermotolerant Absidia Spp. Form a Coherent Group, Mycocladiaceae Fam. Nov. *Mycol. Res.* 111, 1169–1183. doi: 10.1016/j.mycres.2007.07.002

Jacobsen, M. D., Gow, N. A., Maiden, M. C., Shaw, D. J., and Odds, F. C. (2007). Strain Typing and Determination of Population Structure of *Candida Krusei* by Multilocus Sequence Typing. *J. Clin. Microbiol.* 45, 317–323. doi: 10.1128/JCM.01549-06

Kaltseis, J., Rainer, J., and de Hoog, G. S. (2009). Ecology of *Pseudallescheria* and *Scedosporium* Species in Human-Dominated and Natural Environments and

Their Distribution in Clinical Samples. *Med. Mycol.* 47, 398–405. doi: 10.1080/13693780802585317

Kondo, M., Goto, H., and Yamanaka, K. (2018). Case of Scedosporium Aurantiacum Infection Detected in a Subcutaneous Abscess. *Med. Mycol. Case Rep.* 10, 26–27. doi: 10.1016/j.mmcr.2018.01.003

Lackner, M., de Hoog, G. S., Yang, L., Ferreira Moreno, L., Ahmed, S. A., Andreas, F., et al. (2014b). Proposed Nomenclature for Pseudallescheria, Scedosporium and Related Genera. *Fungal Diversity* 67 (1), 1–10. doi: 10.1007/s13225-014-0295-4

Lackner, M., Hagen, F., Meis, J. F., Gerrits van den Ende, A. H., Vu, D., Robert, V., et al. (2014a). Susceptibility and Diversity in the Therapy-Refractory Genus Scedosporium. *Antimicrob. Agents Chemother.* 58 (10), 5877–5885. doi: 10.1128/AAC.03211-14

Lass-Flörl, C., and Cuenca-Estrella, M. J. (2017). Changes in the Epidemiological Landscape of Invasive Mold Infections and Disease. *J. Antimicrob. Chemother.* 72 (suppl_1), i5–i11. doi: 10.1093/jac/dkx028

Litvintseva, A. P., Thakur, R., Vilgalys, R., and Mitchell, T. G. (2006). Multilocus Sequence Typing Reveals Three Genetic Subpopulations of *Cryptococcus Neoformans* Var *Grubii* (Serotype A), Including a Unique Population in Botswana. *Genetics* 172, 2223–2238. doi: 10.1534/genetics.105.046672

Liu, Y. J., Whelen, S., and Hall, B. D. (1999). Phylogenetic Relationship Among Ascomycetes: Evidence From an RNA Polymerase II Subunit. *Mol. Biol. Evol.* 16, 1799–1808. doi: 10.1093/oxfordjournals.molbev.a026092

Lott, T. J., Frade, J. P., and Lockhart, S. R. (2010). MLST Analysis Reveals Both Clonality and Recombination in Populations of *Candida Glabrata* Bloodstream Isolates From US Surveillance. *Eukaryot Cell* 9, 619–625. doi: 10.1128/EC.00002-10

Luplertlop, N., Pumeesat, P., Muangkaew, W., Wongsuk, T., and Alastruey-Izquierdo, A. (2016). Environmental Screening for the Scedosporium Apiospermum Species Complex in Public Parks in Bangkok, Thailand. *PloS One* 11 (7), e0159869. doi: 10.1371/journal.pone.0159869

Maiden, M. C., Bygraves, J. A., Feil, E., Morelli, G., Russell, J. E., Urwin, R., et al. (1998). Multilocus Sequence Typing: A Portable Approach to the Identification of Clones Within Populations of Pathogenic Microorganisms. *Proc. Natl. Acad. Sci. U. S. A.* 95, 3140–3145. doi: 10.1073/pnas.95.6.3140

Meyer, W., Aanensen, D. M., Boekhout, T., Cogliati, M., Diaz, M. R., Espoto, M. C., et al. (2009). Consensus Multi-Locus Sequence Typing Scheme for Cryptococcus Neoformans and *Cryptococcus Gattii*. *Med. Mycol.* 12, 1–14. doi: 10.1080/13693780902953886

Mizusawa, M., Totten, M., and Zhang, S. X. (2021). Case of *Scedosporium Aurantiacum* Infection in the United States. *Mycopathologia* 186 (1), 127–130. doi: 10.1007/s11046-020-00498-x

Mouhajir, A., Poirier, W., Angebault, C., Rahal, E., Bouabid, R., Bougnoux, M.-E., et al. (2020). *Scedosporium* Species in Soils From Various Biomes in Northwestern Morocco. *PloS One* 15 (2), e0228897. doi: 10.1371/journal.pone.0228897

Nakamura, Y., Suzuki, N., Nakajima, Y., Utsumi, Y., Murata, O., Nagashima, H., et al. (2013). *Scedosporium Aurantiacum* Brain Abscess After Near Drowning in a Survivor of a Tsunami in Japan. *Respir. Investig.* 51 (4), 207–211. doi: 10.1016/j.resinv.2013.07.001

Nei, M., and Gojobori, T. (1986). Simple Methods for Estimating the Numbers of Synonymous and Nonsynonymous Nucleotide Substitutions. *Mol. Biol. Evol.* 3, 418–426. doi: 10.1093/oxfordjournals.molbev.a040410

Ngamskulrungroj, P., Serena, C., Gilgado, F., Malik, R., and Meyer, W. (2011). Global VGIIa Isolates are of Comparable Virulence to the Major Fatal Cryptococcus Gattii Vancouver Island Outbreak Genotype. *Clin. Microbiol. Inf.* 17 (2), 252–258. doi: 10.1111/j.1469-0691.2010.03222.x

Odds, F. C., and Jacobsen, M. D. (2008). Multilocus Sequence Typing of Pathogenic *Candida* Species. *Eukaryot Cell* 7, 1075–1084. doi: 10.1128/EC.00062-08

O'Donnell, K., Kistler, H. C., Cigelnik, E., and Ploetz, R. C. (1998). Multiple Evolutionary Origins of the Fungus Causing Panama Disease of Banana: Concordant Evidence From Nuclear and Mitochondrial Gene Genealogies. *Proc. Natl. Acad. Sci. U. S. A.* 95, 2044–2049. doi: 10.1073/pnas.95.5.2044

Pérez-Bercoff, A., Papanicolaou, A., Ramsperger, M., Kaur, J., Patel, H. R., Harun, A., et al. (2015). Draft Genome of Australian Environmental Strain WM 09.24 of the Opportunistic Human Pathogen Scedosporium Aurantiacum. *Genome Announc* 3 (1), e01526–e01514. doi: 10.1128/genomeA.01526-14

Perez-Losada, M., Browne, E. B., Madsen, A., Wirth, T., Viscidi, R. P., and Crandall, K. A. (2006). Population Genetics of Microbial Pathogens Estimated From Multilocus Sequence Typing (MLST) Data. *Infect. Genet. Evol.* 6, 97–112. doi: 10.1016/j.meegid.2005.02.003

Pihet, M., Carrère, J., Cimon, B., Chabasse, D., Delhaes, L., Symoens, F., et al. (2009). Occurrence and Relevance of Filamentous Fungi in Respiratory Secretions of Patients With Cystic Fibrosis - A Review. *Med. Mycol.* 47, 387–397. doi: 10.1080/13693780802609604

Planet, P. J. (2005). Tree Disagreement: Measuring and Testing Incongruence in Phylogenies. *J. Biomed. Inform* 39, 86–102. doi: 10.1016/j.jbi.2005.08.008

Rainer, J., de Hoog, G. S., Wedde, M., Gräser, Y., and Gilges, S. (2000). Molecular Variability of Pseudallescheria Boydii, a Neurotropic Opportunist. *J. Clin. Microbiol.* 38, 3267–3273. doi: 10.1128/JCM.38.9.3267-3273.2000

Rainer, J., Rambach, G., Kaltseis, J., Hagleitner, M., Heiss, S., and Speth, C. (2011). Phylogeny and Immune Evasion: A Putative Correlation for Cerebral Pseudallescheria/Scedosporium Infections. *Mycoses* 54 (suppl_3), 48–55. doi: 10.1111/j.1439-0507.2011.02117.x

Ramirez-Garcia, A., Pellon, A., Rementeria, A., Buldain, I., Barreto-Berguer, E., Rollin-Pinheiro, R., et al. (2018). *Scedosporium* and Lomentospora: An Updated Overview of Underrated Opportunists. *Med. Mycol.* 56 (suppl1), 102–125. doi: 10.1093/mmy/myx113

Rivero-Menendez, O., Cuenca-Estrella, M., and Alastruey-Izquierdo, A. (2020). In Vitro Activity of Olorofim Against Clinical Isolates of *Scedosporium* Species and *Lomentospora Prolificans* Using EUCAST and CLSI Methodologies. *J. Antimicrob. Chemother.* 75 (12), 3582–3585. doi: 10.1093/jac/dkaa351

Rodriguez, M. M., Pastor, F. J., Salas, V., Calvo, E., Mayayo, E., and Guarro, J. (2010). Experimental Murine Scedosporiosis: Histopathology and Azole Treatment. *Antimicrob. Agents Chemother.* 54, 3980–3984. doi: 10.1128/AAC.00046-10

Rokas, A., King, N., Finnerty, J., and Carroll, S. B. (2003a). Conflicting Phylogenetic Signals at the Base of the Metazoan Tree. *Evol. Dev.* 5, 346–359. doi: 10.1046/j.1525-142X.2003.03042.x

Rokas, A., Williams, B. L., King, N., and Carroll, S. B. (2003b). Genome-Scale Approaches to Resolving Incongruence in Molecular Phylogenies. *Nature* 425, 798–804. doi: 10.1038/nature02053

Rougeron, A., Giraud, S., Alastruey-Izquierdo, A., Cano-Lira, J., Rainer, J., Mouhajir, A., et al. (2018). Ecology of Scedosporium Species: Present Knowledge and Future Research. *Mycopathologia* 183 (1), 185–200. doi: 10.1007/s11046-017-0200-2

Rougeron, A., Schuliar, G., Leto, J., Sitterlé, E., Landry, D., Bougnoux, M.-E., et al. (2015). Human-Impacted Areas of France are Environmental Reservoirs of the Pseudallescheria Boydii/Scedosporium Apiospermum Species Complex. *Environ. Microbiol.* 17 (4), 1039–1048. doi: 10.1111/1462-2920.12472

Rozas, J., Ferrer-Mata, A., Sánchez-DelBarrio, J. C., Guirao-Rico, S., Librado, P., Ramos-Onsins, S. E., et al. (2017). DnaSP 6: DNA Sequence Polymorphism Analysis of Large Data Sets. *Mol. Biol. and Evol.* 34, 12, 3299–3302. doi: 10.1093/molbev/msx248

Sahl, J. W., Johnson, J. K., Harris, A. D., Phillippy, A. M., Hsiao, W. W., Thom, K. A., et al. (2011). Genomic Comparison of Multi-Drug Resistant Invasive and Colonizing Acinetobacter Baumannii Isolated From Diverse Human Body Sites Reveals Genomic Plasticity. *BMC Genomics* 12, 291. doi: 10.1186/1471-2164-12-291

Schwarz, C., Vandeputte, P., Rougeron, A., Giraud, S., de Bernonville, T. D., Duvaux, L., et al. (2018). Developing Collaborative Works for Faster Progress on Fungal Respiratory Infections in Cystic Fibrosis. *Med. Mycol.* 56 (suppl.1), 42–56. doi: 10.1093/mmy/myx106

Tajima, F. (1989). Statistical Method for Testing the Neutral Mutation Hypothesis by DNA Polymorphism. *Genetics* 123, 585–595. doi: 10.1093/genetics/123.3.585

Tamura, K., Stecher, G., and Kumar, S. (2021). MEGA 11: Molecular Evolutionary Genetics Analysis Version 11. *Mol. Biol. Evol.* 38 (7), 3022–3027. doi: 10.1093/molbev/msab120

Tavanti, A., Davidson, A. D., Johnson, E. M., Maiden, M. C., Shaw, D. J., Gow, N. A. R., et al. (2005). Multilocus Sequence Typing for Differentiation of Strains of Candida Tropicalis. *J. Clin. Microbiol.* 43, 5593–5600. doi: 10.1128/JCM.43.11.5593-5600.2005

Troke, P., Aguirrebengoa, K., Arteaga, C., Ellis, D., Heath, C. H., Lutsar, I., et al. (2008). Treatment of Scedosporiosis With Voriconazole: Clinical Experience

With 107 Patients. *Antimicrob. Agents Chemother.* 52, 1743–1750. doi: 10.1128/AAC.01388-07

Uraiwan, A., Wolfgang, S., and Stadler, T. (2007). Using Multilocus Sequence Data to Assess Population Structure, Natural Selection, and Linkage Disequilibrium in Wild Tomatoes. *Mol. Biol. Evol.* 24 (10), 2310–2322. doi: 10.1093/molbev/msm162

Van der Mee-Marquet, N., Fourny, L., Arnault, L., Domelier, A., Salloum, M., Lartigue, M. F., et al. (2008). Molecular Characterization of Human-Colonizing Streptococcus Agalactiae Strains Isolated From Throat, Skin, Anal Margin, and Genital Body Sites. *J. Clin. Microbiol.* 46, 2906–2911. doi: 10.1128/JCM.00421-08

Zouhair, R., Defontaine, A., Ollivier, C., Cimon, B., Symoens, F., Hallet, J.-N., et al. (2001). Typing of Scedosporium Apiospermum by Multilocus Enzyme Electrophoresis and Random Amplification of Polymorphic DNA. *J. Med. Microbiol.* 50, 925–932. doi: 10.1099/0022-1317-50-10-925

Zouhair, R., Rougeron, A., Razafimandimby, B., Kobi, A., Bouchara, J. P., and Giraud, S. (2013). Distribution of the Different Species of the Pseudallescheria Boydii/Scedosporium Apiospermum Complex in French Patients With Cystic Fibrosis. *Med. Mycol* 51 (6), 603–613. doi: 10.3109/13693786.2013.770606

Conflict of Interest: The authors declare that the research was conducted in the absence of any commercial or financial relationships that could be construed as a potential conflict of interest.

Publisher's Note: All claims expressed in this article are solely those of the authors and do not necessarily represent those of their affiliated organizations, or those of the publisher, the editors and the reviewers. Any product that may be evaluated in this article, or claim that may be made by its manufacturer, is not guaranteed or endorsed by the publisher.

frontiers in Cellular and Infection Microbiology

ORIGINAL RESEARCH
published: 02 February 2022
doi: 10.3389/fcimb.2022.797017

Genome Sequences of Two Strains of *Prototheca wickerhamii* Provide Insight Into the Protothecosis Evolution

Jian Guo[1†], *Jianbo Jian*[2†], *Lili Wang*[1†], *Lijuan Xiong*[3], *Huiping Lin*[1], *Ziyi Zhou*[1], *Eva C. Sonnenschein*[2*] *and Wenjuan Wu*[1*]

[1] Department of Laboratory Medicine, Shanghai East Hospital, Tongji University School of Medicine, Shanghai, China, [2] Department of Biotechnology and Biomedicine, Technical University of Denmark, Lyngby, Denmark, [3] Department of Laboratory Medicine, Guizhou University The Second Affiliated Hospital of Traditional Chinese Medicine, Guizhou, China

The *Prototheca* alga is the only chlorophyte known to be involved in a series of clinically relevant opportunistic infections in humans and animals, namely, protothecosis. Most pathogenic cases in humans are caused by *Prototheca wickerhamii*. In order to investigate the evolution of *Prototheca* and the genetic basis for its pathogenicity, the genomes of two *P. wickerhamii* strains S1 and S931 were sequenced using Nanopore long-read and Illumina short-read technologies. The mitochondrial, plastid, and nuclear genomes were assembled and annotated including a transcriptomic data set. The assembled nuclear genome size was 17.57 Mb with 19 contigs and 17.45 Mb with 26 contigs for strains S1 and S931, respectively. The number of predicted protein-coding genes was approximately 5,700, and more than 96% of the genes could be annotated with a gene function. A total of 2,798 gene families were shared between the five currently available *Prototheca* genomes. According to the phylogenetic analysis, the genus of *Prototheca* was classified in the same clade with *A. protothecoides* and diverged from *Chlorella* ~500 million years ago (Mya). A total of 134 expanded genes were enriched in several pathways, mostly in metabolic pathways, followed by biosynthesis of secondary metabolites and RNA transport. Comparative analysis demonstrated more than 96% consistency between the two herein sequenced strains. At present, due to the lack of sufficient understanding of the *Prototheca* biology and pathogenicity, the diagnosis rate of protothecosis is much lower than the actual infection rate. This study provides an in-depth insight into the genome sequences of two strains of *P. wickerhamii* isolated from the clinic to contribute to the basic understanding of this alga and explore future prevention and treatment strategies.

Keywords: *Prototheca wickerhamii*, protothecosis, algae, whole genome sequencing, pathogenic

OPEN ACCESS

Edited by:
Min Chen,
Shanghai Changzheng Hospital, China

Reviewed by:
Pei Hao,
Institut Pasteur of Shanghai (CAS), China
Hong-Yu Ou,
Shanghai Jiao Tong University, China
Abdullah M. S. Al-Hatmi,
University of Nizwa, Oman

***Correspondence:**
Wenjuan Wu
wwj1210@126.com
Eva C. Sonnenschein
evaso@bio.dtu.dk

†These authors have contributed equally to this work

Specialty section:
This article was submitted to Fungal Pathogenesis, a section of the journal Frontiers in Cellular and Infection Microbiology

Received: *18 October 2021*
Accepted: *10 January 2022*
Published: *02 February 2022*

Citation:
Guo J, Jian J, Wang L, Xiong L, Lin H, Zhou Z, Sonnenschein EC and Wu W (2022) Genome Sequences of Two Strains of Prototheca wickerhamii Provide Insight Into the Protothecosis Evolution. Front. Cell. Infect. Microbiol. 12:797017. doi: 10.3389/fcimb.2022.797017

INTRODUCTION

The genus *Prototheca* belongs to the predominantly photosynthetic family of the green algae Chlorellaceae but has forfeited the photosynthetic ability (Severgnini et al., 2018; Bakula et al., 2020). All *Prototheca* species possessing colorless plastids evolved from photosynthetic algae that had lost genes related to photosynthesis, yet they retained vestigial plastids (Suzuki et al., 2018). *Prototheca* can cause pathogenic disease in humans and animals with *Prototheca wickerhamii* and *Prototheca zopfii* being the two most common pathogenic species (Kwiecinski, 2015). *P. wickerhamii* has been reported to be the more common human–pathogenic species compared to *P. zopfii*, which infects cattle and dogs (Leimann et al., 2004; Todd et al., 2018). Clinically, *P. wickerhamii* causes protothecosis, usually infects skin and subcutaneous tissue, and can affect both immunocompetent and immunocompromised patients (Todd et al., 2018). In cattle, it has been identified in infected mammary glands (Todd et al., 2018). A previous report described the chain of infection with, *P. wickerhamii*, namely the reservoirs, route of transmission and length of incubation, as unknown or variable (Khan et al., 2018). By 2017, at least 211 cases caused by *P. wickerhamii* had been reported (Bakula et al., 2021). In our laboratory, we have collected 59 *Prototheca* isolates from Chinese clinical patients coming from Shanghai, Beijing, Zhejiang, Sichuan, Jiangsu, Shandong, Jiangxi, Fujian, Guangxi, Guangdong, Yunnan, Chongqing, and Henan. Based on the real-time PCR targeting portion D1/D2 of the 28S rRNA gene, *P. wickerhamii* was found to be the most abundant species in 37 patients with systemic or cutaneous protothecosis.

However, due to the lack of knowledge on the organism and molecular pathogen detection (Khan et al., 2018), protothecosis is difficult to diagnose leading to many patients failing to be treated timely and appropriately (Zeng et al., 2019). Despite the pathogenic potential of *Prototheca* spp., limited scientific knowledge of the genus has hindered the progress on how to prevent or treat infections. Until now, only little genomic data of *Prototheca* exist to support building this understanding. Five nuclear genome sequences are currently available in the NCBI database originating from five *Prototheca* species, namely, *Prototheca ciferrii* SAG2063 (Severgnini et al., 2018), *Prototheca cutis* JCM 15793 (Suzuki et al., 2018), *Prototheca stagnora* JCM 9641 (Suzuki et al., 2018), *Prototheca bovis* SAG 2021 (Severgnini et al., 2018), and *P. wickerhamii* ATCC 16529 (Bakula et al., 2021). However, all the public genomes (except for the one of *P. wickerhamii*) are draft genomes assembled from next-generation sequencing data, which limits the detailed genomic protothecosis research. Using the first closed genome, Bakula et al. could pioneer in describing the putative genes associated with protothecosis and disease development in *P. wickerhamii* (Bakula et al., 2021). Many genes associated with fungal pathogenicity, some potential virulence factors, and putative genes involved in protothecosis were identified in the *P. wickerhamii* genome (Bakula et al., 2021).

Besides its role as pathogen, *Prototheca* also represents an important model to study algal evolution due to the loss of photosynthesis. The taxonomic position of *Prototheca* as well as the number of *Prototheca* species have been debated for a long time (Jagielski et al., 2019). The phylogeny of *Prototheca* has been revised significantly several times because of more information becoming available including phenotypic, chemotaxonomic, and molecular data (Jagielski et al., 2019). The genus *Prototheca* along with *Helicosporidium* and *Auxenochlorella* belong to the green algal family of Trebouxiophyceae (Suzuki et al., 2018), with the polyphyly being reinforced with plastid genome-based phylogeny (Bakula et al., 2020). However, a study of the phylogenetic relationships of *Auxenochlorella protothecoides* and 23 *Prototheca* strains demonstrated inconsistencies with the molecular phylogenetic analyses based upon complete 16S and partial 23S plastid rDNA sequences (Ewing et al., 2014).

In order to investigate the evolution of *Prototheca* and the genetic basis for its pathogenicity, we herein sequenced two clinical isolates of *P. wickerhamii*, analyzed their phylogeny within the green algae, and identified genes potentially involved in the pathogenicity.

METHODS

Sampling and Genomic DNA Extraction

The *P. wickerhamii* strain S1 (mucoid colony) was isolated from a case of an 85-year-old patient who had suffered from cutaneous infections in Shanghai, China. The *P. wickerhamii* strain S931 (rough colony) was isolated from a case of a 24-year-old patient who had suffered from multiple cutaneous infections in Shanghai, China (**Figure S1**). For macroscopic observation of colonies, each strain was streaked out on Sabouraud dextrose agar medium and incubated at 35°C for 3 days. Wet specimens were observed under a differential interference contrast microscope. The strains were harvested from agar culture medium and washed with distilled water, and then the genomic DNA was extracted with the CTAB method as described previously (Jagielski et al., 2017).

Library Preparation and Sequencing

Extracted genomic DNA (gDNA) was prepared for Illumina sequencing as libraries with insert sizes of about 350 bp using the HiSeq X Reagent Kit v2. An amplification-free approach was performed for 150-bp paired-end reads following the manufacturer's protocol (Illumina) and sequenced on a NovaSeq 6000 Sequencing platform. The PCR duplicates, adapter, N content (N content >5%), and low-quality (quality value ≤10, low-quality base >20%) reads were excluded using SOAPnuke version 1.5.3 (Chen et al., 2018). Then, the clean reads were retained for genome survey. A total of 10 μg gDNA was used to select fragment sizes (>10 kb) with a BluePippin BLF7510 cassette (Sage Science, Beverly, MA, USA). The standard Oxford Nanopore Technologies library prep protocol was applied with a ligation sequencing kit SQK-LSK109. Then, DNA fragments were end-repaired, recovered, purified, and sequenced on the GridION X5 platform. The raw reads were removed with a Q value of <7 and a minimum read length <5,000 bp. The retained clean reads were applied to assemble the genome.

Genome Survey and Assembly

To obtain the genome size, heterozygosity, and repeat content, Illumina 150-bp paired-end reads were initially used to estimate the *P. wickerhamii* genome characteristics using a 17 K-mer by JellyFish (Marcais and Kingsford, 2011) and GenomeScope (Vurture et al., 2017). The quality-filtered Nanopore long reads were assembled using CANU v1.8 (Koren et al., 2017) with the parameters corOutCoverage = 40, and minReadLength = 1000 and Necat (Chen et al., 2021) with parameters –ctg_min_length=1000 and –coverage=40, respectively. The primary contigs were polished with raw Nanopore long reads using Racon v1.3.3 (three rounds) (Vaser et al., 2017) and Medaka v0.7.1 (one round) (https://github.com/nanoporetech/medaka). Subsequently, the Illumina short insert size reads were mapped to the polished consensus sequence using BWA-mem (v0.7.17) (Li and Durbin, 2009) and applied to correct the assembled genome by Pilon (v1.23) (Walker et al., 2014) with the default settings.

Genome Annotation and Functional Annotation

The assembled genome was annotated for repeats and genes. Two kinds of methods including homology-based and *de novo* methods were performed in repeat annotation. Firstly, in the homology-based method, the repeat sequence database of RepBase v21.12 (http://www.girinst.org/repbase) (Bao et al., 2015) was applied to identify the similarly repetitive sequences using RepeatModeler v2.0 (Flynn et al., 2020) (http://www.repeatmasker.org/RepeatModeler/)and LTR_FINDER v1.07 (Xu and Wang, 2007) (http://tlife.fudan.edu.cn/ltr_finder/). The *de novo* method was processed by RepeatMasker 3.3.0 (Saha et al., 2008) to predict the repetitive sequences. Three different algorithms (homology-based prediction, RNA-Seq data-based prediction, and *ab initio* prediction) were combined to predict the gene structure. In *ab initio* prediction, the coding regions of genes were predicted with a repeat-masked sequence using AUGUSTUS v3.2.3 (Stanke et al., 2006) and SNAP (Korf, 2004). A total of 9 published homology protein sequences from *Arabidopsis thaliana*, *Auxenochlorella protothecoides*, *Chlamydomonas reinhardtii*, *Chlorella variabilis*, *Coccomyxa subellipsoidae*, *Helicosporidium* sp., *Micractinium conductrix*, *Trebouxia* sp. A1-2, and *Prototheca wickerhamii* type strain ATCC 16529 were aligned to the assembled genome using *TBLASTn* (Kent, 2002). The transcriptome data of *P. wickerhamii* S1 and S931 (see below) were mapped to the genome sequences through *BLAST* and *PASA* software. Finally, the three kinds of evidence used for gene prediction and annotation were integrated with the MAKER (Holt and Yandell, 2011) pipeline. The mitochondrial (mtDNA) and plastid (ptDNA) genomes were annotated with the software of Genes of Organelle from the Reference sequence Analysis (AGORA) (Jung et al., 2018).

For functional annotation of protein-coding genes, protein sequences were aligned to five databases including NR (NCBI non-redundant protein), SwissProt (http://www.gpmaw.com/html/swiss-prot.html), KEGG (http://www.genome.jp/kegg/), KOG (Koonin et al., 2004), and TrEMBL (http://www.uniprot.org) using BLASTp with an E-value of 1 E−5. The protein motifs and domains were identified with *InterPro* (Mulder and Apweiler, 2007) and retrieved using Gene Ontology (GO) (Ashburner et al., 2000) terms. Benchmarking Universal Single-Copy Orthologs (BUSCO V5) (Simao et al., 2015) with the chlorophyta_odb10 database was used to investigate the quality of the genome assembly and gene annotation. To predict putative pathogenicity-related genes, the Pathogen-Host Interaction (PHI) database (Urban et al., 2020) was used to align with protein sequences using BLASTp with an E-value (1 E−5) cutoff.

RNA Extraction and RNA-Seq Data Analysis

A total of six samples (two *P. wickerhamii*-type strains, S1 and S931, with three biological replicates each) of RNA were obtained from cultured cells using the TRIzol reagent (Invitrogen, USA) following the manufacturer's protocol. The algal cells were firstly treated with DNase I to remove DNA contamination, and then oligo(dT) magnetic beads were used to enrich total RNA. The library construction methods were consistent with previous reports (Jian et al., 2017). Finally, the constructed libraries were sequenced with 150-bp paired-end on a NovaSeq 6000 platform. Raw reads were preprocessed using SOAPnuke version 1.5.3 (Chen et al., 2018). The clean reads were then mapped to the reference genome (the newly sequenced genome of S1) to acquire the position information and the unique reads feature of the sequenced samples. The FPKM value of each gene was calculated using Cufflinks (Trapnell et al., 2010). The differentially expressed gene (DEG) analysis were performed with DESeq2 (Love et al., 2014). The false discovery rate (FDR) ≤0.05 and fold change ≥2 were used as the threshold to identify the genes significantly differentially expressed between the replicates.

Gene Family and Phylogenomic Analysis

The single-copy orthologous genes were identified with comparative analysis to examine the conservation of the two newly sequenced genomes and 11 published algae species using OrthoMCL (v2.0.9) (http://orthomcl.org/orthomcl/) (Li et al., 2003). The gene sets of the 11 genomes were processed in two steps. The genes encoding proteins less than 50 amino acids in length were excluded and the longest transcript was retained when there were several spliced transcripts in a gene. The similarity of protein sequences was evaluated by all-versus-all BLASTp (v2.2.26) with an e-value threshold of 1e-10 (Altschul et al., 1990). Single-copy orthologues were extracted from the gene clustering result, and the alignment was performed by the MUSCLE program (v3.8.31, http://www.drive5.com/muscle/) with default parameters (Katoh and Standley, 2013). The phase 1 sites of all single-copy orthologous genes were extracted and concatenated to one super-gene for the phylogeny tree using RAxML (v 8.2.12). Then, the species of *Micromonas commoda* was rooted as outgroup using TreeBest (https://github.com/Ensembl/treebest). The divergence time of species was

calculated with MCMCTree module in PAML (v 4.9, http://abacus.gene.ucl.ac.uk/software/paml.html). Three time-calibrated points were derived from the TimeTree database (http://www.timetree.org/): *M. commode–C. reinhardtii* (792.4–1,019.6 Mya), *O. tauri–C. reinhardtii* (781.1–803.1 Mya), and *C. reinhardtii–C. variabilis* (586.9–604.9 Mya). The expansion and contraction analysis of gene families were performed with CAFE (v3.1) (De Bie et al., 2006).

Comparative Analysis

To test the consensus and variation among the *P. wickerhamii* genomes, the newly and previously assembled genomes were compared with each other using NUCmer 3.1 (MUMmer 3.23 package) (Delcher et al., 2003) and the completeness comparison was performed by MUMmerplot 3.5 (MUMmer 3.23 package) (Delcher et al., 2003) on the NUCmer results after filtering to 1-on-1 alignments and allowing rearrangements with a 1-kbp-length cut.

Ethical Approval

This study was approved by the ethics committee of Shanghai East Hospital, Tongji University School of Medicine (No. 2020-163). The need for informed consents was waived by the Clinical Research Ethics Committee.

RESULTS

Genomic Characterization of *P. wickerhamii* and Genome Assemblies

To obtain the genome characteristics including genome size, heterozygosity, and repeat content, about 4.54 and 4.55 Gb of clean data with Illumina short insert size was generated for *P. wickerhamii* strains S1 and S931, respectively (**Table S1**). Both of the Q20 values of clean reads were higher than 98%, and the Q30 value was approximately 95%. Using jellyfish and GenomeScope (Kmer = 17), the estimated genome sizes were about 18.65 and 17.97 Mb for strain S1 and S931, respectively (**Figures S2, S3**). The heterozygosity was 2.69% for S1 and 3.96% for S931. The estimated genome size was a little higher than the one of the published genome of *P. wickerhamii*-type strain ATCC 16529 with 16.7 Mb. Using Nanopore sequencing on the GridION, in total, 1,328,625 and 681,088 raw reads were generated for S1 and S931, respectively. After filtering out the low-quality reads (Q value of <7 and minimum read length <5,000 bp), a total of 551,989 and 542,630 reads were retained for subsequent assembly. The total clean data were about 4.55 Gb with an average length of 8,235 bp and a maximum length of 153,066 bp for S1. For S931, with a total of 4.90 Gb, the average length was 9,035 bp and the maximum length was 149,724 bp (**Table S2**). The clean Nanopore long reads were used to obtain two primary genome sequences with Canu and Necat (**Tables S3, S4**), and the Necat-based genomes were used for downstream analyses.

Nuclear Genome Acquirement and Annotation

The mitochondrial (mtDNA) and plastid (ptDNA) genomes were obtained from the assembled sequences (**Figure S4** and **Table S5**). After filtering the mtDNA and ptDNA genome sequences out, the length of the final nuclear genome of S1 was approximately 17.57 Mb with 19 contigs (**Table S6**). A final nuclear genome of 17.45 Mb with 26 contigs was generated for S931 (**Table S7**). For strain S1, the contig N50 was 1,639,047 bp with 98.25% of the genome present on 13 contigs, each larger than 500 kb. For S931, the contig N50 was 1,406,360 bp with 93.47% of sequences assembled in 15 contigs of more than 500 kb in size. The characteristics of the two strains of *P. wickerhamii* genomes are shown in **Figure 1**. The assembled genomes suggested that the long contigs were close to the chromosome level. The GC content of both genomes was approximately 64%. The repetitive sequences were initially annotated with homology-based and *de novo* methods. 3.11% and 2.49% of repetitive sequences were identified in S1 and S931, respectively, which might be the reason for *P. wickerhamii* genomes being the smallest and most compact microalgal genomes (**Table S8**). These results are a little higher than that of 2.25% in the genome of *P. wickerhamii* strain ATCC 16529. A total of 5,694 and 5,704 protein-coding genes were predicted in *P. wickerhamii* strains S1 and S931, respectively (**Table 1**), and thereby were slightly less than in strain ATCC 16529. The high quality of the genome and gene annotation was confirmed with the BUSCO V5 analysis based on chlorophyta_odb10 (a total of 1519 gene set). 88.4% and 86.9% of genes were evaluated to be complete for the predicted genes in S1 and S931, respectively (**Table 1** and **Table S9**). The annotation of complete genes was higher in this study compared to *P. wickerhamii* strain ATCC 16529 (79.7%). Potentially, the greater volume of long-read sequencing data (4.5 Gb for S1 and 4.9 Gb for S931) led to more complete genome assemblies as compared to that of strain ATCC 16529 (2.2 Gb). The annotation of gene functions demonstrated that more than 95% of genes were annotated in both of the newly sequenced *P. wickerhamii* genomes (**Table S10**). The enrichment of Gene Ontology (GO) annotation showed a similar distribution of biological processes, cellular components, and molecular functions in strain S1 and S931, and these were the processes with the highest number of genes enriched in the global overview maps of Kyoto Encyclopedia of Genes and Genomes (KEGG) among all the pathways (**Figures S5–S8**).

Phylogenetic Analysis

To gain insights into the evolution of *Prototheca*, the two newly sequenced genomes were compared with 11 other published, algal genomes including *Micromonas commoda*, *Ostreococcus tauri*, *Prasinoderma coloniale*, *Chlamydomonas reinhardtii*, *Micractinium conductrix*, *Chlorella variabilis*, *Auxenochlorella protothecoides*, *Coccomyxa subellipsoidae*, *Prototheca stagnorum*, *Prototheca cutis*, and *P. wickerhamii* strain ATCC 16529. *M. commoda* was used as the outgroup. The gene families were clustered for identifying the single-copy orthologous genes. The number of clustered gene families in these species ranged from 3,662 (*P. stagnorum*) to 8,012 (*C. reinhardtii*) (**Table S11**). The number of unique gene families in the five *Prototheca* strains was less than 10 (**Table S11**). A total of 2,798 gene families were shared between the five pathogenic *Prototheca* strains (**Figure 2**). 1,377, 1,018, 491, and 349 genes were shared in four, three, two,

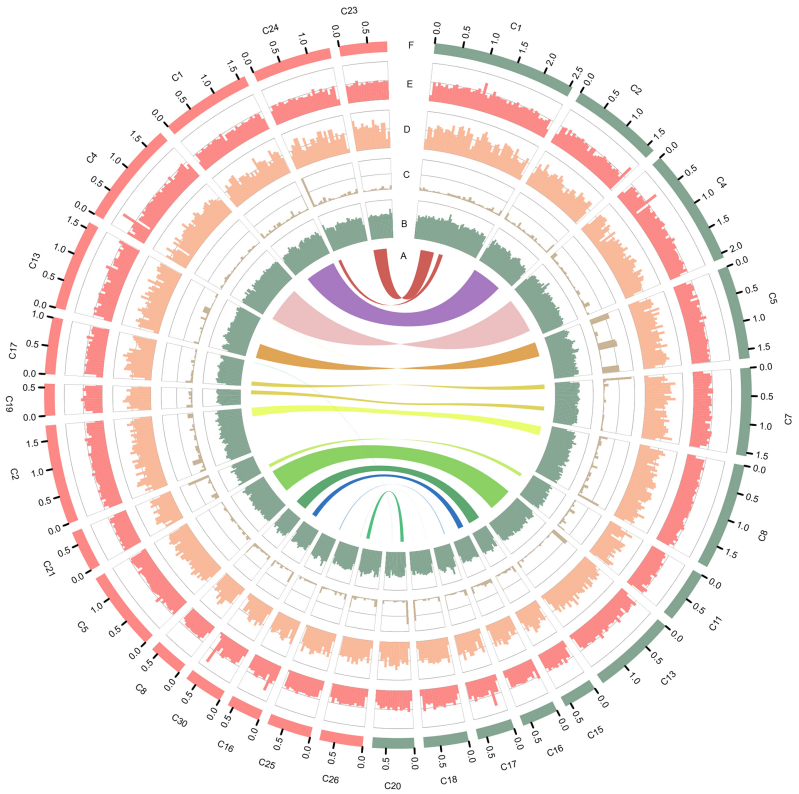

FIGURE 1 | Characteristics of the two types of *P. wickerhamii* genomes. Distribution of genomic features of the *P. wickerhamii* genomes for strain S1 (red) and strain S931 (green). From inside to outside: **(A)** syntenic gene blocks, **(B)** GC content, **(C)** TE density, **(D)** gene number, **(E)** gene length, and **(F)** Contig (>500 kb).

TABLE 1 | Genome statistics of two newly sequenced and one published *P. wickerhamii*.

P. wickerhamii	**Strain S1**	**Strain S931**	**Strain ATCC 16529 (Bakula et al., 2021)**
Assembly length (Mb)	17.57	17.45	16.70
Contig number	19	26	21
N50 contig (bp)	1,639,047	1,406,360	1,578,614
GC content (%)	64.21	64.45	64.16
Number of genes	5,694	5,704	6,081
Complete BUSCOs V5 (gene)	88.40%	86.90%	79.70%
Repetitive DNA in genome assembly (%)	3.11	2.49	2.25

and one strain, respectively. Compared to the eight genomes of non-pathogenic algae, 494 gene families were unique to the five genomes of the pathogenic *Prototheca* strains. A total of 683 gene families were identified specific to *P. wickerhamii* in comparison to *P. stagnorum* and *P. cutis*. Finally, 737 single-copy orthologous gene families were shared by all 13 algal genomes. The phylogenetic tree implied that the genus of *Prototheca* forms a clade with *A. protothecoides* (**Figure 3**). The new sequenced *P. wickerhamii* strains S1 and S931 grouped in a single clade with strain ATCC 16529. Our analysis proposes that the genus of *Prototheca* diverged from *Chlorella* ~498.5 million years ago (Mya) and the species of *P. wickerhamii* separated from the common ancestor approximately 104.9 Mya (**Figure 3**). Following this divergence, 83 gene families showed expansion in species of *P. wickerhamii*, and 722 gene families showed contraction. Of the 83 expanded gene families, a total of 134 genes were enriched in several pathways within the KEGG analysis (**Table S12**). The genes were notably enriched in metabolic pathways, followed by biosynthesis of secondary metabolites and RNA transport (**Table S12**).

Comparative Genomics and Putatively Involved in Pathogenicity With the PHI Database

For comparison of the three strains of *P. wickerhamii*, NUCmer v3.1 generated a total of 799 contig alignments between S1 and S931 averaging at 96.35% identity. 478 contig alignments were generated for S1 and ATCC 16529 with a sequence identity of 96.27%. The results of the sequence alignments showed highly conserved collinearity (**Figure S9**). Within the alignment results, a total of 94,236 SNPs were detected between strains S1 and S931 (**Table S13**). For the three sets of SNP comparisons in *P. wickerhamii*, 59.87%, 61.91%, and 58.60% were transitions in S1 vs. S931, S1 vs. ATCC 16529, and ATCC 16529 vs. S931, respectively, and the rate of transitions was higher than that of transversions (transition/transversion ratios ranged from 1.415 to 1.625) (**Table S13**). The SNP C/T was the most common (~30%) and A/T the least common (below 7.3%) substitution

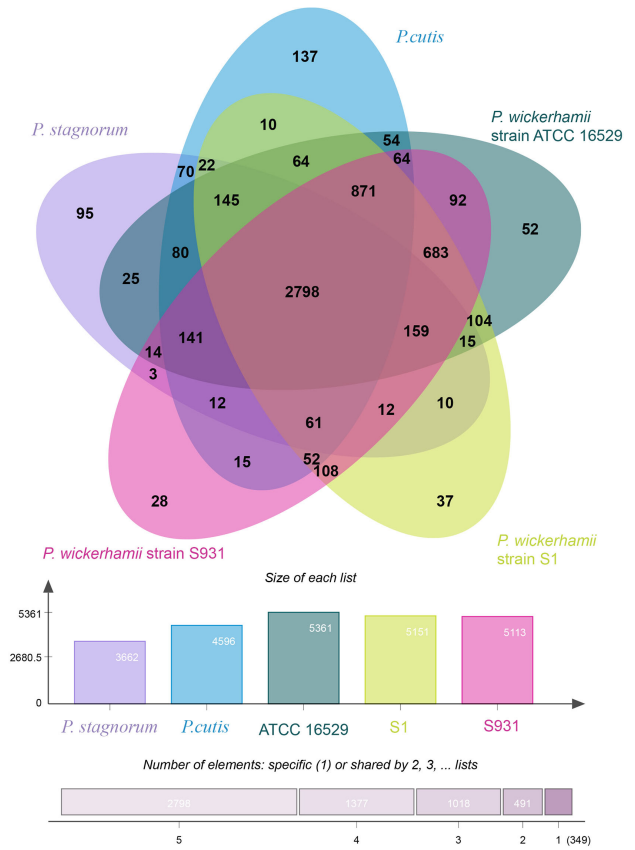

FIGURE 2 | Distribution of gene families in *P. wickerhamii* strain S1, *P. wickerhamii* strain S931, *P. wickerhamii* strain ATCC 16529, *P. cutis, and P. stagnorum*. Homologous genes in the five species were clustered into gene families. Numbers indicate unique and shared gene families in each species.

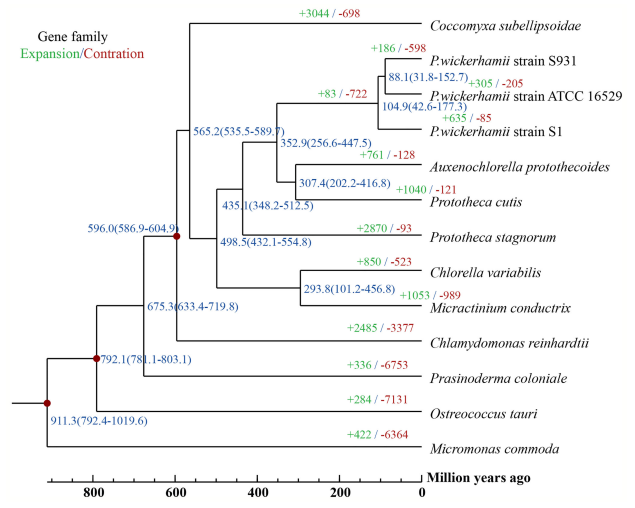

FIGURE 3 | A Phylogenetic tree and gene family expansion and contraction among 13 species. Node labels represent node ages. Expansion/contraction of gene families is shown in green and red.

observed, which is different in comparison to findings in higher plant species (Lu et al., 2021).

To evaluate potential pathogenicity-associated genes in the *Prototheca* genomes, genome-wide protein BLAST analysis against the Pathogen Host Interaction (PHI) database was performed. The abundances of protein-coding genes identified as orthologs to PHI genes were similar among the five *Prototheca* strains and ranged from 1,578 in *P. stagnorum*, 1,744 in *P. wickerhamii* strain S1, 1,775 in *P. wickerhamii* strain ATCC 16529, and 1,789 in *P. wickerhamii* strain S931 to 1,791 *P. cutis*. A total of 2,195 PHI-database genes were matched in all five *Prototheca* genomes: 1,088 genes were annotated with "reduced virulence," 474 with "unaffected pathogenicity," 175 with "loss of pathogenicity," and 35 with both "reduced virulence" and "loss of pathogenicity" (**Supplementary Material 1**). A total of 23 KOG functional categories were annotated with "reduced virulence," "unaffected pathogenicity," and "loss of pathogenicity" in S1 and S931 (**Figure 4**). The most abundant KOG categories were posttranslational modification, protein turnover, chaperones, and signal transduction mechanisms. A total of 62 PHI genes were highly represented with ≥10 hits among all the five genomes. The pathogen gene encoding MoTup1 (PHI:4475), a general transcriptional repressor, resulted in the highest number of 499 total hits in the *Prototheca* genomes. MoTup1 is required for dimorphism and virulence in a fungal plant pathogen (Chen et al., 2015). The second most abundant hits were obtained for CaTUP1 (PHI:211) and tup1 (PHI:6806), which are associated with transcription factors and transcriptional repressors, respectively, suggesting that transcriptional regulation might be important for the *Prototheca* pathogenesis.

Difference in Gene Expression Between Strain S1 and S931

To identify unique features in the pathogenicity of the two *P. wickerhamii* strains S1 and S931, comparative transcriptomic

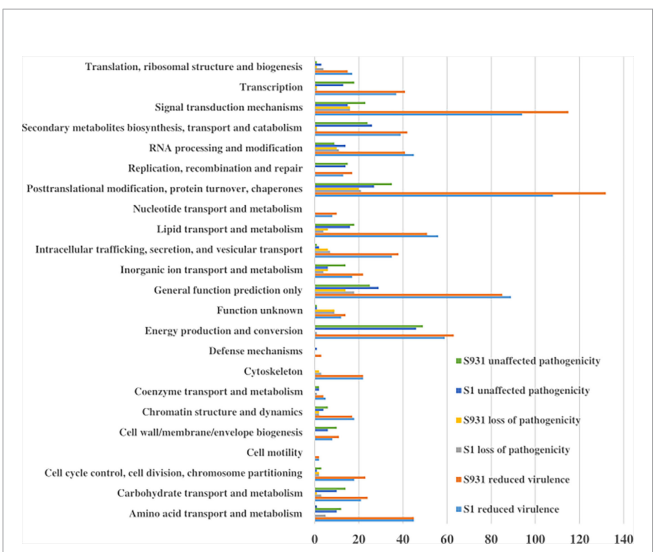

FIGURE 4 | The KOG functional categories for "reduced virulence," "unaffected pathogenicity," and "loss of pathogenicity" in S1 and S931.

analysis of six samples (three biological replicates of each strain, S1 and S931) was performed. A total of 25.9 and 20.4 Gb high-quality data (with the adaptors removed and low-quality data filtered out) were obtained, and approximately 38.55% and 34.91% reads could be mapped to the genes of the *P. wickerhamii* genomes of S1 and S931, respectively. A total of 3,786 differentially expressed genes (DEGs) were identified in the two strains. 1,887 genes were upregulated, and 1,899 genes were downregulated in S1 compared to S931 (**Figure S10**). With integration of the PHI database and InterPro annotation, 413 upregulated and 426 downregulated genes could be annotated in the datasets. The highest upregulated gene (Maker00004366) was annotated with the function of an integral membrane component (GO:0016021) and as *satP* gene (PHI:9230) encoding a symporter involved in the pathogenicity of *Escherichia coli*. The highest downregulated gene (Maker00001286) was annotated with three GOs, namely, protein kinase activity (GO:0004672), ATP binding (GO:0005524), and protein phosphorylation (GO:0006468). This gene was also matched with several PHI genes including PHI:1239 (FGSG_02399), PHI:1230(FGSG_06959), PHI:1186(Sc_Cdc15), PHI:1241(FGSG_00469), and PHI:1257 (FGSG_07121) associated with pathogenicity of *Fusarium graminearum*. These DEGs could play a role in the unique metabolic or pathogenic strategies of each strain during growth and infection.

DISCUSSION

The investigation of molecular epidemiology of *P. wickerhamii* is still limited. There were only a few studies including *P. wickerhamii* drug susceptibility tests and unrooted phylogenetic trees which were based on nuclear rDNA transcriptional units (Falcaro et al., 2021). *In vitro, P. wickerhamii* was generally susceptible to amphotericin and had variable susceptibility to triazoles (McMullan et al., 2016). The *Prototheca* CYP51/ERG11 and fungal CYP51/ERG11 were phylogenetically different from each other (Watanabe et al., 2021). Antifungal azoles had been used for the empirical treatment of protothecosis (Inoue et al., 2018). *In vitro*, the drug susceptibility tests of clinical and environmental isolates of *P. wickerhamii* to itraconazole (ITZ), voriconazole (VRZ), posaconazole (PCZ), and ravuconazole (RVZ) were different. RVZ was more effective than the other azoles against *Prototheca* species (Miura et al., 2020).

Prototheca genomes contain multiple copies of nuclear rDNA transcriptional units, each of which consists of an 18S small subunit (SSU) rDNA, 26S/28S large subunit (LSU) rDNA, ITS1, ITS2, and 5.8S rDNA (Hirose et al., 2013). The analysis of the *P. wickerhamii* 28S rRNA sequences revealed higher heterogeneity than cytb mitochondrial DNA sequences. A partial cytochrome b (CYTB) gene sequences had been used for identification of *P. wickerhamii* previously (Falcaro et al., 2021). The nucleotide sequences were heterogeneously different in rDNA copies of *P. wickerhamii* ITS, which might be useful for the intraspecies genotypic classification (Hirose et al., 2013). The *P. wickerhamii* ITS sequences could be grouped into four distinct clades (A to D). However, all of the strains examined only had the ITS of clades C and D (Hirose et al., 2013). The *P. wickerhamii* strains could be classified into at least two genotypes depending on ITS clades. Genotype 1 represented ITS clades A and B, and genotype 2 represented ITS clades C and D. The SSU rDNA of *P. wickerhamii* were very variable. Thus, the SSU-based intraspecies genotyping would be very difficult.

In this study, we compared two clinical strains of *P. wickerhamii* isolated in China for their rDNA by PCR and nucleotide sequencing. We obtained two *P. wickerhamii* genomes of strain S1 (17.57 Mb) and strain S931 (17.45 Mb). Assessing the assembly with two software tools, the Necat assembly resulted in a higher genome quality and completeness. The newly assembled genomes of both strains were nearly 1 Mb larger than the previously published genome of the type strain ATCC 16529 (16.7 Mb) (Bakula et al., 2021). Also, percentages of repetitive elements were slightly higher than for ATCC 16529 (Bakula et al., 2021). The greater abundance of repetitive elements might explain the higher assembled genome size with a higher level of genome quality and completeness. The small assembled genome size and low content of repetitive elements suggest that the *P. wickerhamii* genome is one of the smallest and most compact microalgal genomes.

The genus of *Prototheca* is the only algae to be involved in a series of clinically relevant opportunistic infections in humans and animals (Kwiecinski, 2015). Most human pathogenic cases are caused by *P. wickerhamii*, which suggests that this species may have undergone an evolutionary specification process. The pathogenicity may come from the horizontal gene transfer or new evolutionary functions acquired. So far, genomic information on *Prototheca* has been limited and previous analysis of plastid genomes suggested that *P. wickerhamii* and its closest photosynthetic relative *A. protothecoides* diverged 6–20 Mya (Yan et al., 2015). In contrast, our analysis based on the nuclear genomes suggests an even earlier divergence from a common ancestor at around 350 Mya. Phylogenetically, *A. protothecoides* is however still placed within the clade of *Prototheca*, which opens up interesting questions about the loss of photosynthesis and the evolution of protothecosis in *Prototheca*.

The three strains of *P. wickerhamii* were classified in the same clade. Although the collinearity of sequence alignment showed high sequence consistency between the strains, the detected SNPs may be used as a resource for the identification.

A comparison of the *Prototheca* genomes against the Pathogen Host Interaction (PHI) identified potential pathogenicity-associated genes that were enriched highly in the KOG functional categories of posttranslational modification, protein turnover, chaperones, and signal transduction mechanisms. These functional genes included those involved in the ATP-binding cassette (ABC) transporter, which could be linked to nutrient uptake, drug resistance, or bacterial pathogenesis. Three DnaJ (PHI:10485, PHI:4733, and PHI:6986) genes were annotated with heat shock protein and enriched in the PI3K 383 and JNK signaling pathways. These results were similar with the previous report in the *P. bovis*-induced infections (Murugaiyan et al., 2016). The pathogen gene encoding MoTup1 resulted in the highest abundance of hits in *Prototheca* and has important regulatory roles in the growth and development of fungi (Chen et al., 2015). These results agree with a

previous study indicating that putative pathogenicity genes in *Prototheca* are similar to those in fungi (Bakula et al., 2021). Also, annotation of the high DEGs in S1 and S931 suggests similarities to fungal pathogenicity. The two types of *P. wickerhamii* strains showed different culture phenotypes. The sporophyte of strain S1 (mucoid colony) was smaller than that of strain S931 (rough colony). The metabolic or pathogenic strategies may be caused by these DEGs.

CONCLUSION

In this study, we assembled the high-quality mitochondrial (mtDNA), plastid (ptDNA), and nuclear genomes of two *P. wickerhamii* strains. Both mtDNA and ptDNA genome sequences were assembled in one circular contig. The nuclear genomes of strain S1 (17.57 Mb with 19 contigs) and S931 (17.45 Mb with 26 contigs) were nearly at the chromosome level. The comparative genomics and evolutionary analysis showed that the genus of *Prototheca* was closely related to *A. protothecoides* and diverged from *Chlorella* 500 Mya. The species-specific differences in the genetics, pathogenicity, and differentially expressed genes of the *P. wickerhamii* strains have been discovered. The high-quality genomes provide a valuable reference for the evolutionary and pathogenicity studies of *Prototheca* and provide genomic resources for the diagnosis of protothecosis.

DATA AVAILABILITY STATEMENT

The datasets presented in this study can be found in online repositories. The names of the repository/repositories and accession number(s) can be found in the article/**Supplementary Material**.

ETHICS STATEMENT

The studies involving human participants were reviewed and approved by the ethics committee of Shanghai East Hospital, Tongji University School of Medicine (No. 2020-163). Written informed consent for participation was not required for this study in accordance with the national legislation and the institutional requirements.

AUTHOR CONTRIBUTIONS

WW and ES: conception and design. JG, JJ, and LW: whole-genome sequencing and data analysis. LX, HL, ZZ, and ES: data analysis and interpretation. All authors: collection and assembly of data, manuscript writing, and final approval of manuscript. All authors contributed to the article and approved the submitted version.

FUNDING

This work was supported by the National Natural Science Foundation [grant number 81971990], Key Discipline of Public Health in Shanghai [grant number GWV-10.1-XK04], Excellent Technology Leader in Shanghai [grant number 20XD1434500], and Novo Nordisk Foundation [grant number NNF20OC0064249].

SUPPLEMENTARY MATERIAL

The Supplementary Material for this article can be found online at: https://www.frontiersin.org/articles/10.3389/fcimb.2022.797017/full#supplementary-material

REFERENCES

Ashburner, M., Ball, C. A., Blake, J. A., Botstein, D., Butler, H., Cherry, J. M., et al. (2000). Gene Ontology: Tool for the Unification of Biology. The Gene Ontology Consortium. *Nat. Genet.* 25, 25–29. doi: 10.1038/75556

Altschul, S. F., Gish, W., Miller, W., Myers, E. W., and Lipman, D. J. (1990). Basic Local Alignment Search Tool. *J. Mol. Biol.* 215, 403–410. doi: 10.1016/S0022-2836(05)80360-2

Bakula, Z., Gromadka, R., Gawor, J., Siedlecki, P., Pomorski, J. J., Maciszewski, K., et al. (2020). Sequencing and Analysis of the Complete Organellar Genomes of Prototheca Wickerhamii. *Front. Plant Sci.* 11, 1296. doi: 10.3389/fpls.2020.01296

Bakula, Z., Siedlecki, P., Gromadka, R., Gawor, J., Gromadka, A., Pomorski, J. J., et al. (2021). A First Insight Into the Genome of Prototheca Wickerhamii, a Major Causative Agent of Human Protothecosis. *BMC Genomics* 22, 168. doi: 10.1186/s12864-021-07491-8

Bao, W., Kojima, K. K., and Kohany, O. (2015). Repbase Update, a Database of Repetitive Elements in Eukaryotic Genomes. *Mobile DNA* 6, 1–6. doi: 10.1186/s13100-015-0041-9

Chen, Y., Chen, Y., Shi, C., Huang, Z., Zhang, Y., Li, S., et al. (2018). SOAPnuke: A MapReduce Acceleration-Supported Software for Integrated Quality Control and Preprocessing of High-Throughput Sequencing Data. *Gigascience* 7, 1–6. doi: 10.1093/gigascience/gix120

Chen, Y., Nie, F., Xie, S. Q., Zheng, Y. F., Dai, Q., Bray, T., et al. (2021). Efficient Assembly of Nanopore Reads *via* Highly Accurate and Intact Error Correction. *Nat. Commun.* 12, 60. doi: 10.1038/s41467-020-20236-7

Chen, Y., Zhai, S., Sun, Y., Li, M., Dong, Y., Wang, X., et al. (2015). MoTup1 is Required for Growth, Conidiogenesis and Pathogenicity of Magnaporthe Oryzae. *Mol. Plant Pathol.* 16, 799–810. doi: 10.1111/mpp.12235

De Bie, T., Cristianini, N., Demut, J. P., and Hahn, M. W. (2006). CAFE: A Computational Tool for the Study of Gene Family Evolution. *Bioinformatics* 22, 1269–1271. doi: 10.1093/bioinformatics/btl097

Delcher, A. L., Salzberg, S. L., and Phillippy, A. M. (2003). Using MUMmer to Identify Similar Regions in Large Sequence Sets. *Curr. Protoc. Bioinf. Chapter 10 Unit* 10, 13. doi: 10.1002/0471250953.bi1003s00

Ewing, A., Brubaker, S., Somanchi, A., Yu, E., Rudenko, G., Reyes, N., et al. (2014). 16S and 23S Plastid rDNA Phylogenies of Prototheca Species and Their Auxanographic Phenotypes. *J. Phycol.* 50, 765–769. doi: 10.1111/jpy.12209

Falcaro, C., Furlanello, T., Binanti, D., Fondati, A., Bonfanti, U., Krockenberger, M., et al. (2021). Molecular Characterization of Prototheca in 11 Symptomatic Dogs. *J. Vet. Diagn. Invest.* 33, 156–161. doi: 10.1177/1040638720976423

Flynn, J. M., Hubley, R., Goubert, C., Rosen, J., Clark, A. G., Feschotte, C., et al. (2020). RepeatModeler2 for Automated Genomic Discovery of Transposable Element Families. *Proc. Natl. Acad. Sci.* 117, 9451–9457. doi: 10.1073/pnas.1921046117

Hirose, N., Nishimura, K., Inoue-Sakamoto, M., and Masuda, M. (2013). Ribosomal Internal Transcribed Spacer of Prototheca Wickerhamii Has Characteristic Structure Useful for Identification and Genotyping. *PLoS One* 8, e81223. doi: 10.1371/journal.pone.0081223

Holt, C., and Yandell, M. (2011). MAKER2: An Annotation Pipeline and Genome-Database Management Tool for Second-Generation Genome Projects. *BMC Bioinf.* 12, 491. doi: 10.1186/1471-2105-12-491

Inoue, M., Miyashita, A., Noguchi, H., Hirose, N., Nishimura, K., Masuda, M., et al. (2018). Case Report of Cutaneous Protothecosis Caused by Prototheca

Wickerhamii Designated as Genotype 2 and Current Status of Human Protothecosis in Japan. *J. Dermatol.* 45, 67–71. doi: 10.1111/1346-8138.14010

Jagielski, T., Bakvba, Z., Gawor, J., Maciszewski, K., Kusber, W.-H., Dyl G, M., et al. (2019). The Genus Prototheca (Trebouxiophyceae, Chlorophyta) Revisited: Implications From Molecular Taxonomic Studies. *Algal Res.* 43, 1–19. doi: 10.1016/j.algal.2019.101639

Jagielski, T., Gawor, J., Bakula, Z., Zuchniewicz, K., Zak, I., and Gromadka, R. (2017). An Optimized Method for High Quality DNA Extraction From Microalga Prototheca Wickerhamii for Genome Sequencing. *Plant Methods* 13, 77. doi: 10.1186/s13007-017-0228-9

Jian, J., Zeng, D., Wei, W., Lin, H., Li, P., and Liu, W. (2017). The Combination of RNA and Protein Profiling Reveals the Response to Nitrogen Depletion in Thalassiosira Pseudonana. *Sci. Rep.* 7, 8989. doi: 10.1038/s41598-017-09546-x

Jung, J., Kim, J. I., Jeong, Y. S., and Yi, G. (2018). AGORA: Organellar Genome Annotation From the Amino Acid and Nucleotide References. *Bioinformatics* 34, 2661–2663. doi: 10.1093/bioinformatics/bty196

Katoh, K., and Standley, D. M. (2013). MAFFT Multiple Sequence Alignment Software Version 7: Improvements in Performance and Usability. *Mol Biol. Evol.* 30, 772–780. doi: 10.1093/molbev/mst010

Kent, W. J. (2002). BLAT–the BLAST-Like Alignment Tool. *Genome Res.* 12, 656–664. doi: 10.1101/gr.229202

Khan, I. D., Sahni, A. K., Sen, S., Gupta, R. M., and Basu, A. (2018). Outbreak of Prototheca Wickerhamii Algaemia and Sepsis in a Tertiary Care Chemotherapy Oncology Unit. *Med. J. Armed Forces India* 74, 358–364. doi: 10.1016/j.mjafi.2017.07.012

Koonin, E. V., Fedorova, N. D., Jackson, J. D., Jacobs, A. R., Krylov, D. M., Makarova, K. S., et al. (2004). A Comprehensive Evolutionary Classification of Proteins Encoded in Complete Eukaryotic Genomes. *Genome Biol.* 5, R7. doi: 10.1186/gb-2004-5-2-r7

Koren, S., Walenz, B. P., Berlin, K., Miller, J. R., Bergman, N. H., and Phillippy, A. M. (2017). Canu: Scalable and Accurate Long-Read Assembly via Adaptive k-mer Weighting and Repeat Separation. *Genome Res.* 27, 722–736. doi: 10.1101/gr.215087.116

Korf, I. (2004). Gene Finding in Novel Genomes. *BMC Bioinf.* 5, 1–9. doi: 10.1186/1471-2105-5-59

Kwiecinski, J. (2015). Biofilm Formation by Pathogenic Prototheca Algae. *Lett. Appl. Microbiol.* 61, 511–517. doi: 10.1111/lam.12497

Leimann, B. C., Monteiro, P. C., Lazera, M., Candanoza, E. R., and Wanke, B. (2004). Protothecosis. *Med. Mycol* 42, 95–106. doi: 10.1080/13695780310001653653

Li, L., Stoeckert, C. J.Jr., and Roos, D. S. (2003). OrthoMCL: Identification of Ortholog Groups for Eukaryotic Genomes. *Genome Res.* 13, 2178–2189. doi: 10.1101/gr.1224503

Li, H., and Durbin, R. (2009). Fast and Accurate Short Read Alignment With Burrows-Wheeler Transform. *Bioinformatics* 25, 1754–1760. doi: 10.1093/bioinformatics/btp324

Love, M. I., Huber, W., and Anders, S. (2014). Moderated Estimation of Fold Change and Dispersion for RNA-Seq Data With Deseq2. *Genome Biol.* 15, 550. doi: 10.1186/s13059-014-0550-8

Lu, Z., Cui, J., Wang, L., Teng, N., Zhang, S., Lam, H. M., et al. (2021). Genome-Wide DNA Mutations in Arabidopsis Plants After Multigenerational Exposure to High Temperatures. *Genome Biol.* 22, 160. doi: 10.1186/s13059-021-02381-4

Marcais, G., and Kingsford, C. (2011). A Fast, Lock-Free Approach for Efficient Parallel Counting of Occurrences of K-Mers. *Bioinformatics* 27, 764–770. doi: 10.1093/bioinformatics/btr011

McMullan, B., Pollett, S., Biswas, C., and Packham, D. (2016). Successful Treatment of Cutaneous Protothecosis With Liposomal Amphotericin and Oral Itraconazole. *Med. Mycol. Case Rep.* 12, 21–23. doi: 10.1016/j.mmcr.2016.08.001

Miura, A., Kano, R., Ito, T., Suzuki, K., and Kamata, H. (2020). *In Vitro* Algaecid Effect of Itraconazole and Ravuconazole on Prototheca Species. *Med. Mycol.* 58, 845–847. doi: 10.1093/mmy/myz119

Mulder, N., and Apweiler, R. (2007). InterPro and InterProScan: Tools for Protein Sequence Classification and Comparison. *Methods Mol. Biol.* 396, 59–70. doi: 10.1007/978-1-59745-515-2_5

Murugaiyan, J., Eravci, M., Weise, C., and Roesler, U. (2016). Label-Free Quantitative Proteomic Analysis of Harmless and Pathogenic Strains of Infectious Microalgae, Prototheca Spp. *Int. J. Mol. Sci.* 18, 59. doi: 10.3390/ijms18010059

Saha, S., Bridges, S., Magbanua, Z. V., and Peterson, D. G. (2008). Empirical Comparison of Ab Initio Repeat Finding Programs. *Nucleic Acids Res.* 36, 2284–2294. doi: 10.1093/nar/gkn064

Severgnini, M., Lazzari, B., Capra, E., Chessa, S., Luini, M., Bordoni, R., et al. (2018). Genome Sequencing of Prototheca Zopfii Genotypes 1 and 2 Provides Evidence of a Severe Reduction in Organellar Genomes. *Sci. Rep.* 8, 14637. doi: 10.1038/s41598-018-32992-0

Simao, F. A., Waterhouse, R. M., Ioannidis, P., Kriventseva, E. V., and Zdobnov, E. M. (2015). BUSCO: Assessing Genome Assembly and Annotation Completeness With Single-Copy Orthologs. *Bioinformatics* 31, 3210–3212. doi: 10.1093/bioinformatics/btv351

Stanke, M., Schöffmann, O., Morgenstern, B., and Waack, S. (2006). Gene Prediction in Eukaryotes With a Generalized Hidden Markov Model That Uses Hints From External Sources. *BMC Bioinf.* 7, 1–11. doi: 10.1186/1471-2105-7-62

Suzuki, S., Endoh, R., Manabe, R. I., Ohkuma, M., and Hirakawa, Y. (2018). Multiple Losses of Photosynthesis and Convergent Reductive Genome Evolution in the Colourless Green Algae Prototheca. *Sci. Rep.* 8, 940. doi: 10.1038/s41598-017-18378-8

Todd, J. R., Matsumoto, T., Ueno, R., Murugaiyan, J., Britten, A., King, J. W., et al. (2018). Medical Phycology 2017. *Med. Mycol* 56, S188–S204. doi: 10.1093/mmy/myx162

Trapnell, C., Williams, B. A., Pertea, G., Mortazavi, A., Kwan, G., Van Baren, M. J., et al. (2010). Transcript Assembly and Quantification by RNA-Seq Reveals Unannotated Transcripts and Isoform Switching During Cell Differentiation. *Nat. Biotechnol.* 28, 511–515. doi: 10.1038/nbt.1621

Urban, M., Cuzick, A., Seager, J., Wood, V., Rutherford, K., Venkatesh, S. Y., et al. (2020). PHI-Base: The Pathogen-Host Interactions Database. *Nucleic Acids Res.* 48, D613–D620. doi: 10.1093/nar/gkz904

Vaser, R., Sovic, I., Nagarajan, N., and Sikic, M. (2017). Fast and Accurate *De Novo* Genome Assembly From Long Uncorrected Reads. *Genome Res.* 27, 737–746. doi: 10.1101/gr.214270.116

Vurture, G. W., Sedlazeck, F. J., Nattestad, M., Underwood, C. J., Fang, H., Gurtowski, J., et al. (2017). GenomeScope: Fast Reference-Free Genome Profiling From Short Reads. *Bioinformatics* 33, 2202–2204. doi: 10.1093/bioinformatics/btx153

Walker, B. J., Abeel, T., Shea, T., Priest, M., Abouelliel, A., Sakthikumar, S., et al. (2014). Pilon: An Integrated Tool for Comprehensive Microbial Variant Detection and Genome Assembly Improvement. *PLoS One* 9, e112963. doi: 10.1371/journal.pone.0112963

Watanabe, T., Ishikawa, T., Sato, H., Hirose, N., Nonaka, L., Matsumura, K., et al. (2021). Characterization of Prototheca CYP51/ERG11 as a Possible Target for Therapeutic Drugs. *Med. Mycol.* 59, 855–863. doi: 10.1093/mmy/myab012

Xu, Z., and Wang, H. (2007). LTR_FINDER: An Efficient Tool for the Prediction of Full-Length LTR Retrotransposons. *Nucleic Acids Res.* 35, W265–W268. doi: 10.1093/nar/gkm286

Yan, D., Wang, Y., Murakami, T., Shen, Y., Gong, J., Jiang, H., et al. (2015). Auxenochlorella Protothecoides and Prototheca Wickerhamii Plastid Genome Sequences Give Insight Into the Origins of Non-Photosynthetic Algae. *Sci. Rep.* 5, 14465. doi: 10.1038/srep14465

Zeng, X., Kudinha, T., Kong, F., and Zhang, Q. Q. (2019). Comparative Genome and Transcriptome Study of the Gene Expression Difference Between Pathogenic and Environmental Strains of Prototheca Zopfii. *Front. Microbiol.* 10, 443. doi: 10.3389/fmicb.2019.00443

Conflict of Interest: The authors declare that the research was conducted in the absence of any commercial or financial relationships that could be construed as a potential conflict of interest.

Publisher's Note: All claims expressed in this article are solely those of the authors and do not necessarily represent those of their affiliated organizations, or those of the publisher, the editors and the reviewers. Any product that may be evaluated in this article, or claim that may be made by its manufacturer, is not guaranteed or endorsed by the publisher.

frontiers in Cellular and Infection Microbiology

ORIGINAL RESEARCH
published: 18 February 2022
doi: 10.3389/fcimb.2022.810604

Molecular Characteristics of Regional Chromoblastomycosis in Guangdong, China: Epidemiological, Clinical, Antifungal Susceptibility, and Serum Cytokine Profiles of 45 Cases

Hongfang Liu[1,2†], Jiufeng Sun[3†], Minying Li[1], Wenying Cai[4], Yangxia Chen[1], Yinghui Liu[1], Huan Huang[1], Zhenmou Xie[1], Weiying Zeng[1] and Liyan Xi[1,4,5]*

[1] Dermatology Hospital, Southern Medical University, Guangzhou, China, [2] Guangdong Dermatology Hospital of Anhui Medical University, Guangzhou, China, [3] Guangdong Provincial Institute of Public Health, Guangdong Provincial Center for Disease Control and Prevention, Guangzhou, China, [4] Sun Yat-sen Memorial Hospital of Zhongshan University, Guangzhou, China, [5] Department of Dermatology and Venerology, Guangzhou First People's Hospital, Guangzhou, China

Chromoblastomycosis (CBM) is a chronic disease caused by several species of dematiaceous fungi. In this study, a regional collection of 45 CBM cases was conducted in Guangdong, China, a hyper-endemic area of CBM. Epidemiology findings indicated that the mean age of cases was 61.38 ± 11.20 years, long duration ranged from 3 months to 30 years, and the gender ratio of male to female was 4.6:1. Thirteen cases (29%) declared underlying diseases. Verrucous form was the most common clinical manifestation (n = 19, 42%). Forty-five corresponding clinical strains were isolated, and 28 of them (62%) were identified as *F. monophora*; the remaining 17 (38%) were identified as *F. nubica* through ITS rDNA sequence analysis. Antifungal susceptibility tests *in vitro* showed low MICs in azoles (PCZ 0.015–0.25 μg/ml, VCZ 0.015–0.5 μg/ml, and ITZ 0.03–0.5 μg/ml) and TRB (0.015–1 μg/ml). Itraconazole combined with terbinafine was the main therapeutic strategy used for 31 of 45 cases, and 68% (n = 21) of them improved or were cured. Cytokine profile assays indicated upregulation of IL-4, IL-7, IL-15, IL-11, and IL-17, while downregulation of IL-1RA, MIP-1β, IL-8, and IL-16 compared to healthy donors ($p < 0.05$). The abnormal cytokine profiles indicated impaired immune response to eliminate fungus in CBM cases, which probably contributed to the chronic duration of this disease. In conclusion, we investigated the molecular epidemiological, clinical, and laboratory characteristics of CBM in Guangdong, China, which may assist further clinical therapy, as well as fundamental pathogenesis studies of CBM.

Keywords: chromoblastomycosis, ITS rDNA, antifungal susceptibility, *Fonsecaea* spp., cytokine

OPEN ACCESS

Edited by:
G. Sybren De Hoog, Radboud University Nijmegen Medical Centre, Netherlands

Reviewed by:
Ludmila Baltazar, Federal University of Minas Gerais, Brazil
Abdullah M.S. Al-Hatmi, University of Nizwa, Oman

***Correspondence:**
Liyan Xi
xiliyan@mail.sysu.edu.cn

†These authors have contributed equally to this work

Specialty section:
This article was submitted to Fungal Pathogenesis, a section of the journal Frontiers in Cellular and Infection Microbiology

Received: *07 November 2021*
Accepted: *24 January 2022*
Published: *18 February 2022*

Citation:
Liu H, Sun J, Li M, Cai W, Chen Y, Liu Y, Huang H, Xie Z, Zeng W and Xi L (2022) Molecular Characteristics of Regional Chromoblastomycosis in Guangdong, China: Epidemiological, Clinical, Antifungal Susceptibility, and Serum Cytokine Profiles of 45 Cases. Front. Cell. Infect. Microbiol. 12:810604. doi: 10.3389/fcimb.2022.810604

INTRODUCTION

Chromoblastomycosis (CBM) is a chronic cutaneous and subcutaneous fungal infection disease caused by several species of dematiaceous fungi, and mainly distributed in tropical and subtropical areas worldwide. In 2017, CBM was first recognized as a neglected tropical disease by the World Health Organization (WHO, 2017). The etiological agents of CBM are mainly related to the genera *Cladophialophora*, *Phialophora*, and *Fonsecaea* (Ameen, 2010). Incidence of CBM usually follows a trauma with a contaminated organic material such as plant thorns, wood, plant debris, grass, and tree cortex, leading to the implantation of the fungus in the subcutaneous tissues, where the fungus changes from mycelial form to its parasitic form composed of muriform cells. The muriform cells are the key to CBM development, which are extremely resistant to the harsh conditions imposed by the host immune system (Queiroz-Telles et al., 2017).

Fonsecaea are the most common pathogens of CBM (Najafzadeh et al., 2011), including four clinical related species, *F. pedrosoi*, *F. nubica*, *F. monophora*, and *F. pugnacius*. Although the morphology of these four species is extremely similar, the pathogenicity is different from each other. *F. pedrosoi* and *F. nubica* appear to be exclusively associated with CBM under skin (De Hoog et al., 2004), whereas *F. monophora* and *F. pugnacius* were found to gain a much wider tissue tropism, e.g., brain, gallbladder and lymph node (Saberi et al., 2003; Surash et al., 2005; de Azevedo et al., 2015). The archived studies indicated that the clinical manifestations of CBM could be classified into 6 types (clinic, nodular, plaque, verrucous, tumor, cicatricial, and mixed form) and three stages (mild, moderate, and severe form) (Queiroz-Telles et al., 2017). The clinic treatment of CBM is quite challenging; there is no universal treatment protocol that could be followed. Many modalities, including antifungals, immunomodulatory therapy, physical methods, photodynamic therapy (PDT), and surgical excision, have been used solely or combined for the treatment of CBM in previous reports (Paniz-Mondolfi et al., 2008; Zhang et al., 2009; Queiroz-Telles and Santos, 2013; de Sousa et al., 2014; Hu et al., 2019; Huang et al., 2019). So far, itraconazole (ITC) and terbinafine (TRB) are the most commonly used antifungal drugs in the treatment of CBM (Lopez and Mendez, 2007; Daboit et al., 2013; Daboit et al., 2014).

The host defense mechanisms in CBM are still poorly understood (Seyedmousavi et al., 2014). Several studies demonstrated that both innate and adaptive immune responses are required for effective containment of infections (Sousa et al., 2011). Initially, Mazo et al. (2005) demonstrated that the severity of CBM correlated with the balance of TH1 and the TH2 immune response. Another study manifested that Treg/Th17 imbalance in CBM patients decreased local immune response to the fungus (Silva et al., 2014). In our previous studies, we found that the melanization of *F. monophora* probably inhibited production of nitric oxide and T helper cell type I cytokines in murine macrophages, and enhanced persistence of the agent in both *in vitro* and *in vivo* (Zhang et al., 2013; Jiang et al., 2018). However, the detailed immune response against fungus remains unclear.

Given the different clinical manifestations of CBM cases, variable causative agents, and poorly understood immune response, there is a great need to explore the real situation in different endemic areas of CBM. In this study, a regional collection of 45 CBM cases was from the Dermatology Hospital of Southern Medical University during 2016 to 2021, aiming to investigate the epidemiology characteristics, evaluate the susceptibility of antifungal agents against isolates *in vitro*, and clarify the cytokine profiles of these CBM cases in Guangdong, China, a hyper-endemic area of CBM.

MATERIALS AND METHODS

Clinical Data of Chromoblastomycosis Cases

All of the 45 diagnosed CBM cases who visited the Dermatology Hospital of Southern Medical University from 2016 to 2021 were enrolled in this study. The detailed clinical data (age, sex, site of predilection, etiologic agent, trauma, underlying disease, time of evolution, severity, lesion type, treatment, and outcome) of CBM cases were collected (**Table S1**, Clinical Data of 45 cases of Chromoblastomycosis). The procedure associated with patients was approved by the Ethics Committee Board of Dermatology Hospital of Southern Medical University.

Isolation and Morphology Identification

The skin lesion of each patient was taken and checked under a microscope when they visited our hospital the first time, and then sent for further culture on sabouraud dextrose agar (SDA) at 26°C for 2 weeks. The suspect colonies were taken and morphologically identified under a microscope. The pure cultured isolates were grown at 26°C on both SDA and potato dextrose agar (PDA) plates for 2 to 3 weeks. Slide cultures were done under the same conditions and checked again with microscopy to confirm the morphology.

Molecular Identification

The morphology-identified pure isolates were cultured again under the above conditions for 2–3 weeks. The fungi were collected (~0.5 g) into a clean microtube (2 ml). The genome DNA was extracted using the protocol adapted from DNA Purification from Yeast (The Gentra Puregene Yeast/Bact. Kit, QIAGEN, Germany). The ITS regions were used for species identification for these isolates. The PCR amplification was performed in T100 Touch Thermal Cycler (Bio-Rad, USA) using primers ITS4 (5′-TCCTCCGCTTATTGATATGC-3′) or ITS1 (TCCGTAGGTGAACCTGCGG) and ITS5 (5′-GGAAGTAAAAGTCGTAACAAGG-3′) in a 50-μl reaction system containing 1 μl of template genome DNA, 25 μl of Taq polymerase (Premix Taq, TaKaRa Taq Version 2.0 plus dye, Japan), 20 μl of ddH_2O, and 2 μl of each primer (10 μM). PCR was conducted with the following conditions: 95°C for 3 min, followed by 34 cycles of 95°C for 30 s, 55°C for 30 s, and 72°C for 1 min and a final extension of 72°C for 5 min. PCR amplicons were

checked using electrophoresis in 1% agarose gel (100 V for 45 min). The positive amplicons were purified and sent to Sangon Biotech (Shanghai, China) for Sanger sequencing as described previously (White et al., 1990; Gauthier, 2007) using the same primers. The homology evaluations were done on the GenBank database using BLAST analysis available at www.ncbi.nlm.nih.gov. All the sequences attained in this study were submitted to the GenBank database under accession numbers listed in **Table S2**, Genbank accession number of 45 clinical strains.

Phylogenetic Analysis

A phylogenetic method was used to explore the relationships among the 45 clinical isolates. ITS sequences were aligned using MUSCLE with a panel of 50 reference strains from the mycobank database (http://www.mycobank.org), and a maximum likelihood (ML) phylogenetic tree was constructed with MEGA 6.0 using the K2+G model with 500 bootstrap replicates. Bootstrap > 70 were considered as consistent support branches.

Antifungal Susceptibility Testing

The Sensititre YeastOne® panel trays containing serial twofold dilutions of anidulafungin (AND, 0.015–8 μg/ml), micafungin (MFG, 0.008–8 μg/ml), caspofungin (CAS, 0.008–8 μg/ml), 5-flucytosine (5-FC, 0.06–64 μg/ml), posaconazole (PCZ, 0.008–8 μg/ml), voriconazole (VCZ, 0.008–8 μg/ml), itraconazole (ITR, 0.015–16 μg/ml), fluconazole (FLU, 0.12–256 μg/ml), and amphotericin B (AMB, 0.12-8 μg/ml) were purchased from Thermo Fisher Company (Shanghai, China). The packages of YeastOne® panels were stored at room temperature until testing was performed. A working conidium suspension of approximately $0.5–5 \times 10^4$ cells/ml was prepared in YeastOne® broth (Trek). Each well of the dried YeastOne® panels was rehydrated with 100 μl of the working conidium suspension delivered by a multichannel pipetting device. The YeastOne® panels were covered with seal strips and incubated at 35°C for 120–144 h in a non-CO_2 incubator. The colorimetric MIC endpoints were determined by visual reading. Fungal growth was evident as a color change from blue (no growth) to red (growth). Colorimetric MIC results for all of the testing drugs were defined as the lowest concentration of antifungal agent that prevented the development of a red color from firstly blue or purple. Because terbinafine (TER) is another commonly used antifungal agent against *Fonsecaea* spp. infection, not involved in YeastOne® method, we used the ClSI method to test its susceptibility according to the reference (M38, Reference Method for Broth Dilution Antifungal Susceptibility Testing of Filamentous Fungi, 3rd Edition). The concentration range of terbinafine was 0.015–8 μg/ml. Reference broth microdilution testing was performed exactly as outlined in the CLSI document with a conidium suspension of 1×10^4 CFU/ml in RPMI 1640 medium buffered to pH 7.0 with 0.165 mol/L morpholinepropanesulfonic acid (MOPS) buffer. The panels were incubated at 35°C and observed for the presence or absence of growth at 120–144 h depending on the growth of each fungus.

Human Serum Cytokine Determination

To evaluate the host immune response to Fonsecaea spp., the serums from 18 of 45 patients and 4 healthy donors were taken before treatment and used for cytokine production screening using protein chip array. The serums of healthy donors were collected from a vaccination project that aimed to collect otherwise healthy donors. The white blood cell, percentage of neutrophil, percentage of lymphocyte, and neutrophil-to-lymphocyte ratio of healthy donors were normal. All protocol of protein chip array reference to Quantibody Human Inflammation Array3 kits to quantitative measurement of 40 human cytokines (RayBiotech, Norcross, GA, USA). This array is a glass slide-based antibody assay that allows us to conduct rapid, accurate expression profiling of 40 human cytokines. Two hundred microliters of each human serum sample was used for this protein chip array. After incubation with serum samples, the cytokines were captured by the antibodies printed on the solid surface of glasses. The slide was blocked, and then washed several times according to the protocol instruction. Then, a second biotin-labeled detection antibody was added to recognize different epitopes of the target cytokines. The signal can be determined through the streptavidin-conjugated Cy3 equivalent dye after scanning by laser fluorescent scanner systems (Axon GenePix, CA, USA). The density of each spot was taken and normalized using Q-analyzer software (no.GSM-CAA-4000-SW).

Statistical Analysis

GraphPad Prism software (version 8.3.0. San Diego, California USA, www.graphpad.com) was used for all statistical analyses. The difference in clinical severity, lesion types, and species distribution was analyzed using Wilcoxon rank sum test and Fisher's exact test. The correlation was tested by Spearman test. Antifungal test data among drugs were tested by Mann–Whitney *U* test and cytokine data were tested by unpaired *t*-test. The error bars indicate standard deviation of the mean. The portion results are presented as the mean ± standard deviation; $p < 0.05$ indicated statistical significance.

RESULTS

Clinical Findings of Chromoblastomycosis Cases

All of the 45 CBM patients come from various cities of Guangdong province. Their clinical characteristics are listed in **Table 1**. The age ranged from 24 to 86 years old (61.38 ± 11.20). The ratio of male to female was 4.6:1. The occupation of 25 cases (56%) was farmer and 17 cases (38%) reported a trauma history. The course of CBM lasted from 3 months to 30 years, while most of the patients (n = 38, 84%) were more than 1 year. Thirteen cases (29%) had underlying diseases, namely, diabetes (n = 3), systemic lupus erythema (n = 2), nephrotic syndrome (n = 1), lung cancer (n = 1), chronic colitis and bronchitis (n = 1), and cardio-cerebral vascular-related diseases (n = 5), and 26 patients (58%) were immunocompetent and denied underlying diseases, while the data of the remaining 7 cases were not available. The most common infection sites occurred in the upper extremity (49%, n = 22), followed by the lower extremity (40%, n = 18) and trunk (11%, n = 5). Verrucous form was the most common clinical presentation for all 45 cases (42%, n = 19), followed by

TABLE 1 | Clinical data of 45 cases of Chromoblastomycosis.

Subject	Type		Data
Age	Average ± STD		61.38 ± 11.20 (24–86 years)
Gender	Male		82% (37/45)
	Female		18% (8/45)
Etiology agent	*F. monophora*		62% (28/45)
	F. nubica		38% (17/45)
Occupation	Farmer		56% (25/45)
	Other		22% (10/45)
	NA		22% (10/45)
Trauma	Y		38% (17/45)
	N		42% (19/45)
	NA		20% (9/45)
Underlying disease	Y		29% (13/45)
	N		58% (26/45)
	NA		13% (6/45)
Duration	Average ± STD		7.10 ± 7.33 years (3 months–30 years)
Sites	Upper extremity		49% (22/45)
	Lower extremity		40% (18/45)
	Trunk		11% (5/45)
Skin lesion	verrucous		42% (19/45)
	Plaque		38% (17/45)
	Cicatricial		7% (3/45)
	Tumorous		2% (1/45)
	Nodular		2% (1/45)
	Mixed form		9% (4/45)
Severity	Mild		29% (13/45)
	Moderate		31% (14/45)
	Severe		40% (18/45)
Treatment	Antifungal agents	ITR+TER	53% (24/45)
		ITR	16% (7/45)
		TER	2% (1/45)
	Combined therapy	ITR+TER+PDT	7% (3/45)
		ITR+TER+Surgery	7% (3/45)
		ITR+Surgery	7% (3/45)
		ITR+TER+Thermotherapy	2% (1/45)
	No treatment		7% (3/45)
Outcome	Cure		7% (3/45)
	Improve		58% (26/45)
	Relapse		11% (5/45)
	Lose follow-up		24% (11/45)
Time of treatment	Months		8.62 ± 9.46 (1–37 months)

NA, not available; ITR, itraconazole; TER, terbinafine; PDT, photodynamic therapy; m, month; y, year.

plaque form (38%, $n = 17$), cicatricial (7%, $n = 3$), tumorous (2%, $n = 1$), nodular (2%, $n = 1$), and mixed form (9%, $n = 4$) of lesions, which were also noted in this study. The classification of severity of CBM was based on type of lesions, size, and extension [3], including 13 mild cases (29%), 14 moderate cases (31%), and 18 severe cases (40%). Oral itraconazole (200 mg/day) in combination with terbinafine (250mg/day) as the initial antifungal therapy was used in 31 cases (69%) solely or combined with other adjunctive therapy (e.g., photodynamic therapy, surgery, and thermotherapy) for 3–6 months. Whether these patients need to be followed by monotherapy of itraconazole or terbinafine as maintenance treatment depended on their clinical outcomes. Among them, 21 cases (68%) improved or were cured. Three patients who received ALA-PDT (5-Aminolaevulinic acid PDT) combined with antifungal agents improved greatly after 3–4 treatment sessions at an interval of 1 week. The duration of treat time recorded in our hospital ranged from 1 to 37 months (mean 8.62 ± 9.46 m). Twenty-six of 45 CBM cases (58%) showed notable improvement, 3 cases had complete remission, 5 cases had relapse, while 11 cases (24%) were lost to follow-up.

Molecular Identification and Phylogenetic Analysis

Among the 45 corresponding clinical isolates identified through ITS rDNA sequence analysis, 28 (62%) were *F. monophora*, and the remaining 17 (38%) were *F. nubica*. The ITS sequencing alignment scores of the fungal isolates herein studied exhibited 99%–100% identity compared with corresponding ITS sequences deposited in the mycobank database (**Figure 1**). There were three major clusters observed in the phylogenetic tree, including *F. pedrosoi*, *F. monophora*, and *F. nubica*. *F. erecta* and *F. brasiliensis* were classified as an outgroup in this study, which indicated a variety of evolution history for different species of *Fonsecaea*. The strains in this study were assigned into the cluster of *F. monophora* ($n = 28$) and *F. nubica* ($n = 17$) with

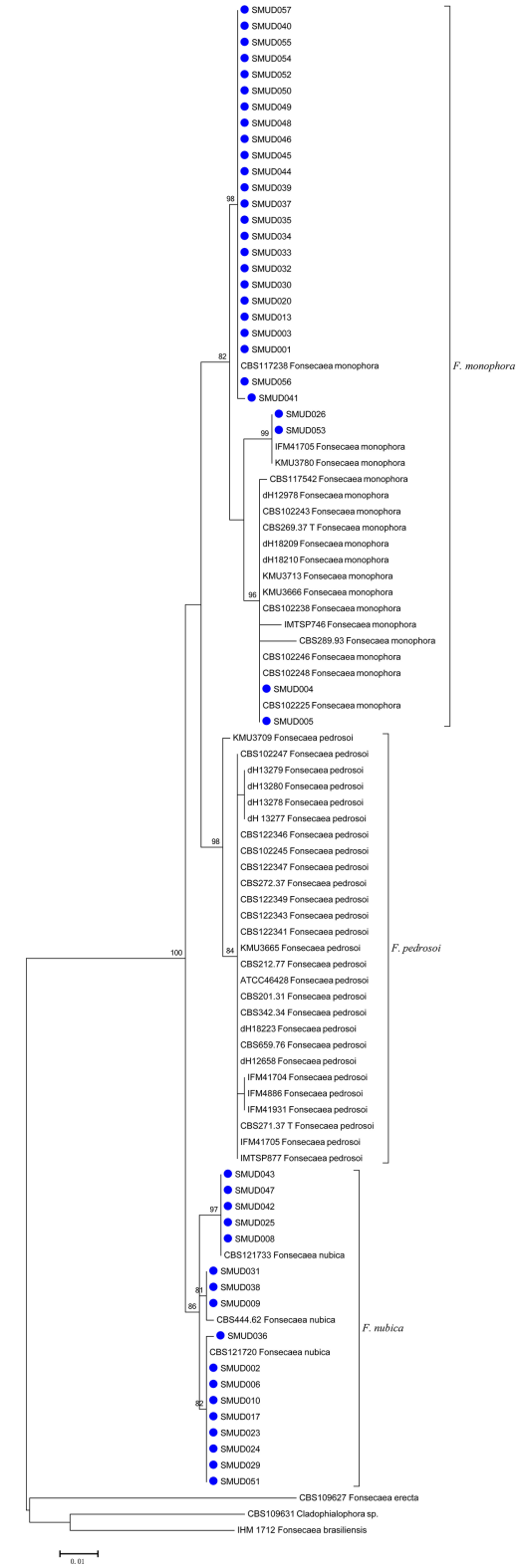

FIGURE 1 | An ITS maximum likelihood (ML) phylogenetic tree of strains isolated in this study. Three species, *F. monophora*, *F. pedrosoi*, and *F. nubica*, were shown in the tree. The tree was constructed with MEGA 6.0 using K2+G model with 500 bootstrap replicates. Bootstrap > 70 were considered as consistent support branches. The strains in this study were marked as a blue dot in tips.

bootstrapsupport, which is consistent with the results of molecular identification.

Correlation Between Clinical Manifestation and Species Distribution

The correlation of clinical severity and species distribution was analyzed using the Wilcoxon rank sum test. Although statistical results showed that *F. monophora* ($n = 11$) caused a more mild form of CBM than *F. nubica* ($n = 2$), not supported by statistical test ($z = -1.458$, $p = 0.145$). There was no difference and correlation between fungal strains and skin lesion, as well as skin lesion and severity tested by Fisher's exact test ($p = 0.846 > 0.05$) and Spearman correlation test ($r = 0.04$) (**Table 2**).

Antifungal Susceptibility Testing

The geometric mean of MICs, MIC ranges, MIC50s, and MIC90s for the *Fonsecaea* isolates is summarized in **Table 3**. PCZ (MIC range 0.015–0.25 μg/ml), VCZ (MIC range 0.015–0.5 μg/ml), and ITZ (MIC range 0.03–0.5 μg/ml) were the azole antifungal agents that showed high activity against the *Fonsecaea* isolates. TRB (MIC range 0.015–1 μg/ml) was also active to these strains, but less effective than in azoles. For echinocandins, most isolates showed less sensitivity to AND (MIC range 2–>8 μg/ml), MFG (MIC range 1–>8 μg/ml), and CAS (MIC range 0.25–>8 μg/ml). The susceptibility profile between *F. monophora* and *F. nubica* showed no differences among the antifungal agents ($p > 0.05$).

Human Serum Cytokine Determination

The Quantibody Human Inflammation Array3 was employed to determine 40 human cytokines that are normally presented as an inflammation response of host cells. We compared the expressed level of cytokines between patients and healthy donors. The results indicated that IL-4, IL-7, IL-15, IL-11, and IL-17 were upregulated (**Figure 2**), while IL-1Ra, MIP-1β, IL-8, and IL-16 were downregulated (**Figure 3**) (unpaired *t*-test, $p < 0.05$). We also compared the expression level of cytokines in the patients with severe form and mild form. Thirty-four cytokines were upregulated, while 6 were downregulated between severe and non-severe patients (**Supplementary Figure S1**). IL-4, a marker cytokine of Th2, was highly induced in severe form cases compared to mild form cases ($p < 0.05$). However, the production of other cytokines showed no significant difference between severe and mild form cases ($p > 0.05$).

DISCUSSION

The age distribution of patients (mean 61.38 ± 11.20 years) in this study was similar to reports from Taiwan (mean 65.9 ± 13.6 years) and Guangdong (59 years, 29 to 83 years) (Fransisca et al., 2017; Yang et al., 2018). The gender ratio (4.6:1) was higher than the report from Taiwan (2.75:1) (Yang et al., 2018) and lower in Guangdong (6.5:1) (Fransisca et al., 2017). The male patients were still the dominant affected population. The skin lesions of most patients (89%) were limited to extremities. The occupation (56% farmers), trauma history (38%), and distribution of lesion sites reemphasize that traumatic inoculation from a contaminated environment is the primary mode of infection in CBM. Fifty-eight percent of patients claimed no underlying diseases, while 8 cases had immunosuppressed diseases including diabetes, systemic lupus erythema, nephrotic syndrome, lung cancer, and chronic colitis. The skin lesion was limited to body sites instead of spreading. We assumed that the local immunity may play an important role to contain the infection. In our study, verrucous form was the most common skin lesion (42%), similar to a report from Taiwan (43%) (Yang et al., 2018). The long duration, bad compliance, and improper therapy may be the main reasons for the high proportion of severe skin lesions (40%). We also supposed long treatment time and expensive medical expense lead to bad compliance, which may be responsible for low healing rate (3 cases) in this cluster of cases.

The combination therapy of oral terbinafine and itraconazole, which was proved to have a synergistic effect against *Fonsecaea* spp. in a previous study (Zhang et al., 2009), was used for the treatment of 31 cases and 68% improved or were cured. This combined therapeutic strategy was supposed to be effective and safe in the management of CBM. Photodynamic therapy as a safe adjunct therapy was also used to treat CBM (Hu et al., 2019; Huang et al., 2019). Three patients who received ALA-PDT improved greatly in 3–4 weeks. However, the high price of the photosensitizer prevented it from being widely used by more patients. In total, 65% of the patients improved or were cured, but we still face the challenges of when will the endpoint of therapy be and how can we reduce relapse.

In Madagascar and Brazil, *F. pedrosoi* is the main causative agent of CBM (Esterre et al., 1996; Silva et al., 1998; Gomes et al., 2016). In Japan, Yaguchi et al. (2007) found 33 isolates previously identified morphologically as *F. pedrosoi* were *F. monophora*

TABLE 2 | Clinical manifestation and species distribution of 45 CBM cases.

Strain	Severity	Type of lesions						Cases
		Verrucous	Plaque	Nodular	Tumorous	Cicatricial	Mixed	
F. monophora	Mild	6	4			1		11
	Moderate	1	5	1				7
	Severe	5	2			1	2	10
F. nubica	Mild		1			1		2
	Moderate	2	5					7
	Severe	5	1		1		1	8
Total		19	18	1	1	3	3	45

TABLE 3 | Minimal inhibitory concentrations (MIC) of 10 antifungal agents against 45 clinical isolates of *Fonsecaea* spp.

Antifungal agent	MIC (μg/ml)											
	Fonsecaea spp.(*n* = 45)				*F. monophora* (*n* = 28)				*F. nubica* (*n* = 17)			
	Range	MIC_{50}	MIC_{90}	GM	Range	MIC_{50}	MIC_{90}	GM	Range	MIC_{50}	MIC_{90}	GM
AND	2–>8	4	>8	3.24	2–>8	2	>8	3.09	2–>8	4	>8	3.50
MFG	1–>8	8	>8	6.35	2–>8	8	>8	6.32	1–>8	8	>8	6.42
CAS	0.25–>8	1	>8	1.74	0.25–>8	1	8	1.48	0.25–>8	2	>8	2.27
5-FC	0.12–8	4	8	5.46	0.25–16	8	8	5.76	0.12–16	4	8	4.96
PCZ	0.015–0.25	0.12	0.25	0.10	0.015–0.25	0.06	0.12	0.10	0.015–0.5	0.12	0.25	0.12
VCZ	0.015–0.5	0.06	0.12	0.09	0.015–0.25	0.06	0.12	0.08	0.015–0.5	0.06	0.12	0.10
ITR	0.03–0.5	0.25	0.25	0.18	0.03–0.25	0.25	0.25	0.18	0.03–0.5	0.12	0.25	0.17
FLU	8–128	32	32	28.62	8–64	32	32	26.00	8–128	32	32	32.94
AMB	1–8	4	8	4.71	1–8	4	8	4.79	1–8	4	8	4.59
TRB	0.015–1	0.25	1	0.35	0.015–1	0.25	1	0.34	0.03–1	0.25	0.5	0.36

MIC refers to the minimal inhibitory concentrations.
The MIC50 and MIC90 values correspond to the minimal inhibitory concentration of the antifungal able to inhibit the growth of 50% and 90% of all fungal isolates, respectively.
GM, Geometrical mean.

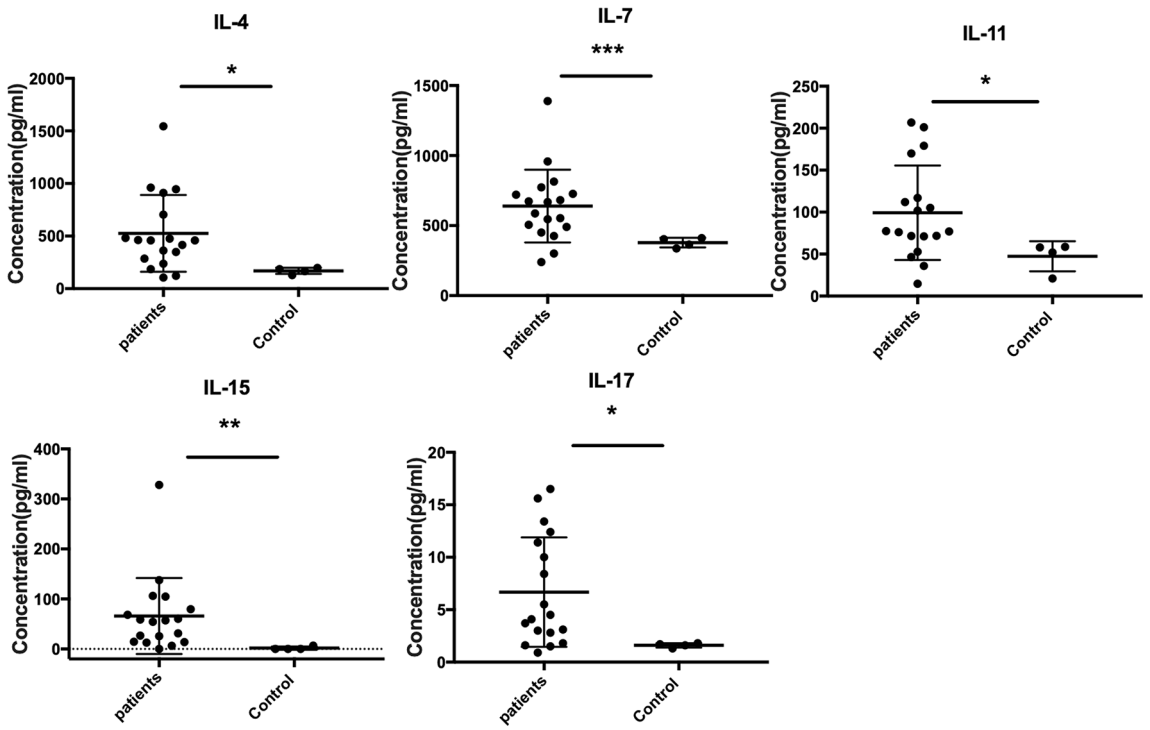

FIGURE 2 | Upregulated expressed cytokines (IL-4, IL-7, IL-15, IL-11, and IL-17) in CBM patients compared to healthy controls (unpaired *t*-test, $p < 0.05$). *P ≤ 0.05, **P ≤ 0.01, ***P ≤ 0.001.

actually. In China, there were more than 500 CBM cases reported since 1952. The predominant agent of CBM was *C. carrionii* in Northern China and *F. monophora* in Southern China (Xi et al., 2009). *F. nubica* is a genetic sibling of *F. monophora*. So far, there are more than 40 strains of *F. nubica* reported in published literature from Brazil and China (Gomes et al., 2016; Fransisca et al., 2017; You et al., 2019). Surprisingly, we did not isolate *F. pedrosoi* in the Guangdong region. These results seemed to confirm again that *F. pedrosoi* was found nearly exclusively in Central and South America, while *F. nubica* and *F. monophora* were distributed worldwide (Esterre et al., 1996; Minotto et al., 2001). Interestingly, incidence of *F. nubica* infection was

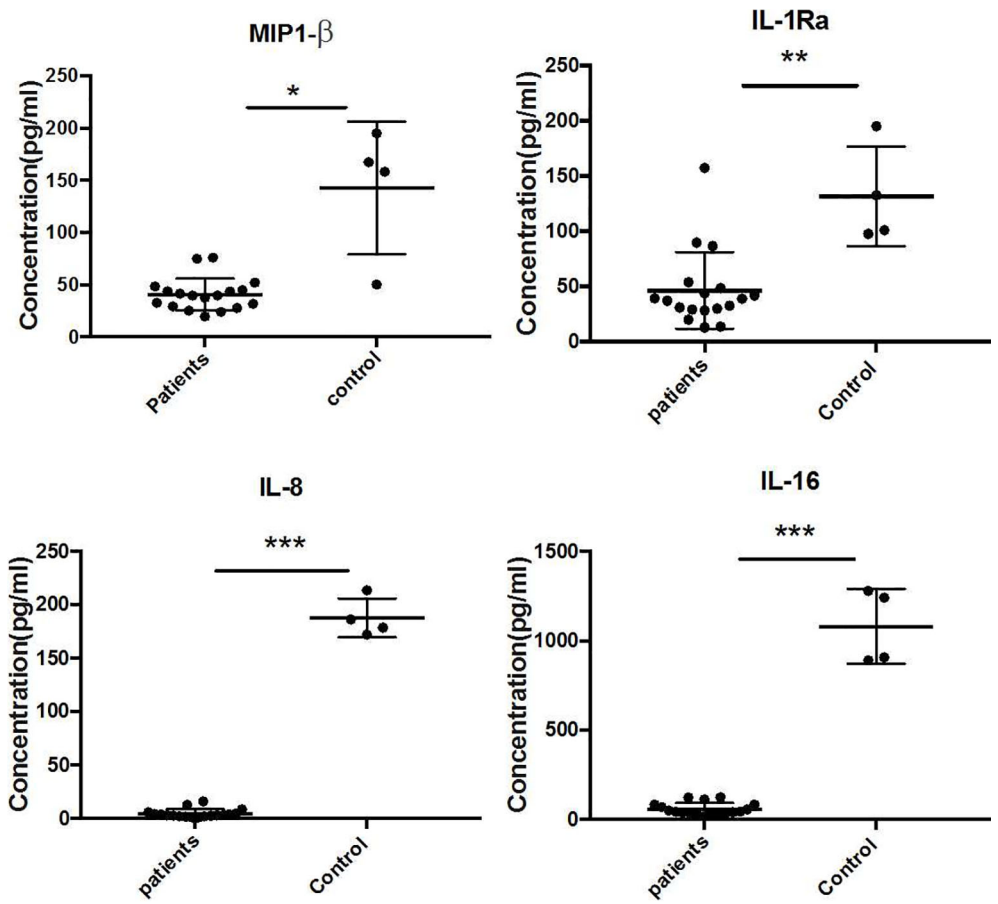

FIGURE 3 | Downregulated expressed cytokines (IL-1Ra, MIP-1β, IL-8, and IL-16) in CBM patients compared to healthy controls (unpaired *t*-test, $p < 0.05$). *P ≤ 0.05, **P ≤ 0.01, ***P ≤ 0.001.

comparable with that of *F. monophora* (17 vs. 28) in this study. Referring to Fransisca's reports in Guangdong (Fransisca et al., 2017) (15 of 60 cases caused by *F. nubica*), we found an increased ratio of *F. nubica* infection. The major difference was the time Fransisca's data were collected (before 2015); our data were collected from 2016 to 2021. Whether the increased ratio of *F. nubica* infection resulted from a change of pathogen profile was still unknown. Long-term surveillance and molecular epidemiology study for all CBM cases are greatly needed in the future.

YeastOne® is a widely used commercial antifungal test product, and it shows accuracy and reproducibility for susceptibility of *Candida* (Cuenca-Estrella et al., 2005; Eschenauer et al., 2014), as well as in filamentous fungi, e.g., *Aspergillus*, *Sporothrix*, dermatophytes, and dematiaceous fungi (Pujol et al., 2002; Siopi et al., 2017; Zheng et al., 2019). Compared to CLSI (the National Committee for Clinical Laboratory Standards reference broth microdilution antifungal susceptibility testing method), this method has the advantages of being time-efficient, cost-effective, simple, and easily handled. Zheng et al. (2019) reported that YeastOne® showed high agreement from 85.3% to 100% compared to CLSI in 9 antifungal agents against *F. pedrosoi*. In our study, all the azoles except fluconazole displayed low MICs, indicating that these azoles may have good therapeutic effects on infection caused by *Fonsecaea*. Although voriconazole had a low MIC range (0.015–0.5 μg/ml) compared to Najafzadeh's report (Najafzadeh et al., 2010), they had similar MIC90 values (0.125 μg/ml vs. 0.25 μg/ml). Most MICs of Azoles obtained were similar to those in other studies of *Fonsecaea* by using CLSI (Najafzadeh et al., 2010). Echinocandins had a limited role in the treatment of CBM for *F. monophora* and *F. nubica*, which was also observed in other studies (Najafzadeh et al., 2010; Badali et al., 2013). There were no significant differences in either MIC90 or MIC50 between *F. monophora* and *F. nubica* in all tested antifungal agents, which was consistent with archived studies (Najafzadeh et al., 2010; Badali et al., 2013; Coelho et al., 2018). The results of our test of susceptibility to *Fonsecaes* spp. *in vitro* using the yeastone® method had high consistency with other reports using the ClSI method, which confirmed that it was an effective alternative method for determining susceptibility of *Fonsecaea* spp.

Previous studies indicated that severe CBM produced high levels of IL-10 and low levels of IFN-γ together with inefficient T-cell proliferation. Meanwhile, patients with the mild form showed intense production of IFN-γ, low levels of IL-10, and efficient T-cell proliferation (Mazo et al., 2005). In our study, we only found that IL-4 was highly produced in severe compared to mild form cases ($p < 0.05$). However, no significant differences were found in cytokines IL-10, IFN-γ, and TNF-alpha comparing severe form to mild form cases, as well as in patients and healthy controls. In addition, we found that IL-7 and IL-15 (Th1 cytokines), IL-11 (proinflammatory cytokine), and IL-17 (Th17 cytokine) significantly increased comparing patients to healthy controls ($p < 0.05$), but there was no significant difference when comparing severe to mild form cases ($p > 0.05$). The antifungal cytokines—Type1 (IL-7 and IL-15), Th17 (IL-7), and proinflammatory (IL-11)—were all significantly enhanced in CBM patients, presumably as a compensatory response to the long-term fungal infection. Surprisingly, we also detected the significantly reduced expression of IL-1Ra, MIP-1β, IL-8, and IL-16 in the serum of CBM patients. The cytokines of MIP-1β, IL-8, and IL-16 played important roles in recruiting macrophages, neutrophils, and CD4 molecules, respectively, which are crucial immune cells against fungal infection (Cruikshank et al., 1994; Maurer and von Stebut, 2004; Remick, 2005). Downregulation of these cytokines indicated impaired immune response to eliminate fungus in CBM cases, which probably contributed to chronic duration of CBM. IL-1Ra (IL-1 receptor antagonist) was a cytokine to inhibit activities of IL-1A, IL-1B. IL-1Ra knock out mice were highly resistant to invasive aspergillosis (Gresnigt et al., 2014), which seemed to be paradoxical to the reduced expression of IL-1Ra in CBM patients. The role that IL-1Ra played in *Fonsecaea* infection still needs further investigation. In this study, we obtained the different cytokine profiles compared to previous studies. The probable explanation was the sample types we used in our study differ from the peripheral blood mononuclear cells (PBMCs) used in archived studies (Mazo et al., 2005). Therefore, future studies will focus on these differently expressed cytokines in both blood and tissues of CBM patients to address the remaining questions.

In conclusion, our study showed a comprehensive clinical and molecular characteristic of a cluster of 45 CBM cases in Guangdong, China, which may represent the regional trends in this subtropical hyper-endemic area of CBM. These data will definitely contribute to better management and clinical therapy, and will help countries still struggling to combat this difficult fungal infection in the West Pacific.

DATA AVAILABILITY STATEMENT

The datasets presented in this study can be found in online repositories. The names of the repository/repositories and accession number(s) can be found in the article/**Supplementary Material**.

ETHICS STATEMENT

The studies involving human participants were reviewed and approved by the Ethics Committee Board of Dermatology Hospital of Southern Medical University. The patients/participants provided their written informed consent to participate in this study.

AUTHOR CONTRIBUTIONS

HL and JS designed the experiments and analyzed the data. HL wrote the manuscript. ML, WC, YC, YL, HH, ZX, and WZ performed the experiments and collected the clinical data. HL and JS are the first co-authors and contributed equally to this article. All works were performed under the guidance of LX. All authors contributed to the article and approved the submitted version.

FUNDING

This study was kindly supported by grants from the National Natural Science Foundation of China (81601746 and 81873960).

SUPPLEMENTARY MATERIAL

The Supplementary Material for this article can be found online at: https://www.frontiersin.org/articles/10.3389/fcimb.2022.810604/full#supplementary-material

Supplementary Figure S1 | The comparison of each cytokines between severe vs mild group, and tested by T test. The p value ($-\log_{10}$ P) and fold change (FC) ($\log_2$ FC), were plot indicated the cytokines with statistical support between these two groups. Purple dot indicated the different makers between two groups with statistical support.

REFERENCES

Ameen, M. (2010). Managing Chromoblastomycosis. *Trop. Doct* 40, 65–67. doi: 10.1258/td.2009.090264

Badali, H., Fernandez-Gonzalez, M., Mousavi, B., Illnait-Zaragozi, M. T., Gonzalez-Rodriguez, J. C., de Hoog, G. S., et al. (2013). Chromoblastomycosis Due to Fonsecaea Pedrosoi and F. Monophora in Cuba. *Mycopathologia* 175, 439–444. doi: 10.1007/s11046-013-9634-3

Coelho, R. A., Brito-Santos, F., Figueiredo-Carvalho, M., Silva, J., Gutierrez-Galhardo, M. C., Do, V. A., et al. (2018). Molecular Identification and Antifungal Susceptibility Profiles of Clinical Strains of Fonsecaea Spp. Isolated From Patients With Chromoblastomycosis in Rio De Janeiro, Brazil. *PLoS Negl. Trop. Dis.* 12, e0006675. doi: 10.1371/journal.pntd.0006675

Cruikshank, W. W., Center, D. M., Nisar, N., Wu, M., Natke, B., Theodore, A. C., et al. (1994). Molecular and Functional Analysis of a Lymphocyte Chemoattractant Factor: Association of Biologic Function With CD4 Expression. *Proc. Natl. Acad. Sci. U.S.A.* 91, 5109–5113. doi: 10.1073/pnas.91.11.5109

Cuenca-Estrella, M., Gomez-Lopez, A., Mellado, E., and Rodriguez-Tudela, J. L. (2005). Correlation Between the Procedure for Antifungal Susceptibility Testing for Candida Spp. Of the European Committee on Antibiotic Susceptibility Testing (EUCAST) and Four Commercial Techniques. *Clin. Microbiol. Infect.* 11, 486–492. doi: 10.1111/j.1469-0691.2005.01166.x

Daboit, T. C., Magagnin, C. M., Heidrich, D., Castrillon, M. R., Mendes, S. D., Vettorato, G., et al. (2013). A Case of Relapsed Chromoblastomycosis Due to Fonsecaea Monophora: Antifungal Susceptibility and Phylogenetic Analysis. *Mycopathologia* 176, 139–144. doi: 10.1007/s11046-013-9660-1

Daboit, T. C., Massotti, M. C., Heidrich, D., Czekster, A. L., Vigolo, S., Collares, M. L., et al. (2014). *In Vitro* Susceptibility of Chromoblastomycosis Agents to Five Antifungal Drugs and to the Combination of Terbinafine and Amphotericin B. *Mycoses* 57, 116–120. doi: 10.1111/myc.12111

de Azevedo, C. M., Gomes, R. R., Vicente, V. A., Santos, D. W., Marques, S. G., Do, N. M., et al. (2015). Fonsecaea Pugnacius, a Novel Agent of Disseminated Chromoblastomycosis. *J. Clin. Microbiol.* 53, 2674–2685. doi: 10.1128/JCM.00637-15

De Hoog, G. S., Attili-Angelis, D., Vicente, V. A., Van Den Ende, A. H., and Queiroz-Telles, F. (2004). Molecular Ecology and Pathogenic Potential of Fonsecaea Species. *Med. Mycol.* 42, 405–416. doi: 10.1080/13693780410001661464

de Sousa, M. G., Belda, W. J., Spina, R., Lota, P. R., Valente, N. S., Brown, G. D., et al. (2014). Topical Application of Imiquimod as a Treatment for Chromoblastomycosis. *Clin. Infect. Dis.* 58, 1734–1737. doi: 10.1093/cid/ciu168

Eschenauer, G. A., Nguyen, M. H., Shoham, S., Vazquez, J. A., Morris, A. J., Pasculle, W. A., et al. (2014). Real-World Experience With Echinocandin MICs Against Candida Species in a Multicenter Study of Hospitals That Routinely Perform Susceptibility Testing of Bloodstream Isolates. *Antimicrob. Agents Chemother.* 58, 1897–1906. doi: 10.1128/AAC.02163-13

Esterre, P., Andriantsimahavandy, A., Ramarcel, E. R., and Pecarrere, J. L. (1996). Forty Years of Chromoblastomycosis in Madagascar: A Review. *Am. J. Trop. Med. Hyg.* 55, 45–47. doi: 10.4269/ajtmh.1996.55.45

Fransisca, C., He, Y., Chen, Z., Liu, H., and Xi, L. (2017). Molecular Identification of Chromoblastomycosis Clinical Isolates in Guangdong. *Med. Mycol.* 55, 851–858. doi: 10.1093/mmy/myw140

Gauthier, M. (2007). *Simulation of Polymer Translocation Through Small Channels: A Molecular Dynamics Study and a New Monte Carlo Approach*. (Canada: University of Ottawa)

Gomes, R. R., Vicente, V. A., Azevedo, C. M., Salgado, C. G., Da, S. M., Queiroz-Telles, F., et al. (2016). Molecular Epidemiology of Agents of Human Chromoblastomycosis in Brazil With the Description of Two Novel Species. *PLoS Negl. Trop. Dis.* 10, e0005102. doi: 10.1371/journal.pntd.0005102

Gresnigt, M. S., Bozza, S., Becker, K. L., Joosten, L. A., Abdollahi-Roodsaz, S., van der Berg, W. B., et al. (2014). A Polysaccharide Virulence Factor From Aspergillus Fumigatus Elicits Anti-Inflammatory Effects Through Induction of Interleukin-1 Receptor Antagonist. *PLoS Pathog.* 10, e1003936. doi: 10.1371/journal.ppat.1003936

Huang, X., Han, K., Wang, L., Peng, X., Zeng, K., and Li, L. (2019). Successful Treatment of Chromoblastomycosis Using ALA-PDT in a Patient With Leukopenia. *Photodiagn Photodyn Ther.* 26, 13–14. doi: 10.1016/j.pdpdt.2019.02.013

Hu, Y., Qi, X., Sun, H., Lu, Y., Hu, Y., Chen, X., et al. (2019). Photodynamic Therapy Combined With Antifungal Drugs Against Chromoblastomycosis and the Effect of ALA-PDT on Fonsecaea *In Vitro*. *PLoS Negl. Trop. Dis.* 13, e0007849. doi: 10.1371/journal.pntd.0007849

Jiang, M., Cai, W., Zhang, J., Xie, T., Xi, L., Li, X., et al. (2018). Melanization of a Meristematic Mutant of Fonsecaea Monophora Increase the Pathogenesis in a BALB/c Mice Infection Model. *Med. Mycol.* 56, 979–986. doi: 10.1093/mmy/myx148

Lopez, M. R., and Mendez, T. L. (2007). Chromoblastomycosis. *Clin. Dermatol.* 25, 188–194. doi: 10.1016/j.clindermatol.2006.05.007

Maurer, M., and von Stebut, E. (2004). Macrophage Inflammatory Protein-1. *Int. J. Biochem. Cell Biol.* 36, 1882–1886. doi: 10.1016/j.biocel.2003.10.019

Mazo, F. G. V., Da, G. D. S. M., Ferreira, K. S., Marques, S. G., Goncalves, A. G., Vagner, D. C. L. S., et al. (2005). Cytokines and Lymphocyte Proliferation in Patients With Different Clinical Forms of Chromoblastomycosis. *Microbes Infect.* 7, 708–713. doi: 10.1016/j.micinf.2005.01.006

Minotto, R., Bernardi, C. D., Mallmann, L. F., Edelweiss, M. I., and Scroferneker, M. L. (2001). Chromoblastomycosis: A Review of 100 Cases in the State of Rio Grande do Sul, Brazil. *J. Am. Acad. Dermatol.* 44, 585–592. doi: 10.1067/mjd.2001.112220

Najafzadeh, M. J., Badali, H., Illnait-Zaragozi, M. T., De Hoog, G. S., and Meis, J. F. (2010). *In Vitro* Activities of Eight Antifungal Drugs Against 55 Clinical Isolates of Fonsecaea Spp. *Antimicrob. Agents Chemother.* 54, 1636–1638. doi: 10.1128/AAC.01655-09

Najafzadeh, M. J., Sun, J., Vicente, V. A., Klaassen, C. H., Bonifaz, A., Gerrits, V. D. E. A., et al. (2011). Molecular Epidemiology of Fonsecaea Species. *Emerg. Infect. Dis.* 17, 464–469. doi: 10.3201/eid1703.100555

Paniz-Mondolfi, A. E., Colella, M. T., Negrin, D. C., Aranzazu, N., Oliver, M., Reyes-Jaimes, O., et al. (2008). Extensive Chromoblastomycosis Caused by Fonsecaea Pedrosoi Successfully Treated With a Combination of Amphotericin B and Itraconazole. *Med. Mycol.* 46, 179–184. doi: 10.1080/13693780701721856

Pujol, I., Capilla, J., Fernandez-Torres, B., Ortoneda, M., and Guarro, J. (2002). Use of the Sensititre Colorimetric Microdilution Panel for Antifungal Susceptibility Testing of Dermatophytes. *J. Clin. Microbiol.* 40, 2618–2621. doi: 10.1128/JCM.40.7.2618-2621.2002

Queiroz-Telles, F., de Hoog, S., Santos, D. W., Salgado, C. G., Vicente, V. A., Bonifaz, A., et al. (2017). Chromoblastomycosis. *Clin. Microbiol. Rev.* 30, 233–276. doi: 10.1128/CMR.00032-16

Queiroz-Telles, F., and Santos, D. W. (2013). Challenges in the Therapy of Chromoblastomycosis. *Mycopathologia* 175, 477–488. doi: 10.1007/s11046-013-9648-x

Remick, D. G. (2005). Interleukin-8. *Crit. Care Med.* 33, S466–S467. doi: 10.1097/01.ccm.0000186783.34908.18

Saberi, H., Kashfi, A., Hamidi, S., Tabatabai, S. A., and Mansouri, P. (2003). Cerebral Phaeohyphomycosis Masquerading as a Parafalcian Mass: Case Report. *Surg. Neurol.* 60, 354–9; discussion 359. doi: 10.1016/s0090-3019(03)00135-6

Seyedmousavi, S., Netea, M. G., Mouton, J. W., Melchers, W. J., Verweij, P. E., and de Hoog, G. S. (2014). Black Yeasts and Their Filamentous Relatives: Principles of Pathogenesis and Host Defense. *Clin. Microbiol. Rev.* 27, 527–542. doi: 10.1128/CMR.00093-13

Silva, A. A., Criado, P. R., Nunes, R. S., Da, S. W., Kanashiro-Galo, L., Duarte, M. I., et al. (2014). *In Situ* Immune Response in Human Chromoblastomycosis–A Possible Role for Regulatory and Th17 T Cells. *PLoS Negl. Trop. Dis.* 8, e3162. doi: 10.1371/journal.pntd.0003162

Silva, J. P., de Souza, W., and Rozental, S. (1998). Chromoblastomycosis: A Retrospective Study of 325 Cases on Amazonic Region (Brazil). *Mycopathologia* 143, 171–175. doi: 10.1023/a:1006957415346

Siopi, M., Pournaras, S., and Meletiadis, J. (2017). Comparative Evaluation of Sensititre YeastOne and CLSI M38-A2 Reference Method for Antifungal Susceptibility Testing of Aspergillus Spp. Against Echinocandins. *J. Clin. Microbiol.* 55, 1714–1719. doi: 10.1128/JCM.00044-17

Sousa, M. G., Reid, D. M., Schweighoffer, E., Tybulewicz, V., Ruland, J., Langhorne, J., et al. (2011). Restoration of Pattern Recognition Receptor Costimulation to Treat Chromoblastomycosis, a Chronic Fungal Infection of the Skin. *Cell Host Microbe* 9, 436–443. doi: 10.1016/j.chom.2011.04.005

Surash, S., Tyagi, A., De Hoog, G. S., Zeng, J. S., Barton, R. C., and Hobson, R. P. (2005). Cerebral Phaeohyphomycosis Caused by Fonsecaea Monophora. *Med. Mycol.* 43, 465–472. doi: 10.1080/13693780500220373

White, T., Bruns, T., Lee, S., Taylor, J., Innis, M., Gelfand, D., et al. (1990). *Amplification and Direct Sequencing of Fungal Ribosomal RNA Genes for Phylogenetics*. Academic Press, Inc 315–322.

WHO (2017). *Report of the Tenth Meeting of the WHO Strategic and Technical Advisory Group for Neglected Tropical Diseases* (Geneva).

Xi, L., Sun, J., Lu, C., Liu, H., Xie, Z., Fukushima, K., et al. (2009). Molecular Diversity of Fonsecaea (Chaetothyriales) Causing Chromoblastomycosis in Southern China. *Med. Mycol.* 47, 27–33. doi: 10.1080/13693780802468209

Yaguchi, T., Tanaka, R., Nishimura, K., and Udagawa, S. (2007). Molecular Phylogenetics of Strains Morphologically Identified as Fonsecaea Pedrosoi From Clinical Specimens. *Mycoses* 50, 255–260. doi: 10.1111/j.1439-0507.2007.01383.x

Yang, C. S., Chen, C. B., Lee, Y. Y., Yang, C. H., Chang, Y. C., Chung, W. H., et al. (2018). Chromoblastomycosis in Taiwan: A Report of 30 Cases and a Review of the Literature. *Med. Mycol.* 56, 395–405. doi: 10.1093/mmy/myx075

You, Z., Yang, X., Yu, J., Zhang, J., and Ran, Y. (2019). Chromoblastomycosis Caused by Fonsecaea Nubica: First Report in Northern China and Literature Review. *Mycopathologia* 184, 97–105. doi: 10.1007/s11046-018-0307-0

Zhang, J., Wang, L., Xi, L., Huang, H., Hu, Y., Li, X., et al. (2013). Melanin in a Meristematic Mutant of Fonsecaea Monophora Inhibits the Production of

Nitric Oxide and Th1 Cytokines of Murine Macrophages. *Mycopathologia* 175, 515–522. doi: 10.1007/s11046-012-9588-x

Zhang, J., Xi, L., Lu, C., Li, X., Xie, T., Zhang, H., et al. (2009). Successful Treatment for Chromoblastomycosis Caused by Fonsecaea Monophora: A Report of Three Cases in Guangdong, China. *Mycoses* 52, 176–181. doi: 10.1111/j.1439-0507.2008.01547.x

Zheng, H., He, Y., Kan, S., Li, D., Lv, G., Shen, Y., et al. (2019). *In Vitro* Susceptibility of Dematiaceous Fungi to Nine Antifungal Agents Determined by Two Different Methods. *Mycoses* 62, 384–390. doi: 10.1111/myc.12895

Conflict of Interest: The authors declare that the research was conducted in the absence of any commercial or financial relationships that could be construed as a potential conflict of interest.

Publisher's Note: All claims expressed in this article are solely those of the authors and do not necessarily represent those of their affiliated organizations, or those of the publisher, the editors and the reviewers. Any product that may be evaluated in this article, or claim that may be made by its manufacturer, is not guaranteed or endorsed by the publisher.

frontiers | Frontiers in Cellular and Infection Microbiology

ORIGINAL RESEARCH
published: 08 July 2022
doi: 10.3389/fcimb.2022.789157

Equine Histoplasmosis in Ethiopia: Phylogenetic Analysis by Sequencing of the Internal Transcribed Spacer Region of rRNA Genes

Gobena Ameni[1,2*†], *Alebachew Messele Kebede*[1†], *Aboma Zewude*[1,2], *Musse Girma Abdulla*[1], *Rahel Asfaw*[1], *Mesfin Mamo Gobena*[1,3], *Martina Kyalo*[4], *Francesca Stomeo*[4], *Balako Gumi*[1] *and Teshale Sori*[3]

[1] *Aklilu Lemma Institute of Pathobiology, Addis Ababa University, Addis Ababa, Ethiopia,* [2] *Department of Veterinary Medicine, College of Food and Agriculture, United Arab Emirates University, Al Ain, United Arab Emirates,* [3] *College of Veterinary Medicine and Agriculture, Addis Ababa University, Debre Zeit, Ethiopia,* [4] *Capacity Building, Biosciences for Eastern and Central Africa-International Livestock Research Institute (BecA-ILRI) Hub, Nairobi, Kenya*

Equine histoplasmosis commonly known as epizootic lymphangitis (EL) is a neglected granulomatous disease of equine that is endemic to Ethiopia. It is caused by *Histoplasma capsulatum* variety *farciminosum*, a dimorphic fungus that is closely related to *H. capsulatum* variety c*apsulatum.* The objective of this study was to undertake a phylogenetic analysis of *H. capsulatum* isolated from EL cases of horses in central Ethiopia and evaluate their relationship with *H. capsulatum* isolates in other countries and/or clades using the internal transcribed spacer (ITS) region of rRNA genes. Clinical and mycological examinations, DNA extraction, polymerase chain reaction (PCR), Sanger sequencing, and phylogenetic analysis were used for undertaking this study. Additionally, sequence data of *Histoplasma* isolates were retrieved from GenBank and included for a comprehensive phylogenetic analysis. A total of 390 horses were screened for EL and 97 were positive clinically while *H. capsulatum* was isolated from 60 horses and further confirmed with PCR, of which 54 were sequenced. BLAST analysis of these 54 isolates identified 29 *H. capsulatum* isolates and 14 isolates from other fungal genera while the remaining 11 samples were deemed insufficient for further downstream analysis. The phylogenetic analysis identified five clades, namely, African, Eurasian, North American 1 and 2, and Latin American A and B. The Ethiopian isolates were closely aggregated with isolates of the Latin American A and Eurasian clades, whereas being distantly related to isolates from North American 1 and 2 clades as well as Latin American B clade. This study highlights the possible origins and transmission routes of Histoplasmosis in Ethiopia.

Keywords: *Histoplasma capsulatum*, internal transcribed spacer region, phylogenetic analysis, equine histoplasmosis, Sanger Sequencing

OPEN ACCESS

Edited by:
G. Sybren De Hoog, Radboud University Nijmegen Medical Centre, Netherlands

Reviewed by:
Govind Vediyappan, Kansas State University, United States
Abdullah M. S. Al-Hatmi, University of Nizwa, Oman

***Correspondence:**
Gobena Ameni
gobena.ameni@aau.edu.et;
gobena.ameni@uaeu.ac.ae

†These authors have contributed equally to this work

Specialty section:
This article was submitted to Fungal Pathogenesis, a section of the journal Frontiers in Cellular and Infection Microbiology

Received: *04 October 2021*
Accepted: *23 March 2022*
Published: *08 July 2022*

Citation:
Ameni G, Messele Kebede A, Zewude A, Girma Abdulla M, Asfaw R, Gobena MM, Kyalo M, Stomeo F, Gumi B and Sori T (2022) Equine Histoplasmosis in Ethiopia: Phylogenetic Analysis by Sequencing of the Internal Transcribed Spacer Region of rRNA Genes. Front. Cell. Infect. Microbiol. 12:789157. doi: 10.3389/fcimb.2022.789157

INTRODUCTION

Equine histoplasmosis is caused by *H. capsulatum* var. *farciminosum* which is a dimorphic fungus that is closely related to *Histoplasma capsulatum* variety *capsulatum* (*H. capsulatum* var. *capsulatum*), which is a causative agent of histoplasmosis in humans. *H. capsulatum* var. *farciminosum* has mycelia and yeast forms; the mycelial form lives in the soil in hot and humid areas while the yeast form is found in the lesions of infected equids. The zoonotic significance of *H. capsulatum* var. *farciminosum* has not been well investigated. However, there were reports of sporadic cases of humans that were not fully established by rigorous laboratory investigations (Al-Ani, 1999). Nonetheless, the World Organization for Animal Health (OIE, 2018) recommends that all laboratory procedures involving *H. capsulatum* var. *farciminosum* should be conducted with appropriate biosafety and containment procedures.

Equine histoplasmosis, commonly known as epizootic lymphangitis (EL), is a contagious chronic disease of equines characterized clinically by a suppurative pyogranulomatous dermatitis and lymphangitis at the early stage, which later becomes ulcerate as the disease progresses (Singh, 1965; Radostits, 1994). In equids, EL can appear in cutaneous, ocular, or/and respiratory forms (Singh, 1965; Ameni, 2007). The cutaneous form occurs as a result of direct or indirect contact between traumatized skin and infected and/or contaminated substances. The conjunctival form is assumed to be transmitted by flies of the *Musca* or *Stomoxys* genera (Singh, 1965), while inhalation of the causative agent leads to the development pulmonary form.

Epidemiologically, EL occurs more frequently in tropical and subtropical regions than in temperate regions, which is due to the favorable environmental condition for the survival of the mycelial form of *H. capsulatum* var. *farciminosum*. It is endemic in north, east, and northeast Africa and in countries bordering the Mediterranean Sea, India, Pakistan, East Africa, and Japan (Selim et al., 1985; Guérin et al., 1992; OIE, 2008). However, there is scarcity of literature on the epidemiology of EL in the equine population of these countries except an indication of their endemicity to the disease. Furthermore, there is little or no information on the epidemiology of human histoplasmosis in the tropical and subtropical regions of the world although the climatic condition is conducive for the replication of *Histoplasma*. Additionally, little effort was made on the isolation and characterization of *H. capsulatum* varieties in general and *H. capsulatum* var. *farciminosum* in particular. Most of the studies conducted so far were performed on human histoplasmosis and its causative agents, i.e., *H. capsulatum* var. *capsulatum* and *H. capsulatum* var. *duboisii*. Hence, studies are needed on the epidemiology of equine histoplasmosis and *H. capsulatum* var. *farciminosum*. A study conducted in Ethiopia between January 2003 and June 2004 on 19,082 carthorses at 28 towns reported a prevalence of 18.8% indicating the widespread occurrence of the disease in Ethiopia (Ameni, 2006). In addition to affecting horses, the disease also affects mules, and a prevalence of 21% was recorded in 309 cart mules in western Ethiopia (Ameni and Terefe, 2004). The infection in mules was observed to be highly associated with tick infestation (Guérin et al., 1992; Ameni and Terefe, 2004).

On top of its economic impact, because of its chronic and debilitating nature, EL is characterized by causing severe welfare problem to equines. The disease poorly responds to treatment. Moreover, EL requires a longer duration, which is not attractive for the owners of equines.

Azoles and amphotericin B are used for the treatment of histoplasmosis in humans and animals in developed countries. However, amphotericin B could not be used in developing countries where EL is most common for its cost (CFSPH. CFSPH, 2019). Instead, EL is treated with cheap drugs such as intravenous sodium iodine or oral potassium iodide, sometimes in conjunction with topical iodide applied to lesions and/or surgical excision. However, iodide has limited efficacy in moderate to severe cases (CFSPH. CFSPH, 2019). Hence, control by vaccination could be an alternative method that requires for the development of a new vaccine. To this effect, identifying the strains of *H. capsulatum* var. *farciminosum* that infect the equine population would contribute to designing of the potential vaccine candidates. The objective of this study was to undertake the phylogenetic analysis of *H. capsulatum* isolated from EL cases of horses in central Ethiopia and evaluate the relationship of the Ethiopian isolates with the isolates from other countries on the basis of the ITS region of rRNA genes.

MATERIALS AND METHODS

Study Animals and Sampling

The screening of the horses for EL was conducted in central Ethiopia using clinical examination. Accordingly, 390 carthorses were examined for the characteristic clinical lesions of EL. The visible parts of the body of each horse were inspected for the presence of nodules and/or ulcers caused by EL. Inspection was made for the cutaneous, ocular, and respiratory forms of the disease. In addition, the contents of the nodular lesions were aspirated with needles and syringes and smeared on glass slides for microscopic examination. Thereafter, the slides were stained with Giemsa stain and then examined at ×100 using oil immersion for the typical yeast form of the organism, which appears as ovoid to globose in shape (Buxton and Fraser, 1977).

Isolation of H. *capsulatum* var. *farciminosum*

The aspirates of the nodular lesions were cultured on Sabouraud Dextrose Agar enriched with 2.5% glycerol for the isolation of the mycelial form while Brain Heart Infusion Agar was used for the isolation of the yeast form. Chloramphenicol (0.5 g/l) was added to each of these two media to avoid the growth of bacterial contaminants. After inoculation of the samples onto the media, incubation was made at 26°C for 8 weeks for the isolation of the mycelial form while the isolation of the yeast form was made at 37°C for 8 weeks. The growth of dry, gray-white, granular wrinkled colonies within 4–8 weeks was considered as positive for the growth. A differentiation between the colonies of the two

forms was made by Giemsa staining (OIE, 2008). As mycelial colonies were abundant, they were used for the extraction of DNA for sequencing.

DNA Extraction and Amplification

The mycelial colonies of 60 culture positive samples were harvested and used for the extraction of DNA for subsequent molecular analysis. DNA extraction was done using the cetyltrimethylammonium bromide (CTAB) method (Mace et al., 2003). The concentration of the DNA was estimated using the NanoDrop ND 1000 spectrophotometer (Thermo Scientific, Wilmington, DE, USA) while the quality of the DNA was evaluated using GelRed®-based 1% gel electrophoresis. A pair of primers (ITS1 and ITS4) (8-11 Munpyeongseo-ro, Daedeok-gu Daejeon, 34302, Republic of Korea) was used for PCR reactions. The primers used were ITS1 (forward primer) with a sequence of TCC GTA GGT GAA CCT GCG G and ITS4 (reverse primer) with a sequence of TCC TCC GCT TAT TGA TAT GC (White et al., 1990). The final concentration of each of the two primers was 0.1 µM/µl. Amplification was carried using a 50-µl reaction volume containing 40 ng of DNA template, PCR buffer containing 50 mM KCl, 10 mM Tris–HCl (pH 8.3), and 3 mM $MgCl_2$, 0.2 mM of each deoxynucleoside triphosphate (dNTPs), 25 pmol of each primer, and 1 U of *Taq* DNA polymerase. PCR was performed in the thermal cycler (Eppendorf Mastercycler) programmed for the first denaturation at 95°C for 5 min followed by 35 cycles of the succeeding step denaturation at 95°C for 45 s, annealing at 58°C for 1 min and extension at 72°C for 1 min, and a final extension period of 72°C of 7 min. The PCR products were electrophoresed in 1.8% agarose (Sigma Chemical Co., St. Louis, MO) using GelRed® at 100 V for 45 min, and the bands were visualized with a UV transilluminator.

Purification of the Amplicon for Sequencing

Amplicons were purified using QIAquick® PCR Purification Kit (Qiagen®, Hilden, Germany) according to the manufacturer's protocols. Following the purification, the concentration and purity of DNA were measured using the NanoDrop spectrophotometer while its integrity was examined using GelRed-based gel electrophoresis. Pure DNA samples with 20 ng/µl or greater concentrations with distinct bands on agarose gel were used for sequencing. Sequencing was conducted at Bioneer Corporation (8-11 Munpyeongseo-ro, Daedeok-gu Daejeon, 34302, Republic of Korea) using the Sanger capillary sequencing method. To this effect, purified PCR products of 60 samples, a positive control, and a pair primer (ITS1 and ITS4) were submitted to Bioneer Corporation through the Biosciences Eastern and Central Africa-International Livestock Research Institute (BecA-ILRI, Kenya) Hub and the sequence data were received.

Sequence Curation

The trace files of all samples were checked for quality and subjected to trimming using a quality score of 0.05 with ambiguous nucleotides, and thereafter the trimmed sequences were saved for further subsequent analysis. Sequence curation was performed using SeqMan Pro 15 DNASTAR Lasergene 15. The forward and reverse sequences of each sample were assembled using the assembly parameters, which included a minimum aligned read length of 50, medium alignment stringency, and conflict votes of A, C, G, and T. Full contigs and consensus sequences were created using these assembly parameters. Trace files which did not fulfil these requirements and those with poor quality to obtain the full-length data were removed from downstream analysis.

Phylogenetic Analysis

For the analysis of the phylogenetic relationship among worldwide isolates, the ITS1-5.8s-ITS2 region sequences of *H. capsulatum* were retrieved from the National Center for Biotechnology Information (NCBI, nig.gov) database. Retrieved GenBank sequences corresponding to *H. capsulatum* were aligned with nucleotide sequences of the isolates of the present study using the Clustal W program. Nucleotide substitutions of the best-fit model for each locus were statistically selected using jModelTest 2.0. Phylogenetic relationships were then estimated using Bayesian methods as implemented in MrBayes v3.2.6. A Tamura-Nei model + gamma model was used as it was assumed to best fit the data. Bayesian support for nodes was inferred in MrBayes using 42 × 106 Markov Chain Monte Carlo (MCMC) steps, with sampling every 200 generations. Convergence was reached after the average standard deviation of the posterior probability was below 0.01 and the value of the potential scale reduction factor reached 1.00. The clade assignment was based on the previous histoplasmosis ITS1–ITS2 nucleotide sequences data published by other studies conducted in Japan, Australia, Mexico, Brazil, Argentina, China, Thailand, and several European and African countries (Kasuga et al., 2003; Landaburu et al., 2014). *Blastomyces dermatitidis* (EF592163.1) that was isolated from USA was included in the phylogenetic analysis as an outgroup in order to improve bootstrap values.

RESULTS

Clinical Cases of Epizootic Lymphangitis

The proportion of EL in the recruited horses was 25% (97/390) in central Ethiopia. However, only 67 horses that had unruptured nodular lesions were used for the aspiration of contents of nodules for culturing of *H. capsulatum*. The observed clinical lesions were characterized by a suppurative, nodular or ulcerating, spreading pyogranulomatous, multifocal dermatitis, and lymphangitis. As it is shown in **Figure 1A**, the disease affects the limbs, the chest wall, and the neck. In all cases, the lesions were nodular and granulomatous in character and spread locally by invasion and *via* the lymphatics. The yeast form *H. capsulatum* was demonstrated by staining the aspirates of the nodules using

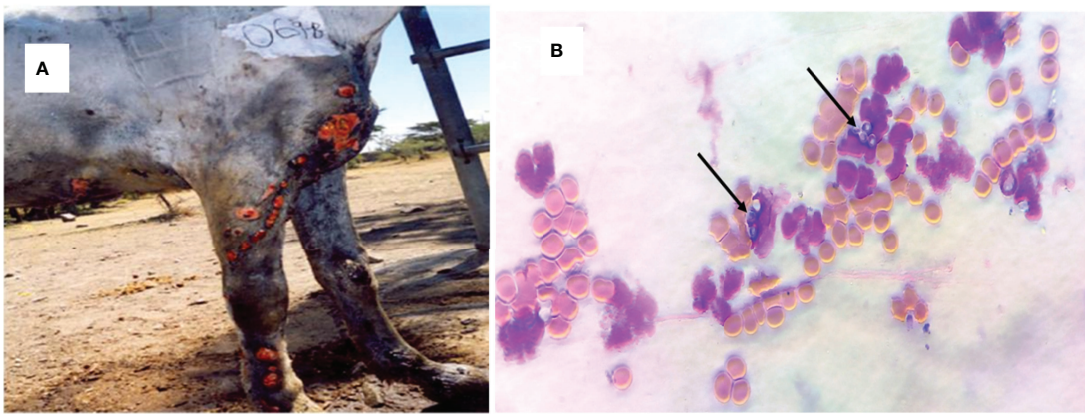

FIGURE 1 | Clinical epizootic lymphangitis case of a carthorse and the yeast form of *H. capsulatum* var. *farciminosum* in central Ethiopia. **(A)** Granulomatous inflammation of the lymphatic vessels, the regional lymph nodes, and the skin of the fore limbs; as the disease progressed, the nodules ulcerated and formed ulcers. **(B)** Giemsa-stained yeast form of *H. capsulatum* var. *farciminosum* obtained from nodular aspirate and observed under microscope at ×100 with oil immersion. The yeast cells are shown by arrow; the purple cells are granulocytes while the orange cells are red blood cells.

Giemsa stain in which it appears as centrally transparent oval shaped and located intracellularly in the macrophages or extracellularly in the nodular content (**Figure 1B**).

Growth of Equine Histoplasma

The growth of mycelial colonies was confirmed in 60 horses. The colonies appeared between 4 and 8 weeks of incubation as gray-white at the early stage, but as the colonies were aging, they became brown in color (**Figure 2A**). The mycelial colonies were abundant and voracious in feeding, emptying the 10-ml Sabouraud Dextrose Agar within a few months. Similarly, the yeast form was grown on the Brain Heart Infusion Agar and the colonies were gray in color and relatively small in size (**Figure 2B**). In the present study, the mycelial colonies were harvested for the extraction of DNA and subsequent molecular activities.

Identification of Histoplasma by PCR and Blasting of the Sequence Data

All the 60 culture-positive samples were also positive with PCR for *Histoplasma*. The molecular weights of the PCR products of all the 54 samples were similar and weigh about 600 bp (**Figures 3A–D**). The qualities and concentration of the 60 PCR products were assessed by further sequencing, but six PCR products failed to fulfill the required quality and concentration for library preparation. Thus, the library of 54 DNA samples was submitted for sequencing excluding the six PCR samples. BLAST analysis of these 54 isolates identified 29 *H.*

FIGURE 2 | Mycelial and yeast colonies of *H. capsulatum* var. *farciminosum* isolated from epizootic lymphangitis cases of horses in central Ethiopia. **(A)** Mycelial colonies on 2.5% glycerol enriched Sabouraud Dextrose Agar grown at 26°C after 4–8 weeks of incubation. The slants show pure mycelial colonies that are abundant, gray/white in color at the early stage but becoming brown as they are aging. **(B)** Yeast colonies grown on the Brain Heart Infusion Agar at 37°C after incubation for 4–8 weeks. The yeast colonies are small in size and whitish gray in color.

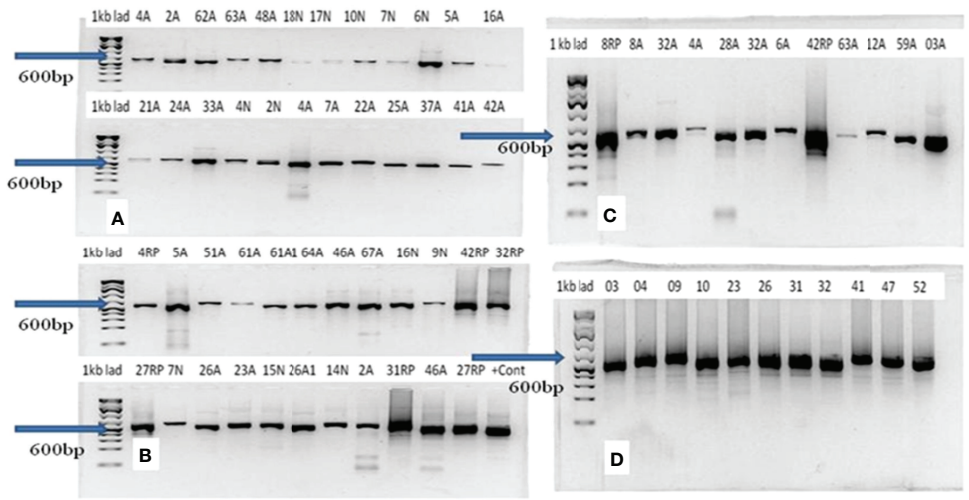

FIGURE 3 | Result of gel electrophoresis of PCR products of *Histoplasma capsulatum* isolated from epizootic lymphangitis cases of horses in central Ethiopia. In each gel **(A–D)**, the left lane is the 1-kb ladder while the remaining 12 lanes (2–13) represent samples. The molecular weights of all PCR products were equal and were about 600 bp as indicated by arrows on each gel.

capsulatum isolates and 14 isolates from other fungal genera (**Table 1**), while the remaining 11 samples were deemed insufficient for further downstream analysis. The alignment of the sequence data of the 29 Ethiopian isolates showed highly conserved ITS regions (**Figure 4**). There were a few gaps at the beginning of the sequences, and uneven sequence lengths were observed because of the deletions of sequences; the longest sequences have 653 bp while the shortest sequences have 553 bp.

Phylogenetic Relationships Between the Ethiopian Isolates and Other Isolates

The sequence data of isolates from different countries were included for the phylogenetic analysis. The accession number and the origin of these isolates are presented in **Table 2**. The phylogenetic analysis identified six clades. These clades include the African, Eurasian, North American 1 and 2, and South American A and B. Almost all the Ethiopian isolates recovered by the present study were grouped under the African clade and were closely clustered with isolates from South American A and Eurasian clades (**Figure 5** and **Supplementary File**). Similarly, one Ethiopian of the two isolates reported from Ethiopia by a previous study and named as EZL 2.1 was also clustered with the new Ethiopian isolates, while the second isolate which was designated EZL 2.2 was further away from the Ethiopian isolates of this study. The Ethiopian isolates were clustered further from the clades of North America 1, North America 2, and South America B.

DISCUSSION

In the present study, *H. capsulatum* was isolated from 60 EL cases of horses in central Ethiopia, of which the DNA samples of the isolates from 54 could qualify for further molecular analysis using sequencing of the ITS region. BLAST analysis of 54-sequence data identified 29 *H. capsulatum* while 14 were identified as other fungal genera including Aspergillus, Eurotium, Penicillium, and Cladosporioides. However, the remaining 11 DNA samples were not deemed of sufficient length to continue downstream analysis and hence were removed. The source of the other fungal genera could not be identified as the cultures were pure and had similar colonies. In addition, as it can be observed from the gels, the PCR products of each sample had a clear single band. Hence, it could be difficult to explain the origin of these fungal genera.

Since the ITS region is a universal to fungal species, it was thus difficult to classify the varieties of *Histoplasma capsulatum* into *H. capsulatum* var. *capsulatum*, *H. capsulatum* var. *farciminosum*, or *H. capsulatum* var. *duboisii*. Therefore, in this study, phylogenetic analysis could group the isolates at the species level of *Histoplasma capsulatum* to evaluate the relationship among the isolates of Histoplasma from different countries. The phylogenetic analysis grouped the global isolates into African, Eurasian, North American 1 and 2, and South American A and B. All of the newly isolated Ethiopian Histoplasma isolates were grouped with the South American A and Eurasian clades. However, they were clustered distantly furthest away from the North American 1 and 2 as well as South American B clades.

In addition to Ethiopia, the African clade was isolated from Egypt, Uganda, and South Africa. This clade is closely related with the Latin American A clade. In addition, the African clade is related to the Eurasian clade. The Eurasian clade was isolated from Europe (Belgium) and Asian countries (Thailand, Japan, Indonesia, India, and China). The South American A clade was originally isolated from the Latin American countries including Cuba, Colombia, Ecuador, and Guatemala covering a broader geographic coverage. The complex genetic population structure of the South American A clade was reported earlier (Teixeira M

TABLE 1 | Histoplasma and other fungal genera identified by blasting the sequence data.

Name of genus	Number (%)	Remark
Aspergillus spp.	4(7.4%)	For the Fasta alignment, please refer to folder "Aspergillus"
Eurotium	3(5.6%	For the Fasta alignment, please refer to folder "Eurotium"
Penicillium	3(5.6%	For the Fasta alignment, please refer to folder "Penicillium"
Cladosporioides	4(7.4%)	For the Fasta alignment, please refer to folder "Cladosporioides"
Histoplasma	32(59.3%)	For the Fasta alignment, please refer to folder "Histoplasma"
Uncultured fungus	8(14.8%)	For the Fasta alignment, please refer to folder "uncultured Fungus clone"

de et al., 2016). Unlike the South American A clade, the South American B clade is limited to isolates from Argentina, as it can observed in the phylogenetic tree of this study. The South American A and B clades were reported by Kasuga and coworkers (Kasuga et al., 2003); however, Sepúlveda and coworkers reported only the South American A clade (Sepúlveda et al., 2017).

Previous studies have reported the North American 1 and North American 2 clades (Kasuga et al., 2003; Sepúlveda et al., 2017). The North American 2 clade was isolated from humans in USA and limited to USA so far, as it has not been reported from other countries. Both the North American 1 and 2 clades are not related to the Ethiopian isolates. This suggests the less likely chance of transmission of *Histoplasma* organisms between Ethiopia and USA. In addition to the present isolates, EZL 2.1 and EZL 2.2 were reported from Ethiopia earlier by other researchers (Scantlebury et al., 2016). In the phylogenetic tree of the present study, EZL 2.1 was grouped closely with the isolates of the present study. However, EZL 2.2 was grouped further from the other Ethiopian isolates.

Different authors classified the clades of *Histoplasma capsulatum* based on different markers. Kasuga and coauthors reported eight different clades using the phylogenetic analysis of 137 isolates based on the DNA sequence variation in four independent protein-coding genes (Kasuga et al., 2003). The authors identified the North American 1 and 2, Latin American A and B, Australian, Netherlands (Indonesia)?, Eurasian, and African clades. As reported by these authors, seven of the eight clades can be considered as recognized phylogenetic species while the Eurasian clade could be classified under the Latin American A clade. A more recent study proposed six additional phylogenetic species of *Histoplasma* within Latin American isolates using 234 isolates by increasing the taxon sampling and using different phylogenetic and population genetic methods (Teixeira M de et al., 2016). Thus, there are different ways of classifying the isolates of *H. capsulatum* by different

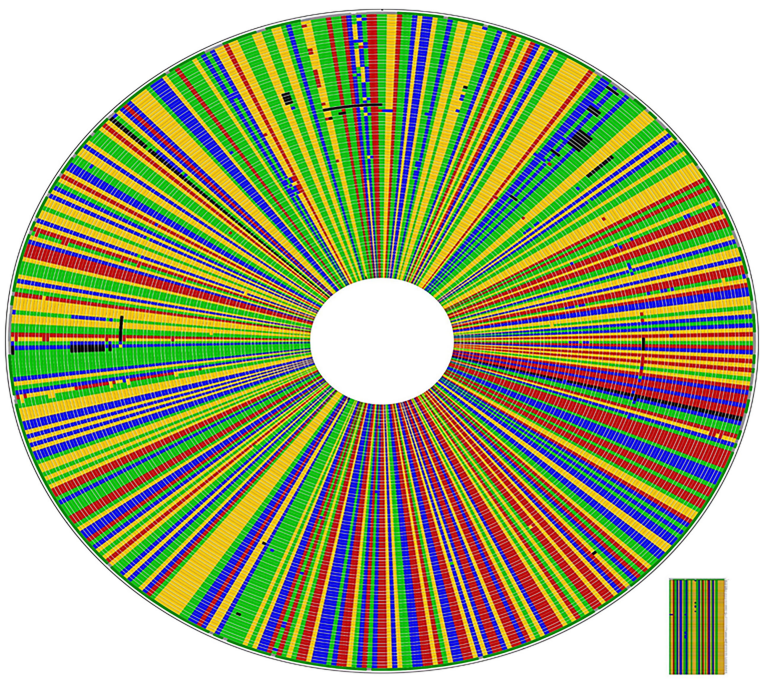

FIGURE 4 | High rate of conservation amongst Ethiopian *Histoplasma capsulatum* in ITS1-5.8s-ITS2 region: CLUSTAL W alignment of the 92 isolates including the 29 generated from this study. The sequences different from the consensus sequences are highlighted by a different color; dark colors indicate gaps.

TABLE 2 | Accession numbers of the *H. capsulatum* isolates included in the phylogenetic analysis and their countries of origin.

Accession number	Strain	Country of origin	Source	Clade
AF322378.1	*Histoplasma capsulatum*	USA	Dog	NAm_1
AB055229.2	*Histoplasma capsulatum*	USA	Human	NAm_2
AB071821.1	*Histoplasma capsulatum*	USA	Human	NAm_2
AB071822.1	*Histoplasma capsulatum*	USA	Human	NAm_2
AF129545.1	*Histoplasma capsulatum*	USA	Human	NAm_2
AF129542.1	*Histoplasma capsulatum*	USA	Human	NAm_1
AB055228.2	*Histoplasma capsulatum*	USA	Human	NAm_1
AF129547.1	*Histoplasma capsulatum*	USA	Human	NAm_1
AF129546.1	*Histoplasma capsulatum*	USA	Human	NAm_1
AF129543.1	*Histoplasma capsulatum*	UK	Human	Eurasia
AF129544.1	*Histoplasma capsulatum*	Thailand	Human	Eurasia
AF129538.1	*Histoplasma capsulatum*	Thailand	Human	Eurasia
AF129539.1	*Histoplasma capsulatum*	Thailand	Human	Eurasia
AF129540.1	*Histoplasma capsulatum*	Japan	Human	Eurasia
AF129541.1	*Histoplasma capsulatum*	Japan	Human	Eurasia
AB055236.2	*Histoplasma capsulatum*	Indonesia	Human	Eurasia
AB055238.2	*Histoplasma capsulatum*	Thailand	Human	Eurasia
AB055239.2	*Histoplasma capsulatum*	Thailand	Human	Eurasia
AB055240.2	*Histoplasma capsulatum*	Thailand	Human	Eurasia
AY623792.1	*Histoplasma capsulatum*	Japan	Dog	Eurasia
AB055244.2	*Histoplasma capsulatum*	Japan	Human	Eurasia
AB055235.2	*Histoplasma capsulatum*	Indonesia	Human	Eurasia
AB071830.1	*Histoplasma capsulatum*	Guatemala	Human	SAm_A
AB071827.1	*Histoplasma capsulatum*	Ecuador	Human	SAm_A
AB071823.1	*Histoplasma capsulatum*	Colombia	Human	SAm_A
AB071840.1	*Histoplasma capsulatum*	China	Human	Eurasia
AB071843.1	*Histoplasma capsulatum*	Australia	Human	Eurasia
KC693546.1	*Histoplasma capsulatum*	Argentina	Skin	SAm_B
KC693545.1	*Histoplasma capsulatum*	Argentina	Larynx biopsy	SAm_B
KC693541.1	*Histoplasma capsulatum*	Argentina	LRC HIV	SAm_B
KC693542.1	*Histoplasma capsulatum*	Argentina	Skin HIV	SAm_B
KC693543.1	*Histoplasma capsulatum*	Argentina	Blood culture HIV	SAm_B
KC693544.1	*Histoplasma capsulatum*	Argentina	Oral mucosa HIV	SAm_B
KC693537.1	*Histoplasma capsulatum*	Argentina	Skin HIV	SAm_B
KC693538.1	*Histoplasma capsulatum*	Argentina	Skin	SAm_B
KC693539.1	*Histoplasma capsulatum*	Argentina	Bone marrow HIV	SAm_B
KC693536.1	*Histoplasma capsulatum*	Argentina	Blood culture HIV	SAm_B
AB055231.2	*Histoplasma capsulatum*	Argentina	human	SAm_B
KC693533.1	*Histoplasma capsulatum*	Argentina	Blood culture HIV	SAm_B
KC693534.1	*Histoplasma capsulatum*	Argentina	Nasal mucosa	SAm_B
KC693535.1	*Histoplasma capsulatum*	Argentina	Oral mucosa	SAm_B
MN912626	*Histoplasma capsulatum*	Ethiopia (this study)	Horse	
MN912624	*Histoplasma capsulatum*	Ethiopia (this study)	Horse	
MN912625	*Histoplasma capsulatum*	Ethiopia (this study)	Horse	
MN912622	*Histoplasma capsulatum*	Ethiopia (this study)	Horse	
MN912623	*Histoplasma capsulatum*	Ethiopia (this study)	Horse	
MN912620	*Histoplasma capsulatum*	Ethiopia (this study)	Horse	
MN912621	*Histoplasma capsulatum*	Ethiopia (this study)	Horse	
MN912618	*Histoplasma capsulatum*	Ethiopia (this study)	Horse	
MN912619	*Histoplasma capsulatum*	Ethiopia (this study)	Horse	
MN912614	*Histoplasma capsulatum*	Ethiopia (this study)	Horse	
MN912615	*Histoplasma capsulatum*	Ethiopia (this study)	Horse	
MN912616	*Histoplasma capsulatum*	Ethiopia (this study)	Horse	
MN912617	*Histoplasma capsulatum*	Ethiopia (this study)	Horse	
MN912612	*Histoplasma capsulatum*	Ethiopia (this study)	Horse	
MN912613	*Histoplasma capsulatum*	Ethiopia (this study)	Horse	
MN912607	*Histoplasma capsulatum*	Ethiopia (this study)	Horse	
MN912611	*Histoplasma capsulatum*	Ethiopia (this study)	Horse	
MN912599	*Histoplasma capsulatum*	Ethiopia (this study)	Horse	
MN912603	*Histoplasma capsulatum*	Ethiopia (this study)	Horse	
MN912604	*Histoplasma capsulatum*	Ethiopia (this study)	Horse	
MN912605	*Histoplasma capsulatum*	Ethiopia (this study)	Horse	
MN912596	*Histoplasma capsulatum*	Ethiopia (this study)	Horse	

(Continued)

TABLE 2 | Continued

Accession number	Strain	Country of origin	Source	Clade
MN912597	*Histoplasma capsulatum*	Ethiopia (this study)	Horse	
MN912598	*Histoplasma capsulatum*	Ethiopia (this study)	Horse	
MN912595	*Histoplasma capsulatum*	Ethiopia (this study)	Horse	
MN912587	*Histoplasma capsulatum*	Ethiopia (this study)	Horse	
MN912588	*Histoplasma capsulatum*	Ethiopia (this study)	Horse	
MN912591	*Histoplasma capsulatum*	Ethiopia (this study)	Horse	
MN912594	*Histoplasma capsulatum*	Ethiopia (this study)	Horse	
EF592163.1	*Blastomyces dermatitidis*			

NAm_1, North America 1 clade; NAm_2, North America 2 clade; SAm_A, South America A clade; SAm_B, South America B clade.

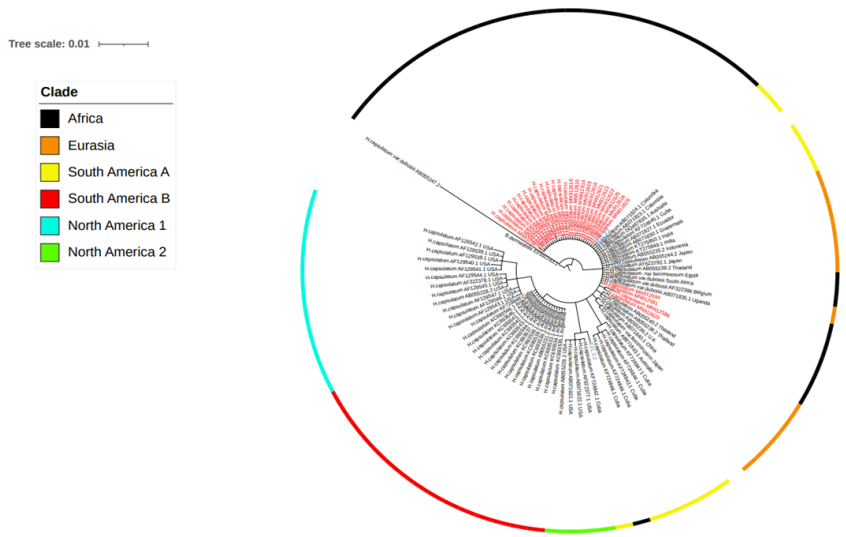

FIGURE 5 | Evolutionary analysis of *Histoplasma capsulatum* isolated from Ethiopia and other countries by maximum likelihood method. The evolutionary history was inferred by using Bayesian inference with the Tamura-Nei model + gamma model. Clades are presented as color tips parallel to sample names which also indicate their countries of origin and NCBI accession number. Sample names written in red color font (Ethiopian) are those generated by the present study, while two Ethiopian isolates that are written in blue font color were generated by previous study in Ethiopia.

authors, which warrants reaching on a consensus single method that can be used for all researchers working on *H. capsulatum*.

Previous studies classified *H. capsulatum* into three varieties (Kasuga et al., 1999). According to this study, *H. capsulatum* var. *capsulatum* causes histoplasmosis in humans primarily affecting the lungs. Furthermore, *H. capsulatum* var. *capsulatum* was also isolated from domestic cats with severe and disseminated mycosis in the lungs (Panciera, 1969; Arunmozhi Balajee et al., 2013). Moreover, histoplasmosis due to *H. capsulatum* var. *capsulatum* was reported in dogs in USA (Brömel and Sykes, 2005). Although *H. capsulatum* var. *capsulatum* was reported from about 60 countries from all continents (Ajello, 1988), it is highly prevalent in the North America and Latin America (Kwon-Chung et al., 1992). There are two clades of *H. capsulatum* var. *capsulatum* in North America which differ in growth phenotypes, restriction fragment length polymorphisms of mitochondria, and genomic DNA (Vincent et al., 1986; Spitzer et al., 1989). The North American 1 isolates were isolated from HIV patients while the North American 2 isolates were isolated from both individuals infected with HIV and individuals not infected with HIV (Spitzer et al., 1990).

H. capsulatum var. *duboisii* is considered to be the causative agent of African histoplasmosis in humans that is characterized by cutaneous, subcutaneous, and osseous lesions (Stelzner and Rippon, 1990), while *H. capsulatum* var. *farciminosum* causes subcutaneous and ulcerated lesions in the skin of horses and mules (Stelzner and Rippon, 1990). Additionally, *H. capsulatum* var. *farciminosum* causes similar lesions in dogs (Ueda et al., 2003). Animal histoplasmosis is widespread throughout Europe, North America, India, and South Asia (Kwon-Chung et al., 1992). In addition, *H. capsulatum* var. *farciminosum* was isolated from soil in caves infested with bats in Israel (Ajello et al., 1977), suggesting the possibility of its transmission by bats which can excrete the fungus through feces or other secretions that can contaminate the soil, thereby facilitating its further transmission to equines. Additionally,

disseminated histoplasmosis was diagnosed in domestic cats and in wild badgers (*Meles meles*) in Austria (Klang et al., 2013) and in Germany (Eisenberg et al., 2013), respectively, suggesting the importance of these species of animals in the epidemiology of histoplasmosis. The morphology of the yeast cells of *H. capsulatum* var. *farciminosum* resembles that of *H. capsulatum* var. *capsulatum* (Panciera, 1969).

This study is the first study in sequencing a relatively large number of *H. capsulatum* var. *farciminosum* isolated from EL cases of horses. In addition, the sequences of Ethiopian isolates were compared with the sequence data of *H. capsulatum* isolates that were retrieved from GenBank. This effort can be considered as the strength of this study. However, the weakness of the study is the use of the internal transcribed spacer (ITS) region of rRNA genes, which is a universal gene in fungal organisms.

CONCLUSION

In conclusion, according to the phylogenetic analysis of the sequences of the ITS region of rRNA genes of *Histoplasma*, the Ethiopian isolates were closely related to the South American A and Eurasian clades while they were distantly clustered further away from the North American 1 and 2 and South American B clades.

DATA AVAILABILITY STATEMENT

The datasets presented in this study can be found in online repositories. The names of the repository/repositories and accession number(s) can be found as follows: https://www.ncbi.nlm.nih.gov/nuccore/MN912587.1/, MN912587-MN912626.

ETHICS STATEMENT

Ethical review and approval were not required for the animal study because the screening cases and sample collection were performed as part of the clinical examination and treatment of epizootic cases of horses in Woliso Town, central Ethiopia. However, consent was obtained from owners for the collection of pus samples. Written informed consent was obtained from the owners for the participation of their animals in this study.

AUTHOR CONTRIBUTIONS

GA and TS designed the study. AZ and AMK contributed in the analysis of the data. MK and FS supervised the preparation of library for sequencing and facilitated the sequencing. RA and MGA contributed in the field sample collection and culturing of the samples. GA was involved in the field sample collection, fungal isolation, and preparation of the library. GA drafted the manuscript while all the other authors edited the manuscript. All authors contributed to the article and approved the submitted version.

FUNDING

The research was financially supported by the National Human Genomic Institute, National Institute of Health (Reference Number U01HG007472).

ACKNOWLEDGMENTS

The authors would like to acknowledge the Biosciences Eastern and Central Africa - International Livestock Research Institute (BecA - ILRI) for providing a laboratory space and technical support.

SUPPLEMENTARY MATERIAL

The Supplementary Material for this article can be found online at: https://www.frontiersin.org/articles/10.3389/fcimb.2022.789157/full#supplementary-material

REFERENCES

Ajello, L. (1988). "Histoplasmosis Capsulati," in *Laboratory Diagnosis of Infectious Diseases: Principles and Practice*. Eds. A. Balows, W. J. Hausler, M. Ohashi, A. Turano and E. H. Lennete (New York, NY: Springer New York), 650–653. doi: 10.1007/978-1-4612-3898-0_65

Ajello, L., Kuttin, E. S., Beemer, A. M., Kaplan, W., and Padhye, A. (1977). Occurrence of Histoplasma Capsulatum Darling, 1906 in Israel, With a Review of the Current Status of Histoplasmosis in the Middle East. *Am. J. Trop. Med. Hyg.* 26 (1), 140–147. doi: 10.4269/ajtmh.1977.26.140

Al-Ani, F. K. (1999). Epizootic Lymphangitis in Horses: A Review of the Literature. *Rev. Sci. Tech. Int. Off. Epizoot.* 18 (3), 691–699. doi: 10.20506/rst.18.3.1186

Ameni, G. (2006) *Epidemiology of Equine Histoplasmosis (Epizootic Lymphangitis) in Carthorses in Ethiopia*.

Ameni, G. (2007). Pathology and Clinical Manifestation of Epizootic Lymphangitis in Cart Mules in Ethiopia. *J. Equine Sci.* 18 (1), 1–4. doi: 10.1294/jes.18.1

Ameni, G., and Terefe, W. (2004). A Cross-Sectional Study of Epizootic Lymphangitis in Cart-Mules in Western Ethiopia. *Prev. Vet. Med.* 66 (1–4), 93–99. doi: 10.1016/j.prevetmed.2004.09.008

Arunmozhi Balajee, S., Hurst, S. F., Chang, L. S., Miles, M., Beeler, E., Hale, C., et al (2013). Multilocus Sequence Typing of Histoplasma Capsulatum in Formalin-Fixed Paraffin-Embedded Tissues From Cats Living in non-Endemic Regions Reveals a New Phylogenetic Clade. *Med. Mycol.* 51 (4), 345–351. doi: 10.3109/13693786.2012.733430

Brömel, C., and Sykes, J. E. (2005). Histoplasmosis in Dogs and Cats. *Clin. Tech. Small Anim. Pract.* 20 (4), 227–232. doi: 10.1053/j.ctsap.2005.07.003

Buxton, A., and Fraser, G. (1977). *Animal Microbiology* Vol. 1, 2 (Oxford: Blackwell Scientific).

CFSPH (2019). *Epizootic lymphangitis*. (Center for Food Security and Public Health, CFSPH. College of Veterinary Medicine, Iowa State University). Available at: https://dr.lib.iastate.edu/handle/20.500.12876/98960.

Eisenberg, T., Seeger, H., Kasuga, T., Eskens, U., Sauerwald, C., and Kaim, U. (2013). Detection and Characterization of Histoplasma Capsulatum in a German Badger (Meles Meles) by ITS Sequencing and Multilocus Sequencing Analysis. *Med. Mycol.* 51 (4), 337–344. doi: 10.3109/13693786.2012.723831

Guérin, C., Abebe, S., and Touati, F. (1992) *Lymphangite Épizootique Du Cheval En Ethiopie. Undefined*. Available at: https://www.semanticscholar.org/paper/Lymphangite-%C3%A9pizootique-du-cheval-en-Ethiopie-Gu%C3%A9rin-Abebe/d629f14af282b519c5b3320b332c3bf59ec54290.

Kasuga, T., Taylor, J. W., and White, T. J. (1999). Phylogenetic Relationships of Varieties and Geographical Groups of the Human Pathogenic Fungus Histoplasma Capsulatum Darling. *J. Clin. Microbiol.* 37 (3), 653–663. doi: 10.1128/JCM.37.3.653-663.1999

Kasuga, T., White, T. J., Koenig, G., Mcewen, J., Restrepo, A., Castañeda, E., et al (2003). Phylogeography of the Fungal Pathogen Histoplasma Capsulatum. *Mol. Ecol.* 12 (12), 3383–3401. doi: 10.1046/j.1365-294X.2003.01995.x

Klang, A., Loncaric, I., Spergser, J., Eigelsreiter, S., and Weissenböck, H. (2013). Disseminated Histoplasmosis in a Domestic Cat Imported From the USA to Austria. *Med. Mycol. Case Rep.* 2, 108–112. doi: 10.1016/j.mmcr.2013.04.004

Kwon-Chung, K. J., and Bennett, J. E. (1992). *Medical Mycology 2nd Edition by Kwon- Hardcover. 2nd edition* (Paris: Lea & Febiger).

Landaburu, F., Cuestas, M. L., Rubio, A., Elías, N. A., Daneri, G. L., Veciño, C., et al (2014). Genetic Diversity of Histoplasma Capsulatum Strains Isolated From Argentina Based on Nucleotide Sequence Variations in the Internal Transcribed Spacer Regions of Rdna. *Mycoses* 57 (5), 299–306. doi: 10.1111/myc.12159

Mace, E. S., Buhariwalla, H. K., and Crouch, J. H. (2003) *A High-Throughput DNA Extraction Protocol for Tropical Molecular Breeding Programs - UQ eSpace*. Available at: https://espace.library.uq.edu.au/view/UQ:406077.

OIE (2008). *Epizootic Lymphangitis* (Paris: OIE - World Organisation for Animal Health). Available at: https://www.oie.int/en/disease/epizootic-lymphangitis/.

OIE (2018). *Epizootic Lymphangitis* (Paris: OIE - World Organisation for Animal Health). Available at: https://www.oie.int/en/disease/epizootic-lymphangitis/.

Panciera, R. J. (1969). Histoplasmic (Histoplasma Capsulatum) Infection in a Horse. *Cornell Vet.* 59 (2), 306–312.

Radostits, O. M. (1994) *Veterinary Medicine: A Textbook of the Diseases of Cattle, Horses, Sheep, Pigs and Goats (Radostits, Veterinary Medicine)*. Available at: https://www.amazon.com/Veterinary-Medicine-textbook-diseases-Radostits/dp/0702027774. 9780702027772: Medicine & Health Science Books @Amazon.com

Scantlebury, C. E., Pinchbeck, G. L., Loughnane, P., Aklilu, N., Ashine, T., Stringer, A. P., et al (2016). Development and Evaluation of a Molecular Diagnostic Method for Rapid Detection of Histoplasma Capsulatum Var. Farciminosum, the Causative Agent of Epizootic Lymphangitis, in Equine Clinical Samples. *J. Clin. Microbiol.* 54 (12), 2990–2999.

Selim, S. A., Soliman, R., Osman, K., Padhye, A. A., and Ajello, L. (1985). Studies on Histoplasmosis Farciminosi (Epizootic Lymphangitis) in Egypt. Isolation of Histoplasma Farciminosum From Cases of Histoplasmosis Farciminosi in Horses and its Morphological Characteristics. *Eur. J. Epidemiol.* 1 (2), 84–89. doi: 10.1007/BF00141797

Sepúlveda, V. E., Márquez, R., Turissini, D. A., Goldman, W. E., and Matute, D. R. (2017). Genome Sequences Reveal Cryptic Speciation in the Human Pathogen Histoplasma Capsulatum. *mBio* 8 (6), e01339-17. doi: 10.1128/mBio.01339-17

Singh, T. (1965). Studies on Epizootic Lymphangitis: Modes Infection and Transmission of Equine Histoplasmosis (Epizootic Lymphangitis). *Int. J. Vet. Sci.* 35, 102–110.

Spitzer, E. D., Keath, E. J., Travis, S. J., Painter, A. A., Kobayashi, G. S., and Medoff, G. (1990). Temperature-Sensitive Variants of Histoplasma Capsulatum Isolated From Patients With Acquired Immunodeficiency Syndrome. *J. Infect. Dis.* 162 (1), 258–261. doi: 10.1093/infdis/162.1.258

Spitzer, E. D., Lasker, B. A., Travis, S. J., Kobayashi, G. S., and Medoff, G. (1989). Use of Mitochondrial and Ribosomal DNA Polymorphisms to Classify Clinical and Soil Isolates of Histoplasma Capsulatum. *Infect. Immun.* 57 (5), 1409–1412. doi: 10.1128/iai.57.5.1409-1412.1989

Stelzner, A., and Rippon, J. W. (1990). Medical Mycology– The Pathogenic Fungi and the Pathogenic Actinomycetes (Third Edition). IX + 797 S., 482 Abb., 58 Tab. Philadelphia–London–Toronto–Montreal–Sydney–Tokyo 1988. W. B. Saunders Company–Harcourt Brace Jovanovich Inc. ISBN: 0-7216-2444-8. *J. Basic Microbiol.* 30 (6), 463–463.

Teixeira M de, M., Patané, J. S. L., Taylor, M. L., Gómez, B. L., Theodoro, R. C., de, H. S., et al (2016). Worldwide Phylogenetic Distributions and Population Dynamics of the Genus Histoplasma. *PloS Negl. Trop. Dis.* 10 (6), e0004732. doi: 10.1371/journal.pntd.0004732

Ueda, Y., Sano, A., Tamura, M., Inomata, T., Kamei, K., Yokoyama, K., et al (2003). Diagnosis of Histoplasmosis by Detection of the Internal Transcribed Spacer Region of Fungal rRNA Gene From a Paraffin-Embedded Skin Sample From a Dog in Japan. *Vet. Microbiol.* 94 (3), 219–224. doi: 10.1016/S0378-1135(03)00104-4

Vincent, R. D., Goewert, R., Goldman, W. E., Kobayashi, G. S., Lambowitz, A. M., and Medoff, G. (1986). Classification of Histoplasma Capsulatum Isolates by Restriction Fragment Polymorphisms. *J. Bacteriol.* 165 (3), 813–818. doi: 10.1128/jb.165.3.813-818.1986

White, T. J., Bruns, T., Lee, S., and Taylor, J. (1990). "Amplification and Direct Sequencing of Fungal Ribosomal Rna Genes for Phylogenetics," in *Pcr Protocols* (Elsevier), 315–322. Available at: https://linkinghub.elsevier.com/retrieve/pii/B9780123721808500421.

Conflict of Interest: The authors declare that the research was conducted in the absence of any commercial or financial relationships that could be construed as a potential conflict of interest.

Publisher's Note: All claims expressed in this article are solely those of the authors and do not necessarily represent those of their affiliated organizations, or those of the publisher, the editors and the reviewers. Any product that may be evaluated in this article, or claim that may be made by its manufacturer, is not guaranteed or endorsed by the publisher.

Advantages of publishing in Frontiers

OPEN ACCESS
Articles are free to read for greatest visibility and readership

FAST PUBLICATION
Around 90 days from submission to decision

HIGH QUALITY PEER-REVIEW
Rigorous, collaborative, and constructive peer-review

TRANSPARENT PEER-REVIEW
Editors and reviewers acknowledged by name on published articles

Frontiers
Avenue du Tribunal-Fédéral 34
1005 Lausanne | Switzerland

Visit us: www.frontiersin.org
Contact us: frontiersin.org/about/contact

REPRODUCIBILITY OF RESEARCH
Support open data and methods to enhance research reproducibility

DIGITAL PUBLISHING
Articles designed for optimal readership across devices

FOLLOW US
@frontiersin

IMPACT METRICS
Advanced article metrics track visibility across digital media

EXTENSIVE PROMOTION
Marketing and promotion of impactful research

LOOP RESEARCH NETWORK
Our network increases your article's readership